CONTENTS

ON APPLICATION OF CONTRACTION PRINCIPLE TO SOLVE TWO-TERM FRACTIONAL DIFFERENTIAL EQUATIONS

Marek BŁASIK*, Małgorzata KLIMEK*

* Institute of Mathematics, Czestochowa University of Technology, ul. Dąbrowskiego 73, 42-200 Częstochowa

marek.blasik@gmail.com, mklimek@im.pcz.pl

Abstract: We solve two-term fractional differential equations with left-sided Caputo derivatives. Existence-uniqueness theorems are proved using newly-introduced equivalent norms/metric on the space of continuous functions. The metrics are modified in such a way that the space of continuous functions is complete and the Banach theorem on a fixed point can be applied. It appears that the general solution is generated by the stationary function of the highest order derivative and exists in an arbitrary interval [0,b].

1. INTRODUCTION

Fractional differential equations (FDE) emerged in applied mathematics as an important tool to describe many processes and phenomena in physics, mechanics, economics, control theory, engineering and bioengineering (compare monographs and review papers (Agrawal et al., 2004; Hilfer, 2000; Kilbas et al., 2006; Magin, 2006; Metzler and Klafter, 2004; West et al., 2003) and the references given therein). During the last decades, the theory of fractional differential equations has become an interesting and meaningful field of mathematics (the results and references are summarized in monographs (Diethelm, 2010; Kilbas et al., 2006; Kilbas and Trujillo, 2001, 2002; Klimek, 2009; Lakshmikantham et al., 2009; Miller and Ross, 1993; Podlubny, 1999)). Since 2010 the FDE theory also was classified in the MSC system: under 34A08 for ordinary fractional differential equations, 34K37 for functional fractional differential equations and under 35R11 for partial fractional differential equations.

Still, in the theory of fractional differential equations, many problems remain open. Even in case of basic existence-uniqueness results, there is an area for investigations concerning the efficient proving methods, corresponding space of solutions choice and the extension of results from basic to more general equations containing many terms with derivatives, both left- and right-sided.

The present paper is devoted to the study of two-term fractional differential equations with left-sided Caputo derivatives. Existence-uniqueness results are obtained for equations of arbitrary fractional order when the highest order derivative is given as a sequential operator i.e. it is a composition of two Caputo derivatives. Let us point out that the equations from this class of sequential FDE were applied in the theory of viscoelasticity (Wang. 2010) and in hydrodynamics (Khan et al., 2009; Shan et al., 2009; Tian et al., 2006).

The proposed method of deriving the solution is an extension of the Bielecki method known from differential equations theory (Bielecki, 1956). He applied equivalent norms/metrics, modified using the exponential function, and the Banach theorem to solve differential equations of integer order. In the paper (El Raheem, 2003), a simple fractional differential equation of the order in the range (0,1) was solved using the same approach. Then, Lakshmikantham and his collaborators (Lakshmikantham et al., 2008, 2009) applied in the modification of norms/metrics the one-parameter Mittag-Leffler function. This allowed them to prove the existence and uniqueness result for equations with the Caputo derivative of order in the range (0,1). Further results for similar equations are given in the paper (Baleanu and Mustafa, 2010). In the papers by Klimek (Klimek, 2011a, b) they were extended to the multi-term FDE dependent on a basic Riemann-Liouville, Caputo or Hadamard derivative.

Here, we study equations with sequential powers of Caputo derivatives of an arbitrary fractional order. Assuming that the nonlinear term obeys the Lipschitz condition, we obtain continuous solutions in an arbitrarily long interval.

The paper is organized as follows. In Section 2 we recall the basic definitions from fractional calculus and introduce a family of norms in the space of functions continuous in a finite interval. They are equivalent to the supremum norm, thus whenever we endow the space of continuous functions with the metric generated by the new norm, we obtain a complete, metric space. We also formulate the lemma on the properties of fractional integration and further apply it to solve fractional differential equations. Section 3 is devoted to the existence-uniqueness result for a two-term fractional differential equation with the composed Caputo derivatives. The analogous results for a general sequential equation with the composed Caputo derivatives are included in Section 4. The paper is closed by a short discussion of the presented method of solving and its possible further applications.

2. PRELIMINARIES

In this section we recall the basic definition from fractional calculus and introduce a class of norms equivalent to the supremum norm on the space of continuous functions. The Riemann-Liouville integral and Caputo derivative are defined as follows (Samko et al., 1993, Kilbas et al., 2006).

Definition 2.1. The left-sided Riemann-Liouville integral of order α, denoted as I_{0+}^{α}, is given by the following formula for $\mathrm{Re}(\alpha) > 0$:

$$I_{0+}^{\alpha} f(t) := \frac{1}{\Gamma(\alpha)} \int_0^t \frac{f(u)du}{(t-u)^{1-\alpha}} . \tag{1}$$

Definition 2.2. Let $\mathrm{Re}(\alpha) \in (n-1, n)$. The left-sided Caputo derivative of order α, denoted as ${}^{c}\mathrm{D}_{0+}^{\alpha}$, is given by the formula:

$${}^{c}D_{0+}^{\alpha} f(t) := \frac{1}{\Gamma(n-\alpha)} \int_0^t \frac{f^{(n)}(u)du}{(t-u)^{\alpha-n+1}} . \tag{2}$$

The definition below describes a generalized exponential function - the Mittag-Leffler function.

Definition 2.3. Let $\gamma > 0,\ \delta > 0$. The two-parameter Mittag-Leffler function is given as the following series

$$E_{\gamma,\delta}(z) = \sum_{k=0}^{\infty} \frac{z^k}{\Gamma(\gamma k + \delta)} . \tag{3}$$

Definition 2.4. We denote as $C[0, \mathrm{b}]$ the space of functions continuous in interval $[0, \mathrm{b}]$. This space with supremum norm $\|g\| = \sup_{t\in[0,b]} |g(t)|$ and the respective generated metric d is a complete metric space.

We shall apply the Mittag-Leffler functions in the construction of a class of norms in space $C[0, \mathrm{b}]$, indexed by positive parameter κ.

Definition 2.5. The following formula defines a one-parameter class of norms and metrics on space $C[0, \mathrm{b}]$

$$\|g\|_{\kappa} := \sup_{t\in[0,b]} \frac{|g(t)|}{E_{\gamma,1}(\kappa t^{\gamma})} \tag{4}$$

$$d_{\kappa}(g,h) := \| g - h \|_{\kappa} . \tag{5}$$

Property 2.6. Supremum norm $\|\cdot\|$ and the norms given by formula (4) are equivalent.

Proof: This property results from the set of inequalities

$$\|g\| \cdot \left(\sup_{t\in[0,b]} E_{\gamma,1}(\kappa t^{\gamma}) \right)^{-1} \le \|g\|_{\kappa} \le \|g\| ,$$

which are fulfilled for any $g \in C[0, \mathrm{b}]$ and $\kappa \in R_+$.

Now, we quote an important result concerning the fractional integrals of the Mittag-Leffler function and their supremum.

Lemma 2.7. The following integration formula is valid for any $\beta, \kappa \in R_+$

$$I_{0+}^{\beta} E_{\beta,1}(\kappa t^{\beta}) = \frac{1}{\kappa}(E_{\beta,1}(\kappa t^{\beta}) - 1) , \tag{6}$$

Let $\beta > \alpha > 0$. Then, constant A exists so that the following inequality is valid for parameter $\kappa \in R_+$

$$\sup_{t\in[0,b]} \frac{I_{0+}^{\beta} E_{\beta-\alpha,1}(\kappa t^{\beta-\alpha})}{E_{\beta-\alpha,1}(\kappa t^{\beta-\alpha})} \le \frac{b^{\alpha}}{\kappa} A . \tag{7}$$

The first part of the above lemma is a straightforward corollary of relation

$${}^{c}D_{0+}^{\beta} E_{\beta,1}(\kappa t^{\beta}) = \kappa E_{\beta,1}(\kappa t^{\beta}).$$

The proof of the second part is rather long and technical so we omit these calculations in the present paper.

3. SOLUTION OF TWO-TERM FRACTIONAL DIFFERENTIAL EQUATION – CASE I

We shall consider a two-term fractional differential equation in an arbitrary finite interval $[0, \mathrm{b}]$ including left -sided Caputo derivatives in a sequential form:

$$(D^{\alpha_2} - a_1 D^{\alpha_1}) f(t) = \psi(t, f(t)) \tag{8}$$

with

$$D^{\alpha_1} f(t) := {}^{c}D_{0+}^{\alpha_1} \tag{9}$$

$$D^{\alpha_2} f(t) := {}^{c}D_{0+}^{\alpha_1} {}^{c}D_{0+}^{\alpha_2-\alpha_1} f(t) ,\ \alpha_2 > \alpha_1 . \tag{10}$$

The preliminary results for equations of this type are discussed in paper (Klimek, Błasik 2011). In the present paper, we shall give full proof of the existence-uniqueness results for the general solution to equation (8) and for the initial value problem in case $\alpha_1, \alpha_2 \in (0,1)$.

In the transformation of the above equation, we shall apply the following composition rule for the Caputo derivative and Riemann-Liouville integral. This rule holds for any function continuous in interval [0,b] and we quote it after the monographs (Samko et al 1993; Kilbas et al 2006).

Property 3.1. Let $f \in C([0, \mathrm{b}], \mathrm{R})$ and $\beta > \alpha$. The following equalities hold for any point $t \in [0, \mathrm{b}]$

$${}^{C}D_{0+}^{\alpha} I_{0+}^{\alpha} f(t) = f(t) \tag{11}$$

$${}^{c}D_{0+}^{\alpha} I_{0+}^{\beta} f(t) = I_{0+}^{\beta-\alpha} f(t) . \tag{12}$$

Assuming the nonlinear term ψ to be a continuous function of two variables and using the above property, we can reformulate equation (8) as follows

$${}^{c}D_{0+}^{\alpha_1} {}^{c}D_{0+}^{\alpha_2-\alpha_1} \left(f(t) - a_1 I_{0+}^{\alpha_2-\alpha_1} f(t) - I_{0+}^{\alpha_2} \psi(t, f(t)) \right) = 0 , \tag{13}$$

provided $f \in C[0, \mathrm{b}]$.

Now, we observe that the function in the brackets belongs to the kernel of sequential derivative D^{α_2}. Let us denote this function as φ_0 and write the corresponding equation for stationary function

$$D^{\alpha_2}(\varphi_0(t)) = {}^{c}D_{0+}^{\alpha_1}\,{}^{c}D_{0+}^{\alpha_2-\alpha_1}(\varphi_0(t)) = 0 \tag{14}$$

which leads to the explicit formula

$$\varphi_0(t) = \sum_{j=0}^{n_{1,2}-1} \frac{c_j \cdot t^j}{\Gamma(j+1)} + \sum_{i=0}^{n_1-1} \frac{d_i \cdot t^{\alpha_2-\alpha_1+i}}{\Gamma(\alpha_2-\alpha_1+i+1)} \tag{15}$$

when the respective orders fulfill the conditions: $\alpha_1 \in (n_1 - 1, n_1)$ and $\alpha_2 - \alpha_1 \in (n_{1,2} - 1, n_{1,2})$.

Equation (13), rewritten using stationary function (15), becomes the fractional integral equation:

$$f(t) - a_1 I_{0+}^{\alpha_2-\alpha_1} f(t) - I_{0+}^{\alpha_2}\psi(t, f(t)) = \varphi_0(t) \tag{16}$$

which in turn coincides with fixed point condition

$$f(t) = T_{\varphi_0} f(t) \tag{17}$$

for mapping $T_{\phi 0}$ generated by stationary function φ_0

$$T_{\varphi_0} f(t) := a_1 I_{0+}^{\alpha_2-\alpha_1} f(t) + I_{0+}^{\alpha_2}\psi(t, f(t)) + \varphi_0(t)\,. \tag{18}$$

Assuming function $\psi \in C([0,b] \times R, R)$ and observing that stationary function φ_0 is continuous in interval $[0,b]$ we conclude that the above mapping transforms any continuous function into its continuous image.

The discussed transformation of the FDE given in (8) into fixed point condition (17) allows us to formulate the following result on the existence of a solution to equation (8).

Proposition 3.2. Let $\alpha_2 > \alpha_1$ and function $\psi \in C([0,b] \times R, R)$ fulfill the Lipschitz condition:

$$|\psi(t,x) - \psi(t,y)| \le M \cdot |x - y| \tag{19}$$

$\forall\, t \in [0,b],\ \forall\, x, y \in R$.

Then, each stationary function of derivative D^{α_2} given in (15) yields a unique solution of equation (8) in the space of functions continuous in interval $[0,b]$. Such a solution is a limit of the iterations of mapping $T_{\phi 0}$:

$$f(t) = \lim_{k\to\infty} (T_{\varphi_0})^k \chi(t)\,, \tag{20}$$

where χ is an arbitrary continuous function.

Proof: We reformulate equation (8) as fixed point condition (17) with mapping $T_{\phi 0}$ defined in (18). We shall consider the properties of this mapping on the space of functions continuous in interval $[0,b]$ endowed with a metric generated by the norm constructed according to Definition 2.5 :

$$\|g\|_\kappa = \sup_{t\in[0,b]} \frac{|g(t)|}{E_{\alpha_2-\alpha_1,1}(\kappa t^{\alpha_2-\alpha_1})}\,. \tag{21}$$

For any two continuous functions g and h, the distance of their images $T_{\phi 0}g$ and $T_{\phi 0}h$ (measured using the metric determined by the above norm) can be estimated as follows

$$\begin{aligned}
&\left\|T_{\varphi_0}h - T_{\varphi_0}g\right\|_\kappa = \\
&= \sup_{t\in[0,b]} \frac{\left|a_1 I_{0+}^{\alpha_2-\alpha_1}(h(t)-g(t)) + I_{0+}^{\alpha_2}(\psi(t,h(t)) - \psi(t,g(t))\right|}{E_{\alpha_2-\alpha_1,1}(\kappa t^{\alpha_2-\alpha_1})} \le \\
&\le \sup_{t\in[0,b]} \frac{|a_1| I_{0+}^{\alpha_2-\alpha_1}|h(t)-g(t)| + I_{0+}^{\alpha_2}|\psi(t,h(t)) - \psi(t,g(t))|}{E_{\alpha_2-\alpha_1,1}(\kappa t^{\alpha_2-\alpha_1})} \le \\
&\le \sup_{t\in[0,b]} \frac{|a_1| \cdot I_{0+}^{\alpha_2-\alpha_1}|h(t)-g(t)| + M \cdot I_{0+}^{\alpha_2}|f(t)-g(t)|}{E_{\alpha_2-\alpha_1,1}(\kappa t^{\alpha_2-\alpha_1})} \le \\
&\le \sup_{t\in[0,b]} \left(\frac{|a_1| \cdot I_{0+}^{\alpha_2-\alpha_1}|h(t)-g(t)| \dfrac{E_{\alpha_2-\alpha_1,1}(\kappa t^{\alpha_2-\alpha_1})}{E_{\alpha_2-\alpha_1,1}(\kappa t^{\alpha_2-\alpha_1})}}{E_{\alpha_2-\alpha_1,1}(\kappa t^{\alpha_2-\alpha_1})} + \right. \\
&\left. + \frac{M \cdot I_{0+}^{\alpha_2}|h(t)-g(t)| \dfrac{E_{\alpha_2-\alpha_1,1}(\kappa t^{\alpha_2-\alpha_1})}{E_{\alpha_2-\alpha_1,1}(\kappa t^{\alpha_2-\alpha_1})}}{E_{\alpha_2-\alpha_1,1}(\kappa t^{\alpha_2-\alpha_1})} \right) = \\
&= \|h-g\|_\kappa \left(\sup_{t\in[0,b]} \left(\frac{|a_1| \cdot I_{0+}^{\alpha_2-\alpha_1} E_{\alpha_2-\alpha_1,1}(\kappa t^{\alpha_2-\alpha_1})}{E_{\alpha_2-\alpha_1,1}(\kappa t^{\alpha_2-\alpha_1})} \right) + \right. \\
&\left. + M \cdot A \cdot \frac{b^{\alpha_1}}{\kappa} \right) = \\
&= \|h-g\|_\kappa \left(\sup_{t\in[0,b]} \left(\frac{\dfrac{|a_1|}{\kappa} \cdot \left(E_{\alpha_2-\alpha_1,1}(\kappa t^{\alpha_2-\alpha_1}) - 1\right)}{E_{\alpha_2-\alpha_1,1}(\kappa t^{\alpha_2-\alpha_1})} \right) + \right. \\
&\left. + M \cdot A \cdot \frac{b^{\alpha_1}}{\kappa} \right) \le \\
&\le \frac{1}{\kappa} \cdot \|h-g\|_\kappa \cdot \left(|a_1| + M \cdot A \cdot b^{\alpha_1}\right).
\end{aligned}$$

In the above calculations, we have applied Lemma 2.7 on the fractional integration of Mittag-Leffler functions. They can be summarized in the form of the following inequality

$$\left\|T_{\varphi_0}h - T_{\varphi_0}g\right\|_\kappa \le L_\kappa \cdot \|h-g\|_\kappa \tag{22}$$

with a constant given by formula

$$L_\kappa = \frac{\left(|a_1| + M \cdot A \cdot b^{\alpha_1}\right)}{\kappa}\,. \tag{23}$$

Relation (22) is fulfilled for any two continuous functions h and g, stationary function φ_0 and the value of parameter κ according to Lemma 2.7. Let us note that the numerator of the fraction defining constant L_k does not depend on the value of κ. Thus, for a parameter κ large enough $L_k \in (0,1)$ and mapping $T_{\phi 0}$ is a contraction in the space of continuous functions $C([0,b]$ endowed with the metric

generated by norm (21). As this space is complete, then using the Banach theorem on a fixed point, we conclude that fixed point *f* exists and fulfills condition (17).
According to the mentioned theorem, the fixed point is a limit of iterations of mapping $T_{\phi 0}$ as described in the thesis of Proposition 3.2 and thanks to the composition rule from Property 3.1 it also solves initial FDE (8).

Let us point out that the presented construction works for any stationary function φ_0 of derivative D^{α_2}. Thus, the obtained solution, connected to φ_0, is an analogue of a general solution from the classical theory of differential equations and it contains $n_{1,2} + n_1$ arbitrary coefficients. To fix the coefficients, we add a set of initial conditions. The next proposition gives the existence-uniqueness result for the case when orders of derivatives are in the range of (0,1).

Proposition 3.3. Let the assumptions of Proposition 3.2 be fulfilled and $\alpha_1, \alpha_2 \in (0,1)$. Then, the unique solution of equation (8) obeying the initial conditions:

$$f(0) = w_0, \quad {}^cD_{0+}^{\alpha_2-\alpha_1} f(0) = w_1$$

exists in the $C([0, b]$ space. Such a solution is a limit of the iterations of mapping $T_{\phi 0}$ generated by the following stationary function

$$\varphi_0(t) = w_0 + (w_1 - a_1 w_0) t^{\alpha_2-\alpha_1}.$$

Proof: From Proposition 3.2 it follows that each stationary function φ_0 generates a unique continuous solution to equation (8). We shall prove that solution f generated by function $w_0 + (w_1 - a_1 w_0) t^{\alpha_2-\alpha_1}$, solves the initial value problem given in Proposition 3.3. First, from (16) we obtain the relation:

$$w_0 = f(0) = \varphi(0) = c_0.$$

Equation (16) and composition rule (12) yield formula

$${}^cD_{0+}^{\alpha_2-\alpha_1} f(t) = a_1 f(t) + I_{0+}^{\alpha_2-\alpha_1} \Psi(t, f(t)) + d_0.$$

Taking $t = 0$, we obtain

$$w_1 = {}^cD_{0+}^{\alpha_2-\alpha_1} f(0) = a_1 f(0) + {}^cD_{0+}^{\alpha_2-\alpha_1} \varphi(0) = a_1 w_0 + d_0.$$

Solving the above equations, we arrive at the following values of coefficients c_0 and d_0 in general formula (15)

$$c_0 = w_0, \; d_0 = w_1 - a_1 w_0$$

and this ends the proof.

4. SOLUTION OF TWO-TERM SEQUENTIAL FRACTIONAL DIFFERENTIAL EQUATION – CASE II

In this section, we shall solve the general two-term sequential FDE in a finite interval. This equation looks as follows:

$${}^cD_{0+}^{\alpha_2-\alpha_1} \, {}^cD_{0+}^{\alpha_1} f(t) = \Psi(t, f(t), {}^cD_{0+}^{\alpha_1} f(t)), \tag{24}$$

where the sequential derivative on the left-hand side is understood differently than that in equation (8). The considered FDE can be rewritten in the vector form

$${}^cD_{0+}^{\alpha_1} f_1(t) = f_2(t) \tag{25}$$

$${}^cD_{0+}^{\alpha_2-\alpha_1} f_2(t) = \Psi(t, f_1(t), f_2(t)), \tag{26}$$

where we denoted $f_1(t) = f(t)$. Such a transformation is typical for the above class of equations (compare monograph by Diethelm (Diethelm, 2010), the references given therein and papers (Kilbas et al., 2001, 2002)). The novelty of our paper is a new method of proof which leads to the existence result for the solution in an arbitrarily long interval $[0, b]$.

Similar to the calculations in the previous section, we transform the above system of FDE into the system of fractional integral equations on the space of continuous functions:

$$f_1(t) = I_{0+}^{\alpha_1} f_2(t) + \varphi_1(t) \tag{27}$$

$$f_2(t) = I_{0+}^{\alpha_2-\alpha_1} \Psi(t, f_1(t), f_2(t)) + \varphi_2(t). \tag{28}$$

Functions φ_1 and φ_2 are the corresponding stationary functions of derivatives ${}^cD_{0+}^{\alpha_1}$ and ${}^cD_{0+}^{\alpha_2-\alpha_1}$:

$${}^cD_{0+}^{\alpha_1} \varphi_1(t) = 0 \tag{29}$$

$${}^cD_{0+}^{\alpha_2-\alpha_1} \varphi_2(t) = 0. \tag{30}$$

The explicit form of the above stationary functions depends on the order of the derivatives. Let $\alpha_1 \in (n_1 - 1, n_1)$ and $\alpha_2 - \alpha_1 \in (n_{1,2} - 1, n_{1,2})$. Then functions φ_1 and φ_2 look as follows

$$\varphi_1(t) = \sum_{j=0}^{n_1-1} \frac{c_j^1 \cdot t^j}{\Gamma(j+1)} \tag{31}$$

$$\varphi_2(t) = \sum_{i=0}^{n_{1,2}-1} \frac{c_i^2 \cdot t^i}{\Gamma(i+1)} \tag{32}$$

with coefficients c_j^1 and c_i^2 being arbitrary real numbers.

We note that the system of fractional integral equations can be reformulated as a fixed point condition for the two-component, real-valued function:

$$[f_1, f_2] = T_{(\varphi_1, \varphi_2)}[f_1, f_2] \tag{33}$$

where the components of the mapping are defined as follows for any two-component continuous function $g = [g_1, g_2]$

$$\left(T_{(\varphi_1, \varphi_2)}[g_1, g_2]\right)_1 := I_{0+}^{\alpha_1} g_2(t) + \varphi_1(t) \tag{34}$$

$$\left(T_{(\varphi_1, \varphi_2)}[g_1, g_2]\right)_2 := I_{0+}^{\alpha_2-\alpha_1} \Psi(t, g_1(t), g_2(t)) + \varphi_2(t). \tag{35}$$

Solving the systems of equations (25, 26) and (27, 28), we shall prove that the mapping given above is a contraction on the space of continuous functions $C([0, b], R^2)$

endowed with the respective norm and metric from the class indexed by positive parameter $\kappa \in R_+$

$$\left\| g \right\|_\kappa := \left\| g_1 \right\|_\kappa + \left\| g_2 \right\|_\kappa \tag{36}$$

$$\left\| g_j \right\|_\kappa := \sup_{t\in[0,b]} \frac{\left| g_j(t) \right|}{E_{\alpha_2-\alpha_1,1}(\kappa t^{\alpha_2-\alpha_1})} . \tag{37}$$

Let us observe that for each positive value of parameter κ, the norm and the respective metric defined by formulas (36, 37) yield a complete metric space as they are equivalent to the standard norm in $C([0,\mathrm{b}], R^2)$:

$$\left\| g \right\| := \left\| g_1 \right\| + \left\| g_2 \right\| \tag{38}$$

$$\left\| g_j \right\| := \sup_{t\in[0,b]} \left| g_j(t) \right| . \tag{39}$$

Proposition 4.1. Let $\alpha_2 > \alpha_1$ and function $\psi \in C([0,\mathrm{b}] \times \mathrm{R}^2, \mathrm{R})$ fulfill the Lipschitz condition:

$$\begin{aligned} &\left|\Psi(t, x_1, x_2) - \Psi(t, y_1, y_2)\right| \le \\ &\le M_1 \cdot \left|x_1 - y_1\right| + M_2 \cdot \left|x_2 - y_2\right| \end{aligned} \tag{40}$$

$$\forall t \in [0,b] \ , \forall\ x_i, x_j \in R \ , j = 1,2 .$$

Then, each pair of stationary functions φ_1, φ_2 of the derivatives given in (31, 32) yields a unique solution of equation (24) in the space of functions continuous in interval $[0,\mathrm{b}]$. Such a solution is a limit of the iterations of mapping $T_{(\varphi_1,\varphi_2)}$:

$$[f_1(t),\ f_2(t)] = \lim_{k\to\infty} (T_{(\varphi_1,\varphi_2)})^k [\chi_1(t), \chi_2(t)] \tag{41}$$

$$f(t) = f_1(t) , \tag{42}$$

where λ_1, λ_2 are arbitrary continuous functions determined in interval $[0,\mathrm{b}]$.

Proof: Let us assume $\alpha_2 - \alpha_1 > \alpha_1$ and estimate the distance between the images of an arbitrary pair of two -component functions $[g_1,\ g_2]$ and $[h_1,\ h_2]$. We obtain the following inequalities

$$\begin{aligned} &\left\| \left(T_{(\varphi_1,\varphi_2)}[g_1, g_2] - T_{(\varphi_1,\varphi_2)}[h_1, h_2] \right)_1 \right\|_\kappa = \\ &= \left\| I_{0+}^{\alpha_1} (g_2 - h_2) \right\|_\kappa \le \\ &\le \left\| g_2 - h_2 \right\|_\kappa \cdot \sup_{t\in[0,b]} \left(\frac{I_{0+}^{\alpha_1} E_{\alpha_1,1}(\kappa t^{\alpha_1})}{E_{\alpha_1,1}(\kappa t^{\alpha_1})} \right) \le \\ &\le \left\| g_2 - h_2 \right\|_\kappa \cdot \sup_{t\in[0,b]} \left(\frac{E_{\alpha_1,1}(\kappa t^{\alpha_1}) - 1}{\kappa \cdot E_{\alpha_1,1}(\kappa t^{\alpha_1})} \right) \le \\ &\le \frac{1}{\kappa} \cdot \left\| g_2 - h_2 \right\|_\kappa \le \frac{1}{\kappa} \cdot \left(\left\| g_1 - h_1 \right\|_\kappa + \left\| g_2 - h_2 \right\|_\kappa \right) \end{aligned}$$

valid for the first component of the image.

The presented calculations can be summarized by the following relation

$$\left\| \left(T_{(\varphi_1,\varphi_2)}[g_1, g_2] - T_{(\varphi_1,\varphi_2)}[h_1, h_2] \right)_1 \right\|_\kappa \le \tag{43}$$

$$\le \frac{1}{\kappa} \cdot \left\| [g_1, g_2] - [h_1, h_2] \right\|_\kappa .$$

Respectively, for the second components of the images we obtain

$$\begin{aligned} &\left\| \left(T_{(\varphi_1,\varphi_2)}[g_1, g_2] - T_{(\varphi_1,\varphi_2)}[h_1, h_2] \right)_2 \right\|_\kappa = \\ &= \left\| I_{0+}^{\alpha_2-\alpha_1} \Psi(t, g_1, g_2) - I_{0+}^{\alpha_2-\alpha_1} \Psi(t, h_1, h_2) \right\|_\kappa \le \\ &\le M_1 \cdot \left\| I_{0+}^{\alpha_2-\alpha_1} \left| g_1 - h_1 \right| \right\|_\kappa + M_2 \cdot \left\| I_{0+}^{\alpha_2-\alpha_1} \left| g_2 - h_2 \right| \right\|_\kappa \le \\ &\le M_1 \cdot \sup_{t\in[0,b]} \frac{I_{0+}^{\alpha_2-\alpha_1} \left| g_1(t) - h_1(t) \right| \dfrac{E_{\alpha_1,1}(\kappa t^{\alpha_1})}{E_{\alpha_1,1}(\kappa t^{\alpha_1})}}{E_{\alpha_1,1}(\kappa t^{\alpha_1})} + \\ &+ M_2 \cdot \sup_{t\in[0,b]} \frac{I_{0+}^{\alpha_2-\alpha_1} \left| g_2(t) - h_2(t) \right| \dfrac{E_{\alpha_1,1}(\kappa t^{\alpha_1})}{E_{\alpha_1,1}(\kappa t^{\alpha_1})}}{E_{\alpha_1,1}(\kappa t^{\alpha_1})} \le \\ &\le M_1 \cdot \left\| g_1 - h_1 \right\|_\kappa \sup_{t\in[0,b]} \frac{I_{0+}^{\alpha_2-\alpha_1} E_{\alpha_1,1}(\kappa t^{\alpha_1})}{E_{\alpha_1,1}(\kappa t^{\alpha_1})} + \\ &+ M_2 \cdot \left\| g_2 - h_2 \right\|_\kappa \sup_{t\in[0,b]} \frac{I_{0+}^{\alpha_2-\alpha_1} E_{\alpha_1,1}(\kappa t^{\alpha_1})}{E_{\alpha_1,1}(\kappa t^{\alpha_1})} \le \\ &\le M_1 \cdot \left\| g_1 - h_1 \right\|_\kappa \cdot \frac{b^{\alpha_2-2\alpha_1}}{\kappa} \cdot A + \\ &+ M_2 \cdot \left\| g_2 - h_2 \right\|_\kappa \cdot \frac{b^{\alpha_2-2\alpha_1}}{\kappa} \cdot A \le \\ &\le \frac{1}{\kappa} \cdot A b^{\alpha_2-2\alpha_1} \cdot \max\{M_1, M_2\} \cdot \left(\left\| g_1 - h_1 \right\|_\kappa + \left\| g_2 - h_2 \right\|_\kappa \right) . \end{aligned}$$

The above calculations yield the following inequality for the second components of images

$$\left\| \left(T_{(\varphi_1,\varphi_2)}[g_1, g_2] - T_{(\varphi_1,\varphi_2)}[h_1, h_2] \right)_2 \right\|_\kappa \le \tag{44}$$

$$\le \frac{1}{\kappa} \cdot A b^{\alpha_2-2\alpha_1} \cdot \max\{M_1, M_2\} \cdot \left\| [g_1, g_2] - [h_1, h_2] \right\|_\kappa .$$

Now using derived relations (43, 44) we are ready to estimate the distance between the images $T_{(\varphi_1,\varphi_2)}[g_1,\ g_2]$ and $T_{(\varphi_1,\varphi_2)}[h_1,\ h_2]$:

$$\begin{aligned} &\left\| T_{(\varphi_1,\varphi_2)}[g_1, g_2] - T_{(\varphi_1,\varphi_2)}[h_1, h_2] \right\|_\kappa \le \\ &\le L_\kappa \cdot \left\| [g_1, g_2] - [h_1, h_2] \right\|_\kappa , \end{aligned}$$

where constant L_k is inversely proportional to the value of parameter κ

$$L_\kappa = \frac{1}{\kappa} \cdot \left(A b^{\alpha_2-2\alpha_1} \cdot \max\{M_1, M_2\} + 1 \right) .$$

As parameters $\alpha_1, \alpha_2, A, b, M_1, M_2$ do not depend on the value of κ, we conclude that for a large enough κ, mapping $T_{(\varphi_1, \varphi_2)}$ is a contraction on space $C([0,\mathrm{b}],\mathrm{R}^2)$. Thus, we can apply the Banach theorem on a fixed point and infer that function $[f_1, f_2] \in C([0,\mathrm{b}],\mathrm{R}^2)$ exists so that the fixed point condition

$$[f_1, f_2] = T_{(\varphi_1,\varphi_2)}[f_1, f_2]$$

is fulfilled. Such a function can be constructed using the iteration limit as described in formulas (41, 42). The first component of the fixed point solves FDE (24) according to relation (42).
The proof in case $\alpha_2 - \alpha_1 \leq \alpha_1$ is analogous.

5. FINAL REMARKS

We developed an efficient method of proving the existence-uniqueness results for two-term fractional differential equations. For equations containing left-sided Caputo derivatives and their composition, we showed that a general solution exists in an arbitrarily long interval and is generated by the stationary function of the highest order derivative. The applied method of equivalent norms/metrics extends the idea given by Bielecki (Bielecki, 1956) for differential equations of integer order. As was shown in former papers (El-Raheem, 2003; Lakshmikantham et al., 2008, 2009; Baleanu and Mustafa, 2010; Klimek, 2011a, b), in FDE theory we should modify the metrics using one- or two-parameter Mittag-Leffler functions. In the present paper, the respective version of the method is given for two-term fractional differential equations considered on the C[0,b] space. However, careful analysis of the obtained results and their proof implies that by using Lemma 2.7, they can be extended to multi-term FDE. Let us also point out that this approach seems appropriate to study and solve fractional differential equations on other function spaces – for instance on the space of differentiable functions.

REFERENCES

1. **Agrawal O. P., Tenreiro-Machado J. A., Sabatier J.** (2004), (Eds.) *Fractional Derivatives and Their Application: Nonlinear Dynamics*, Springer-Verlag, Berlin, vol. 38.
2. **Baleanu D., Mustafa O. G.** (2010), On the global existence of solutions to a class of fractional differential equations, *Comp. Math. Appl*. Vol. 59, 1835-1841.
3. **Bielecki A.** (1956), *Une remarque sur la methode de Banach-Cacciopoli-Tikhonov dans la theorie des equations differentielles ordinaires*, Bull. Acad. Polon. Sci. Cl. III - IV, 261-264.
4. **Diethelm K.** (2010), *The Analysis of Fractional Differential Equations*, Springer-Verlag, Berlin.
5. **El-Raheem Z. F. A.** (2003), Modification of the application of a contraction mapping method on a class of fractional differential equation, *Appl. Math. & Comput.* Vol. 137, 371-374.
6. **Hilfer R.** (2000), (Ed.) *Applications of Fractional Calculus in Physics*, World Scientific, Singapore.
7. **Khan M., Hyder Ali S., Fetecau C., Haitao Qi** (2009), Decay of potential vortex for a viscoleastic fluid with fra-ctional Maxwell model, *Appl. Math. Comput*. Vol. 33, 2526-2533.
8. **Kilbas A. A., Srivastava H. M., Trujillo J. J.** (2006), *Theory and Applications of Fractional Differential Equations*, Elsevier, Amsterdam.
9. **Kilbas A. A., Trujillo J. J.** (2001), Differential equation of fractional order: methods, results and problems. I, *Appl. Anal*. Vol. 78, 153-192.
10. **Kilbas A. A., Trujillo J. J.** (2002), Differential equation of fractional order: methods, results and problems. II, *Appl. Anal*. Vol. 81, 435-493.
11. **Klimek M.** (2009), *On Solutions of Linear Fractional Differential Equations of a Variational Type*, The Publishing Office of the Czestochowa University of Technology, Czestochowa.
12. **Klimek M.** (2011), *On contraction principle applied to nonlinear fractional differential equations with derivatives of order* $\alpha \in (0,1)$, Banach Center Publ., To appear.
13. **Klimek M.** (2011), Sequential fractional differential equations with Hadamard derivative, *Commun. Nonlinear Sci. Numer*. Simulat., doi: 10.1016/j.cnsns.2011.01.018.
14. **Klimek M., Błasik M.** (2011), Existence-uniqueness result for nonlinear two-term sequential FDE, *Proceedings of the 7th European Nonlinear Dynamics Conference ENOC 2011*, Rome 24.07-29.07.2011, To appear.
15. **Lakshmikantham V., Leela, S., Vasundhara Devi J.** (2009), *Theory of Fractional Dynamic Systems*, Cambridge Scientific Publishers, Cambridge.
16. **Lakshmikantham V., Vasundhara Devi J.** (2008), Theory of fractional differential equations in a Banach space, *European J. Pure and Appl. Math.*, Vol. 1, 38-45.
17. **Magin R. L.** (2006), *Fractional Calculus in Bioengineering*, *Redding*, Begell House Publisher.
18. **Metzler R., Klafter J.** (2004), The restaurant at the end of the random walk: recent developments in the description of anomalous transport by fractional dynamics, *J. Phys A*, Vol. 37, R161-R208.
19. **Miller K. S., Ross B.** (1993), *An Introduction to the Fractional Calculus and Fractional Differential Equations*, Wiley and Sons, New York,
20. **Podlubny I.** (1999), *Fractional Differential Equations*, Academic Press, San Diego.
21. **Samko S. G., Kilbas A. A., Marichev O. I.** (1993), *Fractional Integrals and Derivatives*, Gordon & Breach, Amsterdam.
22. **Shan L.**, **Tong D., Xue L.** (2009), Unsteady flow of non -Newtonian visco-elastic fluid in dual porosity media with the fractional derivative. J. *Hydrodyn. B,* Vol. 21, 705-713.
23. **Tian J.**, **Tong D**. (2006), The flow analysis of fluids in fractal reservoir with the fractional derivative, *J. Hydrodyn*., Vol. 18, 287-293.
24. **Wang Z.H., Wang X.** (2010), General solution of the Bagley -Torvik equations with fractional order derivative, *Commun. Nonlinear Sci. Numer. Simulat*.,Vol. 15, 1279-1285.
25. **West B. J., Bologna M., Grigolini P.** (2003), *Physics of Fractional Operators*, Springer-Verlag, Berlin.

ANALYSIS AND APPLICATIONS OF COMPOSED FORMS OF CAPUTO FRACTIONAL DERIVATIVES

Tomasz BŁASZCZYK[*], Ewa KOTELA[**], Matthew R. HALL[***], Jacek LESZCZYŃSKI[**]

[*]Institute of Mathematics, Czestochowa University of Technology, ul. Dabrowskiego 73, 42-200 Czestochowa, Poland
[**]Department of Heating, Ventilation and Air Protection, Czestochowa University of Technology, ul. Dabrowskiego 73, 42-200 Czestochowa, Poland
[***]Nottingham Centre for Geomechanics, Division of Materials, Mechanics and Structures, Faculty of Engineering, University of Nottingham, University Park, NG7 2RD, UK

tomblaszczyk@gmail.com, ekotela@wp.pl, Matthew.Hall@nottingham.ac.uk, jleszczynski@is.pcz.czest.pl

Abstract: In this paper we consider two ordinary fractional differential equations with composition of the left and the right Caputo derivatives. Analytical solution of this type of equations is known for particular cases, having a complex form, and therefore is difficult in practical calculations. Here, we present two numerical schemes being dependent on a fractional order of equation. The results of numerical calculations are compared with analytical solutions and then we illustrate convergence of our schemes. Finally, we show an application of the considered equation.

1. INTRODUCTION

This study is devoted to the analysis of ordinary differential equations containing a composed form of left- and right-sided fractional derivatives, which are defined in any sense, i.e. the Riemann-Liouville and the Caputo ones. Moreover, we consider the equations in a restricted domain. The equations are obtained by modification the minimum action principle and the application of fractional integration by parts. It should be noted that many authors (Agrawal, 2002; Klimek, 2002; Riewe, 1996) elaborated fractional forms of the Euler-Lagrange equations. However, the equations contain only specific compositions of fractional derivatives, i.e. the arbitrary form of Riemann-Liouville (left- or right-sided) composed with the arbitrary form of Caputo (also left- or right-sided). Therefore, in the Euler-Lagrange equations a disadvantage in boundary conditions occurs. The disadvantage reveals an introduction of homogenous conditions for one boundary, where the Riemann-Liouville fractional derivative exists (Blaszczyk et al., 2011; Leszczynski and Blaszczyk, 2010). To omit such problems, we consider a composed form of fractional derivatives, where the left- and the right-sided Caputo operators are used. Moreover, we expect that a fractional differential equation containing the composition of two Caputo derivatives has physical meaning and will be useful in modelling complex processes in nature.

To obtain the analytical solution is one of the fundamental problem that arises from Euler-Lagrange equations. The results, based on the fixed point theorem (Klimek, 2007), are not capable in practice, because the solution is presented in the form of very complex series. Klimek (Klimek, 2008) proposed to use the Mellin transform in order to obtain the analytical solution. However, such solution has complex form, which includes series of special functions. For practical applications we cannot use the analytical solution due to its useless in calculations. Therefore, we will construct some approximate solutions. Some numerical basics can be found in the studies (Blaszczyk, 2009; Blaszczyk, 2010; Blaszczyk & Ciesielski, 2010).

2. FORMULATION OF THE PROBLEM

We consider two ordinary fractional differential equations with composition of the left- and the right-sided Caputo derivatives, which have the following forms

$${}^{C}D_{b-}^{\alpha}\,{}^{C}D_{0+}^{\alpha}T(x)-\lambda T(x)=0, \tag{1}$$

$${}^{C}D_{0+}^{\alpha}\,{}^{C}D_{b-}^{\alpha}T(x)-\lambda T(x)=0, \tag{2}$$

where $x\in[0,b]$ and operators ${}^{C}D_{0+}^{\alpha}$, ${}^{C}D_{b-}^{\alpha}$ are defined as (Kilbas et al., 2006)

$${}^{C}D_{0+}^{\alpha}T(x)=\frac{1}{\Gamma(n-\alpha)}\int_{0}^{x}\frac{T^{(n)}(\tau)}{(x-\tau)^{\alpha-n+1}}\,\mathrm{d}\tau,\quad \text{for } x>0 \tag{3}$$

$${}^{C}D_{b-}^{\alpha}T(x)=\frac{(-1)^{n}}{\Gamma(n-\alpha)}\int_{x}^{b}\frac{T^{(n)}(\tau)}{(\tau-x)^{\alpha-n+1}}\,\mathrm{d}\tau,\quad \text{for x}<b \tag{4}$$

where $n=[\alpha]+1$.

Here, we mean ${}^{C}D_{0+}^{\alpha}$ as the left-sided Caputo derivative and ${}^{C}D_{b-}^{\alpha}$ denotes the right-sided Caputo derivative.

For $\alpha\in(0,1)$ Eqns. (1) and (2) are supplemented by the adequate boundary conditions

$$T(0)=T_0,\quad T(b)=T_b \tag{5}$$

Analytical solutions are known only for some type of Euler-Lagrange equations (Klimek, 2007; Klimek,

2008), and they have very complex form. To omit this problem we propose a numerical approach.

3. NUMERICAL SCHEMES

In order to develop a discrete form of Eqns. (1) and (2), the homogenous grid of nodes is introduced as

$$0 = x_0 < x_1 < \ldots < x_i < x_{i+1} < \ldots < x_N = b, \tag{6}$$

where

$$x_i = x_0 + i\,\Delta x, \tag{7}$$

Function T determined at the point x_i is denoted as $T_i = T(x_i)$. We also assume $\alpha \in (0,1)$.

3.1. Discrete scheme for Eqns. (1) and (2)

We have introduced the discrete form of fractional derivatives for Eqn. (1). The value of the left-sided Caputo derivative at point x_i can be approximated as

$$\begin{aligned} {}^{C}D_{0+}^{\alpha}T(x)\Big|_{x=x_i} &= \frac{1}{\Gamma(1-\alpha)}\int_{x_0}^{x_i}\frac{T'(\tau)}{(x_i-\tau)^{\alpha}}\,d\tau \\ &\cong \frac{1}{\Gamma(1-\alpha)}\sum_{j=0}^{i-1}\frac{T_{j+1}-T_j}{\Delta x}\int_{x_j}^{x_{j+1}}\frac{1}{(x_i-\tau)^{\alpha}}\,d\tau \\ &= (\Delta x)^{-\alpha}\sum_{j=0}^{i}T_j\,v(i,j) \end{aligned} \tag{8}$$

where

$$v(i,j) = \frac{1}{\Gamma(2-\alpha)} \times \begin{cases} (i-1)^{1-\alpha} - i^{1-\alpha} & \text{for } j=0 \\ (i-j+1)^{1-\alpha} - 2(i-j)^{1-\alpha} & \\ +(i-j-1)^{1-\alpha} & \text{for } j=1,\ldots,i-1 \\ 1 & \text{for } j=i \end{cases} \tag{9}$$

Next, denoting $g(x) = {}^{C}D_{0+}^{\alpha}T(x)$ in Eqn. (1) we find the discrete form of the right-sided Caputo derivative

$$\begin{aligned} {}^{C}D_{b-}^{\alpha}\,{}^{C}D_{0+}^{\alpha}T(x)\Big|_{x=x_i} &= {}^{C}D_{b-}^{\alpha}\,g(x)\Big|_{x=x_i} \\ &= \frac{-1}{\Gamma(1-\alpha)}\int_{x_i}^{x_N}\frac{g'(\tau)}{(\tau-x_i)^{\alpha}}\,d\tau \\ &\cong \frac{-1}{\Gamma(1-\alpha)}\sum_{j=i}^{N-1}\frac{g_{j+1}-g_j}{\Delta x}\int_{x_j}^{x_{j+1}}\frac{1}{(\tau-x_i)^{\alpha}}\,d\tau \\ &= (\Delta x)^{-\alpha}\sum_{j=i}^{N}g_j\,w(i,j) \end{aligned} \tag{10}$$

where

$$w(i,j) = \frac{1}{\Gamma(2-\alpha)} \times \begin{cases} 1 & \text{for } j=i \\ (j-i+1)^{1-\alpha} - 2(j-i)^{1-\alpha} & \\ +(j-i-1)^{1-\alpha} & \text{for } j=i+1,\ldots,N-1 \\ (N-i-1)^{1-\alpha} - (N-i)^{1-\alpha} & \text{for } j=N \end{cases} \tag{11}$$

Using formulas (8) and (10) we obtain a system containing the discrete form of Eqn. (1) and boundary conditions as

$$\begin{cases} T_0 = T(x_0) \\ (\Delta x)^{-2\alpha}\sum_{j=i}^{N}\left[w(i,j)\sum_{k=0}^{j}v(j,k)T_k\right] - \lambda T_i = 0, \text{ for } i=1,\ldots,N-1 \\ T_N = T(x_N) \end{cases} \tag{12}$$

Similarly to previous considerations, we write the discrete form of Eqn. (2) as

$$\begin{cases} T_0 = T(x_0) \\ (\Delta x)^{-2\alpha}\sum_{j=0}^{i}\left[v(i,j)\sum_{k=j}^{N}w(j,k)T_k\right] - \lambda T_i = 0, \text{ for } i=1,\ldots,N-1 \\ T_N = T(x_N) \end{cases} \tag{13}$$

To obtain full numerical solutions of Eqns. (1) and (2), we need to solve a system of algebraic equations (12) and (13) respectively.

3.2. Convergence and error analysis

Including discrete forms of Eqns. (1) and (2) we analyse errors and convergence of the numerical schemes. Let us assume $\alpha \in (0,1)$, $x \in [0,1]$, $\lambda = 0$ and boundary conditions as

$$T(0) = 0, \quad T(1) = 1 \tag{14}$$

Then, the solution of Eqn. (1) has the following form

$$T(x) = x^{\alpha} \tag{15}$$

Tab.1 shows errors generated by numerical scheme (12) being dependent on fractional order α and step Δx which was assumed in calculations.

We determine experimental estimation of the convergence row (EOC) as

$$EOC = \log_2\left(\frac{error[N]}{error[2N]}\right), \tag{16}$$

where

$$error[N]=\frac{\frac{1}{2}\left|T(x_0)-T_0\right|+\frac{1}{2}\left|T(x_N)-T_N\right|+\sum_{i=1}^{N-1}\left|T(x_i)-T_i\right|}{N}, \tag{17}$$

In the error calculations we take into account boundary conditions (14).

Tab. 1. Errors and experimental estimation of the convergence row (EOC) generated by the numerical scheme (12)

	$\alpha=0.3$		$\alpha=0.5$		$\alpha=0.7$	
Δx	error	EOC	error	EOC	error	EOC
1/16	1.51e-2		1.46e-2		1.05e-2	
1/32	8.47e-3	0.83	8.19e-3	0.83	6.05e-3	0.79
1/64	4.60e-3	0.88	4.41e-3	0.89	3.34e-3	0.86
1/128	2.44e-3	0.91	2.32e-3	0.93	1.80e-3	0.89

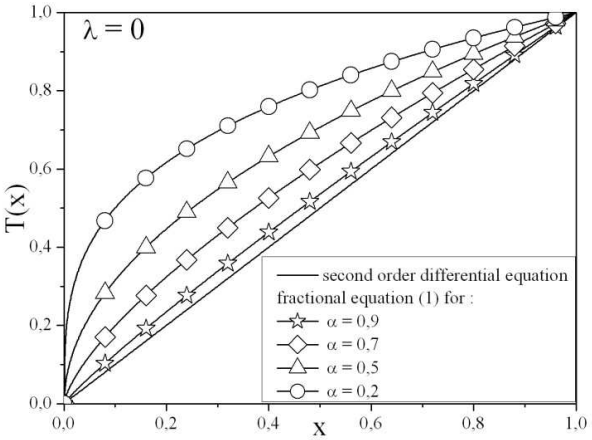

Fig. 1. Numerical solutions of Eqn. (1)

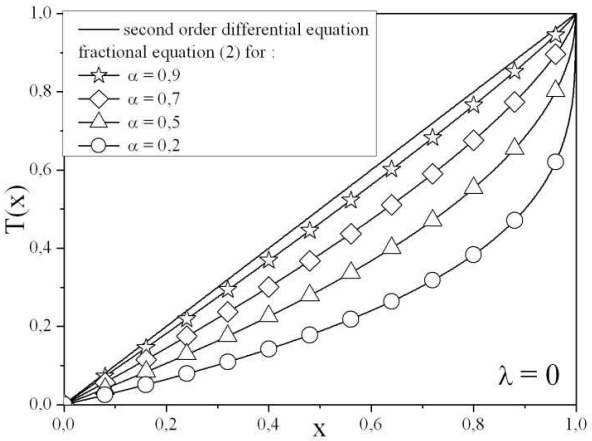

Fig. 2. Numerical solutions of Eqn. (2)

When we solve Eqn. (2) numerically with boundary conditions

$$T(0)=1, \quad T(1)=0 \tag{18}$$

then we obtain identical table of errors. This is resulted by the effect of relation between considered equations and the reflection operator (Blaszczyk and Ciesielski, 2010).

Analyzing values of EOC in table 1 one can observe that the convergence of our numerical schemes is $O(h)$ and does not depend of parameter α.

Next, we calculated some examples for different values of α in order to show graphically how numerical solutions of Eqns. (1) and (2) behave.

In Figure 1 and 2 the solutions of Eqns. (1) and (2) for different values of the parameter α are presented. One can see that both solutions are symmetrical. Analyzing the behavior of solutions we observe that *T(x)* tends to the solution of the classical second order ordinary differential equation for $\alpha \to 1^{-}$.

4. APPLICATION

In order to show a practical application of Eqn. (1) we consider a steady state of heat transfer through the granular layer as presented by Fig. 3.

Using the idea presented in (US Department of Transportation, 2009) the experiment began with five thermocouples placed at depths 25 mm, 85 mm, 145 mm, 252 mm, 327 mm in the granular material which is used for road construction. Grains have specific parameters such as thermal conductivity, specific heat and density. It should be noted that the surface has been exposed to the weather conditions (irradiation, wind speed, relative humidity). Data from the thermocouples (US Department of Transportation, 2009) helped us to create a temperature profile.

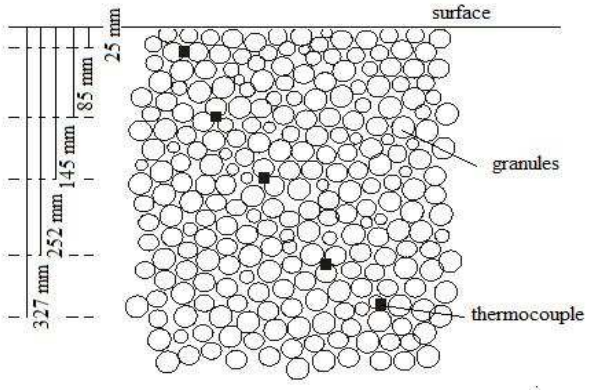

Fig. 3. Experimental setup

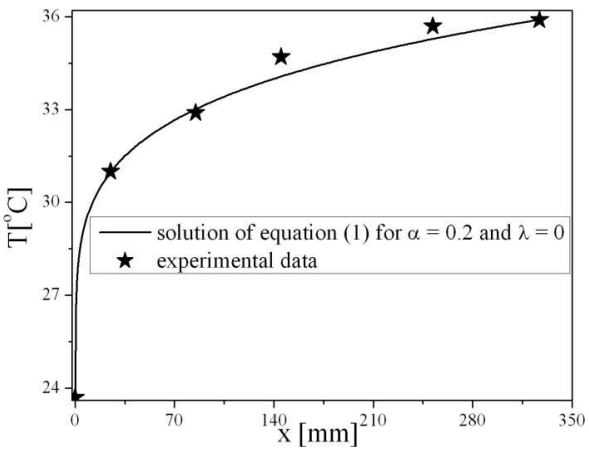

Fig. 4. Comparison of Eqn. (1) with experiment data (US Department of Transportation, 2009)

In order to obtain the experimental results we approximate a temperature profile using the solution of the fractional Eqn. (1). Figure 4 presents comparison between experimental data and numerical results.

Analyzing changes in the temperature profile we can say that the nonlinear profile is observed. Additionally, we can observe a good agreement between the experimental data and the solution of the fractional Eqn. (1).

5. CONCLUSIONS

In this work the fractional differential equations with composition of the left- and the right-sided Caputo derivatives were considered. The analytical solutions of these equations are difficult to apply in practical calculations. Numerical solution is an alternative approach to the analytical one. In this study the numerical schemes were presented in order to obtain the solutions for considered equations. We show that the convergence row of our numerical schemes was $O(h)$ and does not depend on parameter α.

Our studies show that the model based on the fractional differential equation containing composition of the left- and the right-sided Caputo derivatives could reflect a steady state of the temperature profile in granular medium.

REFERENCES

1. **Agrawal O.P.** (2002), Formulation of Euler-Lagrange equations for fractional variational problems, *J. Math. Anal. Appl.*, Vol. 272, 368-379.
2. **Blaszczyk T.** (2009), Application of the Rayleigh-Ritz method for solving fractional oscillator equation, *Scientific Research of the Institute of Mathematics and Computer Science*, Vol. 8, No. 2, 29-36.
3. **Blaszczyk T.** (2010), *Zastosowanie rownania frakcyjnego oscylatora do modelowania efektu pamieci w materii granulowanej*, rozprawa doktorska, Politechnika Czestochowska (in Polish).
4. **Blaszczyk T., Ciesielski M.** (2010), Fractional Euler-Lagrange equations - numerical solutions and applications of reflection operator, *Scientific Research of the Institute of Mathematics and Computer Science*, Vol. 9, No. 2, 17-24.
5. **Blaszczyk T., Kotela E., Leszczynski J.** (2011), Application of the fractional oscillator equation to simulations of granular flow In a silo, *Computer Methods in Materials Science*, Vol. 11, No. 1, 64-67.
6. **Kilbas A.A., Srivastava H.M., Trujillo J.J.** (2006), *Theory and Applications of Fractional Differential Equations*, Elsevier, Amsterdam.
7. **Klimek M.** (2002), Lagrangean and Hamiltonian fractional sequential mechanics, *Czech. J. Phys.*, Vol. 52, 1247-1253.
8. **Klimek M.** (2007), Solutions of Euler-Lagrange equations in fractional mechanics, *AIP Conference Proceedings 956. XXVI Workshop on Geometrical Methods in Physics*. Bialowieza, 73-78.
9. **Klimek M.** (2008), G-Meijer functions series as solutions for certain fractional variational problem on a finite time interval, *Journal Europeen des Systemes Automatises (JESA)*, Vol. 42, 653-664.
10. **Leszczynski J., Blaszczyk T.** (2010), Modeling the transition between stable and unstable operation while emptying a silo, *Granular Matter*, DOI: 10.1007/s10035-010-0240-5.
11. **Riewe F.** (1996), Nonconservative Lagrangian and Hamiltonian mechanics, *Phys. Rev. E*, Vol. 53, 1890-1899.
12. **US Department of Transportation**, Federal Transport Administration, (2009). LTPP Seasonal Monitoring Programme (SMP): Pavement Performance Database (PPDB). [electronic database], Standard Data Release 23.0, DVD Version, USA.

Acknowledgments: This work was supported by the National Centre for Research and Development, as Strategic Project PS/E/2/66420/10 "Advanced Technologies for Energy Generation: Oxy-combustion technology for PC and FBC boilers with CO_2 capture". The support is gratefully acknowledged.

STABILITY OF STATE-SPACE MODELS OF LINEAR CONTINUOUS-TIME FRACTIONAL ORDER SYSTEMS

Mikołaj BUSŁOWICZ*

*Białystok University of Technology, Faculty of Electrical Engineering
ul. Wiejska 45D, Białystok, 15-351 Białystok

busmiko@pb.edu.pl

Abstract: The paper considers the stability problem of linear time-invariant continuous-time systems of fractional order, standard and positive, described by the state space model. Review of previous results is given and some new methods for stability checking are presented. Considerations are illustrated by numerical examples and results of computer simulations.

1. INTRODUCTION

In the last decades, the problem of analysis and synthesis of dynamical systems described by fractional order differential (or difference) equations was considered in many papers and books. For review of the previous results see, for example, the monographs (Caponetto et al., 2010; Das, 2008; Diethelm (2010); Kaczorek, 2009, 2011a; Kilbas et al., 2006; Monje et al., 2010; Ostalczyk, 2008; Podlubny, 1994, 1999; Sabatier et al., 2007).

The problems of stability and robust stability of linear fractional order continuous-time systems were studied among others in Matignon (1996, 1998), Busłowicz (2008a, 2008b, 2009), Petras (2008, 2009), Radwan et al. (2009), Sabatier et al. (2008, 2010), Tavazoei and Heri (2009) and in Ahn et al. (2006), Ahn and Chen (2008), Busłowicz (2008c), Lu and Chen (2009), Tan et al. (2009), Zhuang and Yisheng (2010), respectively.

The new class of the linear fractional order systems, namely the positive systems of fractional order was considered by Kaczorek (2008a, 2008b, 2009, 2011a, 2011b).

The aim of the paper is to give the review of the methods for stability analysis of fractional continuous-time linear systems described by the state-space model and presentation of some new results. The standard and positive fractional order systems will be considered.

2. PROBLEM FORMULATION

Consider a linear continuous-time system of fractional order described by the state equation

$$ {}_0D_t^{\alpha}x(t) = Ax(t) + Bu(t), \tag{1}$$

where $x(t) \in R^n$, $u(t) \in R^m$, $A \in R^{n\times n}$, $B \in R^{n\times m}$ and

$$ {}_0D_t^{\alpha}x(t) = \frac{1}{\Gamma(p-\alpha)}\int_0^t \frac{x^{(p)}(\tau)d\tau}{(t-\tau)^{\alpha+1-p}}, \quad p-1 \le \alpha \le p, \tag{2}$$

is the Caputo definition for fractional α-order derivative, where $x^{(p)}(t) = d^P x(t)/dt^P$, p is a positive integer and

$$ \Gamma(\alpha) = \int_0^{\infty} e^{-t}t^{\alpha-1}dt \tag{3}$$

is the Euler gamma function.

Definition (3) can be written in the equivalent form

$$ \Gamma(\alpha) = \lim_{n\to\infty} \frac{n!n^{\alpha}}{\alpha(\alpha+1)\cdots(\alpha+n)}. \tag{3a}$$

From (2) for $p = 1$ and $p = 2$ we have, respectively

$$ {}_0D_t^{\alpha}x(t) = \frac{1}{\Gamma(1-\alpha)}\int_0^t \frac{x^{(1)}(\tau)}{(t-\tau)^{\alpha}}d\tau, \quad 0 < \alpha < 1, \tag{4}$$

$$ {}_0D_t^{\alpha}x(t) = \frac{1}{\Gamma(2-\alpha)}\int_0^t \frac{x^{(2)}(\tau)d\tau}{(t-\tau)^{\alpha-1}}, \quad 1 < \alpha < 2. \tag{5}$$

The Laplace transform of the Caputo fractional derivative has the form

$$ L\{{}_0D_t^{\alpha}x(t)\} = s^{\alpha}F(s) - \sum_{k=1}^{p} s^{\alpha-k}x^{(k-1)}(0^+). \tag{6}$$

For zero initial conditions, the Laplace transform (6) reduces to

$$ L\{{}_0D_t^{\alpha}x(t)\} = s^{\alpha}F(s). \tag{6a}$$

Definition 1. The fractional system (1) will be called positive (internally) if $x(t) \in \Re_+^n$ for any initial condition $x(0) \in \Re_+^n$ and for all inputs $u(t) \in \Re_+^n$, $t \ge 0$.

Positivity condition of the system (1) is known only in the case of fractional order $\alpha \in (0,1]$. In Kaczorek (2008a, 2008b), see also Kaczorek (2009, 2011a), the following theorem has been proved.

Theorem 1. The fractional system (1) with $0 < \alpha \le 1$ is positive if and only if

$$A \in M_n, \quad B \in \Re_+^{n \times m}, \tag{7}$$

where M_n – the set of $n \times n$ real Metzler matrices (matrices with non-negative off-diagonal entries), $\Re_+^{n \times m}$ – the set of $n \times m$ real matrices with non-negative entries.

Characteristic function of the fractional system (1) is the fractional degree polynomial of the form

$$w(s) = \det(s^\alpha I - A) = a_n s^{n\alpha} + a_{n-1} s^{(n-1)\alpha} + ... + a_0. \tag{8}$$

The associated natural degree polynomial has the form

$$\tilde{w}(\lambda) = a_n \lambda^n + a_{n-1} \lambda^{n-1} + ... + a_1 \lambda + a_0, \quad \lambda = s^\alpha. \tag{9}$$

The polynomial (8) is a multivalued function whose domain is a Riemann surface. In general, this surface has an infinite number of sheets and the fractional polynomial (8) has an infinite number of zeros. Only a finite number of which will be in the main sheet of the Riemann surface. For stability reasons only the main sheet defined by $-\pi < \arg s < \pi$ can be considered (Petras, 2008, 2009).

From the theory of stability of linear fractional order systems given by Matignon (1996, 1998) and Petras (2008, 2009), we have the following theorem.

Theorem 2. The fractional order system (1) is stable if and only if the fractional degree characteristic polynomial (8) has no zeros in the closed right-half of the Riemann complex surface, i.e.

$$w(s) = \det(s^\alpha I - A) \neq 0 \text{ for } \operatorname{Re} s \geq 0, \tag{10}$$

or equivalently, the following condition is satisfied

$$|\arg \lambda_i(A)| > \alpha \frac{\pi}{2}, \quad i = 1,2,..., n, \tag{11}$$

where $\lambda_i(A)$ is the i-th eigenvalues of matrix A.

From Radwan et al. (2009) it follows that the fractional system with the characteristic polynomial (8) is unstable for all $\alpha > 2$. Therefore, in this paper we consider the fractional system (1) of fractional order $\alpha \in (0,2)$.

The stability regions of the system (1), described by (11) are shown in Fig. 1 and 2 for $0 < \alpha \leq 1$ and $1 \leq \alpha < 2$, respectively. Parametric description of the boundary of the stability regions has the form

$$(j\omega)^\alpha = |\omega|^\alpha e^{j\pi\alpha/2}, \quad \omega \in (-\infty, \infty). \tag{12}$$

The polynomial (8) with $\alpha = 1$ is a natural degree polynomial and from (12) for $\alpha = 1$ we have that the imaginary axis of the complex plane is the boundary of the stability region.

The aim of this paper is to give the review of the methods for stability analysis of the fractional system (1) and presentation of some new results. We consider the stability problem of standard and positive fractional order systems.

3. STABILITY OF FRACTIONAL SYSTEMS

The following lemma can be used to checking the condition (11) of Theorem 2.

Lemma 1. The fractional order system (1) is stable if and only if

$$\gamma > \alpha \frac{\pi}{2}, \tag{13}$$

where

$$\gamma = \min_i |\arg \lambda_i(A)| \tag{14}$$

and $\lambda_i(A)$ is the i-th eigenvalue of A.

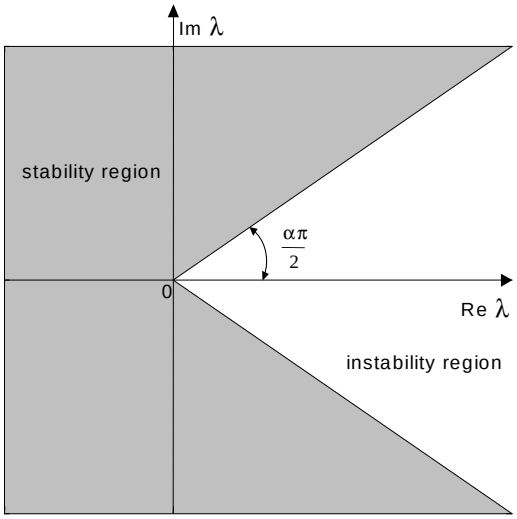

Fig. 1. Stability region for $0 < \alpha \leq 1$

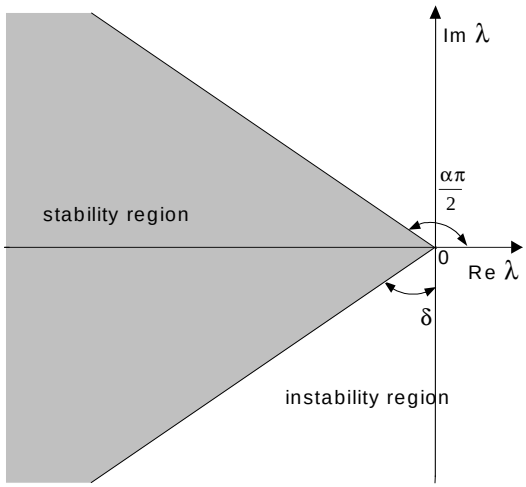

Fig. 2. Stability region for $1 \leq \alpha < 2$

From Theorem 2, Lemma 1 and Fig. 1 and 2 we have the following important lemmas and remark.

Lemma 2. The fractional system (1) is unstable for all $\alpha \in (0,2)$ if the matrix A has at least one non-negative real eigenvalue. In particular, this holds if $\det A = 0$.

Lemma 3. Assume that the state matrix A has no real non-negative eigenvalues. Then the fractional system (1) is stable if and only if $\alpha \in (0, \alpha_0)$, where $\alpha_0 = 2\gamma/\pi$ and γ is computed from (14).

Remark 1. If the fractional system (1) is stable for a fixed $\alpha \in [1,2)$ then it is also stable for all fractional orders $\alpha \in (0,1]$.

3.1. Stability of system of fractional order $\alpha \in [1, 2)$

The system (1) of fractional order $\alpha \in [1,2)$ is stable if and only if all eigenvalues of A lie in the stability region shown in Fig. 2. Hence, this system may be unstable in the case of negative real parts of all eigenvalues of matrix A if $\alpha \arg\lambda_i(A) < \alpha\pi/2, i = 1, 2, \ldots, n$.

The following lemma can be used to stability checking of the fractional system (1) of order $\alpha \in [1,2)$.

Lemma 4 (Anderson et al., 1974; Davison and Ramesh, 1970). The eigenvalues of an $n \times n$ matrix A lie in the sector shown in Fig. 2 if and only if the eigenvalues of $2n \times 2n$ matrix

$$\tilde{A} = \begin{bmatrix} A\cos\delta & -A\sin\delta \\ A\sin\delta & A\cos\delta \end{bmatrix} \tag{15}$$

have negative real parts, where $\delta = (\alpha - 1)\pi/2$.

From the above and the result given in (Hostetter, 1975), see also (Tavazoei and Haeri, 2009) it follows that if $p(s) = \det(sI - A)$ then

$$\det(sI - \tilde{A}) = p(se^{j\delta})\,p(se^{-j\delta}), \quad \delta = (\alpha - 1)\pi/2.$$

Based on Lemma 4, the following theorem has been proved in Tavazoei and Haeri (2009).

Theorem 3. The fractional system (1) with $1 \le \alpha < 2$ is stable if and only if the eigenvalues of the matrix $\tilde{A}$ have negative real parts, where

$$\tilde{A} = \begin{bmatrix} A\sin(\alpha\pi/2) & A\cos(\alpha\pi/2) \\ -A\cos(\alpha\pi/2) & A\sin(\alpha\pi/2) \end{bmatrix}. \tag{16}$$

Proof. Substitution $\delta = (\alpha - 1)\pi/2$ in (15) gives (16). The proof follows directly from Theorem 2 and Lemma 4.

In Molinary (1975) it has been proved that if there exist positive definite Hermitian matrices $P > 0$ and $Q > 0$ such that

$$\beta PA + \beta^* A^{\mathrm{T}} P = -Q, \tag{17}$$

where $\beta = \eta + j\xi$ with $\tan(\pi - \alpha\pi/2) = \eta/\xi$ (equivalently, $\tan(\pi/2 - \delta) = \eta/\xi$), then all eigenvalues of A are within the stable area shown in Fig. 2. From the above and Theorem 2 one obtains the following theorem (see also Ahn et. al. (2006), Sabatier et al. (2008, 2010)).

Theorem 4. The fractional system (1) with $1 \le \alpha < 2$ is stable if and only if there exist positive definite Hermitian matrices $P > 0$ and $Q > 0$ such that (17) holds.

The stability region shown in Fig. 2 is convex. Therefore, to the stability analysis of the system (1) with $1 \le \alpha < 2$ the LMI based conditions can be applied.

In Chilali et al. (1999) it has been shown that the eigenvalues of matrix A lie in the sector shown in Fig. 2 if and only if there exists a matrix $P = P^{\mathrm{T}} > 0$ such that

$$\begin{bmatrix} (AP + PA^{\mathrm{T}})\sin(\theta) & (AP - PA^{\mathrm{T}})\cos(\theta) \\ (PA^{\mathrm{T}} - AP)\cos(\theta) & (AP + PA^{\mathrm{T}})\sin(\theta) \end{bmatrix} < 0, \tag{18}$$

where $\theta = \pi - \alpha\pi/2$.

Substitution $\theta = \pi - \alpha\pi/2$ in (18) gives

$$\begin{bmatrix} (AP + PA^{\mathrm{T}})\sin(\alpha\pi/2) & (AP - PA^{\mathrm{T}})\cos(\alpha\pi/2) \\ (PA^{\mathrm{T}} - AP)\cos(\alpha\pi/2) & (AP + PA^{\mathrm{T}})\sin(\alpha\pi/2) \end{bmatrix} < 0. \tag{19}$$

Hence, we prove the following theorem.

Theorem 5. The fractional system (1) with $1 \le \alpha < 2$ is stable if and only if there exists a matrix $P = P^{\mathrm{T}} > 0$ such that the condition (19) holds.

The same criterion has been obtained by Sabatier et al. (2008, 2010). In this criterion, the condition (19) is written in the equivalent form

$$\begin{bmatrix} (A^{\mathrm{T}}P + PA)\sin(\alpha\pi/2) & (A^{\mathrm{T}}P - PA)\cos(\alpha\pi/2) \\ (PA - A^{\mathrm{T}}P)\cos(\alpha\pi/2) & (A^{\mathrm{T}}P + PA)\sin(\alpha\pi/2) \end{bmatrix} < 0. \tag{19a}$$

To checking the condition (19) (or (19a)), a LMI solver can be used.

3.2. Stability of system of fractional order $\alpha \in (0, 1]$

The system (1) of fractional order $\alpha \in (0,1]$ is stable if and only if all eigenvalues of A lie in the stability region shown in Fig. 1. Hence, this system may be stable in the case when not all eigenvalues of A lie in open left half-plane. Moreover, this system may be stable when all eigenvalues of the matrix A are complex with positive real parts.

From the above we have the following simple sufficient condition for the stability.

Lemma 5. The fractional system (1) with $0 < \alpha \le 1$ is stable if all eigenvalues of A lie in open left half-plane of the complex plane.

Using Lemma 4 and taking into account that the system (1) with $0 < \alpha \le 1$ is unstable if all eigenvalues of A lie in the instability region shown in Fig. 1, we obtain the following theorem.

Theorem 6 (Tavazoei and Haeri, 2009). The fractional system (1) with $0 < \alpha \le 1$ is unstable and all eigenvalues of A lie in the instability region shown in Fig. 1 if and only if the eigenvalues of $\bar{A}$ have negative real parts, where

$$\bar{A} = \begin{bmatrix} -A\sin(\alpha\pi/2) & A\cos(\alpha\pi/2) \\ -A\cos(\alpha\pi/2) & -A\sin(\alpha\pi/2) \end{bmatrix}. \tag{20}$$

Proof. If all eigenvalues of A lie in the instability sector shown in Fig. 1, then all eigenvalues of $-A$ satisfy the inequality

$$|\arg\lambda_i(-A)| > \pi - \alpha\frac{\pi}{2}, \quad i = 1,2,\ldots,n, \tag{21}$$

i.e. lie in sector shown in Fig. 2 if we consider angle $\pi - \alpha\pi/2$ with $\alpha \in (0,1]$ instead of angle $\alpha\pi/2$. Then $\delta = (1 - \alpha)\pi/2$. The proof follows directly from Lemma 4 for $\delta = (1 - \alpha)\pi/2$ and substitution $-A$ instead of A.

Based on instability analysis, the following condition has been given in Sabatier et al. (2008, 2010).

Theorem 7. The fractional system (1) with $0 < \alpha < 1$ is stable if and only if there does not exist any non-negative rank one complex matrix Q such that

$$rAQ + QA^{T}\bar{r} \ge 0, \tag{22}$$

where $r = \sin(\alpha\pi/2) + j\cos(\alpha\pi/2)$ and $\bar{r}$ denotes the complex conjugate of r.

The stability region shown in Fig. 1 is not convex. Therefore, to the stability analysis of the fractional system (1) with $0 < \alpha < 1$ the LMI conditions can not be applied.

In Sabatier et al. (2008, 2010) the following sufficient and necessary and sufficient conditions have been proved.

Theorem 8. The fractional system (1) with $0 < \alpha < 1$ is asymptotically stable if there exists a matrix $P > 0$ such that

$$(A^{1/\alpha})^{\mathrm{T}} P + P(A^{1/\alpha}) < 0. \tag{23}$$

Theorem 9. The fractional system (1) with $0 < \alpha < 1$ is stable if and only if there exists a symmetric matrix $P > 0$ such that

$$\left(-(-A)^{1/(2-\alpha)}\right)^{\mathrm{T}} P + P\left(-(-A)^{1/(2-\alpha)}\right) < 0. \tag{24}$$

Based on the Generalized LMI (GLMI), in Sabatier et al. (2008, 2010) the following criterion has been given.

Theorem 10. The fractional system (1) with $0 < \alpha < 1$ is stable if there exist positive definite complex matrices $X_1 = X_1^*$ and $X_2 = X_2^*$ such that

$$\bar{r}X_1A^{\mathrm{T}} + rAX_1 + rX_2A^{\mathrm{T}} + rAX_2 < 0, \tag{25}$$

where $r = \exp(j(1-\alpha)\pi/2)$.

3.3. Generalization of frequency domain methods

The frequency domain methods for stability analysis of fractional systems described by the transfer function have been proposed in Busłowicz (2008a, 2009), see also Kaczorek (2011a, Chapter 9). These methods can be applied to the system (1) of any fractional order $\alpha \in (0,2)$.

By generalization of the results of Busłowicz (2008a, 2009) to the case of fractional system (1) we obtain the following methods for stability checking.

Theorem 11. The fractional system (1) with characteristic polynomial (8) is stable if and only if

$$\Delta \arg_{0\le\omega<\infty} w(j\omega) = n\pi/2, \tag{26}$$

where $w(j\omega) = w(s)$ for $s = j\omega$, i.e. plot of the function $w(j\omega)$ starts for $\omega = 0$ in the point $w(0) = \det(-A)$ and with ω increasing from 0 to ∞ turns strictly counter-clockwise and goes through n quadrants of the complex plane.

Plot of the function $w(j\omega)$ is called the generalised (to the class of fractional degree polynomials) Mikhailov plot.

Checking the condition (26) is difficult in general (for large values of n), because $w(j\omega)$ quickly tends to infinity as ω grows to ∞.

To remove this difficulty, we consider the rational function

$$\psi(s) = \frac{\det(s^{\alpha}I - A)}{w_r(s)} \tag{27}$$

instead of the polynomial (8), where $w_r(s)$ is stable the reference fractional polynomial of degree αn, i.e.

$$w_r(s) \neq 0 \text{ for } \operatorname{Re} s \ge 0. \tag{28}$$

The reference fractional polynomial can be chosen in the form

$$w_r(s) = (s+c)^{\alpha n}, \quad c > 0. \tag{29}$$

Theorem 12. The fractional system (1) with $0 < \alpha < 2$ is stable if and only if

$$\Delta \arg_{\omega\in(-\infty,\infty)} \psi(j\omega) = 0, \tag{30}$$

where $\psi(j\omega) = \psi(s)$ for $s = j\omega$ and $\psi(s)$ is defined by (27), i.e. plot of the function $\psi(j\omega)$ does not encircle or cross the origin of the complex plane as ω runs from $-\infty$ to ∞.

Plot of the function $\psi(j\omega)$, $\omega \in (-\infty,\infty)$, is called the generalised modified Mikhailov plot.

From (8), (27) and (29) we have

$$\psi(\infty) = \lim_{\omega\to\pm\infty} \psi(j\omega) = 1 \tag{31}$$

and

$$\psi(0) = \frac{\det(-A)}{c^{\alpha n}}. \tag{32}$$

From (32) it follows that $\psi(0) \le 0$ if $\det(-A) \le 0$. Hence, from Theorem 12 we have the following important lemma.

Lemma 6. If $\det(-A) \le 0$ then the fractional system (1) is unstable for all $\alpha \in (0,2)$.

Lemma 6 also follows from the Hurwitz stability test because if $\det(-A) \le 0$ then not all coefficients of the characteristic polynomial of A are non-zero and positive.

3.4. Stability of positive systems

Now we consider the stability problem of the positive system (1) of fractional order $\alpha \in (0,1]$. In this case, according to Theorem 1, the condition (7) holds, i.e. the matrix A has non-negative off-diagonal entries.

Positive linear systems are sub-class of linear systems. Therefore, the stability conditions given in this paper can also be applied to the stability analysis of the positive system (1).

Stability conditions of positive natural number systems, continuous-time and discrete-time, are very simple in comparison with the stability conditions of standard systems (Farina and Rinaldi, 2000; Kaczorek, 2000, 2002). Therefore, we consider the possibilities of simplification of the stability conditions of standard fractional system (1) with $\alpha \in (0,1]$.

From Theorems 1 and 2 it follows that the positive system (1) with $\alpha \in (0,1)$ is stable if and only if all eigenvalues of the Metzler matrix A lie in the stability region shown in Fig. 1.

From (Farina and Rinaldi, 2000; Kaczorek, 2011b) we have that the dominant eigenvalue (eigenvalue with the

largest real part) of the Metzler matrix is real. Therefore, the positive system (1) with $\alpha \in (0,1)$ is stable if and only if all eigenvalues of the Metzler matrix A have negative real parts.

Hence, using the well-known stability conditions of positive systems given in Kaczorek (2000, 2002), we obtain the following simple necessary and sufficient condition for the asymptotic stability.

Lemma 7. The positive system (1) is asymptotically stable for all $\alpha \in (0,1)$ if and only if one of the following equivalent conditions holds:

1. eigenvalues $\lambda_1, \lambda_2, \ldots, \lambda_n$ of the matrix A have negative real parts,
2. all the leading principal minors $\Delta_1, \Delta_2, \ldots, \Delta_n$ of the matrix $-A$ are positive,
3. all the coefficients of the characteristic polynomial of the matrix A are positive.

It is easy to see that if $A \in M_n$ then the matrix (20) is not a Metzler matrix. This means that is not possible simplification of the condition given in Theorem 6 for the positive system (1).

4. ILLUSTRATIVE EXAMPLES

Example 1. Check stability of the system (1) with

$$A = \begin{bmatrix} 0 & 1 \\ -b & -a \end{bmatrix}, \quad a, b \in \Re. \tag{33}$$

Eigenvalues of A are as follows

$$\lambda_{1,2} = \frac{-a \pm \sqrt{a^2 - 4b}}{2}. \tag{34}$$

If $a^2 = 4b$ then $\lambda_{1,2} = -a/2$ Hence, from Lemmas 2 and 3 we have the following:

- if $a < 0$ then eigenvalues of A are positive and the system is unstable for all fractional orders α
- if $a > 0$ then eigenvalues of A are negative and the system is stable for all fractional orders $\alpha \in (0,2)$.

If

$$a^2 > 4b \text{ and } -a + \sqrt{a^2 - 4b} \geq 0 \text{ or } -a - \sqrt{a^2 - 4b} \geq 0, \tag{35}$$

then from Lemma 2 it follows that the system is unstable for all values $\alpha \in (0,2)$.

If

$$a^2 > 4b \text{ and } -a \pm \sqrt{a^2 - 4b} < 0, \tag{36}$$

then from Lemma 5 it follows that the system is stable for all $\alpha \in (0,1)$.

If $a^2 < 4b$ then the matrix (33) has two complex eigenvalues

$$\lambda_{1,2} = \frac{-a \pm j\sqrt{4b - a^2}}{2}. \tag{37}$$

If $a < 0$ then from (14) and (37) we have

$$\gamma = \arctan\sqrt{4\tau - 1}, \quad \tau = b/a^2, \tag{38}$$

and

$$\alpha_0 = \frac{2}{\pi}\gamma = \frac{2}{\pi}\arctan\sqrt{4\tau - 1}. \tag{39}$$

From Lemma 3 it follows that the system with $a^2 < 4b$ and $a < 0$ is stable for any $\alpha \in (0, \alpha_0)$ where α_0 is computed from (39).

Similarly, we can show that if $a > 0$ and $a^2 < 4b$ then the system is stable for any $\alpha \in (0, \alpha_{01})$ where

$$\alpha_{01} = \frac{2}{\pi}\gamma = \frac{2}{\pi}(\pi - \arctan\sqrt{4\tau - 1}), \quad \tau = b/a^2. \tag{40}$$

Plots of $\alpha_0(\tau)$ and $\alpha_{01}(\tau)$ for $\tau \in [1,10]$ are shown in Fig. 3. It is easy to check that $\alpha_0 \to 1$ and $\alpha_{01} \to 1$ if $\tau \to \infty$.

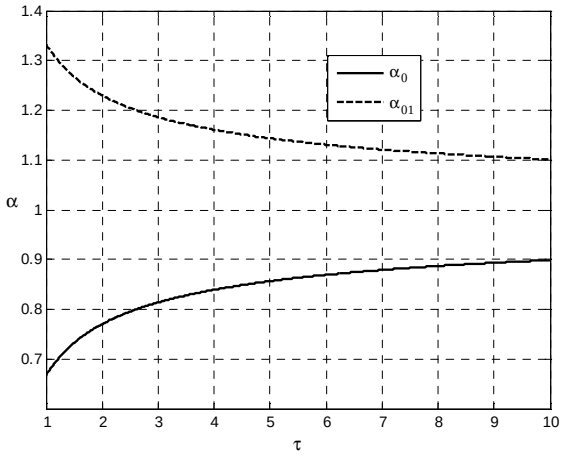

Fig. 3. Plot of the functions (39) and (40) vs. $\tau \in [1,10]$

From Fig. 3 and (39), (40) it follows that $\alpha_0 < \alpha_{01}$ for all fixed τ.

If $\tau = 4$ (i.e. $b = 4a^2$), for example, then the system

- with $a < 0$ is stable if and only if $\alpha \in (0, \alpha_0)$, $\alpha_0 = 0.8391$
- with $a > 0$ is stable if and only if $\alpha \in (0, \alpha_{01})$, where $\alpha_{01} = 1.1609$.

Assume that the output equation and the input matrix of the system (1), (33) are as follows

$$y(t) = Cx(t), \quad C = [1 \quad 0], \quad B = \begin{bmatrix} 0 \\ 1 \end{bmatrix}.$$

Then, the transfer function has the form

$$G(s) = C(s^\alpha I - A)^{-1}B = \frac{1}{\det(s^\alpha I - A)} = \frac{1}{s^{2\alpha} + as^\alpha + b}.$$

Step responses of the system for $b = 4$, $a = 1$ and $b = 4$, $a = -1$ are shown in Figs 4 and 5, respectively, for few values of fractional order α.

Numerical simulations are performed using Ninteger v. 2.3 – Fractional Control Toolbox for MatLab, see Valério (2005).

From Figs 4 and 5 it follows that simulations confirm the above theoretical results that the system with $b = 4a^2$ and $a < 0$ is stable for all positive $\alpha < 0.8391$, whereas

this system with $a > 0$ is stable for all positive $\alpha < 1.1609$.

Now we consider the stability problem of positive system (1) with (33).

From Theorem 1 it follows that the system (1) with A of the form (33) and $\alpha \in (0,1]$ is positive if and only if $b < 0$. If $b < 0$ then from (34) it follows that A has two real eigenvalues, one negative and one positive. Hence, from the above and Lemma 2 we have that the positive system (1) with the matrix (33) with $b < 0$ is unstable for all fractional orders $\alpha \in (0,1]$. In particular, this system is unstable for $\alpha = 1$ (the natural number positive system).

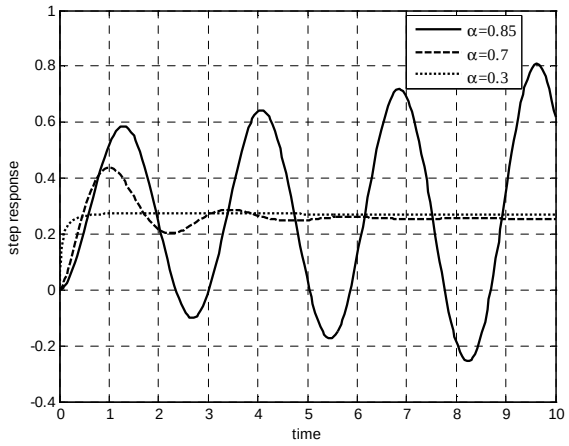

Fig. 4. Step responses of the system with $a = -1$, $b = 4$

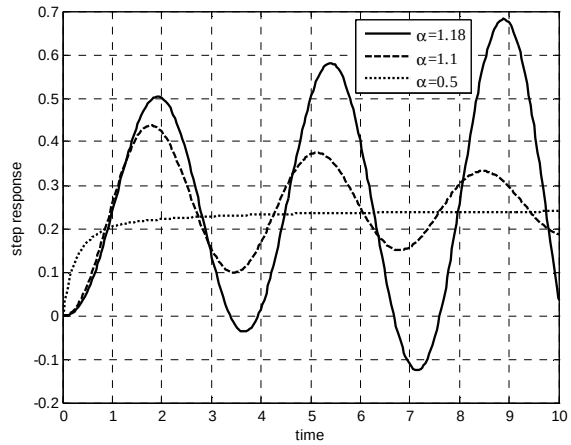

Fig. 5. Step responses of the system with $a = 1$, $b = 4$

Example 2. Consider the fractional system (1) with

$$A = \begin{bmatrix} -1 & 0.8 & 1.1 \\ -0.8 & -2 & 0.9 \\ -0.3 & -1.2 & -1.6 \end{bmatrix}. \tag{41}$$

Check stability of the system for $\alpha = 1.4$ and $\alpha = 1.9$. Plot of the function

$$\psi(j\omega) = \frac{\det((j\omega)^{\alpha} I - A)}{(j\omega + 1)^{3\alpha}}, \quad \omega \in (-\infty, \infty), \tag{42}$$

with $\alpha = 1.4$ and $\alpha = 1.9$ is shown in Figs 6 and 7, respectively.

According to (31) and (32) we have (independently of the value of α)

$$\psi(\infty) = \lim_{\omega \to \pm\infty} \psi(j\omega) = 1, \quad \psi(0) = \det(-A) = 5.1240.$$

From Figs 6, 7 and Theorem 12 it follows that the system with $\alpha = 1.4$ is stable (plot of (42) does not encircle the origin of the complex plane) and with $\alpha = 1.9$ is unstable (plot of (42) encircles the origin of the complex plane).

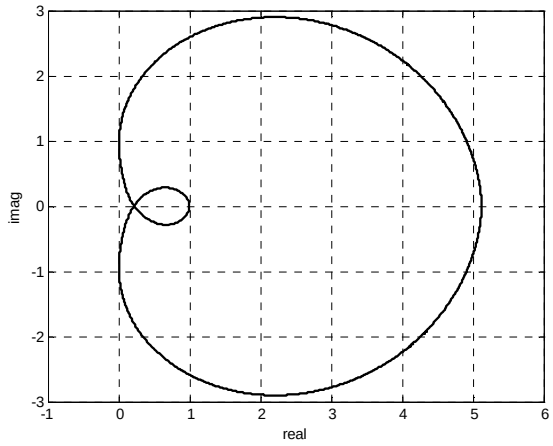

Fig. 6. Plot of the function (42) with $\alpha = 1.4$

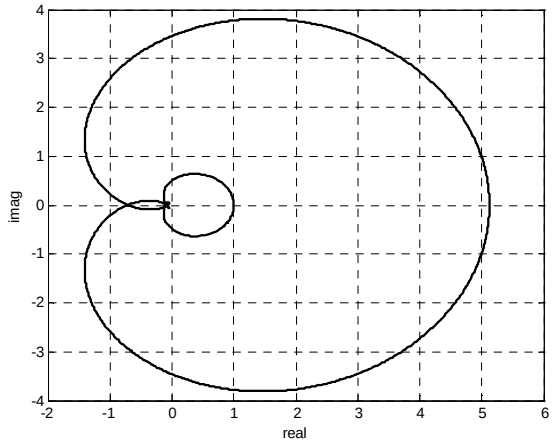

Fig. 7. Plot of the function (42) with $\alpha = 1.9$

Now we apply Theorem 5. Using the LMI toolbox of Matlab, we obtain the following feasible solution of (19):

– for $\alpha = 1.4$

$$P = \begin{bmatrix} 0.7751 & -0.0939 & 0.0750 \\ -0.0939 & 0.4212 & -0.0232 \\ 0.0750 & -0.0232 & 0.4510 \end{bmatrix} \tag{43}$$

– for $\alpha = 1.9$

$$P = \begin{bmatrix} 1.4859 & -0.6659 & 0.5467 \\ -0.6659 & 0.2984 & -0.2450 \\ 0.5467 & -0.2450 & 0.2012 \end{bmatrix}. \tag{44}$$

Computing the leading principal minors of the matrices (43) and (44) we obtain, respectively,

$$\Delta_1 = 0.7751,\ \Delta_2 = 0.3277,\ \Delta_3 = 0.1408,$$

$$\Delta_1 = 1.4850,\ \Delta_2 = -1.676 \cdot 10^{-9},\ \Delta_3 = -3.025 \cdot 10^{-5}.$$

From the above it follows that the matrix (43) is positive definite (all the leading principal minors are positive) and the matrix (44) is not positive definite. This means, according to Theorem 5, that the system with $\alpha = 1.4$ is stable and with $\alpha = 1.9$ is unstable.

Now we apply Lemma 3 to stability checking of the system.

The matrix (41) has the following eigenvalues:

$$\lambda_1 = -0.9538;\ \lambda_{2,3} = -1.8231 \pm j1.4313.$$

From (14) we have $\gamma = 2.4760$ and from Lemma 3 it follows that the system is stable for all $\alpha \in (0, \alpha_0)$ where $\alpha_0 = 2\gamma/\pi = 1.4305$. Hence, the system is stable for $\alpha = 1.4 < \alpha_0$ and unstable for $\alpha = 1.9 > \alpha_0$.

Now we assume $\alpha = 0.5$ and check stability using Theorems 8 and 9.

Computing the feasible solutions of (23) and (24) with $\alpha = 0.5$ we obtain respectively

$$P = \begin{bmatrix} 0.3866 & -0.0039 & 0.1038 \\ -0.0039 & 0.2308 & -0.0216 \\ 0.1038 & -0.0216 & 0.3173 \end{bmatrix}, \tag{45}$$

$$P = \begin{bmatrix} 0.6392 & -0.0125 & 0.1085 \\ -0.0125 & 0.4703 & -0.0301 \\ 0.1085 & -0.0301 & 0.5521 \end{bmatrix}. \tag{46}$$

It is easy to check that the matrices (45) and (46) are positive definite. From Theorems 8 and 9 it follows the system with $\alpha = 0.5$ is stable.

Example 3. Check stability of the system (1) with

$$A = \begin{bmatrix} -1.4 & 0 & 0.1 & 1.8 \\ 0.1 & -1.5 & 1.7 & 0.5 \\ 0.1 & 0.08 & -1.4 & 1.1 \\ 0 & 0.4 & 0.5 & -1.4 \end{bmatrix}. \tag{47}$$

The matrix (47) is a Metzler matrix. Therefore, the system (1), (47) with $\alpha \in (0,1]$ is a positive system. To stability checking of this system we apply simple necessary and sufficient condition given in Lemma 7.

Computing the characteristic polynomial of the matrix (47) we obtain

$$\det(\lambda I - A) = \lambda^4 + 5.7\lambda^3 + 11.284\lambda^2 + 8.0684\lambda + 0.8373.$$

All coefficients of the above polynomial are positive. From Lemma 7 it follows that the positive fractional system (1) with matrix A of the form (47) is stable for any $\alpha \in (0,1]$.

The matrix (47) has the following eigenvalues:

$$\lambda_1 = -0.1239;\ \lambda_2 = -1.5683;\ \lambda_{3,4} = -2.0039 \pm j0.5404.$$

From (14) we have $\gamma = 2.8782$ and $\alpha_0 = 1.8323$. From Lemma 3 it follows that the system (1) with A of the form (47) is stable for any fractional order $\alpha \in (0,\ 1.8323)$.

5. CONCLUDING REMARKS

Review of the existing methods for stability analysis of the system (1) of fractional order $\alpha \in (0,2)$ is given and the new results are presented.

In particular, generalisation of the classical Mikhailov stability criterion to the class of fractional order systems (1) with $\alpha \in (0,2)$ is proposed.

Moreover, it has been shown that:

- the fractional system (1) is unstable for all $\alpha \in (0,2)$ if the matrix A has at least one non-negative real eigenvalue (Lemma 2);
- if A has no real non-negative eigenvalues, then the fractional system (1) is stable if and only if $\alpha \in (0, \alpha_0)$ where $\alpha_0 = 2\gamma/\pi$ and γ is computed from (14) (Lemma 3);
- the positive system (1) is stable for all $\alpha \in (0,1]$ if and only if all coefficients of the characteristic polynomial of the matrix A are positive (Lemma 7).

REFERENCES

1. **Ahn H.-S., Chen Y. Q.** (2008), Necessary and sufficient stability condition of fractional-order interval linear systems, *Automatica*, Vol. 44, 2985-2988.
2. **Ahn H.-S., Chen Y. Q., Podlubny I.** (2006), Robist stability checking of a class of linear interval fractional order systems using Lyapunov inequality, *Proc. 2nd IFAC Workshop on Fractional Differentiation and its Applications*, Porto, Portugal (CD-ROM).
3. **Anderson B. D. O., Bose N. K. and Jury E. I.** (1974), A simple test for zeros of a complex polynomial in a sector, *IEEE Trans. Autom. Control*, Vol. 19, 437-438.
4. **Busłowicz M.** (2008a), Frequency domain method for stability analysis of linear continuous-time fractional systems, In: **Malinowski K. and Rutkowski L.** (Eds.), *Recent Advances in Control and Automation*, Academic Publishing House EXIT, Warsaw, 83-92.
5. **Busłowicz M.** (2008b), Stability of linear continuous-time fractional order systems with delays of the retarded type, *Bull. Pol. Acad. Sci., Tech. Sci.*, Vol. 56, No. 4, 319-324.
6. **Busłowicz M.** (2008c), Robust stability of convex combination of two fractional degree characteristic polynomials, *Acta Mechanica et Automatica*, Vol. 2, No. 2, 5-10.
7. **Busłowicz M.** (2009), Stability analysis of linear continuous-time fractional systems of commensurate order, *Journal of Automation, Mobile Robotics and Intelligent Systems*, Vol. 3, No. 1, 12-17.
8. **Caponetto R., Dongola G., Fortuna L., Petras I.** (2010), Fractional order systems: Modeling and Control Applications, New Jersey: World Scientific.
9. **Chilali M., Gahinet P., Apkarian P.** (1999), Robust pole placement in LMI regions, *IEEE Trans. Autom. Control*, Vol. 44, No. 12, 2257-2270.
10. **Das S.** (2008), *Functional Fractional Calculus for System Identification and Controls*, Springer, Berlin.
11. **Davison E. J., Ramesh N.** (1970), A note on the eigenvalues of a real matrix, *IEEE Trans. Autom. Control*, Vol. 15, 252-253.

12. **Diethelm K.** (2010), *The Analysis of Fractional Differential Equations, An Application-Oriented Exposition Using Differential Operators of Caputo Type*, Springer-Verlag, Berlin Heidelberg.
13. **Farina L., Rinaldi S.** (2000), *Positive Linear Systems: Theory and Applications*, J. Wiley, New York.
14. **Hostetter G. H.** (1975), An improved test for the zeros of a polynomial in a sector, *IEEE Trans. Automat. Control*, Vol. 20, 433–434.
15. **Kaczorek T.** (2000), *Positive 1D and 2D Systems*, Publishing House of Warsaw University of Technology, Warsaw (in Polish).
16. **Kaczorek T.** (2002), *Positive 1D and 2D Systems*, Springer-Verlag, London.
17. **Kaczorek T.** (2008a), Reachability of fractional positive continuous-time linear systems, *Pomiary Automatyka Robotyka*, No. 2, 527-537 (on CD-ROM).
18. **Kaczorek T.** (2008b), Fractional positive continuous-time linear systems and their reachability. *Int. J. Appl. Math. Comput. Sci.*, Vol. 18, No. 2, 223-228.
19. **Kaczorek T.** (2009), *Selected Problems of Fractional Systems Theory*, Publishing Department of Białystok University of Technology, Białystok (in Polish).
20. **Kaczorek T.** (2011a), *Selected Problems of Fractional Systems Theory*, Springer, Berlin (in print).
21. **Kaczorek T.** (2011b), Necessary and sufficient stability conditions of fractional positive continuous-time linear systems, *Acta Mechanica et Automatica* (in print).
22. **Kilbas A. A., Srivastava H. M. Trujillo J. J.** (2006), *Theory and Applications of Fractional Differential Equations*, Elsevier, Amsterdam.
23. **Lu J.-G., Chen G.** (2009), Robust stability and stabilization of fractional-order interval systems: an LMI approach, *IEEE Trans. Autom. Control*, Vol. 54, No. 6, 1294-1299.
24. **Matignon D.** (1996), Stability results on fractional differential equation with applications to control processing, *Proc. of IMACS*, Lille, France, 963-968.
25. **Matignon D.** (1998), Stability properties for generalized fractional differential systems, *Proc. of ESAIM*, 145-158.
26. **Molinary B. P.** (1975), The stabilizing solution of the discrete-algebraic equation, *IEEE Trans. Autom. Control*, Vol. 20, No. 3, 393-399.
27. **Monje C. A., Chen Y.-Q., Vinagre B. M., Xue D.-Y., Feliu V.** (2010), Fractional-order Systems and Controls: Fundamentals and Applications, London: Springer-Verlag.
28. **Ostalczyk P.** (2008), *Epitome of the Fractional Calculus, Theory and its Applications in Automatics*, Publishing Department of Technical University of Łódź, Łódź (in Polish).
29. **Petras I.** (2008), *Stability of fractional-order systems with rational orders*, Institute of Control and Informatization of Production Processes, Technical University of Kosice, Report arXiv:0811.4102v2 [math.DS].
30. **Petras I.** (2009), Stability of fractional-order systems with rational orders: a survey, *Fractional Calculus & Applied Analysis. An International Journal for Theory and Applications*, Vol. 12, No. 3, 269-298.
31. **Podlubny I.** (1994), *Fractional Order Systems and Fractional Order Controllers*, The Academy of Sciences Institute of Experimental Physics, Kosice, Slovak Republic.
32. **Podlubny I.** (1999), *Fractional Differential Equations*, Academic Press, San Diego.
33. **Radwan A.G., Soliman A.M., Elwakil A.S., Sedeek A.** (2009), On the stability of linear systems with fractional-order elements, *Chaos, Solitons and Fractals*, Vol. 40, 2317–2328.
34. **Sabatier J., Agrawal O. P., Machado J. A. T.** (Eds) (2007), *Advances in Fractional Calculus, Theoretical Developments and Applications in Physics and Engineering*, Springer, London.
35. **Sabatier J., Moze M., Farges C.** (2008), On stability of fractional order systems, *Proc. of 3rd IFAC Workshop on Fractional Differentiation and its Applications*, Ankara, Turkey (CD-ROM).
36. **Sabatier J., Moze M., Farges C.** (2010), LMI stability conditions for fractional order systems, *Computers and Mathematics with Applications*, Vol. 59, 1594-1609.
37. **Tan N., Özguven Ö. F., Özyetkin M. M.** (2009), Robust stability analysis of fractional order interval polynomials, *ISA Transactions*, Vol. 48, 166-172.
38. **Tavazoei M. S., Haeri M.** (2009), Note on the stability of fractional order systems, *Mathematics and Computers in Simulation*, Vol. 79, 1566-1576.
39. **Valério D.** (2005), Ninteger v. 2.3 - Fractional Control Toolbox for MatLab, User and programmer manual, Technical University of Lisbona, http://web.ist.utl.pt/duarte.valerio/ ninteger/ninteger.htm.
40. **Zhuang J., Yisheng Z.** (2010), Robust stability for uncertain fractional-order systems, *Proc. of the 29th Chinese Control Conference*, Beijing, China.

Acknowledgement: The work was supported by the Ministry of Science and High Education of Poland under grant No. N N514 638940.

FUZZY PREDICTIVE CONTROL OF FRACTIONAL-ORDER NONLINEAR DISCRETE-TIME SYSTEMS

Stefan DOMEK*

*Department of Control Engineering and Robotics, West Pomeranian University of Technology at Szczecin, ul. Sikorskiego 37, 70-313 Szczecin

stefan.domek@zut.edu.pl

Abstract: At the end of the 19th century Liouville and Riemann introduced the notion of a fractional-order derivative, and in the latter half of the 20th century the concept of the so-called Grünewald-Letnikov fractional-order discrete difference has been put forward. In the paper a predictive controller for MIMO fractional-order discrete-time systems is proposed, and then the concept is extended to nonlinear processes that can be modelled by Takagi-Sugeno fuzzy models. At first nonlinear and linear fractional-order discrete-time dynamical models are described. Then a generalized nonlinear fractional-order TS fuzzy model is defined, for which equations of a predictive controller are derived.

1. INTRODUCTION

The effectiveness of nonlinear process control systems depends to a large extent on the quality of the model used for controller synthesis or tuning. Unfortunately, the choice of an adequate model for a nonlinear process and its parameterization involves difficulties in industrial practice. Therefore, nonlinear process models of relatively simple structure but furnishing a means to synthesize the controller that would ensure satisfactory control performance are still looked for (Domek, 2006).

One of the more effective methods employed to describe real properties exhibited by many industrial processes, inclusive of those with distributed parameters, seems to be the description based on fractional-order derivatives. Many examples illustrating possible applications of such a description may be found in the literature (Domek and Jaroszewski, 2010; Kaczorek, 2009; Lorenz and Kasturiarachi, 2009; Muddu Madakyaru et al., 2009; Ostalczyk, 2000l Podlubny et al., 1997; Riewe, 1997; Sierociuk, 2007; Sjöberg and Kari, 2002; Suarez et al., 2003; Vinagre and Feliu, 2002; Xue and Chen, 2002; Zamani et al., 2007).

In the paper a way of modelling complex nonlinear MIMO processes in state space by means of fuzzy Takagi-Sugeno models of fractional order (Domek, 2006; Takagi and Sugeno, 1985; Tatjewski, 2007) is presented and a generalized predictive algorithm that employs such models is introduced.

2. DYNAMICAL MODELS OF FRACTIONAL ORDER

Let us consider the traditional discrete-time nonlinear process model of integer order in state space, well-known in the form

$$x(t+1) = f\big(x(t), u(t)\big) \tag{1}$$

$$y(t) = g\big(x(t)\big) \tag{2}$$

where $x(t) \in \mathcal{R}^n,\ u(t) \in \mathcal{R}^m,\ y(t) \in \mathcal{R}^p$ denote the state, input and output vectors respectively at time instant $t \in \{0,1,2,\dots\}$ of dimensions $n \times 1,\ m \times 1$ and $p \times 1$ respectively.

Equation (1) can be rewritten with the use of the so-called first-order backward difference for the state $x(t)$:

$$\Delta^1 x(t) = x(t) - x(t-1) \tag{3}$$

as

$$\Delta^1 x(t+1) = f_d\big(x(t), u(t)\big) \tag{4}$$

where

$$f_d\big(x(t), u(t)\big) = f\big(x(t), u(t)\big) - x(t) \tag{5}$$

Now, let us introduce the definition of the real fractional-order α backward difference for the state vector $x(t)$, based on the Grünewald-Letnikov definition (Sierociuk, 2007):

$$\Delta^\alpha x(t) = \sum_{i=0}^{t} (-1)^i \binom{\alpha}{i} x(t-i), \tag{6}$$

$$n-1 < \alpha \le n \in \{1,2,3,\dots\}$$

$$\binom{\alpha}{i} = \begin{cases} 1 & \text{for} \quad i = 0 \\ \frac{\alpha(\alpha-1)\dots(\alpha-i+1)}{i!} & \text{for} \quad i = 1,2,\dots \end{cases} \tag{7}$$

The definition (6) may be written in a generalized form by adopting different orders of backward differences for individual state variables of the state vector $x(t) \in \mathcal{R}^n$:

$$\Delta^{\Upsilon} x(t+1) = [\Delta^{\alpha_1} x_1(t+1) \quad \cdots \quad \Delta^{\alpha_n} x_n(t+1)]^T \tag{8}$$

Then, similarly to eq. (4), the fractional-order generalized model of a nonlinear process may be defined in state space as:

$$\Delta^{\Upsilon} x(t+1) = f_d\big(x(t), u(t)\big) \tag{9}$$

which, in view of eqs. (6), (7) and (8), may be rewritten in the following form:

$$x(t+1) = f_d\big(x(t), u(t)\big) - \sum_{i=1}^{t+1} (-1)^i \Upsilon_i x(t+1-i) \tag{10}$$

$$\Upsilon_i = \operatorname{diag}\left[\binom{\alpha_1}{i} \quad \cdots \quad \binom{\alpha_n}{i}\right] \tag{11}$$

It should be noted that the model (10), (11) in particular may describe properties of a fractional-order linear process. By analogy to the integer-order model (1) – (5), for which the well-known linear version has the form:

$$x(t+1) = \mathbf{A}x(t) + \mathbf{B}u(t) \tag{12}$$

$$y(t) = \mathbf{C}x(t) \tag{13}$$

with the state equation (12) written another way as:

$$\Delta^1 x(t+1) = \mathbf{A}_{\boldsymbol{d}} x(t) + \mathbf{B}u(t) \tag{14}$$

where

$$\mathbf{A}_{\boldsymbol{d}} = \mathbf{A} - \mathbf{I}_n \tag{15}$$

($\mathbf{I}_n \in \mathcal{R}^{n\times n}$ – identity matrix), the fractional-order generalized model of a linear process, in view of eqs. (8), (9) and (15), may be given in state space as:

$$\Delta^{\boldsymbol{\Upsilon}} x(t+1) = \mathbf{A}_{\boldsymbol{d}} x(t) + \mathbf{B}u(t) \tag{16}$$

or alternatively

$$x(t+1) = \mathbf{A}_{\boldsymbol{d}} x(t) + \mathbf{B}u(t) - \sum_{i=1}^{t+1}(-1)^i \boldsymbol{\Upsilon}_{\boldsymbol{i}} x(t+1-i) \tag{17}$$

3. FRACTIONAL-ORDER NONLINEAR FUZZY MODELS

The usefulness of fractional-order models (9) in industrial practice, where processes to be controlled are most often significantly nonlinear, is small. Making use of the nonlinear model (10) is not possible in general, since universal methods for nonlinear controller synthesis based on such models are lacking.

On the other hand, the linear model (16) may be employed to synthesize a nonlinear process controller only if the assumption is made that the control system is operated in a small vicinity of the equilibrium point, for which the model has been defined.

The approach to modelling integer-order nonlinear processes that has been employed for many years is the use of the so-called networks (batteries) of Takagi-Sugeno local models (also called Takagi-Sugeno-Kanga models), originally proposed in Takagi and Sugeno (1985). In these models an antecedent in the form of a fuzzy logical product for each *i*-th fuzzy rule out of *p* rules is adopted (Domek, 2006; Tatjewski, 2007):

$$\text{IF} \quad \left\{ \begin{matrix} x_1(t) \subset S_{j,1} \;\; AND \;\; x_2(t) \subset S_{j,2} \\ AND \;\; ... \;\; AND \;\; x_n(t) \subset S_{j,n} \end{matrix} \right\} \tag{18}$$

where $x_k(t) \subset S_{j,k}$ denotes membership of the state variable $x_k(t)$ to the fuzzy set $S_{j,k}$ with membership function $\mu_{S_{j,k}}(x_k(t))$:

$$\forall x_k \quad \exists \left\{ \mu_{S_{1,k}}, \; \mu_{S_{2,k}}, \; \dots, \; \mu_{S_{p,k}} \right\} \\ \sum_{j=1}^{p} \left(x_k(t) \right) = 1 \cap \mu_{S_{j,k}}(x_k(t)) \geq 0 \tag{19}$$

The consequents of rules in the Takagi-Sugeno models are given by algebraic expressions. For the considered in the paper case of a battery of fractional-order models the following consequents are suggested:

$$\text{THEN} \tag{20}$$

$$\left\{ \begin{matrix} x(t+1) = \mathbf{A}_{\boldsymbol{d,j}} x(t) + \boldsymbol{B_j} u(t) - \sum_{i=1}^{L+1} (-1)^i \boldsymbol{\Upsilon_{i,j}} x(t+1-i) \\ y(t) = \mathbf{C_j} x(t) \end{matrix} \right\}$$

where

$$\Upsilon_{\boldsymbol{i,j}} = \text{diag}\left[\binom{\alpha_{1,j}}{i} \quad \dots \quad \binom{\alpha_{n,j}}{i} \right] \tag{21}$$

and subscript *j* denotes a set of parameters of the *j*-th local model described by a complemented state matrix $\mathbf{A}_{\boldsymbol{d,j}}$, input matrix $\mathbf{B}_{\boldsymbol{j}}$ and output matrix $\mathbf{C}_{\boldsymbol{j}}$ and of fractional orders $\{\alpha_{1,j}, \alpha_{2,j}, \dots, \alpha_{n,j}\}$.

It may be shown (Domek, 2006; Tatjewski, 2007) that the following resultant state equation for the entire network of local models is obtained after performing inference and defuzzification by means of the center of gravity technique (Babuška and Verbrungen, 1996; Domek, 2006):

$$x(t+1) = \frac{\sum_{j=1}^{p} w_j(t) x_j(t+1)}{\sum_{j=1}^{p} w_j(t)} \sum_{j=1}^{p} \widetilde{w}_j(t) \left[\mathbf{A}_{\boldsymbol{d,j}} x(t) + \right. \\ \left. \mathbf{B}_{\boldsymbol{j}} u(t) - \sum_{i=1}^{L+1} (-1)^i \boldsymbol{\Upsilon}_{\boldsymbol{i,j}} x(t+1-i) \right] \tag{22}$$

$$y(t) = \frac{\sum_{j=1}^{p} w_j(t) y_j(t)}{\sum_{j=1}^{p} w_j(t)} = \sum_{j=1}^{p} \widetilde{w}_j(t) \, \mathbf{C}_{\boldsymbol{j}} x(t) \tag{23}$$

where weight coefficients determining the so-called degree of activation of individual rules are defined by means of the fuzzy product operator (Babuška and Verbrungen, 1996):

$$w_j(t) = \prod_{k=1}^{n} \mu_{S_{j,k}}(x_k(t)) \tag{24}$$

With eqs. (22) – (24) in view, the fractional-order nonlinear process (9) may be described in state space by a fuzzy-tuned fractional-order quasi-linear model of the form (17) creating a fuzzy network of Takagi-Sugeno (TS) local models:

$$x(t+1) = \mathbf{A}_{\boldsymbol{d}}^{t} x(t) + \mathbf{B}^{t} u(t) - \sum_{i=1}^{L+1} (-1)^i \boldsymbol{\Upsilon}_{\boldsymbol{i}}^{t} x(t+1-i) \tag{25}$$

$$y(t) = \mathbf{C}^{t} x(t) \tag{26}$$

where

$$\mathbf{A}_{\boldsymbol{d}}^{t} = \mathbf{A}_{\boldsymbol{d}}(x(t)) = \sum_{j=1}^{p} \widetilde{w}_j(t) \, \mathbf{A}_{\boldsymbol{d,j}} \tag{27}$$

$$\mathbf{B}^{t} = \mathbf{B}(x(t)) = \sum_{j=1}^{p} \widetilde{w}_j(t) \, \mathbf{B}_{\boldsymbol{j}} \tag{28}$$

$$\mathbf{C}^{t} = \mathbf{C}(x(t)) = \sum_{j=1}^{p} \widetilde{w}_j(t) \, \mathbf{C}_{\boldsymbol{j}} \tag{29}$$

$$\boldsymbol{\Upsilon}_{\boldsymbol{i}}^{t} = \boldsymbol{\Upsilon}_{\boldsymbol{i}}^{t}(x(t)) = \sum_{j=1}^{p} \widetilde{w}_j(t) \, \boldsymbol{\Upsilon}_{\boldsymbol{i,j}} \tag{30}$$

To identify the parameters and the order of fractional-order local dynamic models (20), (21), use can be made, for example, of Sierociuk (2007), Sierociuk and Dzieliński (2006). In Wnuk (2004) there are many remarks to be found concerning choosing the number of local models, dividing the operating area into local partitions, establishing the individual membership functions and validating the adopted assumptions for fuzzy modeling.

4. A FRACTIONAL-ORDER PREDICTIVE CONTROLLER

One of the more effective and frequently employed in industry control methods, especially for multivariable and nonlinear processes, based on the process model is the predictive control (Domek, 2006; Maciejowski, 2002; Tatjewski, 2007). First attempts to utilize fractional-order derivatives in predictive control have been described, among others, in Domek and Jaroszewski (2010), Muddu

Madakyaru et al. (2009) and Romero et al. (2008). There have been applied selected methods of discrete approximation for fractional-order processes (Xue et al., 2006).

In order to determine the manipulated variable $u(t)$ let us adopt the quadratic cost function over a finite horizon in its general the matrix form:

$$\boldsymbol{J}(t) = [Y(t)_{\rightarrow} - Y^r(t)_{\rightarrow}]^T[Y(t)_{\rightarrow} - Y^r(t)_{\rightarrow}] + \lambda\,[\Delta U_0(t)_{\rightarrow}]^T[\Delta U_0(t)_{\rightarrow}]\,, \quad \lambda \geq 0 \tag{31}$$

where

$$Y^r(t)_{\rightarrow} = \begin{bmatrix} y^r(t+N_1|t) \\ y^r(t+N_1+1|t) \\ \vdots \\ y^r(t+N_2|t) \end{bmatrix} \tag{32}$$

denotes the reference trajectory vector, which starts always from the current value of the plant output and has the form of a smoothed reference signal,

$$Y(t)_{\rightarrow} = \begin{bmatrix} y(t+N_1|t) \\ y(t+N_1+1|t) \\ \vdots \\ y(t+N_2|t) \end{bmatrix} \tag{33}$$

is the output prediction vector, whereas the vector $\Delta\widehat{U}(t)_{\rightarrow}$ can take the following forms depending on the used algorithm version:

$$\Delta U_0(t)_{\rightarrow} = [\Delta_0 u(t|t) \quad \Delta_0 u(t+1|t) \quad \cdots \quad \Delta_0 u(t+N_u-1|t)]^T \tag{34}$$

with increments of the manipulated variable related to the component determined for the t–1 instant

$$\Delta_0 u(t+j|t) = u(t+j|t) - u(t-1)\,,$$
$$0 \leq j \leq N_u - 1 \tag{35}$$

with an additional assumption respectively

$$\Delta u_0(t+j|t) = 0\,, \quad \text{for} \quad N_u \leq j \leq N_2 - 1 \tag{36}$$

4.1. Synthesis of a fractional-order linear predictive controller

To determine the optimal manipulated variable we have to find the dependence of the process output prediction vector (33) on the vector of future manipulated variables (34). For the process defined by the model (17) the solution is given by Sierociuk (2007):

$$x(t) = \boldsymbol{\Phi}^{\boldsymbol{\Upsilon}}(t)x(0) + \sum_{i=0}^{t-1} \boldsymbol{\Phi}^{\boldsymbol{\Upsilon}}(i)\mathbf{B}u(t-i-1), \quad t = 1,2,\ldots \tag{37}$$

where the matrix $\boldsymbol{\Phi}^{\boldsymbol{\Upsilon}}(t)$ is defined by the recurrence relation

$$\boldsymbol{\Phi}^{\boldsymbol{\Upsilon}}(t+1) = (\mathbf{A}_D+\boldsymbol{\Upsilon}_1)\boldsymbol{\Phi}^{\boldsymbol{\Upsilon}}(t) - \sum_{i=2}^{t+1}(-1^i)\boldsymbol{\Upsilon}_i\boldsymbol{\Phi}^{\boldsymbol{\Upsilon}}(t-i+1), \quad i = 2,3,\ldots \tag{38}$$

with

$$\boldsymbol{\Phi}^{\boldsymbol{\Upsilon}}(1) = (\mathbf{A}_D+\boldsymbol{\Upsilon}_1), \quad \boldsymbol{\Phi}^{\boldsymbol{\Upsilon}}(0) = \mathbf{I}_n \tag{39}$$

Hence, in view of eqs. (13) and (37), we get

$$y(t) = \mathbf{C}\left[\boldsymbol{\Phi}^{\boldsymbol{\Upsilon}}(t)x(0) + \sum_{i=0}^{t-1} \boldsymbol{\Phi}^{\boldsymbol{\Upsilon}}(i)\mathbf{B}u(t-i-1)\right] + \mathbf{D}u(t) \tag{40}$$

and consequently, assuming for simplicity $\mathbf{D} = \mathbf{0}$, the prediction of the output for the $t+j$ instant may be found at the t instant in the following form:

$$y(t+j|t) = \mathbf{C}\left[\boldsymbol{\Phi}^{\boldsymbol{\Upsilon}}(j)x(t) + \sum_{i=0}^{j-1} \boldsymbol{\Phi}^{\boldsymbol{\Upsilon}}(i)\mathbf{B}u(t+j-i-1)\right] \tag{41}$$

or equivalently

$$y(t+j|t) = \mathbf{C}\left[\boldsymbol{\Phi}^{\boldsymbol{\Upsilon}}(j)x(t) + \sum_{i=0}^{j-1} \boldsymbol{\Phi}^{\boldsymbol{\Upsilon}}(j-i-1)\mathbf{B}u(t+i)\right] \tag{42}$$

Hence, the prediction of the natural process response becomes

$$y^0(t+j|t) = \mathbf{C}\left[\boldsymbol{\Phi}^{\boldsymbol{\Upsilon}}(j)x(t) + \sum_{i=0}^{j-1} \boldsymbol{\Phi}^{\boldsymbol{\Upsilon}}(i)\mathbf{B}u(t-i)\right] \tag{43}$$

and that of the forced response becomes

$$y^c(t+j|t) = \mathbf{C}\left[\sum_{i=0}^{j-1} \boldsymbol{\Phi}^{\boldsymbol{\Upsilon}}(j-i-1)\mathbf{B}\Delta_0 u(t+i)\right] \tag{44}$$

Writing the future values of the natural response (43) within the prediction horizon in the vector form

$$Y^0(t)_{\rightarrow} = \begin{bmatrix} y^0(t+N_1|t) \\ y^0(t+N_1+1|t) \\ \vdots \\ y^0(t+N_2|t) \end{bmatrix} \tag{45}$$

$$Y^0(t)_{\rightarrow} = \underline{\mathbf{C}} \cdot \left(\begin{bmatrix} \boldsymbol{\Phi}^{\boldsymbol{\Upsilon}}(N_1) \\ \vdots \\ \boldsymbol{\Phi}^{\boldsymbol{\Upsilon}}(N_2) \end{bmatrix} x(t) + \begin{bmatrix} \sum_{i=0}^{N_1-1} \boldsymbol{\Phi}^{\boldsymbol{\Upsilon}}(i) \\ \vdots \\ \sum_{i=0}^{N_2-1} \boldsymbol{\Phi}^{\boldsymbol{\Upsilon}}(i) \end{bmatrix} \mathbf{B}u(t-1) \right) \tag{46}$$

the output prediction vector (33), in view of eqs. (43) and (44), assumes the following form:

$$Y(t)_{\rightarrow} = \mathbf{E}\,\Delta U_0(t)_{\rightarrow} + Y^0(t)_{\rightarrow} \tag{47}$$

where the so-called process dynamics matrix for the vector (34) is given by:

$$\mathbf{E} = \underline{\mathbf{C}} \cdot \underline{\mathbf{E}} \cdot \underline{\mathbf{B}} \tag{48}$$

with the matrix $\underline{\mathbf{E}} \in \mathcal{R}^{n\cdot(N_2-N_1+1)\times n\cdot N_u}$:

$$\underline{\mathbf{E}} = \begin{bmatrix} \sum_{i=0}^{N_1-1} \boldsymbol{\Phi}^{\boldsymbol{\Upsilon}}(i) & \cdots & \cdots & \cdots & \mathbf{0}_n \\ \vdots & \vdots & \ddots & \vdots & \vdots \\ \vdots & \cdots & \mathbf{A}_D+\boldsymbol{\Upsilon}_1 & \mathbf{I}_n & \vdots \\ \sum_{i=0}^{N_u-1} \boldsymbol{\Phi}^{\boldsymbol{\Upsilon}}(i) & \cdots & \cdots & \mathbf{A}_D+\boldsymbol{\Upsilon}_1 & \mathbf{I}_n \\ \sum_{i=0}^{N_u} \boldsymbol{\Phi}^{\boldsymbol{\Upsilon}}(i) & \cdots & \cdots & \cdots & \mathbf{A}_D+\boldsymbol{\Upsilon}_1 \\ \vdots & \vdots & \vdots & \vdots & \vdots \\ \sum_{i=0}^{N_2-1} \boldsymbol{\Phi}^{\boldsymbol{\Upsilon}}(i) & \cdots & \cdots & \cdots & \sum_{i=0}^{N_2-N_u} \boldsymbol{\Phi}^{\boldsymbol{\Upsilon}}(i) \end{bmatrix} \tag{49}$$

and the block matrices $\underline{\mathbf{B}} \in \mathcal{R}^{n\cdot N_u \times m\cdot N_u}$

and $\underline{\mathbf{C}} \in \mathcal{R}^{p\cdot(N_2-N_1+1)\times n\cdot(N_2-N_1+1)}$:

$$\underline{\mathbf{B}} = \begin{bmatrix} \mathbf{B} & \cdots & \mathbf{0} \\ \vdots & \ddots & \vdots \\ \mathbf{0} & \cdots & \mathbf{B} \end{bmatrix}, \qquad \underline{\mathbf{C}} = \begin{bmatrix} \mathbf{C} & \cdots & \mathbf{0} \\ \vdots & \ddots & \vdots \\ \mathbf{0} & \cdots & \mathbf{C} \end{bmatrix} \tag{50}$$

In view of eqs. (31) and (47), the optimal control becomes [3]:

$$\Delta U_{opt}(t)_{\rightarrow} = \mathbf{P}[Y^r(t)_{\rightarrow} - Y^0(t)_{\rightarrow}] \tag{51}$$

where the controller gain matrix is:

$$\mathbf{P} = \left(\mathbf{E}^T\mathbf{E}+\lambda\cdot\mathbf{I}_{m\cdot N_u}\right)^{-1}\mathbf{E}^T \tag{52}$$

In view of the fact that, according to the principle of the moving horizon, only the first component of the computed control vector is utilized at the given instant *t*, we get finally from eqs. (35), (51) and (52):

$$u(t|t) = u(t-1) + \mathbf{p}[Y^r(t)_{\rightarrow} - Y^0(t)_{\rightarrow}] \quad (53)$$

where $\mathbf{p}$ is the first row of the gain matrix $\mathbf{P}$.

In the proposed predictive controller, as with the classic predictive control, it is possible to determine the optimal control in the presence of constraints imposed on the control signal, its increments and/or process output. In such a situation, in view of eqs. (46) – (50), the quadratic programming (QP) problem should be solved numerically at each step *t* (Domek, 2006; Maciejowski, 2002).

4.2. A fuzzy, fractional-order, state model predictive controller

The above presented synthesis of the fractional-order linear predictive controller can be extended in a relatively simple way to nonlinear processes by employing the proposed fuzzy TS model. In such an event a fractional-order linear predictive controller is to be determined at each step for the current quasi-linear process (25), (26). Another natural approach is utilizing the above presented method to synthesize a controller for linear processes, design of local linear controllers for each *j*-th local submodel (20) and employing all found controllers in the consequents of the rules (18), (19). Therefore, a fuzzy network (battery) of local controllers is obtained in such a way.

5. CONCLUDING REMARKS

In the paper an approach to synthesis of a fractional-order nonlinear predictive controller for fractional-order nonlinear MIMO processes is presented. The approach is based on utilizing the proposed fuzzy TS model of the fractional-order nonlinear process. The individual state variables in the generalized model are assumed to be of different orders. A more simple case is represented by the model of identical orders, the particular case of which is the integer-order model including the linear model. In such a case the proposed predictive controller reduces to the known SMPC controller (Maciejowski, 2002).

REFERENCES

1. **Babuška R., Verbrungen H. B.** (1996) An overview of fuzzy modelling for control, *Control Eng. Practice*, 4(11), 1593–1606.
2. **Domek S.** (2009), *Robust predictive control of nonlinear processes (in Polish)*, Wydawnictwo Politechniki Szczecińskiej, Szczecin.
3. **Domek S., Jaroszewski K.** (2010), *Model predictive controller for fractional order systems*, In: A. Grzech,P. Świątek, J. Drapała (Eds): Advances in System Science, Computer Science, EXIT, Warszawa, 9–18.
4. **Kaczorek T.** (2009), Positive 2D fractional linear systems, *COMPEL: Int. Journal for Computation and Mathematics in Electrical and Electronic Engineering*, Vol. 28, No. 2, 341–352.
5. **Lorenz A., Kasturiarachi A.** (2009), *The theory and application of fractional derivatives*, The annual meeting of the The Mathematical Association of America – MathFest.
6. **Maciejowski J. M.** (2002), *Predictive control with constraints*, Englewood Cliffs, Prentice Hall.
7. **Mäkilä P. M., Partington J. R.** (2003), On linear models for nonlinear systems, *Automatica*, 39, 1–13.
8. **Muddu Madakyaru M., Narang A., Patwardhan S. C**. (2009), Development of ARX models for predictive control using fractional order and orthonormal basis filter parametrization, *Ind. Eng. Chem. Res*., Vol. 48, No. 19, 8966–8979.
9. **Ostalczyk P.** (2000), The non-integer difference of the discrete-time function and its application to the control system synthesis, *Int. J. Syst. Sci*., Vol. 31, No. 12, 1551–1561.
10. **Podlubny I., Dorcak L., Kostial I.** (1997), On fractional derivatives, fractional-order systems and $PI^{\lambda}D^{\mu}$-controllers, *Proc. 36th IEEE Conf. on Decision and Control, San Diego*, 4985–4990.
11. **Riewe F.** (1997), Mechanics with fractional derivatives, *Physical Review*, E, Vol. 55, No. 3, 3581–3592.
12. **Romero M., Vinagre B. M., De Madrid Á. P. (**2008), GPC Control of a Fractional–Order Plant: Improving Stability and Robustness, *Proc. 17th IFAC World Congress, Seoul*, 14266–14271.
13. **Shantanu D.** (2008), *Functional fractional calculus for system identification and controls*, Springer Verlag, Berlin.
14. **Sierociuk D.** (2007), *Estimation and control of discrete fractional –order dynamic systems described in the state space (In Polish)*, PhD Thesis. Warsaw University of Technology, Warszawa.
15. **Sierociuk D., Dzieliński A.** (2006), Fractional Kalman filter algorithm for the states, parameters and order of fractional system estimation, *Int. J. Appl. Math. Comp. Sci.*, Vol. 16, No. 1, 129–140.
16. **Sjöberg M., Kari L.** (2002), Non-linear behavior of a rubber isolator system using fractional derivatives, *Vehicle Syst. Dynam*., Vol. 37, No. 3, 217–236.
17. **Suarez J. I., Vinagre B. M., Chen Y. Q.** (2003), Spatial path tracking of an autonomous industrial vehicle using fractional order controllers, *Proc. 11th Int. Conf. Advanced Robotics*, Coimbra, CD-ROM.
18. **Takagi T., Sugeno M.** (1985), Fuzzy identification of systems and its application to modeling and control, *IEEE Trans. Systems, Man, and Cybernetics*, 15, 116–132.
19. **Tatjewski P.** (2007), *Advanced control of industrial processes*, Structures and algorithms, Springer, London.
20. **Vinagre M., Feliu V.** (2002), Modeling and control of dynamic systems using fractional calculus: Application to electrochemical processes and flexible structures, *Proc. 41st IEEE Conf. Decision and Control*, Las Vegas, 214–239.
21. **Wnuk P.** (2004), *Identification algorithms for fuzzy models*, PhD Thesis, Warsaw University of Technology, Warszawa.
22. **Xue D., Chen Y.** (2002), A comparative introduction of four fractional order controllers, *Proc. 4th IEEE World Congress on Intelligent Control and Automation, Shanghai*, 3228–3235.
23. **Xue D., Zhao C., Chen Y.** (2006), A modified approximation method of fractional order system, *Proc. IEEE ICMA*, Luoyang, 1043–1048.
24. **Zamani M., Karimi-Ghartemani M., Sadati N.** (2007), FOPID controller design for robust performance using particle swarm optimization, Fractional Calculus & Applied Analysis, *Int. Journal for Theory and Applications*, Vol. 10, No. 2, 169–187.

THE INFLUENCE OF GEOMETRY OF THE SPECIMEN AND MATERIAL PROPERTIES ON THE Q-STRESS VALUE NEAR THE CRACK TIP FOR SEN(T) SPECIMEN

Marcin GRABA*

*Kielce University of Technology, Faculty of Mechatronics and Machine Design,
Chair of Fundamentals of Machine Design, Al. 1000-lecia PP 7, 25-314 Kielce, Poland

mgraba@tu.kielce.pl

Abstract: In the paper the short theoretical backgrounds about elastic-plastic fracture mechanics were presented and the O'Dowd-Shih theory was discussed. Using ADINA System program, the values of the Q-stress determined for various elastic-plastic materials for SEN(T) specimen – single edge notched plates in tension – were presented. The influence of kind of the specimen, crack length and material properties (work-hardening exponent and yield stress) on the Q-parameter were tested. The numerical results were approximated by the closed form formulas. Presented in the paper results are complementary of the two papers published in 2007 (Graba, 2007) and in 2010 (Graba, 2010), which show and describe influence of the material properties and crack length for the Q-stress value for SEN(B) and CC(T) specimens respectively. Presented and mentioned papers show such catalogue of the Q-stress value, which may be used in engineering analysis for calculation of the real fracture toughness.

1. INTRODUCTION TO ELASTIC-PLASTIC FRACTURE MECHANICS

In 1968 J. W. Hutchinson (ADINA 8.4.1, 2006a) published the fundamental paper, which characterized stress fields in front of a crack for non-linear Ramberg-Osgood (R-O) material in the form:

$$\sigma_{ij} = \sigma_0 \left(\frac{J}{\alpha \sigma_0 \varepsilon_0 I_n r} \right)^{\frac{1}{1+n}} \tilde{\sigma}_{ij}(\theta, n) \tag{1}$$

where r and θ are polar coordinates of the coordinate system located at the crack tip, σ_{ij} are the components of the stress tensor, J is the *J*-integral, n is R-O exponent, α is R-O constant, σ_0 is yield stress, ε_0 is strain related to σ_0 through $\varepsilon_0 = \sigma_0/E$. Functions $\tilde{\sigma}_{ij}(n,\theta)$, $I_n(n)$ must be found by solving the fourth order non-linear homogenous differential equation independently for plane stress and plane strain (Hutchinson, 1968). Equation (1) is commonly called the "HRR solution" (Fig. 1).

The HRR solution includes the first term of the infinite series only. The numerical analysis shown, that results obtained using the HRR solution are different from the results obtained using the finite element method (FEM) - see Fig. 2. To eliminate this difference, it's necessary to use more terms in the HRR solution.

In 1985 Li and et. (Li and Wang, 1985) proposed the another stress field description, which was used two terms in the Airy function. They obtained the second term of the asymptotic expansion for the two materials described by two different work-hardening exponent: n=3 and n=10. Next, they compared their results with the HRR fields and FEM results. Their analysis shown, that using the two term solution to describe the stress field near the crack tip, brings closer analytical results to FEM results. Two term solution much better describes the stress field near the crack tip, and the value of the second term, which may not to be negligible depends on the material properties and the geometry specimen.

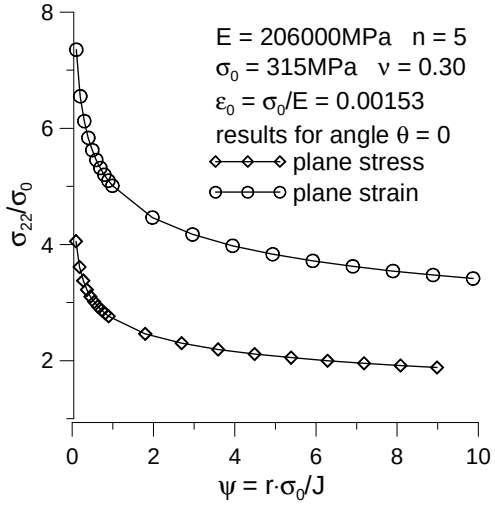

Fig. 1. The crack opening stress distribution for elastic-plastic materials, obtained using the HRR solution

In 1993 Yang and et. (Yang et al., 1993) using the Airy function with the separate variables in the infinite series form, proposed, that stress field near the crack tip may be described by the Eq. (2) in the infinite series form:

$$\frac{\sigma_{ij}}{\sigma_0} = \sum_{k=1}^{+\infty} A_k \bar{r}^{s_k} \tilde{\sigma}_{ij}^{(k)}(\theta) \tag{2}$$

where k is the number of the series terms, A_k is the amplitude for the k series term, $\bar{r}$ is the normalized distance from the crack tip, s_k is power exponent for the k series term, and $\tilde{\sigma}_{ij}^{(k)}$ is "stress" function.

Using only three terms of the infinite series, Eq. (2) may be written in the following form:

$$\frac{\sigma_{ij}}{\sigma_0} = A_1 \bar{r}^{\,s} \tilde{\sigma}_{ij}^{(1)}(\theta) + A_2 \bar{r}^{\,t} \tilde{\sigma}_{ij}^{(2)}(\theta) + \frac{A_2^2}{A_1} \bar{r}^{\,2t-s} \tilde{\sigma}_{ij}^{(3)}(\theta) \qquad (3)$$

where the $\tilde{\sigma}_{ij}^{(k)}$ functions must be found by solving the fourth order non-linear homogenous differential equation independently for plane stress and plane strain, s is the power exponent, which is identical to the one in the HRR solution (s may be calculated as s=-1/(n+1)), t is the power exponent for the second term of the asymptotic expansion, which must be found numerically by solving the fourth order non-linear homogenous differential equation independently for plane stress and plane strain, $\bar{r}$ is the normalized distance from the crack tip calculated as $\bar{r} = r/(J/\sigma_0)$, A_1 is the amplitude of the first term of the infinite series evaluated as $A_1 = (\alpha \varepsilon_0 I_n)^{-1/(n+1)}$, and A_2 is the amplitude of the second term, which is calculated by fitting the Eq. (3) to the numerical results of the stress fields close to crack tip.

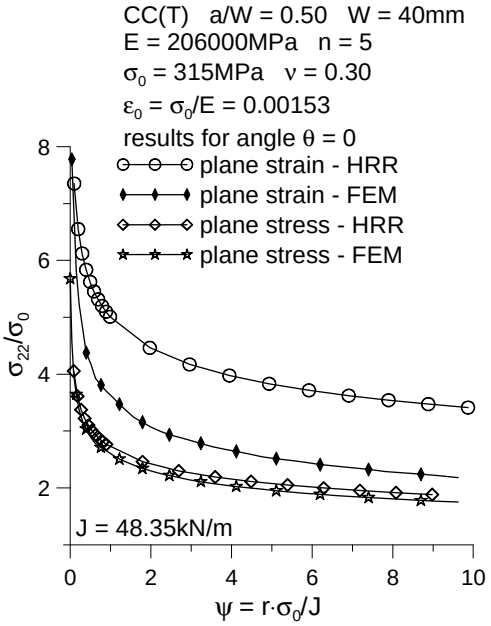

Fig. 2. Comparison the FEM results and HRR solution for plane stress and plane strain for center cracked plate in tension (CC(T))

In 1993 Shih et al. (1993) proposed simplified solution. They assumed, that the FEM results are exact and computed the difference between the numerical and HRR results. They proposed, that the stress field near the crack tip, may be described using only two terms, by following equation:

$$\frac{\sigma_{ij}}{\sigma_0} = \left(\frac{J}{\alpha \varepsilon_0 \sigma_0 I_n r} \right)^{1/(n+1)} \tilde{\sigma}_{ij}(\theta; n) + Q \left(\frac{r}{J/\sigma_0} \right)^{q} \hat{\sigma}_{ij}(\theta; n) \qquad (4)$$

where $\hat{\sigma}_{ij}(\theta, n)$ are functions evaluated numerically, q is the power exponent, which value changes in the range (0; 0.071), and Q is the parameter, which is the amplitude of the second term asymptotic solution. The Q-parameter is commonly called the "Q-stress".

O'Dowd and Shih (1991, 1992), tested the Q-parameter in the range J/σ_0<r<5J/σ_0 near the crack tip. They showed, that the Q-parameter weakly depend on crack tip distance in the range of the ±π/2 angle. O'Dowd and Shih proposed only two terms to describe the stress field near the crack tip:

$$\sigma_{ij} = (\sigma_{ij})_{HRR} + Q \sigma_0 \hat{\sigma}_{ij}(\theta) \qquad (5)$$

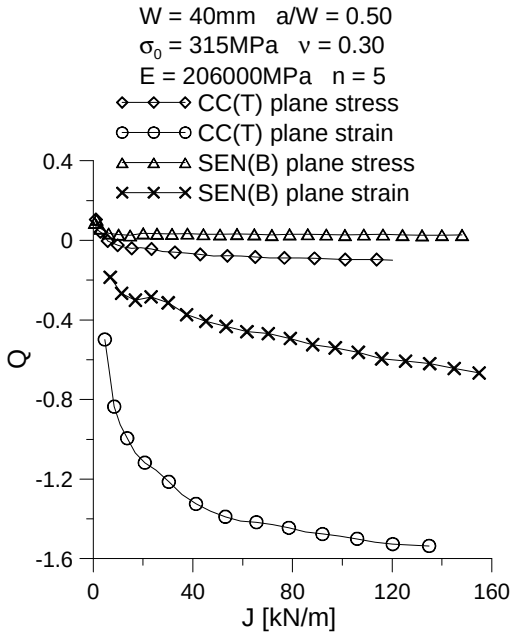

Fig. 3. The comparison of the J-Q trajectories for CC(T) and SEN(B)

To avoid the ambiguity during the calculation of the Q-stress, O'Dowd and Shih (O'Dowd, Shih, 1991), (O'Dowd, Shih, 1992) have suggested, where the Q-stress may be evaluated. It was assumed, that the Q-stress should be computed at distance from crack tip, which is equal to r=2J/σ_0 for θ=0 direction. O'Dowd and Shih postulated, that for θ=0 the function $\hat{\sigma}_{\theta\theta}(\theta = 0)$ is equal to 1. That's why, the Q-stress may be calculated from following relationship:

$$Q = \frac{(\sigma_{\theta\theta})_{FEM} - (\sigma_{\theta\theta})_{HRR}}{\sigma_0} \text{ for } \theta=0 \text{ and } \frac{r\sigma_0}{J} = 2 \qquad (6)$$

where $(\sigma_{\theta\theta})_{FEM}$ is the stress value calculated using FEM and $(\sigma_{\theta\theta})_{HRR}$ is stress value evaluated form HRR solution. During analysis, O'Dowd and Shih shown, that in the range of θ=±π/4, the following relationships take place: $Q\hat{\sigma}_{\theta\theta} \approx Q\hat{\sigma}_{rr}$, $\hat{\sigma}_{\theta\theta}/\hat{\sigma}_{rr} \approx 1$ and $Q\hat{\sigma}_{r\theta} \approx 0$ (because $Q\hat{\sigma}_{r\theta} << Q\hat{\sigma}_{\theta\theta}$). Thus, the Q-stress value determines the level of the hydrostatic stress. For plane stress, the Q-parameter is equal to zero, but for plane strain, the Q- parameter is in the most cases smaller than zero (Fig. 3).

2. DISCUSSION ABOUT ENGINEERING APPLICATIONS OF THE *J-Q* THEORY

To describe the stress field near the crack tip for elastic-plastic materials, the HRR solution is most often used (Eq. 1). However the results obtained are usually overesti-

mated and analysis is conservative. The HRR solution includes the first term of the infinite series only.

The numerical analysis shown, that results obtained using the HRR solution are different from the results obtained using the finite element method (FEM) – see Fig. 2. To eliminate this difference, it's necessary to use more terms in the HRR solution, for example the J-A_2 theory suggested by Yang and et. (Yang et al., 1993), or the O'Dowd and Shih approach – the J-Q theory (O'Dowd, and Shih, 1991).

For using the O'Dowd approach, engineer needs only the Q-stress distribution, which must be calculated numerically. That's why O'Dowd approach is easier and pleasanter in use in contrast to J-A_2 theory. Using the J-A_2 theory proposed by Yang and el., first engineer must solve fourth order nonlinear differential equation to determine the $\tilde{\sigma}_{ij}^{(k)}$ function and the t power exponent. Next, the engineer using FEM results calculated the A_2 amplitude by fitting the Eq. 3 to numerical results.

The J-Q theory found application in European Engineering Programs, like SINTAP (Sintap, 1999) or FITNET (Fitnet, 2006). The Q-stress are applied under construction the fracture criterion and to assessment the fracture toughness of the structural component. Thus O'Dowd theory has practical application in engineering issues.

Sometimes using the J-Q theory may be limited, because there is no value of the Q-stress for given material and specimen. Using any fracture criterion, for example proposed by O'Dowd (O'Dowd, 1995), or another criterion, the engineer can estimate fracture toughness quit a fast, if the Q-stress are known. Literature doesn't announce the Q-stress catalogue and Q-stress value as function of external load, material properties or geometry of the specimen. In some articles, the engineer may find the J-Q graphs for certain group of material.

The best solution will be, origin the catalogue of the J-Q graphs for materials characterized by various yield strength, different work-hardening exponent. Such catalogue should take into consideration the influence of the external load, kind of the specimen (SEN(B) specimen – bending, SEN(T) specimen – tension) and geometry of the specimen, too. For SEN(B) and CC(T) specimens, such catalogues were presented by Graba in 2007 (Graba, 2007) and in and 2010 (Graba, 2010) respectively.

In the next parts of the paper, the values of the Q-stress will be determined for various elastic-plastic materials for single edge notched specimens in tension (SEN(T)). The SEN(T) specimen is the basic structural element, which is used in the FITNET procedures to modeling real constructions. All results will be approximated by the closed form formulas.

3. DETAILS OF NUMERICAL ANALYSIS

In the numerical analysis, the single edge notched specimens in tension (SEN(T)) were used (Fig. 4). Dimensions of the specimens satisfy the standard requirement which is set up in FEM calculation - $L \geq 2W$, where W is the width of the specimen and L is the measuring length of the specimen. Computations were performed for plane strain using small strain option. The relative crack length was equal to a/W={0.20, 0.50, 0.70} where a is a crack length and the width of specimens W was equal to 40mm. For this case, the measuring length L satisfied the condition $L \geq 80$mm.

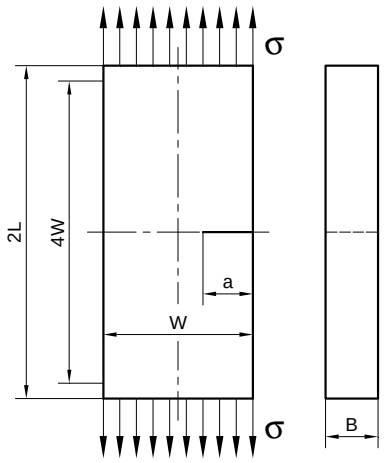

Fig. 4. The single edge notched specimen in tension (SEN(T)) used in the numerical analysis

The choice of the SEN(T) specimen was intentional, because the SEN(T) specimens are used in the FITNET procedures to modeling real structural elements. Also in FITNET procedures, the limit load and stress intensity factors solutions for SEN(T) specimens are presented. However in the EPRI procedures (Kumar et al., 1981), the hybrid method for calculation the J-integral is given. Also some laboratory test in order to determine the critical values of the J-integral, may be done using the SEN(T) specimen.

Computations were performed using ADINA SYSTEM 8.4 (Adina, 2006a, b). Due to the symmetry, only a half of the specimen was modeled. The finite element mesh was filled with the 9-node plane strain elements with nine (3×3) Gauss integration points. The size of the finite elements in the radial direction was decreasing towards the crack tip, while in the angular direction the size of each element was kept constant. The crack tip region was modeled using 50 semicircles. The first of them, was at least 20 times smaller then the last one. It also means, that the first finite element behind to crack tip is smaller 2000 times than the width of the specimen. The crack tip was modeled as quarter of the arc which radius was equal to $r_w=1\cdot10^{-6}$m (it's $(0.000025\times W)$. The whole SEN(T) specimen was modeled using 323 finite elements and 1353 nodes. External load was applied to bottom edge of the specimen. The example finite element model for SEN(T) specimen used in the numerical analysis is presented on Fig. 5.

In the FEM simulation, the deformation theory of plasticity and the von Misses yield criterion were adopted. In the model the stress–strain curve was approximated by the relation:

$$\frac{\varepsilon}{\varepsilon_0} = \begin{cases} \sigma/\sigma_0 & \text{for } \sigma \leq \sigma_0 \\ \alpha(\sigma/\sigma_0)^n & \text{for } \sigma > \sigma_0 \end{cases} \tag{7}$$

where α=1. The tensile properties for the materials which were used in the numerical analysis are presented below

in the Tab.1. In the FEM analysis, calculations were done for sixteen materials, which were differed by yield stress and the work hardening exponent.

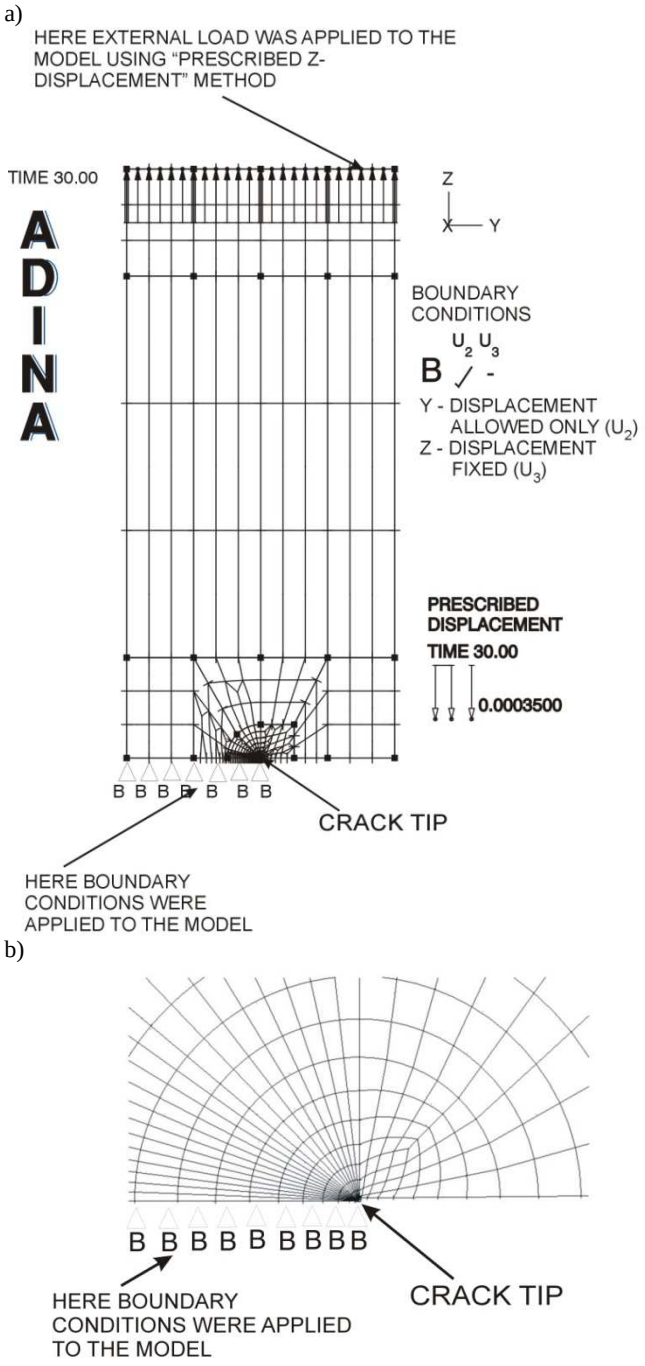

Fig. 5. a) The finite element model for SEN(T) specimen used in the numerical analysis; b) The finite elements mesh near crack tip using in the numerical analysis

Tab. 1. The mechanical properties of the materials used in numerical analysis and the HRR parameters for plane strain

σ_0 [MPa]	E [MPa]	ν	$\varepsilon_0=\sigma_0/E$	α	n	$\tilde{\sigma}_{\theta\theta}(\theta=0)$	I_n
315	206000	0.3	0.00153	1	3	1.94	5.51
500			0.00243		5	2.22	5.02
1000			0.00485		10	2.50	4.54
1500			0.00728		20	2.68	4.21

The J-integral were calculated using two methods. The first method, called the "virtual shift method", uses concept of the virtual crack growth to compute the virtual energy change. The second method is based on the J–integral definition:

$$J=\int_C \left[w dx_2 - \boldsymbol{t}(\partial \boldsymbol{u}/\partial x_1) ds\right] \tag{8}$$

where w is the strain energy density, $\boldsymbol{t}$ is the stress vector acting on the contour C drawn around the crack tip, $\boldsymbol{u}$ denotes displacement vector and ds is the infinitesimal segment of contour C.

In summary, in the numerical analysis 48 SEN(T) specimens were used, which were differed by crack length and material properties.

4. ANALYSIS OF THE NUMERICAL RESULTS

The analysis of the results obtained was made in the range $J/\sigma_0<r<6J/\sigma_0$ near the crack tip, and its shown, that the Q-stress decrease if the distance from the crack tip increase (Fig. 6). If the external load increases, the Q-stress decreases and the difference between Q-stress calculated in the following measurement points increase (Fig. 6). If the crack length decrease then Q-stress reaches more negative value for the same J-integral level (Fig. 7).

For the sake of the fact, that the Q-parameter, which is used in fracture criterion is calculated at distance equal to $r=2J/\sigma_0$, it's necessary to notice some comments about obtained results. If the yield stress increases, the Q-parameter increase too, and it reflects for all SEN(T) specimen with different crack length a/W (Fig. 8). For smaller yield stress the J-Q trajectories shape up well lower and it's observed faster changes of the Q-parameter if the external load is increase (Fig. 8).

For SEN(T) specimens, the ambiguous behavior of the J-Q trajectories depending of the work-hardening exponent is observed. For specimens with short cracks (a/W=0.20) and the same yield stress, for smaller values of the work-hardening exponent n (e.g. $n\leq5$), the Q-stress become less negative (Fig. 9). For specimens with the normative crack length (a/W=0.50) or with the long cracks (a/W=0.70), the cutting of the J-Q trajectories was observed (Fig. 10 and Fig. 11) - first the higher values of the Q-stress were observed for specimen characterized by strongly hardening material, but for increasing external load the reversal of the trend took place and the higher Q-stress were observed for specimens characterized by weakly hardening material.

For short cracks the Q-stress value drops more rapidly then for long ones in the range of the small external load (Fig. 7). For specimen with long cracks (a/W=0.70), the another nature of the J-Q trajectories was observed than for specimen with relative cracks length $a/W\leq0.50$ (Fig. 7). It may be a consequence of the absence in the analysis of the stress field, the consideration of the bending stress near the crack tip, which was discussed by Chao et al., (2004).

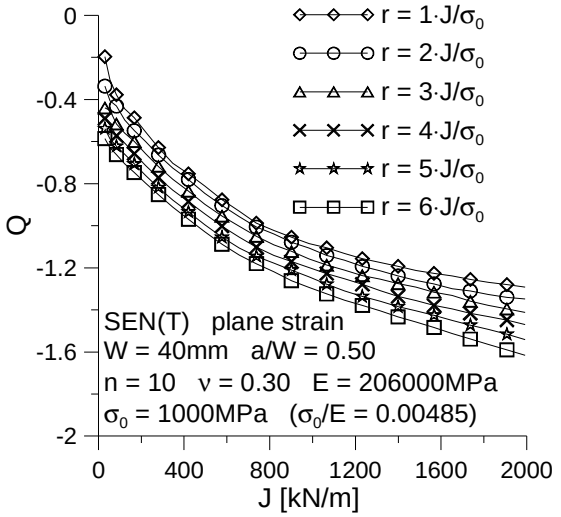

Fig. 6. "The *J-Q* family curves" for SEN(T) specimen calculated at six distances *r* from crack tip

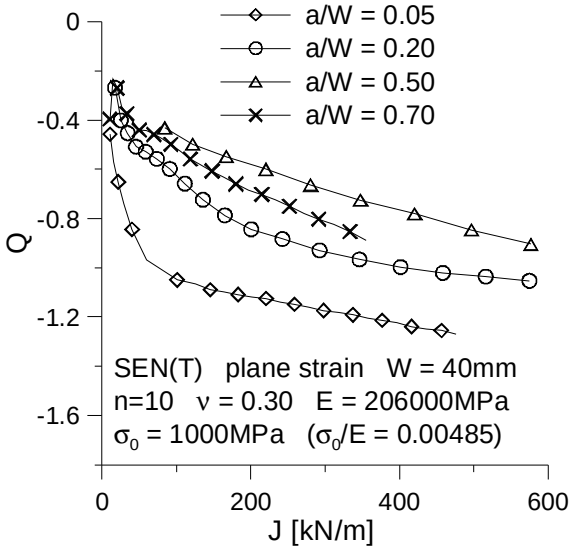

Fig. 7. The influence of the crack length on *J-Q* trajectories for SEN(T) specimens

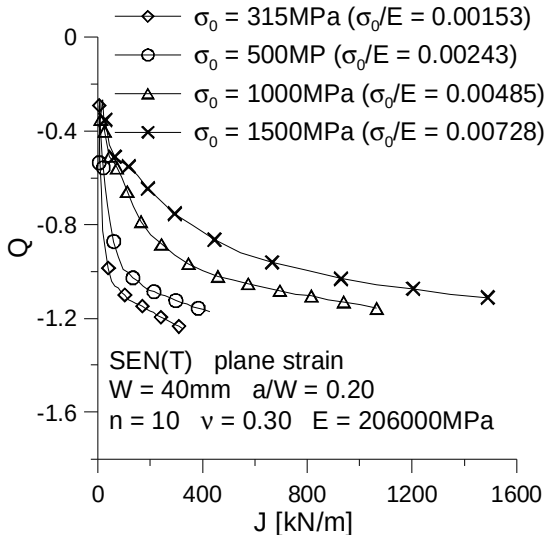

Fig. 8. The influence of the yield stress on *J-Q* trajectories for SEN(T)

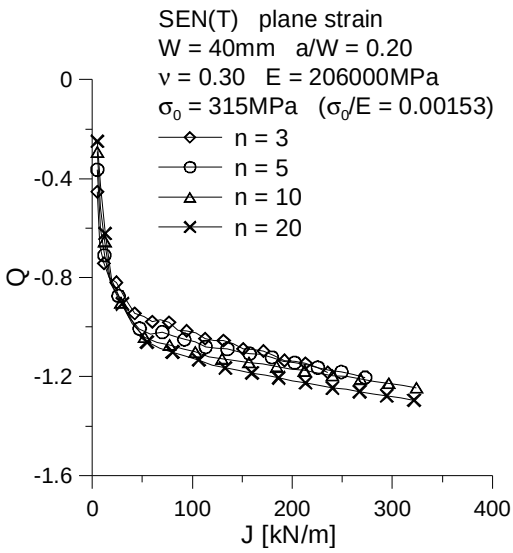

Fig. 9. The influence of the work hardening exponent on *J-Q* trajectories for SEN(T) specimens (a/W=0.20, σ_0=315MPa)

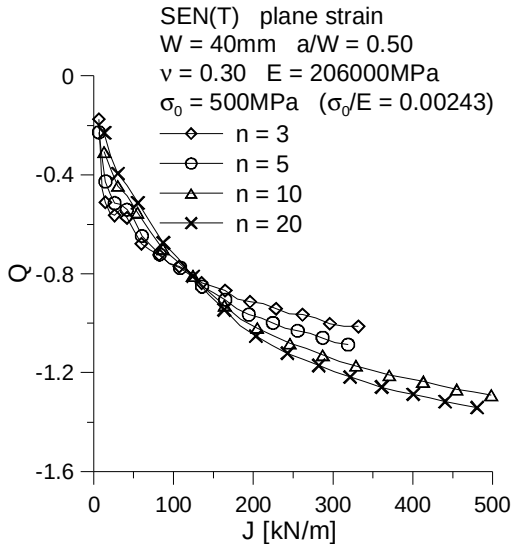

Fig. 10. The influence of the work hardening exponent on *J-Q* trajectories for SEN(T) specimens (a/W=0.50, σ_0=500MPa)

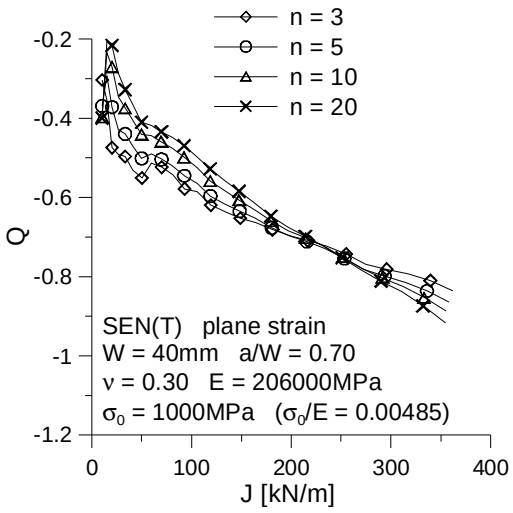

Fig. 11. The influence of the work hardening exponent on *J-Q* trajectories for SEN(T) specimens (a/W=0.70, σ_0=1000MPa)

5. APPROXIMATION OF THE NUMERICAL RESULTS

In the literature the mathematic formulas, to calculate the *Q*-stress taking into consideration the level of external load, material properties and geometry of the specimen are not known for the most of the cases. Presented in the paper numerical computations provided with the *J-Q* catalogue and the universal formula (9), which allows to calculate the *Q*-stress and take into consideration all the parameters influencing the value of the *Q*-stress. All results, were presented in the Q=f(log($J/(a\cdot\sigma_0)$)) graph forms. Next all graphs were approximated by the simple mathematical formulas, taking the material properties, external load and geometry specimen into consideration. All the approximations were made for results obtained at the distance $r=2.0\cdot J/\sigma_0$. Each of the obtained trajectories Q=f(log($J/(a\cdot\sigma_0)$)), was approximated by the third order polynomial in the form:

$$Q(J,a,\sigma_0)=A+B\cdot\left(\log\left(\frac{J}{(a\cdot\sigma_0)}\right)\right)+ +C\cdot\left(\log\left(\frac{J}{(a\cdot\sigma_0)}\right)\right)^2+D\cdot\left(\log\frac{J}{(a\cdot\sigma_0)}\right)^3 \quad (9)$$

where the *A*, *B*, *C*, *D* coefficients depend on the work-hardening exponent *n*, yield stress σ_0 and crack length *a*/*W*. The rank of the fitting the formula (9) to numerical results for the worst case was equal R^2=0.95. For different work hardening exponents *n*, yield stresses σ_0 and ratios *a*/*W*, which were not include in the numerical analysis, the coefficients *A*, *B*, *C* and *D* may be evaluated using the linear or quadratic approximation. Results of the approximation (all coefficients of the approximation numerical results by Eq. (9)) are presented in Tables 2-4.

Tab. 2. The coefficients of equation (9) for SEN(T) specimen with the crack length *a*/*W*=0.20

σ_0 = 315MPa			σ_0/E = 0.00153		
n	*A*	*B*	*C*	*D*	R^2
3	-2.476	-2.221	-1.165	-0.228	0.993
5	-2.128	-1.722	-0.999	-0.223	0.997
10	-1.752	-0.991	-0.604	-0.163	0.998
20	-1.677	-0.683	-0.379	-0.121	0.997
σ_0 = 500MPa			σ_0/E = 0.00243		
n	*A*	*B*	*C*	*D*	R^2
3	-1.618	-0.876	-0.397	-0.087	0.986
5	-1.105	0.104	0.119	-0.008	0.996
10	-1.365	-0.139	0.029	-0.026	0.996
20	-1.465	-0.145	0.075	-0.017	0.996
σ_0 = 1000MPa			σ_0/E = 0.00485		
n	*A*	*B*	*C*	*D*	R^2
3	-1.875	-1.438	-0.651	-0.119	0.958
5	-1.198	0.007	0.217	0.037	0.990
10	-1.065	0.552	0.622	0.116	0.995
20	-1.163	0.533	0.654	0.122	0.996
σ_0 = 1500MPa			σ_0/E = 0.00728		
n	*A*	*B*	*C*	*D*	R^2
3	-1.601	-1.099	-0.477	-0.089	0.982
5	-1.469	-0.537	-0.056	-0.002	0.990
10	-1.401	-0.078	0.328	0.080	0.996
20	-1.486	-0.085	0.364	0.088	0.996

Tab. 3. The coefficients of equation (9) for SEN(T) specimen with the crack length *a*/*W*=0.50

σ_0 = 315MPa			σ_0/E = 0.00153		
n	*A*	*B*	*C*	*D*	R^2
3	-2.743	-1.606	-0.456	-0.059	0.990
5	-2.909	-1.516	-0.334	-0.038	0.990
10	-0.621	1.913	1.291	0.205	0.996
20	0.238	3.364	2.03142	0.320	0.996
σ_0 = 500MPa			σ_0/E = 0.00243		
n	*A*	*B*	*C*	*D*	R^2
3	-3.927	-3.615	-1.435	-0.209	0.982
5	-3.383	-2.414	-0.728	-0.088	0.995
10	-2.009	-0.132	0.435	0.094	0.997
20	-1.810	0.450	0.811	0.160	0.997
σ_0 = 1000MPa			σ_0/E = 0.00485		
n	*A*	*B*	*C*	*D*	R^2
3	-4.009	-4.031	-1.629	-0.229	0.977
5	-2.662	-1.869	-0.545	-0.059	0.997
10	-2.773	-1.760	-0.403	-0.032	0.996
20	-2.971	-1.789	-0.312	-0.006	0.997
σ_0 = 1500MPa			σ_0/E = 0.00728		
n	*A*	*B*	*C*	*D*	R^2
3	-2.612	-2.335	-0.943	-0.138	0.994
5	-2.505	-1.895	-0.629	-0.078	0.999
10	-2.559	-1.688	-0.420	-0.035	0.996
20	-2.357	-1.041	0.048	0.059	0.997

Fig. 12 presents the comparison of the numerical results and their approximation for *J-Q* trajectories for several cases of the SEN(T) specimens. Fig.s 13-15 presents in the graphical form some numerical results obtained for SEN(T) specimens in plain strain. All results are presented using the *J-Q* trajectories.

Tab. 4. The coefficients of equation (9) for SEN(T) specimen with the crack length *a*/*W*=0.70

σ_0 = 315MPa			σ_0/E = 0.00153		
n	*A*	*B*	*C*	*D*	R^2
3	-6.051	-4.762	-1.512	-0.179	0.989
5	-3.287	-0.872	0.171	0.049	0.991
10	0.290	3.710	2.045	0.294	0.993
20	4.424	8.931	4.175	0.574	0.993
σ_0 = 500MPa			σ_0/E = 0.00243		
n	*A*	*B*	*C*	*D*	R^2
3	-8.575	-8.072	-2.818	-0.341	0.989
5	-10.470	-9.908	-3.417	-0.410	0.997
10	-11.036	-9.958	-3.227	-0.365	0.998
20	-0.753	2.846	1.979	0.325	0.993
σ_0 = 1000MPa			σ_0/E = 0.00485		
n	*A*	*B*	*C*	*D*	R^2
3	-6.703	-6.471	-2.323	-0.286	0.985
5	-7.237	-6.937	-2.456	-0.301	0.996
10	-7.642	-7.198	-2.481	-0.297	0.998
20	-8.527	-8.058	-2.747	-0.325	0.997
σ_0 = 1500MPa			σ_0/E = 0.00728		
n	*A*	*B*	*C*	*D*	R^2
3	-5.580	-5.462	-2.021	-0.256	0.976
5	-5.819	-5.576	-2.011	-0.250	0.995
10	-5.990	-5.608	-1.961	-0.238	0.998
20	-7.453	-7.315	-2.617	-0.322	0.999

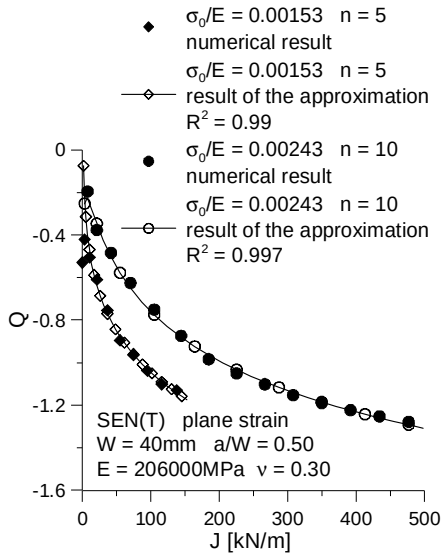

Fig. 12. Comparison of the numerical results and their approximation for *J*-*Q* trajectories for SEN(T) specimens with relative crack length a/W=0.50: σ_0={315, 500}MPa, n={5, 10}

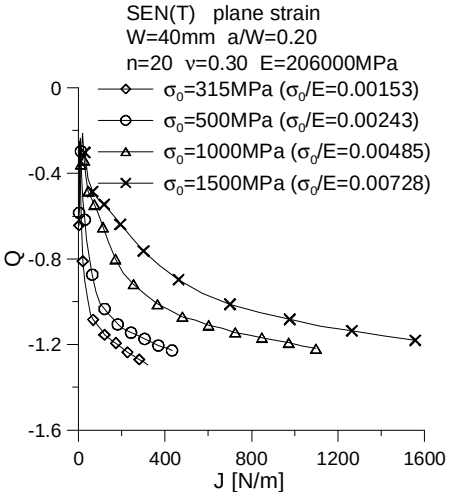

Fig. 13. Sample numerical results obtained for SEN(T) specimens: the influence of the yield stress on *J*-*Q* trajectories for specimens with crack length a/W=0.20 and for power exponents n=20

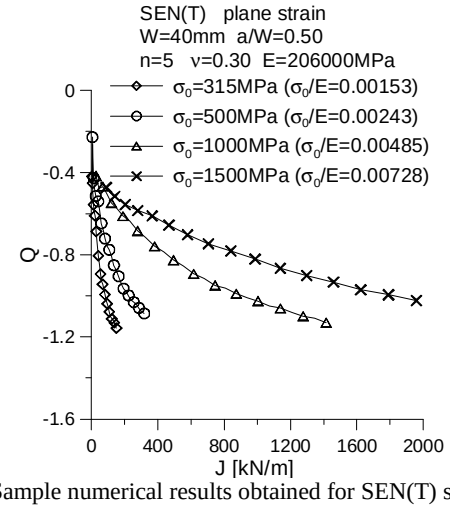

Fig. 14. Sample numerical results obtained for SEN(T) specimens: the influence of the yield stress on *J*-*Q* trajectories for specimens with crack length a/W=0.50 and for power exponents n=5

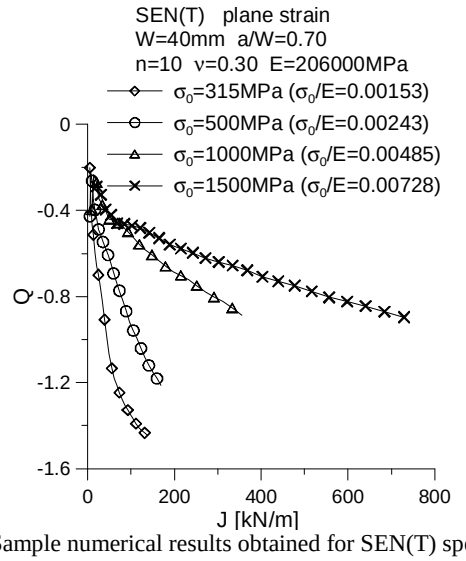

Fig. 15. Sample numerical results obtained for SEN(T) specimens: the influence of the yield stress on *J*-*Q* trajectories for specimens with crack length a/W=0.70 and for power exponents n=10

6. SUMMARY

In the paper the values of the Q-stress were determined for various elastic-plastic materials for single edge notched specimens in tension (SEN(T)). The influence of the yield strength, the work-hardening exponent and the crack length on the *Q*-parameter was tested. The numerical results were approximated by the closed form formulas. The most important results are summarized as follows:

- the *Q*-stress depends on geometry and external the load; different values of the *Q*-stress are obtained for center cracked plane in tension (CC(T)) and different for the SEN(T) specimen, which are characterized by the same material properties;
- the *Q*-parameter is a function of the material properties; its value depends on the work-hardening exponent n and the yield stress σ_0;
- if the crack length decrease then *Q*-stress reaches more negative value for the external load.

REFERENCES

1. **ADINA 8.4.1** (2006a), ADINA: User Interface Command Reference Manual - Volume I: ADINA Solids & Structures Model Definition, *Report ARD 06-2*, ADINA R&D, Inc.
2. **ADINA 8.4.1** (2006b), ADINA: Theory and Modeling Guide - Volume I: ADINA, *Report ARD 06-7*, ADINA R&D, Inc.
3. **FITNET** (2006), FITNET Report, (European Fitness-for-service Network), Edited by M. Kocak, S. Webster, J. J. Janosch, R. A.Ainsworth, R.Koers, *Contract No. G1RT-CT-2001-05071*.
4. **Graba M**. (2007)**,** Wpływ stałych materiałowych na rozkład naprężeń Q przed wierzchołkiem pęknięcia w materiałach sprężysto - plastycznych, *IV MSMZMiK - Augustów 2007*, materiały konferencyjne, 109-114;
5. **Graba M**. (2010)**,** Wpływ stałych materiałowych na rozkład naprężeń *Q* przed wierzchołkiem pęknięcia w materiałach sprężysto-plastycznych dla płyty z centralną szczeliną poddanej rozciąganiu, *Acta Mechanica et Automatica*, Vol. 4, No. 2, 54-62.

6. **Hutchinson J. W.** (1968), Singular Behaviour at the End of a Tensile Crack in a Hardening Material, *Journal of the Mechanics and Physics of Solids*, 16, 13-31.
7. **Kumar V., German M. D., Shih C. F.** (1981), An Engineering Approach for Elastic-Plastic Fracture Analysis, *EPRI Report* NP-1931, Electric Power Research Institute, Palo Alto, CA., 1981.
8. **Li Y., Wang Z.** (1985), High-Order Asymptotic Field of Tensile Plane-Strain Nonlinear Crack Problems, *Scientia Sinica (Series A)*, Vol. XXIX, No. 9, 941-955.
9. **O'Dowd N. P.** (1995), Applications of two parameter approaches in elastic-plastic fracture mechanics, *Engineering Fracture Mechanics*, Vol. 52, No. 3, 445-465.
10. **O'Dowd N. P., Shih C. F.** (1991), Family of Crack-Tip Fields Characterized by a Triaxiality Parameter – I. Structure of Fields, *J. Mech. Phys. Solids*, Vol. 39, No. 8, -1015.
11. **O'Dowd N. P., Shih C. F.** (1992), Family of Crack-Tip Fields Characterized by a Triaxiality Parameter – II. Fracture Applications, J. *Mech. Phys. Solids*, Vol. 40, No. 5, 939-963.
12. **Shih C. F., O'Dowd N. P., Kirk M. T.** (1993), A Framework for Quantifying Crack Tip Constraint, *Constraint Effects in Fracture*, ASTM STP 1171, E.M. Hackett, K,-H. Schwalbe, R. H. Dodds, Eds., American Society for Testing and Materials, Philadelphia, 2-20.
13. **SINTAP** (1999), SINTAP: Structural Integrity Assessment Procedures for European Industry. Final Procedure, *Brite-Euram Project No BE95-1426* – Rotherham: British Steel.
14. **Yang S., Chao Y. J., Sutton M. A.** (1993), Higher Order Asymptotic Crack Tip in a Powe –Law Hadening Material, *Engineering Fracture Mechanics*, Vol. 45, No. 1, 99. 1 – 20.
15. **Chao Y. J., Zhu X. K., Kim Y., Lar P. S., Pechersky M. J., Morgan M. J.** (2004), Characterization of Crack-Tip Field and Constraint for Bending Specimens under Large-Scale Yielding, *International Journal of Fracture*, 127, 2004, 283-302.

Acknowledgments: The support of the Faculty of Mechatronics and Machine Design at Kielce University of Technology through scientific projects **No. 1.22/8.57 and No. 1.22/7.14** is acknowledged by the author.

Author of the paper, were involved in apprenticeship scholarships for young doctors (PhD) in the project "Capacity Development Program Educational Kielce University of Technology: training in advanced areas of technology," co-financed by the European Social Fund under the Human Capital Operational Programme, Priority IV, Activity 4.1, Sub-activity 4.1.1, no contract UDA-POKL.04.01.01-00-395/09-00; running time: 15 February 2010 - 31 December 2010.

PARTITION OF HEAT IN 2D FINITE ELEMENT MODEL OF A DISC BRAKE

Piotr GRZEŚ*

*Phd student, Katedra Mechaniki i Informatyki Stosowanej, Wydział Mechaniczny, Politechnika Białostocka, ul. Wiejska 45 C, 15-351 Białystok

p.grzes@doktoranci.pb.edu.pl

Abstract: In this paper nine of formulas (theoretical and experimental) for the heat partition ratio were employed to study the temperature distributions of two different geometrical types of the solid disc brake during emergency brake application. A two-dimensional finite element analysis incorporating specific values of the heat partition ratios was carried out. The boundary heat flux uniformly distributed over the circumference of a rubbing path to simulate the heat generated at the pad/disc interface was applied to the model. A number of factors over the heat partition ratio that affects the temperature fields are included and their importance is discussed.

1. INTRODUCTION

Frictional heating problem is an important issue during operation of the brake system. When the sliding mutual process occurs the mechanical energy is converted into thermal energy, chemical bonding energy and phase transition energy at the interface of two mating bodies. Nonetheless thermal energy is prevalent. Thus it is essential to develop critical temperature above which various undesirable effects such as softening or sintering of materials, premature wear, friction coefficient fluctuations or breakdown of the system may take place (Olesiak et al., 1997; Yi et al., 2002).

Various techniques have been so far developed for the calculation of maximum temperatures in sliding systems. Analytical methods for solution of thermal problem of friction during braking are limited to the contact of two semi-spaces or the plane-parallel strip and semi-space (Chichinadze et al., 1979; Balakin 1999; Grylytskyy, 1996; Yevtushenko and Kuciej, 2010). More accurate for the finite object, transform techniques have been used, but numerous mathematical difficulties implies simplifications in geometry. The finite element method among numerical techniques is held as one of the most suitable for thermal problem investigation. Review of FEM-solutions of thermal problems of friction during braking are given in article of Yevtushenko and Grześ (2010).

The calculation of temperature during braking requires appropriate model where sufficient number of variables are included to obtain reliable outcomes. One of the input parameters for FEM-calculations of temperature in pad/disc brake system is the heat partition ratio (Pereverzeva and Balakin, 1992; Evtushenko et al., 2000). The separation of heat between two sliding bodies depends primarily on the relative velocity, the thermophysical properties of materials, the interface contact length, the amount of wear debris (third body) whose magnitude varies during the process. The settlement of the heat partition at the interface of two sliding bodies within the years was somewhat complex and remains in fact unsolved.

The problem of the heat partition in a three-dimensional FE model of a pad/disc brake system subjected to non-axisymmetric thermal load was studied in article of Yevtushenko and Grześ (2011).

In this paper the finite element analysis of frictional heating problem in an axisymmetric arrangement of the disc brake model to assess the impact of separation of total heat generated between members of sliding system was carried out. Irresistible advantages of this numerical technique approach were reported within the past years. Nevertheless several disadvantages, namely partition of heat during frictional heating process became apparent. This study aims to compare the temperatures obtained with the use of nine various formulas, both experimental and theoretical for the heat partition ratio. The comparison of outcomes of the thermal finite element analysis with experimental data of two different circumstances of braking action (Nosko et al, 2009; Zhu et al., 2009) dimensions and properties of materials was accomplished as well.

2. FRICTION HEAT DISTRIBUTION BETWEEN A PAD AND A DISC

The thermal energy is generated at the interface as the heat fluxes with the specified intensity, and at the same time is divided into contact surfaces of two bodies. In order to analyze thermal processes, the heat partition ratio denoted γ is employed, e.g. if the heat flux with the intensity of $q_1 = \gamma q$ enters into body "1", the intensity of heat flux entered into body "2" equals $q_2 = (1 - \gamma)q$. Noticeably $q = q_1 + q_2$, where the power of friction equals $q = fVp$, and f denotes the coefficient of friction, V is the relative velocity of sliding bodies, p is the contact pressure. The heat partition ratio term was introduced in 1937 by Blok (1937), who considered sliding of single roughness with square (a x a) or circular (with radius a) shape and the lateral surface of cylinder (narrow layer of contact zone) along surface of semi-space. The dimensions of contact area in comparison to whole dimen-

sions of contacting bodies were insignificant, because the semi-space was considered. It was assumed that the heat generation takes place directly on contact surface, and heat expansion process is unidirectional perpendicular to contact surface. The intensity of heat flux was constant with time and independent of spatial distribution, according to the same law as the contact pressure. Dividing virtually contacting bodies, two problems of frictional heating are obtained, namely: with the surface of semi-space heating with the intensity of q_1 (for roughness), and with the local surface of semi-space heating where the intensity of heat flux q_2 is moving. The magnitude of heat partition ratio for low sliding velocities ($V \le 8k_2/25a$ or $Pe \le 0.32$) Blok specifies as follows

$$\gamma = \frac{K_1}{K_1 + K_2}, \tag{1}$$

where: K – thermal conductivity, subscripts 1 and 2 indicate the first and the second body, respectively.

It was concluded, that for high sliding velocities ($V > 8k_2/a$ or Pe > 8) of the roughness, the maximum temperature on the friction surface, according to the rod model, is obtained near the edge of the roughness, opposite to sliding direction. In the case of lateral surface of cylinder sliding over the plane surface of semi-space Blok defines high velocity as $V > 40k_2/a$ (Pe ≥ 40). In order to find the coefficient γ, Blok equates the maximum temperatures on the contact area of roughness and semi-space. As a result, the following formula for the heat partition ratio is obtained:

$$\gamma = \frac{K_1}{K_1 + K_2\sqrt{\pi Pe/16}} \cong \frac{K_1}{K_1 + 0.44K_2\sqrt{Pe}} \tag{2}$$

where: Pe – Peclet number.

The cases of sliding with constant velocity of semi-infinite rod of rectangular or quadrate profile over the surface of semi-space were considered by Jaeger (1942). Unlike to Blok, Jaeger, defining γ, compared the mean temperatures on the contact surface. In case of the rod of quadrate cross-section (a x a) with a thermally insulated lateral surface, and one tip sliding with constant high speed (Pe > 20) over the surface of semi-space, Jaeger obtained the following formula to calculate heat partition ratio

$$\gamma = \frac{1.25K_1}{1.25K_1 + K_2\sqrt{Pe/2}} \cong \frac{K_1}{K_1 + 0.56K_2\sqrt{Pe}} \tag{3}$$

From formula (3) it results that an increase in sliding velocity (the Peclet number Pe) evokes decrease of γ and, consequently, the amount of heat which heats the rod. Jaeger explains this fact by two sources of heating the semi-space: heat generated as a result of friction, and heat previously heating layers of the rod. At the same time, the tip of the rod is heated only by frictional heating, and cooled by forthcoming "cooler" areas of semi-spaces. The higher speed of sliding there is, the more amount of heat absorbed by the semi-space.

Jaeger also improves formula (3) for the case of convectional heat transfer with constant heat transfer coefficient h between lateral surface of rod and ambient environment:

$$\gamma = \frac{\sqrt{K_1}}{\sqrt{K_1} + 0.67K_2\sqrt{Pe/Bi}} \tag{4}$$

where: Bi – Biot number.

From the formula (4) it may be concluded that the increase of heat transfer coefficient h leads to an increase of the amount of heat directed into the rod.

One of typically used formulas to calculate the heat partition ratio in braking systems is the Charron's formula (1943)

$$\gamma = \frac{\sqrt{K_1\rho_1 c_1}}{\sqrt{K_1\rho_1 c_1} + \sqrt{K_2\rho_2 c_2}}, \tag{5}$$

where: ρ – density, c – specific heat capacity,

The Charron's formula (5), which is recommended to use for calculating the temperature of clutches and brakes, when the coefficient of mutual overlap η equals approximately to one.

$$\eta = \frac{\theta_0}{2\pi}, \tag{6}$$

where: θ_0 – cover angle of pad. If $\eta << 1$, then correction of Charron's formula has the form (Newcomb, 1958-59)

$$\gamma = \frac{\eta K_1\sqrt{k_2}}{\eta K_1\sqrt{k_2} + K_2\sqrt{k_1}} = \frac{\eta}{\eta + \varepsilon}. \tag{7}$$

In order to comply real thickness of the friction pair d_i, which cumulate the heat generated during friction, the following formula for determination of the heat partition ratio was proposed by Hasselgruber (1963):

$$\gamma = \frac{d_1 c_1\sqrt{k_1}}{d_1 c_1\sqrt{k_1} + d_2 c_2\sqrt{k_2}},\ d_i \le \delta_i,\ i = 1,2, \tag{8}$$

where the efficient depth of heating δ (the distance at which the temperature is equal 5% of the maximum temperature on the contact surface) equals (Chichinadze et al., 1964):

$$\delta_i = 1.73\sqrt{k_i t_s},\ i = 1,2 \tag{9}$$

If the thicknesses d_i of the braking elements are greater then thicknesses of thermal layers δ_i (9), then it is necessary to replace d_i on δ_i, i = 1, 2 in the formula (8). Consequently, substituting the thicknesses δ_i (9) into the formula (8), we obtain

$$\gamma = \frac{c_1 k_1}{c_1 k_1 + c_2 k_2},\ \delta_i > d_i,\ i = 1,2. \tag{10}$$

Transformation of formula (8) to comply effective saturated heat of bodies volume V_i, was made by Chichinadze et al. (1979):

$$\gamma = \frac{V_1 c_1\sqrt{k_1}}{V_1 c_1\sqrt{k_1} + V_2 c_2\sqrt{k_2}},\ d_i \le \delta_i,\ i = 1,2, \tag{11}$$

where $V_i = S_i d_i$, S_i – nominal contact area of body $i = 1, 2$. If $\delta_i > d_i$, then replacing in the formula (11) d_i on δ_i (8), we find

$$\gamma = \frac{\eta c_1 k_1}{\eta c_1 k_1 + c_2 k_2},\ \delta_i > d_i,\ i = 1,2, \tag{12}$$

where the coefficient of mutual overlap η was defined by the formula (6).

The frictional heat generation in the pad/disc tribosystem, using the solution of thermal problem of friction for two layers with thickness d_i, $i = 1, 2$ on the assumption that $q_i = const.$, $i = 1, 2$ and the external surfaces are insulated was studied in article (Ginzburg, 1973). From the condition of equality of temperatures on a surface of contact the time-dependent formula for calculation of the heat partition ratio is obtained:

$$\gamma(t) = \frac{\eta K_1 d_2 \theta(\tau_2)}{\eta K_1 d_2 \theta(\tau_2) + K_2 d_1 \theta(\tau_1)},\ 0 \le t \le t_s, \tag{13}$$

where

$$\theta(\tau_i) = \frac{1}{3} + \tau_i + 2\sum_{n=1}^{\infty} (-1)^{n+1} \frac{\cos(\pi n)}{(\pi n)^2} \exp[-(\pi n)^2 \tau_i]$$
$$\tau_i = \frac{k_i t}{d_i}, d_i \le \delta_i, i = 1,2 \tag{14}$$

If $\tau_i > 0.3$, then the function $\theta(\tau_i)$ (14) may be written in the following form

$$\theta(\tau_i) \approx \frac{1}{3} + \tau_i,\ i = 1,2 \tag{15}$$

As above, in case when $d_i > \delta_i$, it is necessary in the formula (13) to replace the thicknesses of friction pair d_i with appropriate effective thicknesses δ_i, $i = 1, 2$ (9).

Tab. 1. Heat partition ratios

Curve number	Number of the formula and type of a brake	Author
1	(1) A, B	Blok, 1937
2	(2) A, B	Blok, 1937
3	(3) A, B	Jaeger, 1942
4	(4) A, B	Jaeger, 1942
5	(5) A, B	Charron, 1943
6	(7) A, B	Newcomb, 1958-59
7	(10) A, (8) B	Hasselgruber, 1963
8	(12) A, (11) B	Chichinadze et al., 1979
9	(13) A, B	Ginzburg, 1973

The thermal conductivity of the pad material is considerably less than the thermal conductivity of the disc material, i.e. $K_1 << K_2$. For that reason, the temperature increases on the external surface of the pad near the moment of standstill t_s, and it differs slightly from the initial period. As a result, pad may be considered as the semi-infinite body (the semi-space), and disc – as the strip. Then from the formula (13) it follows

$$\gamma(t) = \frac{\eta K_1 d_2 \theta(\tau_2)}{\eta K_1 d_2 \theta(\tau_2) + 2K_2 d_1 \sqrt{\frac{\tau_1}{\pi}}},\ 0 \le t \le t_s \tag{16}$$

The formulas shown in this section are found by various ways and differ significantly from each other. Therefore, comparison of the results of the numerical analysis obtained with their help with appropriate experimental data is the actual problem.

3. STATEMENT OF THE PROBLEM

When the friction force acts on the members of brake system being in sliding contact, the energy conversion should be considered as an essential. The work done is converted into heat and the vehicle decelerates with the certain rate. The disc brake system consists primarily of two major parts, namely: rotating axisymmetric disc and immovable non-axisymmetric pads (Fig. 1). The generated thermal energy dissipated by the conduction from disc/pad interface to adjacent components of brake system, and by convection to atmosphere due to Newton's law. Obviously the third of mode of heat transfer takes place as well, nonetheless by virtue of relatively low temperatures attained during slipping and short time of the operation is neglected.

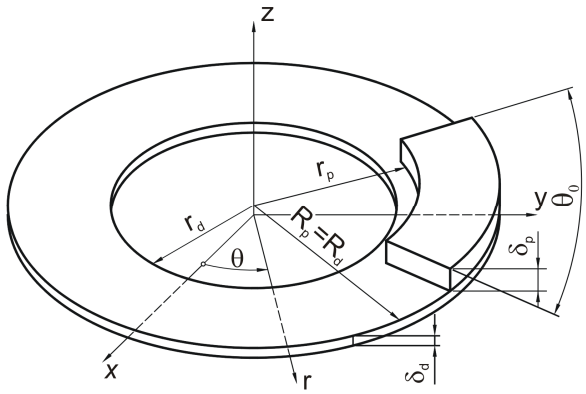

Fig. 1. A schematic diagram of a disc brake system

In actual thermal load of a disc is non-axisymmetric, which stems from the geometry of a pad covering rubbing path partly. Thereby, for the selected spot on the circumference of the friction surface the temperature will differ periodically with time. Such a distribution both in depth and circumferential direction can be obtained by means of the three-dimensional model.

Despite the fact of comprehensive outcomes possible to obtain by means of the spatial model of a disc, hitherto have been made calculations of transient temperatures using two-dimensional configurations of the same phenomenon make a case for theirs application (Talati and Jalalifar, 2009). The accuracy of such an approximation increases, when the Peclet number is higher for considered tribosystem. In an automotive disc brakes the Peclet numbers almost always are in order of 10^3 (Chichinadze et al., 1979). Therefore, the transient heat conduction problem for the disc

and the pad has been analysed in the axisymmetric statement (uniformly distributed heat source over the rubbing path of the disc), assuming boundary thermal flux acting on the lateral surfaces of a disc.

An analytical solution of one-dimensional boundary-value problem of heat conductivity for tribosystem, consisting of a plane-parallel strip and semi-space, was obtained by Nosko et al. (2009). The temperature evolution at mean radius of pad contact surface was illustrated. The frictional heating phenomenon of a brake shoe including spread of heat on its depth during hoist's emergency braking was studied by Zhu et al. (2009). The integral transform method was adopted in the three-dimensional analysis.

In the proposed article two types of a real disc brake system including disc and pad volume during single braking action with a special respect to different heat partition ratios were studied. In order to validate further transient numerical analysis, dimensions, material properties and operating parameters were adopted from the experimental data Nosko et al. (2009) and Zhu et al. (2009).

For the purpose of thermal analysis, it is assumed that the contact pressure p is constant during entire process of braking and the angular velocity decreases linearly with time

$$\omega(t) = \omega_0\left(1-\frac{t}{t_s}\right),\ 0 \le t \le t_s\,. \tag{17}$$

where: ω – angular velocity, ω – initial angular velocity, t – time, t_s – braking time.

In order to calculate transient temperature distributions in the pad and the disc, the following heat conduction equation for an axisymmetric problem given in the cylindrical coordinate system was employed:

$$\begin{aligned}
&\frac{\partial^2 T}{\partial r^2}+\frac{1}{r}\frac{\partial T}{\partial r}+\frac{\partial^2 T}{\partial z^2}=\frac{1}{k_p}\frac{\partial T}{\partial t}, r_p \le r \le R_p,\\
&0 < z < \delta_p, t > 0;\\
&\frac{\partial^2 T}{\partial r^2}+\frac{1}{r}\frac{\partial T}{\partial r}+\frac{\partial^2 T}{\partial z^2}=\frac{1}{k_d}\frac{\partial T}{\partial t}, r_d \le r \le R_d,\\
&0 < z < \delta_d, t > 0,
\end{aligned} \tag{18}$$

where: T – temperature, r, z – radial, axial coordinate respectively, k – thermal diffusivity, r, R – internal and external radius, respectively. The bottom indexes p and d, denote the pad and the disc, respectively.

Taking account of the symmetry of a given problem, the insulation on mid-plane of the disc as well as the inner surface represented by the edge of two-dimensional model was established. On the remained surfaces of the brake models the forced convection takes place with the constant value of heat transfer coefficient. It is also assumed that the material properties of the pad and the disc are isotropic and independent of temperature.

$$q_p(r,t) = \gamma f p r \omega(t), r_p \le r \le R_p, 0 \le t \le t_s, \tag{19}$$

$$q_d(r,t) = \frac{\theta_0}{2\pi}(1-\gamma) f p r \omega(t), r_d \le r \le R_d, 0 \le t \le t_s\,. \tag{20}$$

where: q – intensity of the heat flux, γ– heat partition ratio, f – friction coefficient, p – contact pressure.

From the formulas (19) and (20) it follows that the intensities of thermal fluxes, which enter the pad and the disc respectively, depends directly on value of the heat partition ratio γ. Consequently, it is essential to specify its influence on the temperature at the pad/disc interface.

4. FE FORMULATION

The understanding of overall formulation (18)–(20) is crucial for the solution of a considered thermal problem of friction by means of the approximate time-stepping procedures for axisymmetric transient governing equations of heat conductivity. The main idea of two-dimensional discretization of the boundary-value heat conductivity problem consists in the following reference (Lewis et al., 2004). Using the Galerkin's method we write Eq. (18) in the matrix form:

$$[\mathbf{C}]\left\{\frac{\mathrm{d}\mathbf{T}}{\mathrm{d}t}\right\}+[\mathbf{K}]\{\mathbf{T}\}=\{\mathbf{Q}\}, \tag{21}$$

where: [**C**] – heat capacity matrix, [**K**] – heat conductivity matrix, {**Q**} – thermal force matrix.

The solution of the first order ordinary differential equation (21) was obtained using the Crank-Nicolson method with approximation relations (Crank and Nicolson, 1947)

$$\frac{1}{\Delta t}[\{\mathbf{T}\}_{t+\Delta t}-\{\mathbf{T}\}_t]=(1-\beta)\left\{\frac{\mathrm{d}\mathbf{T}}{\mathrm{d}t}\right\}_t+\beta\left\{\frac{\mathrm{d}\mathbf{T}}{\mathrm{d}t}\right\}_{t+\Delta t}, \tag{22}$$

where: $\{\mathbf{T}\}_t$ – temperature vector at time t. The weight parameter $0.5 < \beta \le 1$ was chosen from the conditions of achievement of necessary accuracy of integration and stable scheme. Taking the relation (22) into account, from Eq. (21) we obtain the system of linear algebraic equations

$$\begin{aligned}
&([\mathbf{C}]+\beta\Delta t[\mathbf{K}])\{\mathbf{T}\}_{t+\Delta t}=([\mathbf{C}]-(1-\beta)[\mathbf{K}]\Delta t)\{\mathbf{T}\}_t,\\
&+(1-\beta)\Delta t\{\mathbf{Q}\}_t+\beta\Delta t\{\mathbf{Q}\}_{t+\Delta t}
\end{aligned} \tag{23}$$

for determination of the temperature $\{\mathbf{T}\}_{t+\Delta t}$ in the time moment $t + \Delta t$.

The temperature distributions in the pad and disc were analyzed using the finite element method based programme. In the thermal analysis of disc brake an appropriate finite element division is indispensable. In this study four-node quadratic elements were used for the finite element analysis. In order to avoid inaccurate or unstable results, a proper initial time step Δt associated with spatial mesh size Δx (smallest element dimension) is essential

$$\Delta t = \Delta x^2 \frac{\rho_{p,d} c_{p,d}}{10 K_{p,d}} \tag{24}$$

where: Δx – mesh size (smallest element dimension).

5. NUMERICAL ANALYSIS

The temperature distributions of two types of a real disc brake system including disc and pad volume during single braking action regarding different heat partition ratios were studied (Tab. 1).

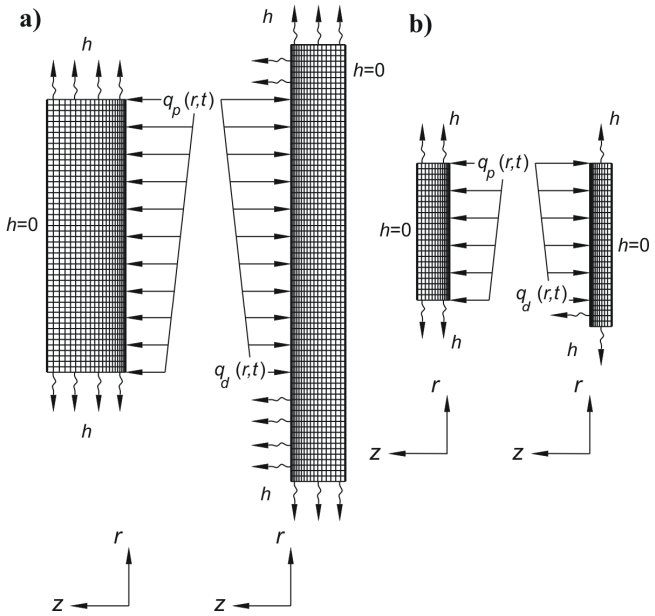

Fig. 2. FE models with the boundary conditions, a) A type, b) B Type

The FE element models with the boundary conditions are shown in Fig. 2. In order to validate further transient numerical analysis, the thermophysical material properties, dimensions and operating parameters have been adopted from the experimental data of Nosko et al. (2009) (the A type) and Zhu et al. (2009) (the B type), and are presented in Tab. 2. In the A type the brake pad is made of polymeric material of the type 145-40, and the brake disc is made of cast iron of the type 15-32. The materials of brake pad and brake disc in the B type are asbestos-free and 16Mn, respectively.

The heat transfer coefficient of 100 W/(m^{2}K) was assumed. The FE model of A type of a disc brake consists of 3680 elements and 3864 nodes for the disc and 12800 elements and 13065 nodes for the pad, and the B type model consists of 660 elements and 732 nodes for the disc and 2000 elements and 2121 nodes for the pad. The temperature evolutions on the contact surface for two types of disc brake employing nine of formulas for the heat partition ratio were determined and compared with the experimental outcomes for the A type (Nosko et al., 2009) and B type (Zhu et al., 2009). Conformity of numbers of the curves presented on the following figures to formulas for calculation of heat partition ratio, is shown in Tab. 1.

The evolution of temperature on the contact surface of the pad and the disc are shown in Figs. 3 and 4, respectively. The character of evolution of temperature is the following: with the beginning of braking the temperature sharply raises, reaches the maximum value and, after this, it decreases to the minimum level in the stop time moment.

The change of temperature in time on the friction surface of the pad in A type of brake is shown in Fig. 3a. We see, that the evolution of contact temperature calculated with use of Charron's formula (5) (the curve 5) and of Ginzburg formula (13) (the curve 9) significantly differs, both qualitatively and quantitatively, from experimental curve (Nosko et al. 2009). The curve denoted as 7 (Hasselgruber H., 1963) coincides with the experimental curve from the initial instant of time until $t = 0.08$ s, then surpasses the experimental values of temperatures. The maximum temperature reached of curve 7 equals $T = 304.3\,°C$, whereas the maximum value of temperature of the experiment equals approximately $T = 250\,°C$, and appears earlier. Then, it decreases considerably to standstill. Most of the solutions illustrated in Fig. 3a range beneath experimental curve of temperature. The cooling conditions have no impact on the temperature values on the average radius, due to comparatively large distance from the outer surface of the disc. A slightly different plot of temperature evolution on friction surface of pad in the B type of brake is observed in Fig. 3b.

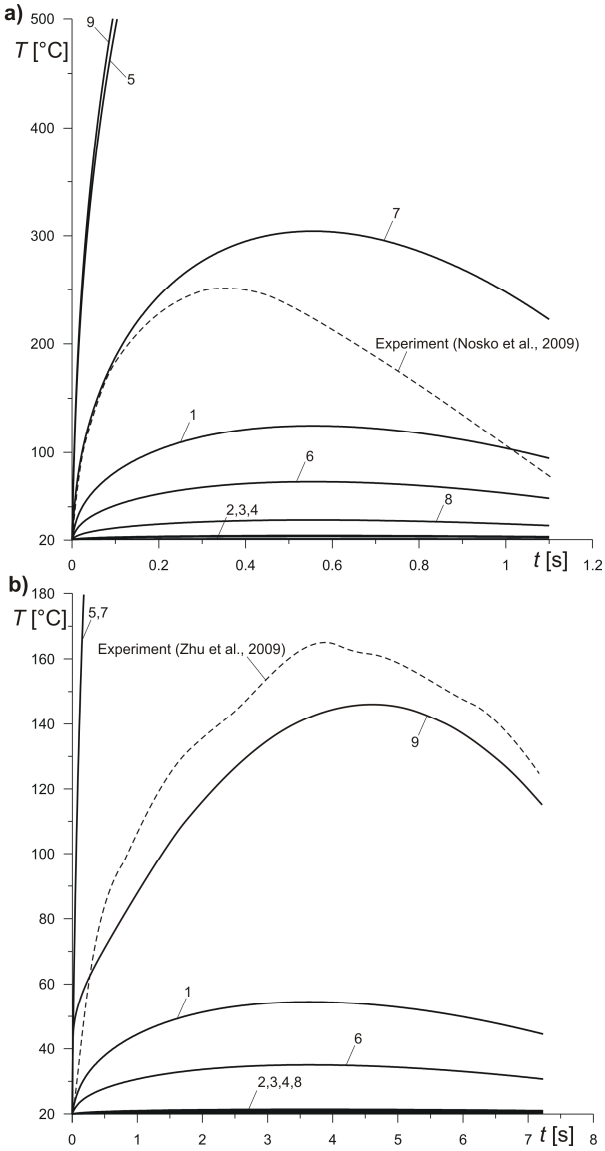

Fig. 3. Evolution of temperature at the mean radius of contact surface of a pad: a) A type, b) B type

Tab. 2. Operation and geometrical parameters

Parameters	A type (Nosko et al., 2009)		B type (Zhu et al., 2009)	
	Disc	Pad	Disc	Pad
thermal conductivity, K (W/mK)	59	0.64	53.2	0.295
specific heat, c (J/kgK)	500	1100	473	2530
density, ρ (kg/m^3)	7100	2500	7866	2206
inner radius, r (m)	0.03	0.05	0.1325	0.1375
outer radius, R (m)	0.11	0.1	0.1625	0.1625
mean radius of pad, r_m (m)		0.075		0.15
cover angle of pad, θ_0 (rad)		0.384		0.167
thickness, δ (m)	0.01	0.015	0.004	0.006
pressure, p (Pa)	4×10^6		1.38×10^6	
braking time, t_s (s)	1.1		7.23	
initial angular velocity, ω_0 (s^{-1})	200		66.667	
coefficient of friction, f	0.38		0.4	
initial temperature, T_0 (°C)	20		20	
ambient temperature, T_a (°C)	20		20	
time step, Δt (s)	0.0002	0.001	0.0002	0.005
Peclet number, Pe	4136.7		3014.6	
Biot number, Bi	0.00777		0.00810	

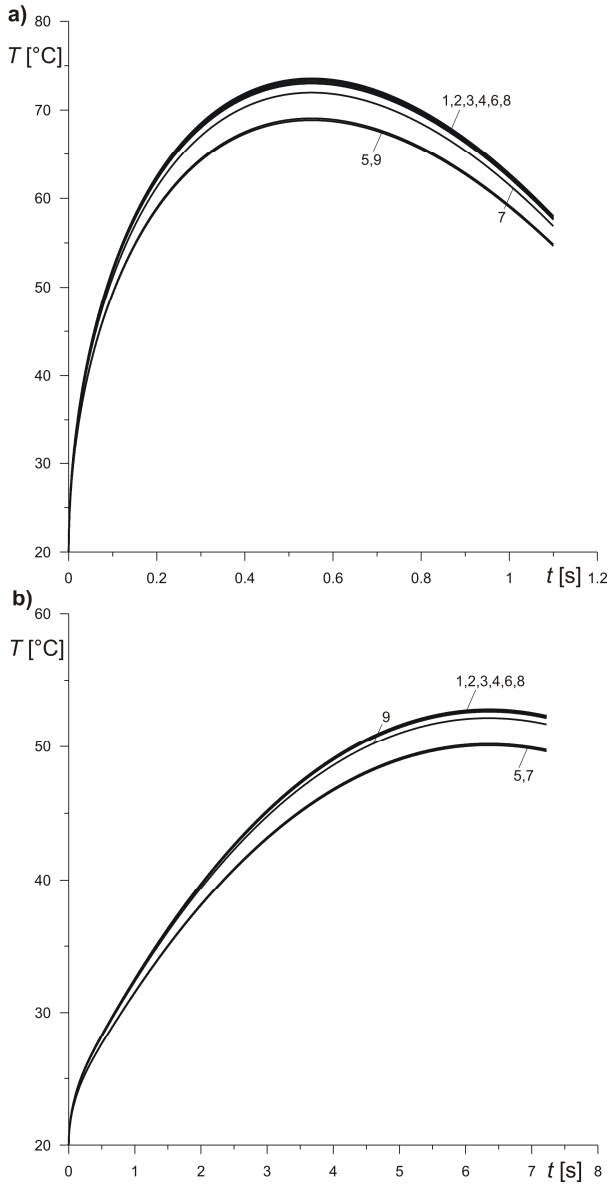

Fig. 4. Evolution of temperature at the mean radius of contact surface of a disc: a) A type, b) B type

However, curve denoted 5 is similar to the same one as in Fig. 3a. Previously correct temperature curve 7, currently provides overlapped values relating to the experimental data. The character of the temperature changes is the same as in A type (Fig. 3a), except the curve denoted 9 (Ginzburg, 1973), which results from the variable in time heat partition ratio. In this case the sharp rise of the temperature at the initial period of braking is noticeable. At time $t = 0.05$ s temperatures of the curve 9 and the experimental one coincide, to separate after this moment till standstill.

In Fig. 4a the temperature evolutions of the disc friction surface of A type obtained from the numerical analysis including different representations of heat partition ratios are plotted against time. For A type of a brake it is important to know the location of the curve 7, because it is the curve, as seen from Fig. 3a, which gives the best coincidence of experimental data. We see in Fig. 4a, that the temperature curve denoted 7 lays between the curves 5, 9 and 1-4, 6, 8. The closeness of the last six curves can be explained by the fact that the value of the heat partition ratio calculated with their help, equals nearly zero. It means, that almost all heat energy, generated on the surface of friction, is absorbed by the disc, whereas influence of a portion of heat entering the pad is negligibly small. The curves 5 and 9 give the worst approximation of the experimental data. Thus, the analysis of evolution of temperature on surfaces of the pad and the disc, allows to come to the conclusion that the most authentic results for A type brake can be obtained with use of the Hasselgruber's formula (10).

The evolutions of temperature on the contact surface of the disc in B type of brake at the mean radius of rubbing path are shown in Fig. 4b. The curve 9, which better coincides with experimental data in Fig. 3b, is located between curves 5 and 7 (the worst coincidence to experimental data) and curves 1-4,6,8. The temperature reaches the maximum value after time ranged between $t = 6.34$ s for curve 9 and $t = 6.35$ s for curve 3 and decreases slightly after that moment. This may indicate that the disc is heated in the entire

volume, and cooling by the absorption to adjacent area is difficult.

The highest value of temperature on the contact surface of the disc of type B equals $T = 52.8\,°C$ (the curve 4) and is reached at time $t = 6.34\,s$ (the curve 4). The lowest temperature $T = 50.07\,°C$ is reached after $t = 6.34\,s$ (the curve 5). The discrepancy between the peak values of temperatures of the curves 4,8,3,2,6,1 equals 0.34 %. The analysis of evolution of temperature on friction surfaces of the pad and the disc in B type of brake show, that the most authentic distribution of temperature can be find, using the time-dependent ratio of heat partition given by Ginzburg's formula (13).

6. CONCLUSIONS

In this paper two-dimensional finite element analysis was carried out to study the effect of use of different heat partition ratios on the contact temperatures of the disc brake components during single braking process. The calculated temperatures on the friction surfaces of the brake system were compared with experimental results (Nosko et al, 2009; Zhu et al., 2009), which allow us make the following conclusions:

- the heat partition ratio is a key factor when analyze the pad friction surface temperature, which is conditioned by the substantial variation of its value in each case of applied formulas;
- the investigation of the pad/disc contact surface temperatures provides an important information about its maximum value reached during frictional heating, nevertheless the obtained results reveal that the material with lower thermal conductivity is more susceptible to the selection of the heat partition ratio included in the expression of the intensity of a heat flux calculation;
- the thickness of the pad plays a significant role as well. Its slender growth may firmly change the actual value of heat partition ratio entering the pad and the disc respectively, whereas in actual, temperatures of the pad alter only in the immediate vicinity of the contact surface;
- relatively small thickness (B type) demonstrates that the entire volume may be nearly uniformly heated from the initial moment of operation without causing significant temperature gradients.

REFERENCES

1. **Adamowicz A., Grześ P.** (2011), Analysis of disc brake temperature distribution during single braking under non-axisymmetric load, *Applied Thermal Engineering*, (in press).
2. **Balakin V. A., Sergienko V. P.** (1999), *Heat calculations of brakes and friction units*, MPRI of NASB, Gomel, (in Russian).
3. **Blok H.** (1937), Theoretical field study of temperature rise at surfaces of actual contact under oiliness lubricating conditions, *Proc. Inst. Mech. Eng. London*, Vol. 45, 222-235.
4. **Charron F.** (1943), Partage de la chaleur entre deux corps frottants, *Publ. scient. et techn. Ministere air.*, No. 182.
5. **Chichinadze A. V.** (1964), *Determination of average temperature of a surface of friction at short-term braking, Friction of hard bodies*, Nauka, Moscow.
6. **Chichinadze A. V., Braun E. D., Ginsburg A. G. et al.** (1979), *Calculation, test and selection of frictional couples*, Nauka, Moscow (in Russian).
7. **Crank J., Nicolson P.** (1947), A practical method for numerical evaluation of solutions of partial differential equations of the heat conduction type, *Proc. Camb. Phil. Soc.*, Vol. 43, 50-67.
8. **Evtushenko O. O., Ivanyk E. H., Horbachova N. V.** (2000), Analytic methods for thermal calculation of brakes (review), *Materials Science*, Vol. 36, No. 6, 857-862.
9. **Farlow S. J.** (1982), *Partial differential equations for Scientists and Engineers*, John Wiley & Sons, New York.
10. **Ginzburg A. H.** (1973), *Theoretical and experimental bases for calculation of unitary process of braking by means of system of the equations of thermal dynamics of friction, In: Optimum use of frictional material in units of friction of machines*, Nauka, Moscow (in Russian).
11. **Grylytskyy D. V.** (1996), *Thermoelastic contact problems in tribology*, Institute of the Maintenance and Methods of Training of the Ministry of Education of Ukraine, Kiev, (in Ukrainian).
12. **Hasselgruber H.** (1963), Der Schaltvorgang einer Trockenreibung Kupplung bei kleinster Erwärmung, *Konstruction*, Vol. 15, No. 2, 41-45.
13. **Hwang P., Wu X.** (2010), Investigation of temperature and thermal stress in ventilated disc brake based on 3D thermo-mechanical coupling model, *J. Mech. Sci. Technol.*, Vol. 24, 81-84.
14. **Jaeger J. C.** (1942), Moving surfaces of heat and the temperature at sliding surfaces, *Proc. Roy. Soc. N.S.W.*, Vol. 76, 203-224.
15. **Lewis R. W., Nithiarasu P., Seetharamu K. N.** (2004), *Fundamentals of the finite element method for Heat and Fluid Flow*, John Wiley & Sons, New York.
16. **Newcomb T. P.** (1958-59), Transient Temperatures in Brakes Drums and Linings, *Proc. Auto. Div. Instn mech. Engrs*, , 227.
17. **Nosko A. L., Belyakov N. S., Nosko A. P.** (2009), Application of the generalized boundary condition to solving thermal friction problems, *J. Friction and Wear*, Vol. 30, No. 6, 455–462.
18. **Olesiak Z., Pyryev Yu., Yevtushenko A.** (1997), Determination of temperature and wear during braking, *Wear*, Vol. 210, 163-169.
19. **Pereverzeva O. V., Balakin V. A.** (1992), Distribution of heat between rubbing bodies, *J. Friction and Wear*, Vol. 13, No. 3, 507-516.
20. **Talati F., Jalalifar S.** (2009), Analysis of heat conduction in a disk brake system, *Heat Mass Transfer*, Vol. 45, 1047-1059.
21. **Yevtushenko A., Grześ P.** (2010), FEM-modeling of the frictional heating phenomenon in the pad/disc tribosystem (a review), *Numerical Heat Transfer Part A*, Vol. 58, No. 3, 207-226.
22. **Yevtushenko A., Grześ P.** (2011), Finite element analysis of heat partition in a pad/disc brake system, *Numerical Heat Transfer Part A*, Vol. 59, No. 7, 521-542.
23. **Yevtushenko A. A, Kuciej M.** (2010), Influence of the convective cooling and the thermal resistance on the temperature of the pad/disc tribosystem, *Int. Comm. Heat Mass Trans.*, Vol. 37, No. 4, 337-342.
24. **Yi Y.-B., Barber J. R., Hartsock D. L.** (2002), *Thermoelastic instabilities in automotive disc brakes – Finite element analysis and experimental verification. In: J.A.C.Martins and Manuel D. P. Monteiro Marques eds., Contact Mechanics*, Kluwer, Dordrecht, pp. 187–202.
25. **Zhu Z.-C., Peng Y.-Z., Chen G.-A.** (2009), Three-dimensional transient temperature field of brake shoe during hoist's emergency braking, *Appl. Therm. Eng.*, Vol. 29, 932-937.

POSITIVITY AND REACHABILITY OF FRACTIONAL ELECTRICAL CIRCUITS

Tadeusz KACZOREK*

*Faculty of Electrical Engineering, Białystok University of Technology, ul. Wiejska 45D, 15-351 Białystok

kaczorek@isep.pw.edu.pl

Abstract: Conditions for the positivity of fractional linear electrical circuits composed of resistors, coils, condensators and voltage (current) sources are established. It is shown that: 1) the fractional electrical circuit composed of resistors, coils and voltage source is positive for any values of their resistances, inductances and source voltages if and only if the number of coils is less or equal to the number of its linearly independent meshes, 2) the fractional electrical circuit is not positive for any values of its resistances, capacitances and source voltages if each its branch contains resistor, capacitor and voltage source, It is also shown that the fractional positive electrical circuits of *R, C, e* type are reachable if and only if the conductances between their nodes are zero and the fractional positive electrical circuits of *R, L, e* type are reachable if and only if the resistances belonging to two meshes are zero.

1. INTRODUCTION

A dynamical system is called positive if its trajectory starting from any nonnegative initial state remains forever in the positive orthant for all nonnegative inputs. An overview of state of the art in positive systems theory is given in the monographs (Farina and Rinaldi 2000; Kaczorek 2002). Variety of models having positive behavior can be found in engineering, economics, social sciences, biology and medicine, etc..

The notion of controllability and observability and the decomposition of linear systems have been introduced by Kalman (1960, 1963). These notions are the basic concepts of the modern control theory (Antsaklis, Michel 2006; Kaczorek 1999, 2002; Kailath 1980; Rosenbrock 1970; Wolovich 1970). They have been also extended to positive linear systems (Farina and Rinaldi 2000; Kaczorek 2002). The decomposition of the pair (*A*,*B*) and (*A*,*C*) of the positive discrete-time linear system has been addressed in Kaczorek (2010b).

The reachability of linear systems is closely related to the controllability of the systems. Specially for positive linear systems the conditions for the controllability are much stronger than for the reachability (Kaczorek 2002). Tests for the reachability and controllability of standard and positive linear systems are given in Kaczorek (2008b, 2002; Klamka 1991). The stability, robust stability and stabilization of positive linear systems have been investigated in (Busłowicz 2008a, 2008b, 2008c, 2009, 2010; Kaczorek 2002, 2011c). Analysis of fractional electrical circuits has been addressed in Kaczorek (2010a, 2011a, 2011b).

In this paper the necessary and sufficient conditions for the positivity and reachability of fractional linear electrical circuits composed of resistors, coils, condensators (supercondensators) and voltage (current) sources will be established.

The paper is organized as follows. In section 2 the state equations of the fractional linear electrical circuits and their solutions are presented. The positive fractional linear electrical circuits composed of resistors, condensators, coils and voltage sources are analyzed in section 3. The reachability of the fractional positive electrical circuits is investigated in section 4. Concluding remarks are given in section 5.

The following notation will be used: $\Re$ – the set of real numbers, $\Re^{n\times m}$ – the set of $n\times m$ real matrices, $\Re_+^{n\times m}$ – the set of $n\times m$ matrices with nonnegative entries and $\Re_+^n = \Re_+^{n\times 1}$, M_n – the set of $n\times n$ Metzler matrices (real matrices with nonnegative off-diagonal entries), I_n – the $n\times n$ identity matrix.

2. FRACTIONAL STATE EQUATIONS AND THEIR SOLUTIONS

In this paper the following Caputo definition of the derivative-integral of fractional order will be used (Kaczorek 2008a, 2011c)

$$\frac{d^\alpha f(t)}{dt^\alpha} = \frac{1}{\Gamma(n-\alpha)}\int_0^t \frac{f^{(n)}(\tau)}{(t-\tau)^{\alpha+1-n}}d\tau \tag{2.1}$$

$n-1<\alpha<n$, $n\in N=\{1,2,...\}$ where

$$\Gamma(x)=\int_0^\infty t^{x-1}e^{-t}dt\ ,\ \mathrm{Re}(x)>0 \tag{2.2}$$

is the gamma function and

$$f^{(n)}(\tau)=\frac{d^n f(\tau)}{d\tau^n} \tag{2.3}$$

is the classical *n* order derivative.

Let the current $i_C(t)$ in a supercondensator (shortly condensator) with the capacity C be the α order derivative of its charge $q(t)$ (Kaczorek 2010a, 2011c)

$$i_C(t) = \frac{d^\alpha q(t)}{dt^\alpha},\ 0 < \alpha < 1 \tag{2.4}$$

Using $q(t) = Cu_C(t)$ we obtain

$$i_C(t) = C\frac{d^\alpha u_C(t)}{dt^\alpha} \tag{2.5}$$

where $u_C(t)$ is the voltage on the condensator.

Similarly, let the voltage $u_L(t)$ on coil (inductor) with the inductance L be the β order derivative of its magnetic flux $\Psi(t)$ (Kaczorek 2010a, 2011c)

$$u_L(t) = \frac{d^\beta \Psi(t)}{dt^\beta},\ 0 < \beta < 1 \tag{2.6}$$

Taking into account that $\Psi(t) = Li_L(t)$ we obtain

$$u_L(t) = L\frac{d^\beta i_L(t)}{dt^\beta} \tag{2.7}$$

where $i_L(t)$ is the current in the coil.

Consider an electrical circuit composed of resistors, n capacitors and m voltage sources. Using the equation (2.5) and the Kirchhoff's laws we may describe the transient states in the electrical circuit by the fractional differential equation

$$\frac{d^\alpha x(t)}{dt^\alpha} = Ax(t) + Bu(t),\ 0 < \alpha < 1 \tag{2.8}$$

where $x(t) \in \Re^n$, $u(t) \in \Re^m$, $A \in \Re^{n\times n}$, $B \in \Re^{n\times m}$. The components of the state vector $x(t)$ and input vector $u(t)$ are the voltages on the condensators and source voltages respectively.

Consider an electrical circuit composed of resistors, n coils and m sources. Similarly, using the equation (2.6) and the Kirchhoff's laws we may describe the transient states in the electrical circuit by the fractional differential equation

$$\frac{d^\beta x(t)}{dt^\beta} = Ax(t) + Bu(t),\ 0 < \beta < 1 \tag{2.9}$$

where $x(t) \in \Re^n$, $u(t) \in \Re^m$, $A \in \Re^{n\times n}$, $B \in \Re^{n\times m}$. In this case the components of the state vector $x(t)$ are the currents in the coils.

Theorem 2.1. Solution of the equation (2.8) satisfying the initial condition $x(0) = x_0$ has the form

$$x(t) = \Phi_0(t)x_0 + \int_0^t \Phi(t-\tau)Bu(\tau)d\tau \tag{2.10}$$

where

$$\Phi_0(t) = \sum_{k=0}^{\infty}\frac{A^k t^{k\alpha}}{\Gamma(k\alpha+1)},\quad \Phi(t) = \sum_{k=0}^{\infty}\frac{A^k t^{(k+1)\alpha-1}}{\Gamma[(k+1)\alpha]},\quad 0 < \alpha < 1 \tag{2.11}$$

Proof is given in Kaczorek (2008a, 2011c) .

Now let us consider electrical circuit composed of resistors, capacitors, coils and voltage (current) source. As the state variables (the components of the state vector $x(t)$ we choose the voltages on the capacitors and the currents in the coils. Using the equations (2.5), (2.7) and Kirchhoff's laws we may write for the fractional linear circuits in the transient states the state equation

$$\begin{bmatrix} \dfrac{d^\alpha x_C}{dt^\alpha} \\ \dfrac{d^\beta x_L}{dt^\beta} \end{bmatrix} = \begin{bmatrix} A_{11} & A_{12} \\ A_{21} & A_{22} \end{bmatrix}\begin{bmatrix} x_C \\ x_L \end{bmatrix} + \begin{bmatrix} B_1 \\ B_2 \end{bmatrix}u,\ 0 < \alpha, \beta < 1 \tag{2.12a}$$

where the components $x_C \in \Re^{n_1}$ are voltages on the condensators, the components $x_L \in \Re^{n_2}$ are currents in the coils and the components of $u \in \Re^m$ are the source voltages

$$A_{ij} \in \Re^{n_i \times n_j},\ B_i \in \Re^{n_i \times m},\ i, j = 1,2\ . \tag{2.12b}$$

Some examples of electrical circuits described by the equation (2.12) are given in (Kaczorek 2010c, 2011c).

Theorem 2.2. The solution of the equation (2.12) for $0 < \alpha < 1$, $0 < \beta < 1$ with initial conditions

$$x_C(0) = x_{10} \text{ and } x_L(0) = x_{20} \tag{2.13}$$

has the form

$$x(t) = \Phi_0(t)x_0 + \int_0^t [\Phi_1(t-\tau)B_{10} + \Phi_2(t-\tau)B_{01}]u(\tau)d\tau \tag{2.14a}$$

where

$$x(t) = \begin{bmatrix} x_C(t) \\ x_L(t) \end{bmatrix},\ x_0 = \begin{bmatrix} x_{10} \\ x_{20} \end{bmatrix},\ B_{10} = \begin{bmatrix} B_1 \\ 0 \end{bmatrix},\ B_{01} = \begin{bmatrix} 0 \\ B_2 \end{bmatrix}$$

$$T_{kl} = \begin{cases} I_n & \text{for } k = l = 0 \\ \begin{bmatrix} A_{11} & A_{12} \\ 0 & 0 \end{bmatrix} & \text{for } k = 1, l = 0 \\ \begin{bmatrix} 0 & 0 \\ A_{21} & A_{22} \end{bmatrix} & \text{for } k = 0, l = 1 \\ T_{10}T_{k-1,l} + T_{01}T_{k,l-1} & \text{for } k + l > 0 \end{cases} \tag{2.14b}$$

$$\Phi_0(t) = \sum_{k=0}^{\infty}\sum_{l=0}^{\infty} T_{kl}\frac{t^{k\alpha+l\beta}}{\Gamma(k\alpha+l\beta+1)}$$

$$\Phi_1(t) = \sum_{k=0}^{\infty}\sum_{l=0}^{\infty} T_{kl}\frac{t^{(k+1)\alpha+l\beta-1}}{\Gamma[(k+1)\alpha+l\beta]}$$

$$\Phi_2(t) = \sum_{k=0}^{\infty}\sum_{l=0}^{\infty} T_{kl}\frac{t^{k\alpha+(l+1)\beta-1}}{\Gamma[k\alpha+(l+1)\beta]}$$

Proof is given in Kaczorek (2010c, 2011c).

The extension of Theorem 2.2 to systems consisting of n subsystems with different fractional order is given in Kaczorek (2011b).

3. POSITIVE FRACTIONAL ELECTRICAL CIRCUITS

Definition 3.1. The fractional electrical circuit (2.8) (or (2.9), (2.12)) is called the (internally) positive fractional system if the state vector $x(t) \in \Re_+^n$, $t \geq 0$ for any initial conditions $x_0 \in \Re_+^n$ and all $u(t) \in \Re_+^m$, $t \geq 0$.

Definition 3.2. A square real matrix $A = [a_{ij}]$ is called the Metzler matrix if its off-diagonal entries are nonnegative, i.e. $a_{ij} \geq 0$ for $i \neq j$ (Kaczorek, 2002, 2011c).

Theorem 3.1. The fractional electrical circuit (2.8) is (internally) positive if and only if

$$A \in M_n, \quad B \in \Re_+^{n \times m} \tag{3.1}$$

where M_n is the set of $n \times n$ Metzler matrices.

Proof is given in Kaczorek (2002, 2011c).

From Theorem 3.1 applied to the fractional circuit (2.12) it follows that the electrical circuit is positive if and only if

$$A_{kk} \in M_{n_k},\ k = 1,2;\ A_{12} \in \Re_+^{n_1 \times n_2},\ A_{21} \in \Re_+^{n_2 \times n_1},$$
$$B_1 \in \Re_+^{n_1 \times m},\ B_2 \in \Re_+^{n_2 \times m} \tag{3.2}$$

3.1. Fractional *R, C, e* type electrical circuits

Theorem 3.2. The fractional electrical circuit is not positive if each its branch contains resistors, condensator and voltage source.

The proof is similar to the proof of Theorem 3.1 in Kaczorek (2011a).

Consider the fractional electrical circuit shown on Figure 3.1 with given conductances $G_k, k = 0, 1, \ldots, n$; capacitances C_j, $j = 1, \ldots, n$ and source voltages e.

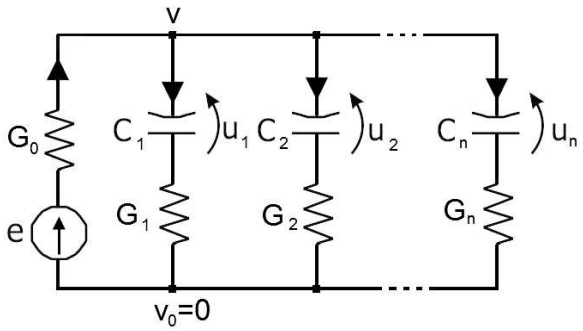

Fig. 3.1. Fractional electrical circuit

Using (2.5) and the Kirchhoff's laws we may write the equations

$$C_k \frac{d^\alpha u_k}{dt^\alpha} = G_k (v - u_k),\ k = 1,\ldots,n \tag{3.3}$$

and

$$G_0 (e - v) = \sum_{j=1}^{n} G_j (v - u_j). \tag{3.4}$$

From (3.4) we have

$$v = \frac{1}{G}\left(G_0 e + \sum_{j=1}^{n} G_j u_j \right),\ G = \sum_{i=0}^{n} G_i . \tag{3.5}$$

Substitution of (3.5) into (3.3) yields

$$\frac{d^\alpha}{dt^\alpha}\begin{bmatrix} u_1 \\ \vdots \\ u_n \end{bmatrix} = A \begin{bmatrix} u_1 \\ \vdots \\ u_n \end{bmatrix} + Be \tag{3.6}$$

where

$$A = \begin{bmatrix} -\dfrac{G_1 G - G_1^2}{C_1 G} & \dfrac{G_1 G_2}{C_1 G} & \cdots & \dfrac{G_1 G_n}{C_1 G} \\ \dfrac{G_2 G_1}{C_2 G} & -\dfrac{G_2 G - G_2^2}{C_2 G} & \cdots & \dfrac{G_2 G_n}{C_2 G} \\ \vdots & \vdots & \ddots & \vdots \\ \dfrac{G_n G_1}{C_n G} & \dfrac{G_n G_2}{C_n G} & \cdots & -\dfrac{G_n G - G_n^2}{C_n G} \end{bmatrix}, \tag{3.7}$$

$$B = \begin{bmatrix} \dfrac{G_0 G_1}{C_1 G} \\ \vdots \\ \dfrac{G_0 G_n}{C_n G} \end{bmatrix}.$$

From (3.7) it follows that $A \in M_n$ and $B \in \Re_+^n$. Therefore, the following theorem has been proved.

Theorem 3.3. The fractional electrical circuit shown on Fig. 3.1 is positive for any values of the conductances $G_k, k = 0, 1, \ldots, n$; capacitances C_j, $j = 1, \ldots, n$ and source voltage e.

In general case let us consider the fractional electrical circuit composed of q conductances $G_k, k = 1, \ldots, q$; r capacitances C_i, $i = 1, \ldots, r$ and m source voltages e_j, $j = 1, \ldots, m$. Let n be the number of linearly independent nodes of the electrical circuit and $n > r$.

Using the Kirchhoff's laws we may write the equation

$$\frac{d^\alpha}{dt^\alpha}\begin{bmatrix} u_1 \\ \vdots \\ u_r \end{bmatrix} = A_r \begin{bmatrix} u_1 \\ \vdots \\ u_r \end{bmatrix} + A_n \begin{bmatrix} v_1 \\ \vdots \\ v_n \end{bmatrix} + B_m \begin{bmatrix} e_1 \\ \vdots \\ e_m \end{bmatrix} \tag{3.8}$$

where u_i is the voltage on the i-th (i = 1, …, r) capacitor, v_j is the voltage of the j-th node (j = 1,…,n), $A_r \in \Re^{r \times r}$ is the diagonal Metzler matrix, $A_n \in \Re^{r \times n}$ and $B_m \in \Re^{r \times m}$.

Using the node method we obtain

$$G\begin{bmatrix} v_1 \\ \vdots \\ v_n \end{bmatrix} = -F\begin{bmatrix} u_1 \\ \vdots \\ u_r \end{bmatrix} - H\begin{bmatrix} e_1 \\ \vdots \\ e_m \end{bmatrix} \tag{3.9}$$

where $G \in \Re^{n \times n}$ is a Metzler matrix, $F \in \Re^{n \times r}$ and $H \in \Re^{n \times m}$.

Taking into account that $-G^{-1} \in \Re_+^{n \times n}$ from (3.9) we obtain

$$\begin{bmatrix} v_1 \\ \vdots \\ v_n \end{bmatrix} = -G^{-1}F\begin{bmatrix} u_1 \\ \vdots \\ u_r \end{bmatrix} - G^{-1}H\begin{bmatrix} e_1 \\ \vdots \\ e_m \end{bmatrix}. \tag{3.10}$$

Substitution of (3.10) into (3.8) yields

$$\frac{d^{\alpha}}{dt^{\alpha}}\begin{bmatrix} u_1 \\ \vdots \\ u_r \end{bmatrix} = A\begin{bmatrix} u_1 \\ \vdots \\ u_r \end{bmatrix} + B\begin{bmatrix} e_1 \\ \vdots \\ e_m \end{bmatrix} \tag{3.11}$$

where

$$A = A_r - A_n G^{-1} F\ ,\ B = B_m - A_n G^{-1} H\ . \tag{3.12}$$

The electrical circuit described by the equation (3.11) is positive if and only if the matrix A is a Metzler matrix and the matrix B has nonnegative entries. Therefore, the following theorem has been proved.

Theorem 3.4. The linear electrical circuit composed of q resistors, r capacitors and m source voltages is positive if and only if $r < n$ and

$$A_r - A_n G^{-1} F \in M_r\ ,\ B_m - A_n G^{-1} H \in \Re_+^{r\times m}. \tag{3.13}$$

3.2. Fractional *R, L, e* type electrical circuits

Consider the electrical circuit shown on Figure 3.2 with given resistances R_1, R_2, R_3 inductances L_1, L_2, L_3 and source voltages e_1, e_2.

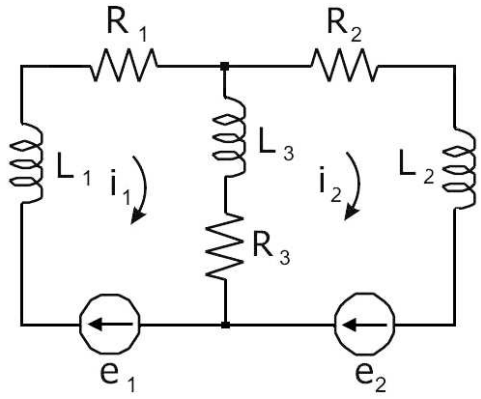

Fig. 3.2. Fractional electrical circuit

Using (2.7) and the mesh method for the electrical circuit we obtain the following equations

$$\begin{bmatrix} L_{11} & -L_{12} \\ -L_{21} & L_{22} \end{bmatrix}\frac{d^{\beta}}{dt^{\beta}}\begin{bmatrix} i_1 \\ i_2 \end{bmatrix} = \begin{bmatrix} -R_{11} & R_{12} \\ R_{21} & -R_{22} \end{bmatrix}\begin{bmatrix} i_1 \\ i_2 \end{bmatrix} + \begin{bmatrix} e_1 \\ e_2 \end{bmatrix} \tag{3.14a}$$

where

$$\begin{aligned} &R_{11} = R_1 + R_3,\ \ R_{12} = R_{21} = R_3,\ \ R_{22} = R_2 + R_3, \\ &L_{11} = L_1 + L_3,\ \ L_{12} = L_{21} = L_3,\ \ L_{22} = L_2 + L_3. \end{aligned} \tag{3.14b}$$

Note that the inverse matrix

$$L^{-1} = \begin{bmatrix} L_{11} & -L_{12} \\ -L_{21} & L_{22} \end{bmatrix}^{-1} = \frac{1}{L_1(L_2 + L_3) + L_2 L_3}\begin{bmatrix} L_{22} & L_{12} \\ L_{21} & L_{11} \end{bmatrix} \tag{3.15}$$

has positive entries. From (3.14) we have

$$\frac{d^{\beta}}{dt^{\beta}}\begin{bmatrix} i_1 \\ i_2 \end{bmatrix} = A\begin{bmatrix} i_1 \\ i_2 \end{bmatrix} + B\begin{bmatrix} e_1 \\ e_2 \end{bmatrix} \tag{3.16}$$

where

$$\begin{aligned} A = L^{-1}\begin{bmatrix} -R_{11} & R_{12} \\ R_{21} & -R_{22} \end{bmatrix} &= \frac{1}{L_1(L_2 + L_3) + L_2 L_3} \\ &\cdot\begin{bmatrix} -L_2(R_1 + R_3) - L_3 R_1 & L_2 R_3 - L_3 R_2 \\ L_1 R_3 - L_3 R_1 & -L_1(R_2 + R_3) - L_3 R_2 \end{bmatrix}, \end{aligned} \tag{3.17}$$

$$B = L^{-1} \in \Re_+^{2\times 2}.$$

From (3.17) it follows that $A \in M_2$ if and only if

$$L_2 R_3 \geq L_3 R_2 \ \text{ and } \ L_1 R_3 \geq L_3 R_1\ . \tag{3.18}$$

Therefore, the fractional electrical circuit is positive if and only if $A \in M_2$ i.e. the condition (3.18) is met.

In general case let us consider the fractional n-mesh electrical circuit with given resistances $R_k, k = 1, \ldots, q$, inductances $L_1, \ldots, L_r$ for $r \geq n$ and $m \leq n$ mesh source voltages $e_{jj}, j = 1, \ldots, m$. Denote by $i_1, \ldots, i_n$ the mesh currents. In a similar way as for the electrical circuit shown on Fig 3.2 using the mesh method we obtain the equation

$$L\frac{d^{\beta}}{dt^{\beta}}\begin{bmatrix} i_1 \\ \vdots \\ i_n \end{bmatrix} = A'\begin{bmatrix} i_1 \\ \vdots \\ i_n \end{bmatrix} + \begin{bmatrix} e_{11} \\ \vdots \\ e_{mm} \end{bmatrix} \tag{3.19a}$$

where

$$\begin{aligned} L &= \begin{bmatrix} L_{11} & -L_{12} & \ldots & -L_{1,n} \\ -L_{21} & L_{22} & \ldots & -L_{2,n} \\ \vdots & \vdots & \ddots & \vdots \\ -L_{n,1} & -L_{n,2} & \ldots & L_{nn} \end{bmatrix}, \\ A' &= \begin{bmatrix} -R_{11} & R_{12} & \ldots & R_{1,n} \\ R_{21} & -R_{22} & \ldots & R_{2,n} \\ \vdots & \vdots & \ddots & \vdots \\ R_{n,1} & R_{n,2} & \ldots & -R_{nn} \end{bmatrix}. \end{aligned} \tag{3.19b}$$

Note that $-L \in M_n$, $A' \in M_n$ and $L^{-1} \in \Re_+^{n\times n}$.

Premultiplying (3.19a) by L^{-1} we obtain

$$\frac{d^{\beta}}{dt^{\beta}}\begin{bmatrix} i_1 \\ \vdots \\ i_n \end{bmatrix} = A\begin{bmatrix} i_1 \\ \vdots \\ i_n \end{bmatrix} + B\begin{bmatrix} e_{11} \\ \vdots \\ e_{mm} \end{bmatrix} \tag{3.20a}$$

where

$$A = L^{-1}A'\ ,\ B = L^{-1} \in \Re_+^{n\times n}\ . \tag{3.20b}$$

The fractional electrical circuit is positive if and only if the matrix $L^{-1}A'$ is a Metzler matrix, i.e.

$$L^{-1}A' \in M_n\ . \tag{3.21}$$

Therefore, the following theorem has been proved.

Theorem 3.4. The fractional linear electrical circuit composed of resistors, coils and voltage sources is positive for $r > n$ if its resistances and inductances satisfy the condition (3.21).

Remark 3.1. In the case $r = n$ if it is possible to choose the n linearly independent meshes so that to each mesh belongs only one coil. Then the matrix $L = diag[L_1, ..., L_n]$ and the condition (3.21) is met for any values of the resistances and inductances of the electrical circuit.

Remark 3.2. Note that it is impossible to choose the n linearly independent meshes so that to each mesh belongs only one coil if all branches belonging to the same node contain the coils. In this case we can eliminate one of the branch currents using the fact that the sum of the currents in the coils is equal to zero.

From Theorem 3.4 and Remark 3.1 we have the following important theorem.

Theorem 3.5. The fractional linear electrical circuit composed of resistors, coils and voltage sources is positive for almost all values of the resistances, inductances and source voltages if and only if the number of coils is less or equal to the number of its linearly independent meshes and the directions of the mesh currents are consistent with the directions of the mesh source voltages.

3.3. Fractional *R, L, C* type electrical circuits

Consider the fractional electrical circuit shown on Figure 3.3 with given resistance *R*, inductance *L*, capacitance *C* and source voltage *e*.

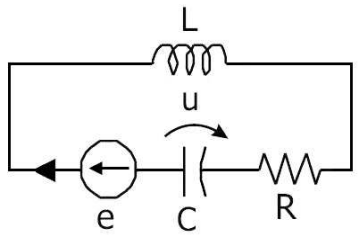

Fig. 3.3. Fractional electrical circuit

Using the Kirchhoff's laws we can write the equations

$$i = C\frac{d^{\alpha}u}{dt^{\alpha}}$$
$$e = Ri + L\frac{d^{\beta}i}{dt^{\beta}} + u \qquad (3.22)$$

which can be written in the form

$$\begin{bmatrix} \frac{d^{\alpha}u}{dt^{\alpha}} \\ \frac{d^{\beta}i}{dt^{\beta}} \end{bmatrix} = A\begin{bmatrix} u \\ i \end{bmatrix} + Be \qquad (3.23a)$$

where

$$A = \begin{bmatrix} 0 & \frac{1}{C} \\ -\frac{1}{L} & -\frac{R}{L} \end{bmatrix}, \quad B = \begin{bmatrix} 0 \\ \frac{1}{L} \end{bmatrix}. \qquad (3.23b)$$

The matrix A has negative off-diagonal entry (-1/*L*) and it is not a Metzler matrix for any values of *R*, *L*, *C*. Therefore, the fractional electrical circuit is not positive one for any values of the resistances *R*, inductance *L*, capacitance *C*.

In general case we have the following theorem.

Theorem 3.6. The fractional electrical circuits of *R*, *L*, *C* type is not positive for almost all values of its resistances, inductances, capacitances and source voltages if at least one its branch contains inductance and capacitance.

Proof. It is well-known that the linear independent meshes of the electrical circuits can be chosen so that the branch containing the inductance *L* and capacitance *C* belongs to the first one. The equation for the first mesh contains the following term

$$e_{11} = L\frac{d^{\beta}i_1}{dt^{\beta}} + u_1 + ... \qquad (3.24)$$

where e_{11} and i_1 are the source voltage and current of the first mesh and u_1 is the voltage on the capacitance *C*. From (3.24) and $i_1 = C((d^{\alpha}u_1)/dt^{\alpha})$ it follows that the matrix A of the electrical circuit has at least one negative off-diagonal entry. Therefore the matrix A is not a Metzler matrix and the electrical circuit is not positive one.

Consider the electrical circuit shown on Fig. 3.4 with given resistances $R_k, k = 1, ..., n$, inductances $L_2,\ L_4 ..., L_{n_2}$, capacitances $C_1,\ C_3 ..., C_{n_1}$ and source voltages $e_1,\ e_2 ..., e_n$.

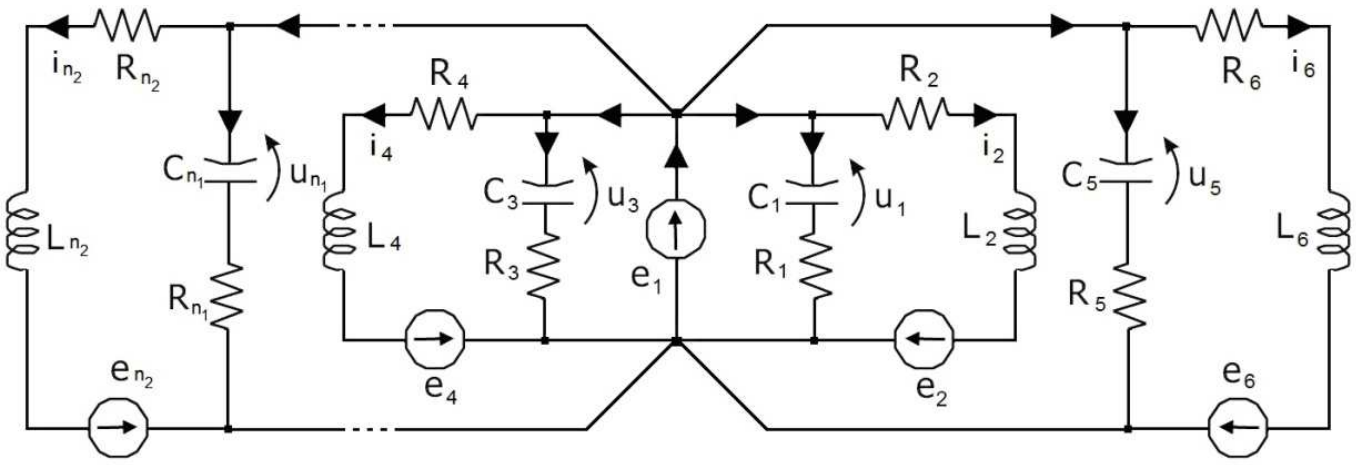

Fig. 3.4. Fractional electrical circuit

Using the Kirchhoff's laws we can write the equations

$$e_1 = R_k C_k \frac{d^\alpha u_k}{dt^\alpha} + u_k \quad \text{for} \quad k = 1,3,...,n_1 \tag{3.25a}$$

$$e_1 + e_j = L_j \frac{d^\beta i_j}{dt^\beta} + R_j i_j \quad \text{for} \quad j = 2,4,...,n_2 \tag{3.25b}$$

which can be written in the form

$$\begin{bmatrix} \frac{d^\alpha u}{dt^\alpha} \\ \frac{d^\beta i}{dt^\beta} \end{bmatrix} = A \begin{bmatrix} u \\ i \end{bmatrix} + Be \tag{3.26a}$$

where

$$u = \begin{bmatrix} u_1 \\ u_3 \\ \vdots \\ u_{n_1} \end{bmatrix}, \quad i = \begin{bmatrix} i_2 \\ i_4 \\ \vdots \\ i_{n_2} \end{bmatrix}, \quad u = \begin{bmatrix} e_1 \\ e_2 \\ e_4 \\ \vdots \\ e_n \end{bmatrix} \tag{3.26b}$$

and

$$A = \text{diag}[-\frac{1}{R_1 C_1}, -\frac{1}{R_3 C_3}, ..., -\frac{1}{R_{n_1} C_{n_1}}, -\frac{R_2}{L_2}, -\frac{R_4}{L_4}, ..., -\frac{R_{n_2}}{L_{n_2}},] \in M_n,$$

$$B = \begin{bmatrix} B_1 \\ B_2 \end{bmatrix} \in \Re_+^{n \times \left(\frac{n_2}{2}+1\right)}, \quad B_1 = \begin{bmatrix} \frac{1}{R_1 C_1} & 0 & 0 & ... & 0 \\ \frac{1}{R_3 C_3} & 0 & 0 & ... & 0 \\ \vdots & \vdots & \vdots & ... & \vdots \\ \frac{1}{R_{n_1} C_{n_1}} & 0 & 0 & ... & 0 \end{bmatrix}, \tag{3.26c}$$

$$B_2 = \begin{bmatrix} \frac{1}{L_2} & \frac{1}{L_2} & 0 & ... & 0 \\ \frac{1}{L_4} & 0 & \frac{1}{L_4} & ... & 0 \\ \vdots & \vdots & \vdots & \ddots & \vdots \\ \frac{1}{L_{n_2}} & 0 & 0 & ... & \frac{1}{L_{n_2}} \end{bmatrix}.$$

The electrical circuit described by the equation (3.26) is positive for all value of the resistances $R_k, k = 1, ..., n$, inductances L_k, $k = 2, 4, ..., n_2$, capacitances C_k, $k = 1, 3, ..., n_1$. Therefore, the following theorem has been proved.

Theorem 3.7. The fractional linear electrical circuit of the structure shown on Fig. 3.4 is positive for any values of its resistances, inductances and capacitances.

4. REACHABILITY OF FRACTIONAL POSITIVE LINEAR ELECTRICAL CIRCUITS

Consider the fractional positive linear electrical circuit described by the equations (2.8), (2.9) and (2.12).

Definition 4.1. The fractional positive electrical circuit (2.8) is called reachable in time t_f if for any given final state $x_f \in \Re_+^n$ there exists an input $u(t) \in \Re_+^m$, for $t \in [0, t_f]$ that steers the state of the circuit from zero initial state $x(0) = 0$ to the final state x_f, i.e. $x(t_f) = x_f$. If every state $x_f \in \Re_+^n$ is reachable in time t_f, then the circuit is called reachable in time t_f. The fractional positive electrical circuit is called reachable if for every $x_f \in \Re_+^n$ there exist time t_f and input $u(t) \in \Re_+^m$, for $t \in [0, t_f]$ which steers the state of the circuit from $x(0) = 0$ to x_f.

A real square matrix is called monomial if each its row and each its column contains only one positive entry and the remaining entries are zero.

Theorem 4.1. The fractional positive electrical circuit (2.8) is reachable in time t_f if the matrix

$$R(t_f) = \int_0^{t_f} \Phi(\tau) B B^T \Phi^T(\tau) d\tau, \; t_f > 0 \tag{4.1}$$

is monomial. The input that steers the state of the electrical circuit in time t_f from $x(0) = 0$ to the state x_f is given by the formula

$$u(t) = B^T \Phi^T(t_f - t) R^{-1}(t_f) x_f \quad \text{for} \; t \in [0, t_f]. \tag{4.2}$$

The proof is given in Kaczorek (2010a).

Theorem 4.2. If the matrix $A = diag[a_1, a_2, ... a_n] \in \Re^{n \times n}$ and $B \in \Re_+^{n \times m}$ for $m = n$ are monomial matrices then the fractional positive electrical circuit (2.8) is reachable.

Proof. From (2.11) it follows that if A is diagonal then the matrix $\Phi(t)$ and $\Phi(t)B$ are also monomial for monomial matrix B. From (4.1) written in the form

$$R(t_f) = \int_0^{t_f} \Phi(\tau) B [\Phi(\tau) B]^T d\tau \tag{4.3}$$

it follows that the matrix (4.3) is monomial. Therefore, by Theorem 4.1 the fractional system is reachable.

Example 4.1. Consider the fractional electrical circuit shown on Figure 4.1 with given conductances $G_1, G_2, G'_1, G'_2, G_{12}$, capacitance C_1, C_2 and source voltages e_1, e_2.

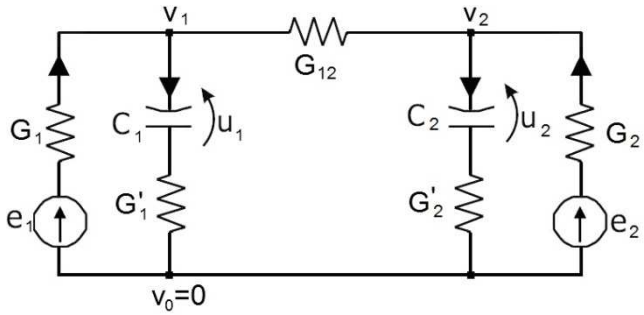

Fig. 4.1. Fractional electrical circuit

Using the Kirchhoff's laws we can write the equations

$$C_k \frac{d^\alpha u_k}{dt^\alpha} = G'_k (v_k - u_k), \quad k = 1,2 \tag{4.4}$$

and

$$G \begin{bmatrix} v_1 \\ v_2 \end{bmatrix} = -\begin{bmatrix} G'_1 & 0 \\ 0 & G'_2 \end{bmatrix} \begin{bmatrix} u_1 \\ u_2 \end{bmatrix} - \begin{bmatrix} G_1 & 0 \\ 0 & G_2 \end{bmatrix} \begin{bmatrix} e_1 \\ e_2 \end{bmatrix} \tag{4.5}$$

where

$$G=\begin{bmatrix} -(G_1+G'_1+G_{12}) & G_{12} \\ G_{12} & -(G_2+G'_2+G_{12}) \end{bmatrix} \tag{4.6}$$

is an Metzler matrix and $-G^{-1}\in \Re_+^{2\times 2}$. From (4.5) we obtain

$$\begin{bmatrix} v_1 \\ v_2 \end{bmatrix} = -G^{-1}\begin{bmatrix} G'_1 & 0 \\ 0 & G'_2 \end{bmatrix}\begin{bmatrix} u_1 \\ u_2 \end{bmatrix} - G^{-1}\begin{bmatrix} G_1 & 0 \\ 0 & G_2 \end{bmatrix}\begin{bmatrix} e_1 \\ e_2 \end{bmatrix}. \tag{4.7}$$

Substitution of (4.7) into

$$\frac{d^\alpha}{dt^\alpha}\begin{bmatrix} u_1 \\ u_2 \end{bmatrix} = \begin{bmatrix} -\frac{G'_1}{C_1} & 0 \\ 0 & -\frac{G'_2}{C_2} \end{bmatrix}\begin{bmatrix} u_1 \\ u_2 \end{bmatrix} + \begin{bmatrix} \frac{G'_1}{C_1} & 0 \\ 0 & \frac{G'_2}{C_2} \end{bmatrix}\begin{bmatrix} v_1 \\ v_2 \end{bmatrix} \tag{4.8}$$

we obtain

$$\frac{d^\alpha}{dt^\alpha}\begin{bmatrix} u_1 \\ u_2 \end{bmatrix} = A\begin{bmatrix} u_1 \\ u_2 \end{bmatrix} + B\begin{bmatrix} e_1 \\ e_2 \end{bmatrix}. \tag{4.9}$$

where

$$A=\begin{bmatrix} -\frac{G'_1}{C_1} & 0 \\ 0 & -\frac{G'_2}{C_2} \end{bmatrix} - \begin{bmatrix} \frac{G'_1}{C_1} & 0 \\ 0 & \frac{G'_2}{C_2} \end{bmatrix} G^{-1}\begin{bmatrix} G'_1 & 0 \\ 0 & G'_2 \end{bmatrix},$$
$$B=-\begin{bmatrix} \frac{G'_1}{C_1} & 0 \\ 0 & \frac{G'_2}{C_2} \end{bmatrix} G^{-1}\begin{bmatrix} G_1 & 0 \\ 0 & G_2 \end{bmatrix}. \tag{4.10}$$

From (4.10) it follows that A is a Metzler matrix and the matrix B has nonnegative entries. Therefore, the fractional electrical circuit is positive for all values of the conductances and capacitances.

We shall show that the fractional positive electrical circuit shown on Fig 4.1 is reachable if and only if $G_{12}=0$.

Note that the matrix (4.6) is diagonal if and only if $G_{12}=0$. In this case from (4.10) it follows that A is a diagonal Metzler matrix and B is a diagonal matrix with positive diagonal entries. Therefore, by Theorem 4.2 the fractional positive electrical circuit is reachable.

In general case let us consider the fractional electrical circuit shown on Fig 4.2 with conductances $G_k, G'_k, G_{kj},\ k,j=1,\dots,n$; capacitances $C_k,\ k=1,\dots,n$ and source voltages $e_k,\ k=1,\dots,n$.

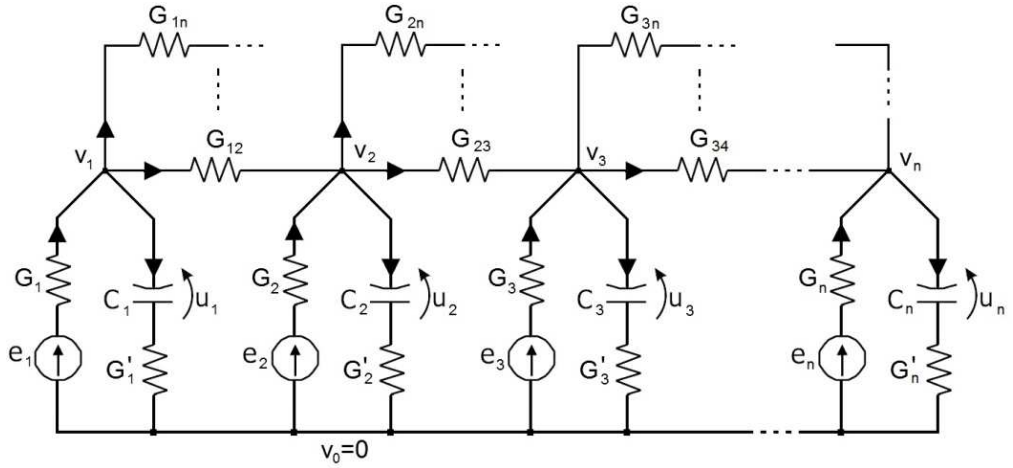

Fig. 4.2. Fractional electrical circuit

Theorem 4.3. The fractional electrical circuit shown on Fig. 4.2 is positive for all values of the conductances, capacitances and source voltages.

Proof. Using the Kirchhoff's laws and the node method for the electrical circuit we may write the equations

$$\frac{d^\alpha}{dt^\alpha}\begin{bmatrix} u_1 \\ \vdots \\ u_n \end{bmatrix} = -C^{-1}G'\begin{bmatrix} u_1 \\ \vdots \\ u_n \end{bmatrix} + C^{-1}G'\begin{bmatrix} v_1 \\ \vdots \\ v_n \end{bmatrix} \tag{4.11a}$$

and

$$\bar{G}\begin{bmatrix} v_1 \\ \vdots \\ v_n \end{bmatrix} = -G'\begin{bmatrix} u_1 \\ \vdots \\ u_n \end{bmatrix} - G\begin{bmatrix} e_1 \\ \vdots \\ e_n \end{bmatrix} \tag{4.11b}$$

where

$$C^{-1}=\mathrm{diag}[C_1^{-1},\dots,C_n^{-1}],\quad G'=\mathrm{diag}[G_1',\dots,G_n'],$$
$$G=\mathrm{diag}[G_1,\dots,G_n], \tag{4.11c}$$
$$\bar{G}=\begin{bmatrix} -G_{11} & G_{12} & \dots & G_{1,n} \\ G_{12} & -G_{22} & \dots & G_{2,n} \\ \vdots & \vdots & \dots & \vdots \\ G_{1,n} & G_{2,n} & \dots & -G_{n,n} \end{bmatrix}$$

G_{ii} is the sum of conductances of all branches belonging to the i-th node, $i=1,\dots,n$.

The matrix $\bar{G}\in M_n$ and $-\bar{G}^{-1}$ has nonnegative entries. Substituting (4.11b) into (4.11a) we obtain

$$\frac{d^{\alpha}}{dt^{\alpha}}\begin{bmatrix} u_1 \\ \vdots \\ u_n \end{bmatrix} = A\begin{bmatrix} u_1 \\ \vdots \\ u_n \end{bmatrix} + B\begin{bmatrix} e_1 \\ \vdots \\ e_n \end{bmatrix} \tag{4.12a}$$

where

$$A = -C^{-1}G'[I_n + \bar{G}^{-1}G'] \in M_n \tag{4.12b}$$

and

$$B = -C^{-1}G'\bar{G}^{-1}G \in \Re_+^{n\times n} \tag{4.12c}$$

since the matrices C^{-1}, G', G and $-\bar{G}^{-1}$ have nonnegative entries. Therefore, the electrical circuit is positive.

Theorem 4.4. The fractional positive electrical circuit shown on Fig. 4.2 is reachable if and only if

$$G_{k,j} = 0 \quad \text{for} \quad k \neq j \quad \text{and} \quad k, j = 1,...n.. \tag{4.13}$$

Proof. The matrix $\bar{G}$ defined by (4.11c) is diagonal if and only if the condition (4.13) is met. In this case the matrices $\bar{G}^{-1}G'$, A and B are also diagonal and from (4.12) we obtain

$$\frac{d^{\alpha}u_k}{dt^{\alpha}} = \frac{1}{C_k}(G_k'G_{k,k}^{-1}G_k' - G_k)u_k + \frac{1}{C_k}G_kG_{k,k}^{-1}G_ke_k, \quad k = 1,...,n \tag{4.14a}$$

where

$$G_{k,k} = G_k + G'_k, \quad k = 1,...,n. \tag{4.14b}$$

Note that the subsystem (4.14a) is reachable. Therefore, the positive electrical circuit is reachable if and only if the condition (4.13) is satisfied.

Example 4.2. Consider the fractional electrical circuit shown on Figure 4.3 with given resistances R_1, R_2, R_3, inductances L_1, L_2 and source voltages e_1, e_2.

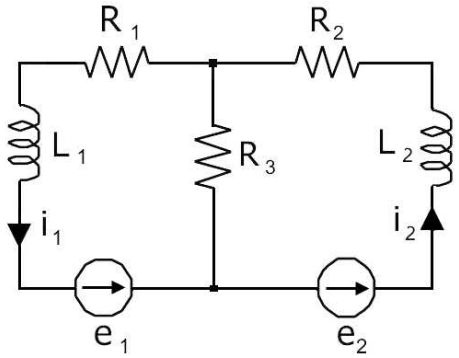

Fig. 4.3. Fractional electrical circuit

Using the Kirchhoff's laws we can write the equations

$$\begin{aligned} e_1 &= R_3(i_1 - i_2) + R_1i_1 + L_1\frac{d^{\beta}i_1}{dt^{\beta}} \\ e_2 &= R_3(i_2 - i_1) + R_2i_2 + L_2\frac{d^{\beta}i_2}{dt^{\beta}} \end{aligned} \tag{4.15}$$

which can be written in the form

$$\frac{d^{\beta}}{dt^{\beta}}\begin{bmatrix} i_1 \\ i_2 \end{bmatrix} = A\begin{bmatrix} i_1 \\ i_2 \end{bmatrix} + B\begin{bmatrix} e_1 \\ e_2 \end{bmatrix} \tag{4.16a}$$

where

$$A = \begin{bmatrix} -\frac{R_1+R_3}{L_1} & \frac{R_3}{L_1} \\ \frac{R_3}{L_2} & -\frac{R_2+R_3}{L_2} \end{bmatrix}, \quad B = \begin{bmatrix} \frac{1}{L_1} & 0 \\ 0 & \frac{1}{L_2} \end{bmatrix}. \tag{4.16b}$$

The fractional electrical circuit is positive since the matrix A is Metzler matrix and the matrix B has nonnegative entries.

We shall show that the fractional positive circuit is reachable if $R_3 = 0$. In this case

$$A = \begin{bmatrix} -\frac{R_1}{L_1} & 0 \\ 0 & -\frac{R_2}{L_2} \end{bmatrix}. \tag{4.17}$$

and

$$e^{A\tau} = \begin{bmatrix} e^{-\frac{R_1}{L_1}\tau} & 0 \\ 0 & e^{-\frac{R_2}{L_2}\tau} \end{bmatrix} \tag{4.18}$$

and from (4.1) we obtain

$$R_f = \int_0^{t_f} e^{A\tau}BB^Te^{A^T\tau}d\tau = \int_0^{t_f}\begin{bmatrix} \frac{1}{L_1^2}e^{-\frac{2R_1}{L_1}\tau} & 0 \\ 0 & \frac{1}{L_2^2}e^{-\frac{2R_2}{L_2}\tau} \end{bmatrix}d\tau \tag{4.19}$$

The matrix (4.19) is monomial and by Theorem 4.1 the fractional positive electrical circuit is reachable if $R_3 = 0$.

Now let us consider the fractional n-mesh electrical circuit with given resistances R_k, $k = 1, \dots, q$, inductances L_i, $i = 1, \dots, n$ and m-mesh source voltages e_{jj}, $j = 1, \dots, m$. It is assumed that to each linearly independent mesh belongs only one inductance. In this case the matrix L defined by (3.19b) is diagonal one and the condition (3.21) is met.

Theorem 4.5. The fractional positive n-meshes electrical circuit with only one inductance in each linearly independent mesh is reachable if

$$R_{ij} = 0 \text{ for } i \neq j, \ i, j = 1,...,n \tag{4.20}$$

where R_{ij} are entries of the matrix A' defined by (3.19b).

Proof. If the condition (4.20) is met then the Metzler matrix A' is diagonal. The matrix L defined by (3.19b) is also diagonal since by assumption only one inductance belongs to each linearly independent mesh. In this case the matrix $A = L^{-1}A'$ is diagonal Metzler matrix and $B = L^{-1} \in \Re_+^{n\times n}$ is also diagonal. For diagonal Metzler matrix A and diagonal B the matrix $e^{A\tau}B$ is also diagonal and the matrix R_f defined by (4.1) is monomial. By Theorem 4.1 the positive electrical circuit is reachable.

Remark 4.1. The condition (4.20) is met if the resistance of the branch belonging to two linearly independent meshes is zero. This result is consistent with the one obtained in Example 4.2.

Consider the fractional electrical circuit shown on Fig. 4.4 with given resistances R_k, $k = 1,...,5$, inductances L_1, L_2, capacitance C and source voltage e.

Using the Kirchhoff's laws we can write the equations

$$\begin{aligned} e_1 &= R_1 i_1 + L_1 \frac{d^\beta i_1}{dt^\beta} - R_5 i_2 + (R_3 + R_5) i_3 \\ L_2 \frac{d^\beta i_2}{dt^\beta} &+ u + (R_2 + R_3) i_3 - R_2 i_1 = 0 \\ C \frac{d^\alpha u}{dt^\alpha} &= i_2 \end{aligned} \tag{4.21a}$$

and

$$(R_2 + R_4) i_1 + (R_4 + R_5) i_2 - (R_2 + R_3 + R_4 + R_5) i_3 = 0 . \tag{4.21b}$$

From (4.21b) we have

$$i_3 = \frac{(R_2 + R_4) i_1 + (R_4 + R_5) i_2}{R_2 + R_3 + R_4 + R_5} \tag{4.22}$$

Substituting (4.22) into (4.21a) we obtain

$$\begin{bmatrix} \frac{d^\beta i_1}{dt^\beta} \\ \frac{d^\beta i_2}{dt^\beta} \\ \frac{d^\alpha u}{dt^\alpha} \end{bmatrix} = A \begin{bmatrix} i_1 \\ i_2 \\ u \end{bmatrix} + Be \tag{4.23a}$$

where

$$A = \begin{bmatrix} -\frac{R_1}{L_1} - \frac{(R_2 + R_4)(R_3 + R_5)}{L_1 (R_2 + R_3 + R_4 + R_5)} & \frac{R_2 R_5 - R_3 R_4}{L_1 (R_2 + R_3 + R_4 + R_5)} & 0 \\ \frac{R_2 R_5 - R_3 R_4}{L_2 (R_2 + R_3 + R_4 + R_5)} & -\frac{(R_2 + R_3)(R_4 + R_5)}{L_2 (R_2 + R_3 + R_4 + R_5)} & -\frac{1}{L_2} \\ 0 & \frac{1}{C} & 0 \end{bmatrix}, \quad B = \begin{bmatrix} \frac{1}{L_1} \\ 0 \\ 0 \end{bmatrix}. \tag{4.23b}$$

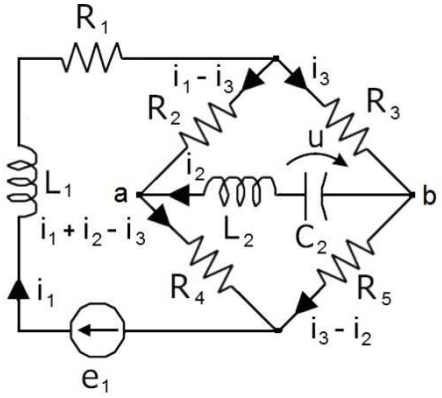

Fig. 4.4. Fractional electrical circuit

From (4.23b) it follows that the matrix A is not a Metzler matrix if

$$R_2 R_5 = R_3 R_4 \tag{4.24}$$

If the condition (4.24) is met then the voltage between the points a, b is equal to zero and $u_2 = 0, L_2 \frac{di_2}{dt} = 0$, $i_2 = 0$. In this case the equation (4.23a) takes the form

$$\frac{di_1}{dt} = \left(-\frac{R_1}{L_1} - \frac{(R_2 + R_4)(R_3 + R_5)}{L_1 (R_2 + R_3 + R_4 + R_5)} \right) i_1 + \frac{1}{L_1} e_1 \tag{4.25}$$

The fractional electrical circuit described by the equation (4.25) is positive. Therefore, we have the following corollary.

Corollary 4.1. If the resistances of the electrical circuit satisfy the condition (4.24) then the fractional electrical circuit is positive.

In general case we have.

Corollary 4.2. Fractional nonpositive electrical circuit for some special choice of the parameters (resistances) can be positive one.

Using (4.23b) it is easy to check that

$$\text{rank}[B \quad AB \quad A^2 B] = 3 \tag{4.26}$$

if and only if the condition (4.24) is not satisfied. Therefore, we have the following corollary.

Corollary 4.3. The fractional standard (nonpositive) electrical circuit shown on Fig. 4.4 is reachable if and only if the condition (4.24) is not satisfied.

From (4.25) it follows that the reduced fractional positive electrical circuit is reachable.

These considerations can be extended for general case of *R*, *L*, *C*, *e* type electrical circuits.

5. CONCLUDING REMARKS

The conditions for the positivity of fractional linear electrical circuits composed of resistors, coils, condensators and voltage (current) sources have been established. It has been shown that:

1. The fractional electrical circuits composed of resistors coils and voltage sources (shortly called *R*, *L*, *e* type) are positive for any values of their resistances, induc-

tances and source voltages if and only if the number of coils is less or equal to the number of its linearly independent meshes (Theorem 3.5).
2. The fractional electrical circuits composed of resistors, condensators and voltage sources (shortly called *R*, *C*, *e* type) are not positive for any values of its resistances, capacitances and voltage sources if each their branch contains resistor capacitor and voltage source (Theorem 3.2).
3. The fractional nonpositive electrical circuits of the *R*, *L*, *C*, *e* type can be positive for some special choice of their parameters (Corollary 4.2).

The conditions for the reachability of the fractional positive electrical circuits have been established. It has been shown that the fractional positive electrical circuit of *R*, *C*, *e* type are reachable if and only if the conductances between their nodes are zero (Theorem 4.4) and the fractional positive electrical circuits of *R*, *L*, *e* type are reachable if and only if the resistances belonging to two meshes are zero (Theorem 4.5). The fractional standard (nonpositive) electrical circuits of *R*, *C*, *L*, *e* type are usually reachable and are unreachable only for some special choice of the parameters.

The considerations have been illustrated by examples of linear electrical circuits.

Some of these results can be also extended for the controllability and observability of the fractional linear electrical circuit. Open problem are extension of these considerations for the following classes of the fractional systems:
1. disturbed parameters linear systems;
2. nonlinear electrical circuits.

REFERENCES

1. **Antsaklis P.J., Michel A.N.** (2006), *Linear Systems*, Birkhauser, Boston.
2. **Busłowicz M.** (2008a), Frequency domain method for stability analysis of linear continuous-time fractional systems, In: **Malinowski K. and Rutkowski L.** (Eds.), *Recent Advances in Control and Automation*, Academic Publishing House EXIT, Warsaw, 83-92.
3. **Busłowicz M.** (2008b), Stability of linear continuous-time fractional order systems with delays of the retarded type, *Bull. Pol. Acad. Sci., Tech. Sci.*, Vol. 56, No. 4, 319-324.
4. **Busłowicz M.** (2008c), Robust stability of convex combination of two fractional degree characteristic polynomials, *Acta Mechanica et Automatica*, Vol. 2, No. 2, 5-10.
5. **Busłowicz M.** (2009), Stability analysis of linear continuous-time fractional systems of commensurate order, *Journal of Automation, Mobile Robotics and Intelligent Systems*, Vol. 3, No. 1, 12-17.
6. **Busłowicz M.** (2010), Robust stability of positive discrete-time linear systems of fractional order, *Bull. Pol. Acad. Sci. Techn.* Vol. 58, no. 4, 567-572.
7. **Farina L., Rinaldi S.** (2000), *Positive Linear Systems; Theory and Applications*, J. Wiley, New York.
8. **Kaczorek T.** (1999), *Linear Control Systems*, Vol. 1, J. Wiley, New York.
9. **Kaczorek T.** (2002), *Positive 1D and 2D Systems*, Springer Verlag, London.
10. **Kaczorek T.** (2008a), Fractional positive continuous-time systems and their reachability, *Int. J. Appl. Math. Comput. Sci.* vol. 18, no. 2, 223-228.
11. **Kaczorek T.** (2008b), Reachability and controllability to zero tests for standard and positive fractional discrete-time systems, *Journal Européen des Systèmes Automatisés, JESA*, Vol. 42, No. 6-8, 2008, 770-781.
12. **Kaczorek T.** (2010a), Analysis of fractional electrical circuits in transient states, *LOGITRANS, Szczyrk, Poland 2010 and also (in Polish) Electrical Review*, vol. 86, no. 6, 191-195.
13. **Kaczorek T.** (2010b), Decomposition of the pair (A,B) and (A,C) of the positive discrete-time linear systems, *Archives of Control Sciences*, Vol. 20, No. 3, 253-273.
14. **Kaczorek T.** (2010c), Positive linear systems with different fractional orders, *Bull. Pol. Acad. Sci. Techn.* Vol. 58, no. 3, 453-458.
15. **Kaczorek T.** (2011a), Positive electrical circuits and their reachability, *Proc. Conf. Computer Applications in Electrical Engineering*, April 11-13, Poznan, Poland.
16. **Kaczorek T.** (2011b), Positive linear systems consisting of n subsystems with different fractional orders, *IEEE Trans. Cir. and Syst.* vol. 58, no.7.
17. **Kaczorek T.** (2011c), *Selected Problems of Fractional Systems Theory*, Springer-Verlag, Berlin 2011.
18. **Kailath T.** (1980), *Linear Systems*, Prentice-Hall, Englewood Cliffs, New York.
19. **Kalman R.E.** (1960), On the General Theory of Control Systems, *Proc. Of the First Intern. Congress on Automatic Control*, Butterworth, London, 481-493.
20. **Kalman R.E.** (1963), Mathematical Descriptions of Linear Systems, *SIAM J. Control*, Vol. 1, 152-192.
21. **Klamka J.** (1991), *Controlability of Dynamila Systems*, Kluwer Academic Publ. Dortreht.
22. **Rosenbrock H.H.** (1970), *State-Space and Multivariable Theory*, J. Wiley, New York.
23. **Wolovich W.A.** (1970), *Linear Multivariable Systems*, Springer-Verlag New York.

This work was supported by Ministry of Science and Higher Education in Poland under work No. N N514 6389 40.

NECESSARY AND SUFFICIENT STABILITY CONDITIONS OF FRACTIONAL POSITIVE CONTINUOUS-TIME LINEAR SYSTEMS

Tadeusz KACZOREK*

*Faculty of Electrical Engineering, Białystok University of Technology, ul. Wiejska 45D, 15-351 Białystok

kaczorek@isep.pw.edu.pl

Abstract: Necessary and sufficient conditions for the asymptotic stability of fractional positive continuous-time linear systems are established. It is shown that the matrix A of the stable fractional positive system has not eigenvalues in the part of stability region located in the right half of the complex plane.

1. INTRODUCTION

A dynamical system is called positive if its trajectory starting from any nonnegative initial state remains forever in the positive orthant for all nonnegative inputs. An overview of state of the art in positive theory is given in the monographs (Farina and Rinaldi, 2000; Kaczorek, 2002). Variety of models having positive behavior can be found in engineering, economics, social sciences, biology and medicine, etc.

Simple conditions for practical stability of discrete-time linear systems have been proposed by Busłowicz and Kaczorek (2009) and next have been extended to robust stability of fractional discrete-time linear systems in Busłowicz (2010). The stability and stabilization of positive fractional linear systems by state-feedbacks have been analyzed in Kaczorek (2010, 2011b). The Hurwitz stability of Metzler matrices has been investigated in Narendra and Shorten (2010) and some new tests for checking the asymptotic stability of positive standard and fractional linear systems have been proposed in Kaczorek (2011a).

In this paper necessary and sufficient conditions for the asymptotic stability of fractional positive continuous-time linear systems will be established. It will be shown that the matrix A of the stable fractional positive system has not eigenvalues in the part of stability region located in the right half of the complex plane.

The paper is organized as follows. In section 2 basic definitions and theorems concerning the fractional positive continuous-time linear systems and their stability are recalled. The main result of the paper is given in section 3 where it is shown that the matrix A of the stable fractional positive system has not eigenvalues in the part of stability region located in the right half complex plane and the necessary and sufficient stability conditions are established. Concluding remarks are given in section 4.

The following notation will be used: $\Re$ – the set of real numbers, $\Re^{n\times m}$ – the set of $n\times m$ real matrices, $\Re_+^{n\times m}$ – the set of $n\times m$ matrices with nonnegative entries and $\Re_+^n=\Re_+^{n\times 1}$, M_n – the set of $n\times n$ Metzler matrices (real matrices with nonnegative off-diagonal entries), I_n – the $n\times n$ identity matrix.

2. PRELIMINARIES

Consider the continuous-time linear system

$$ {}_0D_t^{\alpha}x(t)=Ax(t),\ 0<\alpha<1 \tag{2.1}$$

where $x(t)\in\Re^n$ is the state vector and $A\in\Re^{n\times m}$,

$$ {}_0D_t^{\alpha}x(t)=\frac{d^{\alpha}x(t)}{dt^{\alpha}}=\frac{1}{\Gamma(1-\alpha)}\int_0^t\frac{\dot{x}(\tau)}{(t-\tau)^{\alpha}}d\tau,\quad \dot{x}(\tau)=\frac{dx(\tau)}{d\tau} \tag{2.2}$$

is the Caputo definition of $\alpha\in\Re$ order derivative and

$$ \Gamma(\alpha)=\int_0^{\infty}e^{-t}t^{\alpha-1}dt \tag{2.3}$$

is the Euler gamma function.

The fractional system (2.1) will be called (internally) positive if $x(t)\in\Re_+^n$, $t\geq 0$ for any initial conditions $x(0)=x_0\in\Re_+^n$.

Theorem 2.1. (Kaczorek, 2011b) The fractional system (2.1) is positive if and only if

$$ A\in M_n \tag{2.4}$$

where M_n is the set of $n\times n$ Metzler matrices.

Theorem 2.2. (Kaczorek, 2011b) The solution of equation (2.1) with initial conditions $x_0\in\Re^n$ is given by

$$ x(t)=\Phi_0(t)x_0 \tag{2.5}$$

where

$$ \Phi_0(t)=E_{\alpha}(At^{\alpha})=\sum_{k=0}^{\infty}\frac{A^kt^{k\alpha}}{\Gamma(k\alpha+1)} \tag{2.6}$$

and $E_{\alpha}(At^{\alpha})$ is the Mittage-Leffler matrix function.

The fractional positive system (2.1) will be called asymptotically stable (shortly stable) if

$$ \lim_{t\to\infty}\Phi_0(t)x_0=0\ \text{ for all }\ x_0\in\Re_+^n \tag{2.7}$$

The characteristic polynomial of the matrix A of the fractional system (2.1) has the form

$$p_A(\lambda) = \det[I_n\lambda - A] = \lambda^n + a_{n-1}\lambda^{n-1} + ... + a_1\lambda + a_0, \quad \lambda = s^\alpha \tag{2.8}$$

Theorem 2.3. (Kaczorek, 2011b) The fractional system (2.1) is stable if and only if

$$\min_i |\arg \lambda_i| > \alpha\frac{\pi}{2} \tag{2.9}$$

where λ_i is the i-th eigenvalue of the matrix A.

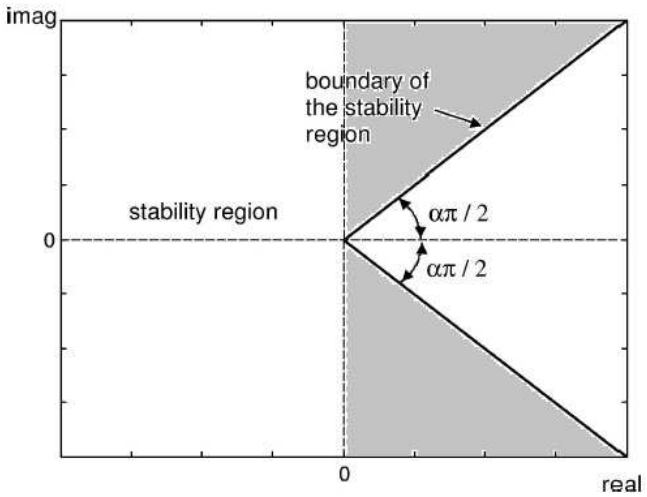

Fig. 2.1. Stability region

Theorem 2.4. (Kaczorek, 2011b) The fractional system (2.1) is unstable if at least one diagonal entry of the matrix A is positive.

3. MAIN RESULT

In this section necessary and sufficient stability conditions of the fractional positive system (2.1) will be established.

Theorem 3.1. The fractional positive system (2.1) for $0 < \alpha < 1$ is (asymptotically) stable if and only if

$$\mathrm{Re}\,\lambda_i < 0 \text{ for } i = 1,..., n \tag{3.1}$$

Proof. By Theorem 2.1 the fractional system (2.1) is positive if and only if A is a Metzler matrix. It is well-known (Farina and Rinaldi, 2000; Mitkowski, 2008) that the dominant eigenvalue $\lambda_d = \lambda_1$ i.e.

$$\lambda_d > \mathrm{Re}\,\lambda_i \text{ for } i = 2,..., n \tag{3.2}$$

of the Metzler matrix A is real. Therefore, the fractional positive system (2.1) is stable if and only if the condition (3.1) is satisfied.

From Theorem 3.1 we have the following important corollary.

Corollary 3.1. The matrix A of stable fractional positive system (2.1) has not eigenvalues in the part of stability region located in the right half complex plane (dark region on Fig. 2.1).

Let $A = [a_{ij}] \in \Re^{n\times m}$ be a Metzler matrix with negative diagonal entries ($a_{ii} < 0,\ i = 1, ..., n$).

Let define

$$A_n^{(0)} = A = \begin{bmatrix} a_{11}^{(0)} & ... & a_{1,n}^{(0)} \\ \vdots & ... & \vdots \\ a_{n,1}^{(0)} & ... & a_{n,n}^{(0)} \end{bmatrix} = \begin{bmatrix} a_{11}^{(0)} & b_{n-1}^{(0)} \\ c_{n-1}^{(0)} & A_{n-1}^{(0)} \end{bmatrix},$$

$$A_{n-1}^{(0)} = \begin{bmatrix} a_{22}^{(0)} & ... & a_{2,n}^{(0)} \\ \vdots & ... & \vdots \\ a_{n,2}^{(0)} & ... & a_{n,n}^{(0)} \end{bmatrix}, \tag{3.3a}$$

$$b_{n-1}^{(0)} = [a_{12}^{(0)} \quad ... \quad a_{1,n}^{(0)}],\ c_{n-1}^{(0)} = \begin{bmatrix} a_{21}^{(0)} \\ \vdots \\ a_{n,1}^{(0)} \end{bmatrix}$$

and

$$A_{n-k}^{(k)} = A_{n-k}^{(k-1)} - \frac{c_{n-k}^{(k-1)} b_{n-k}^{(k-1)}}{a_{k+1,k+1}^{(k-1)}} = \begin{bmatrix} a_{k+1,k+1}^{(k)} & ... & a_{k+1,n}^{(k)} \\ \vdots & ... & \vdots \\ a_{n,k+1}^{(k)} & ... & a_{n,n}^{(k)} \end{bmatrix} = \begin{bmatrix} a_{k+1,k+1}^{(k)} & b_{n-k-1}^{(k)} \\ c_{n-k-1}^{(k)} & A_{n-k-1}^{(k)} \end{bmatrix},$$

$$A_{n-k-1}^{(k)} = \begin{bmatrix} a_{k+2,k+2}^{(k)} & ... & a_{k+2,n}^{(k)} \\ \vdots & ... & \vdots \\ a_{n,k+2}^{(k)} & ... & a_{n,n}^{(k)} \end{bmatrix}, \tag{3.3b}$$

$$b_{n-k-1}^{(k)} = [a_{k+1,k+2}^{(k)} \quad ... \quad a_{k+1,n}^{(k)}],\ c_{n-k-1}^{(k)} = \begin{bmatrix} a_{k+2,k+1}^{(k)} \\ \vdots \\ a_{n,k+1}^{(k)} \end{bmatrix}$$

for $k = 1,\ldots,n-1$.

Let us denote by $R[i + j \times c]$ the following elementary column operation on the matrix A: addition to the i-th column the j-th column multiplied by a scalar c. It is well-known that using these elementary operations we may reduce the matrix

$$A = \begin{bmatrix} a_{11} & a_{12} & ... & a_{1,n} \\ a_{21} & a_{22} & ... & a_{2,n} \\ \vdots & \vdots & ... & \vdots \\ a_{n,1} & a_{n,2} & ... & a_{n,n} \end{bmatrix} \tag{3.4}$$

to the lower triangular form

$$\tilde{A} = \begin{bmatrix} \tilde{a}_{11} & 0 & ... & 0 \\ \tilde{a}_{21} & \tilde{a}_{22} & ... & 0 \\ \vdots & \vdots & \ddots & \vdots \\ \tilde{a}_{n,1} & \tilde{a}_{n,2} & ... & \tilde{a}_{n,n} \end{bmatrix}. \tag{3.5}$$

To check the stability of the fractional positive system (2.1) the following theorem is recommended.

Theorem 3.2. The fractional positive linear system (2.1) for $0 < \alpha < 1$ is (asymptotically) stable if and only if one of the equivalent conditions is satisfied:

1. All principal minors $\Delta_i,\ i = i = 1, ..., n$ of the matrix $-A = [-a_{ij}]$ are positive, i.e.

$$\Delta_1 = -a_{11} > 0,$$
$$\Delta_2 = \begin{vmatrix} -a_{11} & -a_{12} \\ -a_{21} & -a_{22} \end{vmatrix} > 0, \qquad (3.6)$$
$$\vdots$$
$$\Delta_n = \det[-A] > 0$$

2. The diagonal entries of the matrices (3.3)

$$A_{n-k}^{(k)} \text{ for } k = 1,\ldots,n-1 \qquad (3.7)$$

are negative,

3. The diagonal entries of the lower triangular matrix (3.5) are negative, i.e.

$$\tilde{a}_{kk} < 0 \text{ for } k = 1,\ldots,n \qquad (3.8)$$

Proof is given in Kaczorek (2011a).

Example 3.1. Consider the fractional system (2.1) with the matrix

$$A = \begin{bmatrix} -2 & 0 & 1 \\ 1 & -3 & 0 \\ 2 & 1 & -a \end{bmatrix}. \qquad (3.9)$$

Find the values of a for which the fractional positive system is stable. The fractional system is positive for all values of the entry a.

Using the conditions (3.6) for (3.9) we obtain

$$\Delta_1 = -a_{11} = 2 > 0,$$
$$\Delta_2 = \begin{vmatrix} -a_{11} & -a_{12} \\ -a_{21} & -a_{22} \end{vmatrix} = \begin{vmatrix} 2 & 0 \\ -1 & 3 \end{vmatrix} = 6 > 0 \qquad (3.10a)$$

and

$$\det[-A] = \begin{vmatrix} 2 & 0 & -1 \\ -1 & 3 & 0 \\ -2 & -1 & a \end{vmatrix} = 6a - 7 > 0 \text{ for } a > 7/6. \qquad (3.10b)$$

Therefore, the fractional positive system is stable for $a > 7/6$.

Using the conditions (3.7) for (3.9) we obtain

$$A_2^{(1)} = \begin{bmatrix} -3 & 0 \\ 1 & -a \end{bmatrix} + \frac{1}{2}\begin{bmatrix} 1 \\ 2 \end{bmatrix}[0 \quad 1] = \begin{bmatrix} -3 & 0.5 \\ 1 & 1-a \end{bmatrix}$$
$$A_1^{(2)} = [1-a] + \frac{1 \cdot 0.5}{3} = \frac{7}{6} - a. \qquad (3.11)$$

The condition 2) of Theorem 3.2 is satisfied and the fractional positive system is stable for $a > 7/6$.

Similarly, using the elementary column operations to the matrix (3.9) we obtain

$$A = \begin{bmatrix} -2 & 0 & 1 \\ 1 & -3 & 0 \\ 2 & 1 & -a \end{bmatrix} \xrightarrow{R[3+1\times 0.5]} \begin{bmatrix} -2 & 0 & 0 \\ 1 & -3 & 0.5 \\ 2 & 1 & 1-a \end{bmatrix}$$
$$\xrightarrow{R\left[3+2\times\frac{1}{6}\right]} \begin{bmatrix} -2 & 0 & 0 \\ 1 & -3 & 0 \\ 2 & 1 & \frac{7}{6}-a \end{bmatrix}. \qquad (3.12)$$

The condition 3) of Theorem 3.2 is also satisfied and the fractional positive system is asymptotically stable for $a > 7/6$.

The characteristic polynomial of the matrix (3.9)

$$p_A(\lambda) = \det[I_3\lambda - A] = \begin{vmatrix} \lambda+2 & 0 & -1 \\ -1 & \lambda+3 & 0 \\ -2 & -1 & \lambda+a \end{vmatrix} \qquad (3.13)$$
$$= \lambda^3 + (5+a)\lambda^2 + (5a+4)\lambda + 6a - 7$$

has all positive coefficients if and only if $a > 7/6$. This also confirm Kaczorek (2011a) that the fractional positive system is stable if $a > 7/6$.

4. CONCLUDING REMARKS

Necessary and sufficient conditions for the asymptotic stability of fractional positive continuous-time linear systems have been established (Theorem 3.1). It has been shown (Corollary 3.1) that the matrix A of the stable fractional positive system has not eigenvalues in the part of stability region (Fig. 2.1) located in the right half of the complex plane. These considerations can be extended to positive fractional continuous-time linear systems with delays.

REFERENCES

1. **Busłowicz M.** (2010), Robust stability of positive discrete-time linear systems of fractional order, *Bull. Pol. Acad. Sci. Techn.*, vol. 58, no. 4, 567-572.
2. **Busłowicz M. and Kaczorek T.** (2009), Simple conditions for practical stability of positive fractional discrete-time lineart stystems, *Int. J. Appl. Math. Comput. Sci.*, Vol. 19, no. 2, 263-169.
3. **Farina L. and Rinaldi S.** (2000), *Positive Linear Systems; Theory and Applications*, J. Wiley, New York.
4. **Kaczorek T.** (2002), *Positive 1D and 2D Systems*, Springer Verlag, London.
5. **Kaczorek T.** (2010), Stability and stabilization of positive fractional linear systems by state-feedbacks, *Bull. Pol. Acad. Sci. Techn.*, vol. 58, no. 4, 517-554.
6. **Kaczorek T.** (2011a), New stability tests of positive standard and fractional linear systems, *Submitted to Circuits and Systems*.
7. **Kaczorek T.** (2011b), *Selected Problems of Fractional System Theory*, Springer Verlag, Berlin.
8. **Mitkowski W.** (2008), Dynamical properties of Metzler systems, *Bull. Pol. Acad. Sci. Techn.*, Vol. 56, no. 4, 309-312.
9. **Narendra K.S. and Shorten R.** (2010), Hurwitz Stability of Metzler Matrices, *IEEE Trans. Autom. Contr.*, Vol. 55, no. 6 June, 1484-1487.

Acknowledgments: This work was supported
by Ministry of Science and Higher Education in Poland
under work No. N N514 6389 40.

LOCAL CONTROLLABILITY OF FRACTIONAL DISCRETE-TIME SEMILINEAR SYSTEMS

Jerzy KLAMKA*

*Silesian University of Technology, Institute of Automatic Control, ul. Akademicka 16; 44-100 Gliwice

jerzy.klamka@polsl.pl

Abstract: In the paper unconstrained local controllability problem of finite-dimensional fractional discrete-time semilinear systems with constant coefficients is addressed. Using general formula of solution of difference state equation sufficient condition for local unconstrained controllability in a given number of steps is formulated and proved. Simple illustrative example is also presented.

1. INTRODUCTION

Controllability is one of the fundamental concepts in modern mathematical control theory. This is qualitative property of control systems and is of particular importance in control theory. The basic concepts of controllability, reachability and the weaker notion of stabilizability play an essential, fundamental role in dynamical systems analysis and in the solutions of many different important optimal control problems.

Many dynamical systems are such that the control does not affect the complete state of the dynamical system but only a part of it. Therefore, it is very important to determine whether or not control of the complete state of the dynamical system is possible. Roughly speaking, controllability generally means, that it is possible to steer dynamical system from an arbitrary initial state to an arbitrary final state using the set of admissible controls.

During last few years many results concerning theory of fractional control systems both discrete-time and continuous-time have been published in the literature (see e.g. (Kaczorek, 2007a, 2007b, 2009; Klamka, 2002, 2008)). However, it should be pointed out, that the most controllability results are known only for linear fractional control systems both without delays or with delays in control or state variables.

Controllability problems studied in this paper concern semilinear fractional discrete-time control systems. More precisely, in the present paper unconstrained local controllability problem of finite-dimensional fractional discrete-time semilinear systems is addressed. Using general formula of solution of difference state equation, sufficient condition for local controllability in a given number of steps is formulated and proved. The present paper extends for semilinear discrete-time fractional control systems with constant coefficients controllability results given in Kaczorek (2007a, 2007b, 2009) and Klamka (2002, 2008) for linear fractional systems.

The paper is organized as follows. In section 2 using results presented in (Kaczorek, 2007b), general solution of the difference state equation for finite-dimensional fractional linear systems is recalled. Sufficient condition for local unconstrained controllability of the semilinear fractional discrete-time control system with constant parameters is established in section 3. Section 4 contains simple numerical example, which illustrates theoretical considerations. Finally, concluding remarks and propositions for future works are given in section 5.

2. FRACTIONAL SYSTEMS

The set of nonnegative integers will be denoted by Z_+. Let $x_k \in R^n$, $u_k \in R^m$, $k \in Z_+$. In this paper well known extended definition of the fractional difference of the form (Kaczorek, 2007a, 2007b, 2009; Klamka, 2002, 2008)

$$\Delta^{\alpha} x_k = \sum_{j=0}^{j=k} (-1)^j \binom{\alpha}{j} x_{k-j} \quad \text{for } n-1 < \alpha < n \in N = \{1,2,\ldots\}, k \in Z_+ \tag{1}$$

will be used, where $\alpha \in R$ is the order of the fractional difference and

$$\binom{\alpha}{j} = \begin{cases} 1 & \text{for} \quad j = 0 \\ \dfrac{\alpha(\alpha-1)\cdots(\alpha-j+1)}{j!} & \text{for } j = 1,2,\ldots \end{cases} \tag{2}$$

where $\binom{\alpha}{j}$ is so called generalized Newton symbol. Let us observe, that in the case when $\alpha = n$ we have well known standard Newton symbol

$$\binom{\alpha}{j} = \frac{n!}{j!(n-j)!}$$

Let us consider the fractional discrete-time linear system, described by the semilinear difference state-space equation

$$\Delta^{\alpha} x_{k+1} = Ax_k + Bu_k + f(x_k, u_k) \tag{3}$$

where $x_k \in R^n$, $u_k \in R^m$ are the state and input and A and B are $n \times n$ and $n \times m$ constant matrices, f: $R^n \times R^m \rightarrow R^n$ is nonlinear function differentiable near zero in the space $R^n \times R^m$ and such that $f(0,0) = 0$.

Let us observe, that semilinear discrete-time control system is described by the difference state equation, which contains both pure linear and pure nonlinear parts in the right hand side of the state equation.

Using definition of fractional difference (1) we may write semilinear difference equation (3) in the equivalent form

$$x_{k+1} + \sum_{j=1}^{j=k+1} (-1)^j \binom{\alpha}{j} x_{k-j+1} = Ax_k + Bu_k + f(x_k, u_k)$$

Next, using standard linearization method (Klamka, 1995) it is possible to find the associated linear difference state equation

$$x_{k+1} + \sum_{j=1}^{j=k+1} (-1)^j \binom{\alpha}{j} x_{k-j+1} = Ax_k + Bu_k + Fx_k + Gu_k$$

where $n \times n$ dimensional matrix

$$F = \frac{d}{dx} f(x,u)\Big|_{\substack{x=0,\\ u=0}}$$

and $n \times m$ dimensional matrix

$$G = \frac{d}{du} f(x,u)\Big|_{\substack{x=0,\\ u=0}}$$

Moreover, for simplicity of notation let us denote $A + F = C$ and $D = B + G$.

Thus we have

$$x_{k+1} + \sum_{j=1}^{j=k+1} (-1)^j \binom{\alpha}{j} x_{k-j+1} = Cx_k + Du_k \tag{4}$$

Lemma 1. (Kaczorek, 2007b) The solution of linear difference equation (4) with initial condition $x_0 \in R^n$ is given by

$$x_k = \Phi_k x_0 + \sum_{i=0}^{i=k-1} \left(\Phi_{k-i-1} D u_i\right) \tag{5}$$

where $n \times n$ dimensional state transition matrices Φ_k, $k = 0,1,2,\ldots$ are determined by the recurrent formula

$$\Phi_{k+1} = (C + I_n \alpha)\Phi_k + \sum_{i=2}^{i=k+1} (-1)^{j+1} \binom{\alpha}{i} \Phi_{k-i+1} \tag{6}$$

with $\Phi_0 = I_n$, where I_n is $n \times n$ dimensional identity matrix and by assumption matrices $\Phi_k = 0$ for $k < 0$.

Moreover, it should be pointed out, that the matrices Φ_k, $k = 0,1,2,\ldots$ defined above are extensions for fractional linear discrete-time control systems, the well known state transition matrices (see e.g. (Klamka, 1991)) for standard linear discrete-time control systems.

3. CONTROLLABILITY

First of all, in order to define global and local controllability concepts for semilinear and linear finite-dimensional discrete-time control systems let us introduce the notion of reachable set or in other words attainable set in q steps (Kaczorek, 2007a, 2007b, 2009; Klamka, 1991, 1995, 2002, 2008).

Definition 1. For fractional semilinear system (3) or linear system (4) reachable set in q steps from initial condition $x_0 = 0$ is defined as follows:

$$K_q = \{x(q) \in R^n: x(q) \text{ is a solution of semilinear system (3) or linear system (4) in step } q \text{ for sequence of admissible controls } u_0, u_1, \ldots u_k, \ldots, u_{q-1}\} \tag{7}$$

Definition 2. The fractional semilinear discrete-time control system (3) is locally controllable in q-steps if there exists a neighborhood of zero $N \subset R^n$, such that

$$K_q = N \tag{8}$$

Definition 3. The fractional linear discrete-time linear control system (4) is globally controllable in q-steps if

$$K_q = N \tag{9}$$

For linear control system (4) let us introduce the $n \times qm$ dimensional controllability matrix

$$H_q = [D, (\Phi_1 D), (\Phi_2 D), \ldots, (\Phi_i D), \ldots, (\Phi_{q-1} D)] \tag{10}$$

In order to prove sufficient condition for local controllability of semilinear discrete-time fractional control systems (3), we shall use certain result taken directly from nonlinear functional analysis. This result concerns so called nonlinear covering operators.

Lemma 2. (Robinson, 1986) Let $W: Z \rightarrow Y$ be a nonlinear operator from a Banach space Z into a Banach space Y and $W(0) = 0$. Moreover, it is assumed, that operator W has the Frechet derivative $dW(0): Z \rightarrow Y$, whose image coincides with the whole space Y. Then the image of the operator W will contain a neighborhood of the point $W(0) \in Y$.

Now, we are in the position to formulate and prove the main result on the local unconstrained controllability in the interval $[0, q]$ for the nonlinear discrete-time system (1). This result is known for semilinear or nonlinear continuous-time control system and is given in Klamka (1995), as a sufficient condition for local controllability.

Theorem 1. Semilinear discrete-time control system (3) is locally controllable in q steps if the associated linear discrete-time control system (4) is globally controllable in q-steps.

Proof. Proof of the Theorem 1 is based on Lemmas 1 and 2. Let the nonlinear operator W transform the space of admissible control sequence $\{u(i): 0 \le i \le q\}$ into the space of solutions at the step q for the semilinear discrete-time fractional control system (3).

More precisely, the nonlinear operator

$$W: R^m \times R^m \times \ldots \times R^m \rightarrow R^n$$

asssociated with semilinear control system (3) is defined as follows (Klamka, 1995):

$$W\{u(0), u(1), u(2),..., u(i),..., u(q-1)\} = x_{sem}(q)$$

where $x_{sem}(q)$ is the solution at the step q of the semilinear discrete-time fractional control system (3) corresponding to an admissible controls sequence $u_q = \{u(i): 0 \le i < q\}$.

Therefore, for zero initial condition Frechet derivative at point zero of the nonlinear operator W denoted as dW(0) is a linear bounded operator defined by the following formula

$$dW(0)\{u(0), u(1), u(2),..., u(i),..., u(q-1)\} = x_{lin}(q)$$

where $x_{lin}(q)$ is the solution at the step q of the linear system (4) corresponding to an admissible controls sequence $u_q = \{u(i): 0 \le i < q\}$ for zero initial condition.

Since from the assumption nonlinear function $f(0,0) = 0$, then for zero initial condition the nonlinear operator W transforms zero in the space of admissible controls into zero in the state space i.e., $W(0) = 0$.

Moreover, let us observe, that if the associated linear discrete-time fractional control system (4) is globally controllable in the interval $[0, q]$, then by Definition 1 the image of the Frechet derivative dW(0) covers whole state space R^n.

Therefore, by the result stated at the beginning of the proof, the nonlinear operator W covers some neighborhood of zero in the state space R^n. Hence, by Definition 2 semilinear discrete-time fractional control system (3) is locally controllable in the interval $[0, q]$. This completes the proof.

Now, for the convenience, let us recall some well known (see e.g. (Kaczorek, 2007a, 2007b, 2009; Klamka, 1991, 2002, 2008)) facts from the controllability theory of linear finite-dimensional discrete-time fractional control systems.

Theorem 2. (Klamka, 2008) The fractional discrete-time linear system (4) is globally controllable in q steps if and only if

$$rank\, H_q = n \tag{11}$$

Taking into account the form of controllability matrix, from Theorem 2 immediately follows the simple Corollary.

Corollary 1. (Klamka, 2008) The fractional linear control system (4) is controllable in q steps if and only if $n \times n$ dimensional constant matrix $H_q H_q^T$ is invertible, i.e. there exists the inverse matrix $(H_q H_q^T)^{-1}$.

Corollary 2. The fractional semilinear control system (3) is controllable in q steps if equality (11) holds or equivalently if $n \times n$ dimensional constant matrix $H_q H_q^T$ is invertible, i.e. there exists the inverse matrix $(H_q H_q^T)^{-1}$.

4. EXAMPLE

Let us consider the semilinear fractional discrete-time control system with constant coefficients of the form (3) for $0 \le \alpha \le 1$ with the following matrices and vectors in the difference state equation

$$A = \begin{bmatrix} 1 & 0 \\ 0 & 1 \end{bmatrix}, \quad B = \begin{bmatrix} 0 \\ 1 \end{bmatrix}, \quad f(x,u) = f(x_1, x_2, u) = \begin{bmatrix} e^u - 1 \\ 2\sin x_1 \end{bmatrix} \tag{12}$$

Hence we have

$$f(0,0,0) = \begin{bmatrix} 0 \\ 0 \end{bmatrix}$$

$$F = \frac{d}{dx} f(x_1, x_2, u)\Big|_{\substack{x=0 \\ u=0}} = \begin{bmatrix} 0 & 0 \\ 2 & 0 \end{bmatrix}$$

$$G = \frac{d}{du} f(x_1, x_2, u)\Big|_{\substack{x=0 \\ u=0}} = \begin{bmatrix} 1 \\ 0 \end{bmatrix}$$

Hence we have

$$C = A + F = \begin{bmatrix} 1 & 0 \\ 2 & 1 \end{bmatrix}, \quad D = B + G = \begin{bmatrix} 1 \\ 1 \end{bmatrix}$$

Using formula (6) for $k = 0$ we obtain

$$\Phi_1 = (C + I\alpha)\Phi_0 = \begin{bmatrix} 1+\alpha & 0 \\ 2 & 1+\alpha \end{bmatrix}$$

Controllability matrix (10) for $q = 2$ has the form

$$H_2 = [D, (\Phi_1 D)] = \begin{bmatrix} 1 & 1+\alpha \\ 1 & 3+\alpha \end{bmatrix}$$

Therefore, since $rank\, H_2 = 2 = n$ then taking into account Theorem 2 the fractional associated linear discrete-time system with constant coefficients is globally controllable in two steps, hence by Theorem 1 the semilinear fractional discrete-time system (12) is locally controllable in two steps.

For comparison let us consider linear fractional discrete system (4) with the matrices A and B given equalities (12). In this case using formula (6) for $k = 0$ we have

$$\Phi_1 = (A + I\alpha)\Phi_0 = \begin{bmatrix} 1+\alpha & 0 \\ 0 & 1+\alpha \end{bmatrix}$$

Controllability matrix (10) for $q = 2$ has the form

$$H_2 = [B, (\Phi_1 B)] = \begin{bmatrix} 0 & 0 \\ 1 & 1+\alpha \end{bmatrix}$$

Therefore, since $rank\, H_2 = 1 < n$ then taking into account Corollary 1 the fractional linear discrete-time system with constant coefficients is not globally controllable in two steps and consequently in any number of steps.

5. CONCLUDING REMARKS

In the present paper unconstrained local controllability problem of finite-dimensional fractional discrete-time semilinear systems has been addressed. Using linearization method and solution formula for linear difference equation sufficient condition for unconstrained local controllability in q steps of the discrete-time fractional control system has been established as rank condition of suitably defined con-

trollability matrix. In the proof of the main result certain theorem taken directly from nonlinear functional analysis has been used. Moreover, simple illustrative numerical example has been also presented.

There are many possible extensions of the results given in the paper. First of all it is possible to consider semilinear infinite-dimensional fractional control systems. Moreover, it should be mentioned, that controllability considerations presented in the paper can be extended for fractional discrete-time linear systems with multiple delays both in the controls and in the state variables.

REFERENCES

1. **Kaczorek T.** (2007), Reachability and controllability to zero of positive fractional discrete-time systems, *Machine Intelligence and Robotic Control*, Vol. 6, No. 4, 356-365.
2. **Kaczorek T.** (2007), Rechability and controllability to zero of cone fractional linear systems, *Archives of Control Sciences.* Vol. 17, No. 3, 357-367.
3. **Kaczorek T.** (2009), *Selected Problems of Fractional Systems Theory*, Publishing Department of Białystok University of Technology, Białystok (in Polish).
4. **Klamka J.** (1991), *Controllability of Dynamical Systems*, Kluwer Academic Publishers, Dordrecht.
5. **Klamka J.** (1995), Constrained controllability of nonlinear systems, *IMA Journal of Mathematical Control and Information*, Vol. 12, 245-252.
6. **Klamka J.** (2002), Controllability of nonlinear discrete systems. *International Journal of Applied Mathematics and Computer Science*. Vol. 12, No. 2, 173-180.
7. **Klamka J.** (2008), Controllability of fractional discrete-time systems with delay, *Zeszyty Naukowe Politechniki Śląskiej. Seria: Automatyka*, zeszyt 151, 67-72.
8. **Robinson S. M.** (1986), Stability theory for systems of inequalities. Part II: differentiable nonlinear systems, *SIAM Journal on Numerical Analysis*, Vol. 13, 1261-1275.

Acknowledgement: This paper was supported by NCBR under grant no. O ROO 0132 12.

FPGA BASED ACTIVE MAGNETIC BEARINGS CONTROLLER

Zbigniew KULESZA*

*Faculty of Mechanical Engineering, Bialystok University of Technology, ul. Wiejska 45 C, 15-351 Bialystok

z.kulesza@pb.edu.pl

Abstract: The article discusses main problems of implementing the PID control law in the FPGA integrated circuit. Consecutive steps of discretizing and choosing the fixed-point representation of the continuous, floating-point PID algorithm are described. The FPGA controller is going to be used in the active hetero-polar magnetic bearings system consisting of two radial and one axial bearings. The results of the experimental tests of the controller are presented. The dynamic performance of the controller is better when compared with the dSPACE controller, that was used so far. The designed hardware and software, the developed implementation procedure and the experience acquired during this stage of the whole project are going to be used during the implementation of more sophisticated control laws (e.g. robust) in the FPGA for AMB controllers.

1. INTRODUCTION

Reconfigurable hardware is becoming a promising alternative to both application specific integrated circuit (ASIC) and digital signal processors (DSP) for control applications (Chen and Lin, 2002; Krach et al., 2003; Osornio-Rios et al., 2008). As a reconfigurable hardware, Field Programmable Gate Array, or FPGA, is gaining popularity. FPGA-based systems have been applied in applications ranging from signal processing, image processing, to network processors and robotics, just to name a few. The speed and size of the FPGAs are comparable with the ASICs, but FPGAs are more flexible and their design cycle is shorter because of their reconfigurability. FPGAs applications go beyond the simple implementation of digital logic. They can be used for implementations of specific architectures for speeding up some algorithm. A given algorithm, implemented into FPGA could have 100-1000 times higher performance than its implementation on a DSP or microprocessor. This is because FPGA has a natural parallel architecture for high-speed computation.

Active magnetic bearing (AMB) is a collection of electromagnets used to levitate the object via feedback control (Chiba et al., 2005). The obvious feature of the AMB is a contact-free motion control, which leads to lower rotating losses, higher speeds, elimination of lubrication system, and long life. Since an active magnetic bearing is inherently nonlinear and unstable, feedback control is indispensable to stabilize the system. A conventional PID controller is often employed as a feedback compensator and this method often yields enough stability and performance. This technique works efficiently as long as the system remains in the vicinity of the linearizing point and the uncertainties and disturbances are small. More sophisticated methods, including robust control, can improve the dynamic properties of the AMB system, especially in case of strong nonlinearities (Gosiewski and Mystkowski, 2008; Hung et al., 2003).

The view of the examined hetero-polar AMB system (Gosiewski and Mystkowski, 2008) is presented in Fig. 1. The rotor is supported by two radial and one axial magnetic bearings. The bearings include the necessary position sensors and power amplifiers. The magnetic force along each axis is generated by a pair of opposing electromagnets. The displacements of the shaft along axes are measured by five eddy-current sensors.

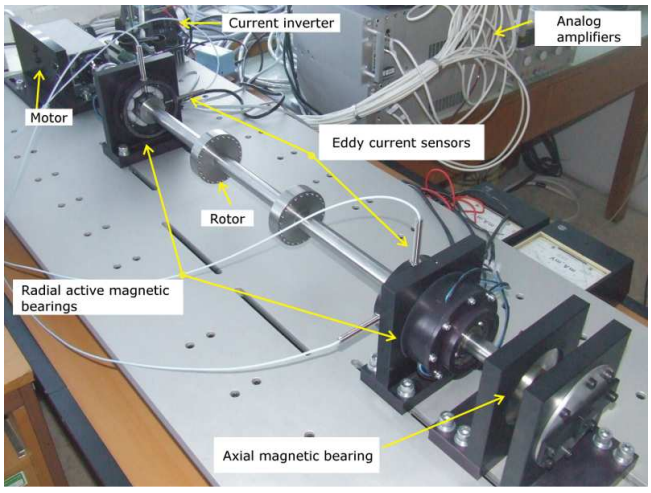

Fig. 1. View of the active magnetic bearing system

The aim of this paper is to discuss the problems of implementation of the PID algorithm for the AMB system in the FPGA. This task is a part of a bigger project concerning the design of an electromechanical flywheel energy storage. The flywheel is going to levitate in active magnetic bearing system and one of the tasks here is to design a stand-alone, FPGA-based controller. The implementation of the PID algorithm is the first stage of the design of such controller. The next will be the implementation of more sophisticated control laws, H_∞ robust, for example.

2. REQUIREMENTS

The controller should have five separate control channels to control each axis of the whole AMB system. Since the measured and control signals are analog, necessary A/D and D/A converters must be designed. The signals can change from -10 V to +10 V. The PID algorithm must be based on integer or fixed-point mathematics. This is because the FPGA used in this project has 400,000 gates and no floating point unit. Certainly, it is also possible to implement the floating point mathematics in the FPGA but this would absorb almost all its resources.

3. HARDWARE

The PID controller for the AMB system is designed with the use of two Spartan-3 LC Development Boards from Memec (2004). Spartan-3 LC board is equipped with Xilinx Spartan-3 family, XC3S400-4 PQ208CES, FPGA chip (Spartan-3, 2006). The FPGA has 400,000 gates and this is quite enough to implement three PID controller algorithms. The chip has sixteen configurable, 18-bit embedded multipliers, sixteen, 18-kbit embedded RAM blocks and two hundred and sixty four user defined input/output signals. The Spartan-3 LC board utilizes the Xilinx XCF02S Platform Flash In-System Programmable (ISP) PROM, allowing designers to store an FPGA design in non-volatile memory.

Fig. 2. Active magnetic bearings controller hardware

The board is also equipped with two push-button and four slide switches, two LEDs, one seven-segment LED display, RS232 and USB ports and two P160 connectors. FPGA can be clocked with external 50 MHz clock. There are no A/D or D/A converters on the board so we were forced to design the external converters board and power supplies for them and the whole controller. We designed and made five A/D and D/A converters boards – one for each channel of the controller. This additional boards communicate with the Spartan-3 LC board through P160 connectors and expansion boards. Each of the five boards is made of one AD976 analog to digital 16-bit converter and one two-channel AD5547 digital to analog 16-bit converter from Analog Devices (16-Bit, 100 kSPS/200 kSPS BiCMOS A/D Converters AD976/AD976A, 1999; Dual Current Output, Parallel Input, 16-/14-Bit Multiplying DACs with 4-Quadrant Resistors AD6647/AD5557, 2004). The sampling frequency of the converters is limited to 200 kSPS.

The view of the disassembled hardware of the AMB controller is shown in Fig. 2.

4. CONTROLLER ALGORITHM IMPLEMENTATION

4.1. Difference recurrence equation

The following transfer function of the PID controller has been adopted for the AMB controller:

$$G(s)=\frac{Y(s)}{U(s)}=k_p\left(1+\frac{1}{T_i s}+\frac{T_d s}{Ts+1}\right), \tag{1}$$

where parameters k_p, T_i, T_d, T can change in the following ranges:

$k_p = 0.1,\ldots,10.0$, $T_i = 0.01,\ldots,2.0$,

$T_d = 0.001,\ldots,0.05$, $T = 0.00001,\ldots,1.0$.

For further calculations, we will assume, that $k_p = 1{,}5$; $T_i = 0{,}1$; $T_d = 0{,}001$; and $T = 0{,}0001$. Transfer function, (Eq. 1) can be transformed to the following form:

$$G(s)=\frac{Y(s)}{U(s)}=\frac{a_2 s^2+a_1 s+a_0}{b_2 s^2+b_1 s+b_0}, \tag{2}$$

where: $a_2 = k_p T_i (T_d + T)$, $a_1 = k_p (T_i + T)$, $a_0 = k_p$, $b_2 = T_i T$, $b_1 = T_i$, $b_0 = 0$.

Transfer function (Eq. 2) can be also transformed to the following linear differential equation:

$$b_2\frac{d^2y}{dt^2}+b_1\frac{dy}{dt}+b_0 y=a_2\frac{d^2u}{dt^2}+a_1\frac{du}{dt}+a_0 u\,. \tag{3}$$

In order to avoid hazards that could arise in the combinatorial system, the controller algorithm should be realized as the synchronic digital system, this is the subsequent calculation steps should be taken in accordance with the clock signal. To realize this, Eq. (2) must be converted to the difference recurrence equation and discretized with the constant sample period h. The discretization process involves determining the difference representations of the subsequent differentials. Below are given the formulas for the first and second differentials of some continuous, differentiable function $x(t)$.

$$\frac{dx}{dt}\approx\frac{x(i)-x(i-1)}{h}, \tag{4}$$

$$\begin{aligned}\frac{d^2x}{dt^2}&=\frac{\frac{dx(i)}{dt}-\frac{dx(i-1}{dt}}{h}\\&\approx\frac{\frac{x(i)-x(i-1)}{h}-\frac{x(i-1)-x(i-2)}{h}}{h}\\&=\frac{x(i)-2x(i-1)+x(i-2)}{h^2}\end{aligned}. \tag{5}$$

After using the above formulas (Eqs. 4 and 5) for the first and second differentials of functions $y(t)$ and $u(t)$, Eq. 3 can be written as follows:

$$\begin{aligned} &B_2 y(i-2)+B_1 y(i-1)+B_0 y(i) \\ &\quad = A_2 u(i-2)+A_1 u(i-1)+A_0 u(i) \end{aligned}, \tag{6}$$

where:

$$A_0 = \frac{a_2}{h^2}+\frac{a_1}{h}+a_0,\ A_1 = -2\frac{a_2}{h^2}-\frac{a_1}{h},\ A_2 = \frac{a_2}{h^2},$$

$$B_0 = \frac{b_2}{h^2}+\frac{b_1}{h}+b_0,\ B_1 = -2\frac{b_2}{h^2}-\frac{b_1}{h},\ B_2 = \frac{b_2}{h^2}.$$

In order to calculate the value of the output signal $y(i)$ for the i-th time step, Eq. 6 should be written in the following recurrence form:

$$\begin{aligned} y(i) = c_1 y(i-1)+c_2 y(i-2)+c_3 u(i) \\ +c_4 u(i-1)+c_5 u(i-2) \end{aligned}, \tag{7}$$

where:

$$c_1 = -\frac{B_1}{B_0} = \frac{h+2T}{h+T},\ c_2 = -\frac{B_2}{B_0} = \frac{-T}{h+T},$$

$$c_3 = \frac{A_0}{B_0} = \frac{k_p(T_i T + T_i h + Th + T_d T_i)}{T_i(h+T)},$$

$$c_4 = \frac{A_1}{B_0} = \frac{-k_p(2T_i T + T_i h + Th + 2T_d T_i)}{T_i(h+T)},$$

$$c_5 = \frac{A_2}{B_0} = \frac{k_p(T+T_d)}{h+T}.$$

For the above given k_p, T_i, T_d, T parameters, we obtain: $c_1 = 1{,}952;\ \ c_2 = -0{,}952;\ c_3 = 15{,}780;\ c_4 = -31{,}489;\ c_5 = 15{,}708.$

Equation 7 allows us to calculate the output signal $y(i)$ on the basis of the actual values of the input signal $u(i)$ and the previous values of the output $y(i-1)$, $(i-2)$, and the input $u(i-1)$, $u(i-2)$ signals.

In case of hetero-polar AMB system the output signal $y(i)$ should be summed with the so called steady-state point signal $y_0(i)$ (Gosiewski and Mystkowski, 2008). This means that the PID controller should generate two output signals $y_1(i)$ and $y_2(i)$ (see Fig. 11) calculated in the following way:

$$y_1(i) = y_0(i)+y(i),\quad y_2(i) = y_0(i)-y(i), \tag{8}$$

where $y_0(i)$ is the steady-state point signal that is proportional to the steady-state point current i_0.

4.2. Fixed-point representation of the signals and parameters

As was mentioned above, the controller algorithm (Eqs. 7 and 8) should be calculated using the fixed-point numbers. To do this we should choose the fixed-point representation of input signal $u(i)$, output signals $y(i)$, $y_1(i)$, $y_2(i)$ and parameters $c_1, \ldots, c_5$. It is especially true for output $y(i)$ and parameters $c_1, \ldots, c_5$ as the bit-widths of signals $u(i)$ and $y_1(i)$, $y_2(i)$ are determined by the bit resolution of the A/D and D/A converters which are $w_u = 16$ and $w_y = 16$ in this case. By conducting many simulation experiments for the controller algorithms written in the floating- and fixed-point representations it was established that in order to achieve the satisfactory accuracy the following widths should be used:

$w_c = 52$, $w_{fc} = 42$ for parameters $c_1, \ldots, c_5$,

$w_u = 16$, $w_{fu} = 0$ for input signal $u(i)$,

$w_y = 52$, $w_{fy} = 35$ for output signal $y(i)$,

$w_{y_1} = 16$, $w_{fy_1} = 0$ and $w_{y_2} = 16$, $w_{fy_2} = 0$

for output signals $y_1(i)$ and $y_2(i)$.

In the above given formulas the notation $w_c = 52$, $w_{fc} = 42$ means for example that the width of the fractional part of the parameter c_1 is 42 bits, the width of its integral part is 10 bits and the whole width (integral and fractional) is 52 bits.

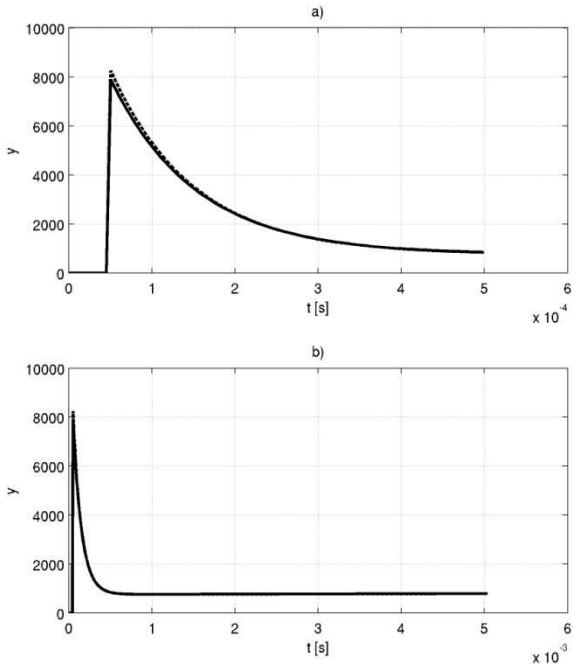

Fig. 3. Step response of the floating-point (continuous line) and the fixed-point (dashed line) representations of the PID AMB controller: a) simulation time $t = 5 \times 10^{-4}$ s, b) simulation time $t = 5 \times 10^{-3}$ s; sample period$h = 5{,}04 \times 10^{-6}$s

As we can see the output signal $y(i)$ is represented with the use of 52 bits from which 35 are used to represent its fractional part, but this is true only when calculating its value according to Eq. 7. When calculating outputs y_1 and y_2 according to Eq. 8, only 16-bit integral part of y is used. This signal is obtained by cutting off the fractional part of signal y.

Input $u(i)$ and output $y(i)$, $y_1(i)$, $y_2(i)$ signals as well as controller parameters $c_1, \ldots, c_5$ can have negative values and they are coded using the two's complement notation in which the most significant bit is the sign bit. In the hexadecimal notation that is used during coding the controller algorithm in VHDL the calculated values of the parameters are as follows:

`c1=x"007CEDDE131B8"`, `c2=x"FFC31221ECE48"`, `c3=x"03F1F140357E2"`, `c4=x"F820B9FEC6256"`, `c5=x"03ED54D03B45A"`.

Step responses of the PID controller in floating- and fixed-point representations for the above given bit-widths and various simulation times, obtained in Matlab with the use of the Fixed-Point Toolbox, are shown in Fig. 3.

4.3. 52-bit fixed-point multiplier

As we can see from Eq. 7 the calculations of the controller algorithm involve 4 summations of 104-bit wide and 5 multiplications of 52-bit wide fixed-point numbers. The multiplication can be implemented in the FPGA in various ways. The simplest is by using the basic resources, these are the so called Control Logic Blocks (CLBs). This method is also the most resource-consuming. The basic resources of the XC3S200 chip do not allow to realize even one such 52-bit operation. This is why it was decided to use the specialized 18-bit multiplication blocks embedded in the XC3S200 [8]. As we established the implementation of the 52-bit multiplication requires nine 18-bit wide embedded multiplication blocks. The whole operation is coded in VHDL using the MULT18x18 components and is placed in the mult03 entity.

To illustrate the problem the subsequent operations of the exemplary 50-bit and 40-bit wide numbers multiplication taken by 18-bit multipliers are shown in Fig. 4 (first bit is omitted as it is responsible for the sign only).

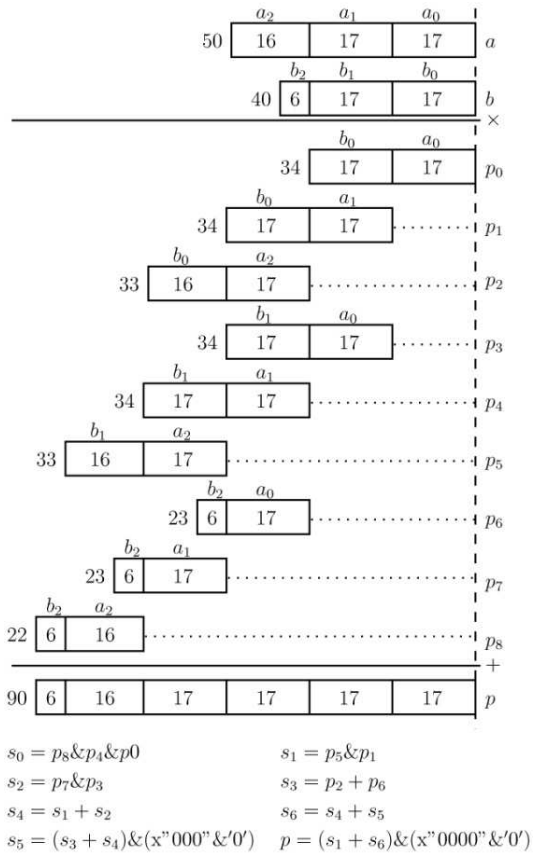

Fig. 4. Subsequent operations of the 50-bit and 40-bit wide numbers multiplication

4.4. Controller architecture

Control system for two radial and one axial AMB bearings consists of two Spartan-3 LC development boards. The first board is connected with three A/D and D/A converters boards and the second – with two A/D and D/A boards. The VHDL project for each XC3S400 FPGA consists of three PID controller cores divided into three separate channels. One of the channels is not used. That is why the whole control system for the AMBs consisits of five separate PID control channels. Although each controller runs the same PID algorithm (as of Eqs. 7, 8), the parameters k_p, T_i, T_d, T can be quite different.

Schematic diagram of the designed AMB control system is shown in Fig. 5.

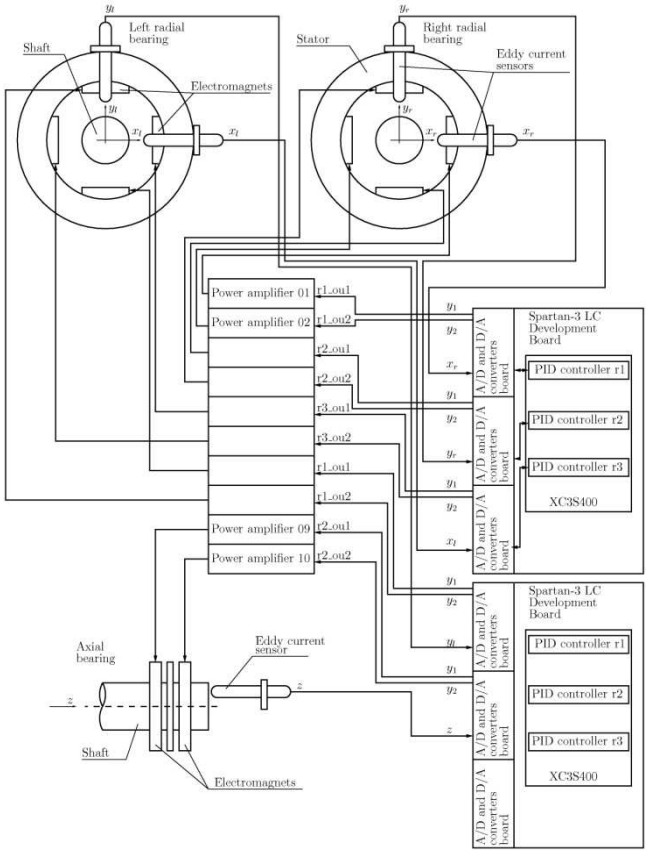

Fig. 5. Schematic diagram of the AMB control system

5. TEST RESULTS

The designed hetero-polar AMB PID controller was tested using Agilent 33220A 20MHz signals generator and Agilent 54624A oscilloscope. The resulting step responses of the controller itself (with no control loop) are shown in Figs. 6 and 7. The parameters are: $k_p = 2$; $T_i = 0{,}02$; $T_d = 0{,}001$; and $T = 1$.

The Bode plots for the first channel of the designed controller are shown in Fig. 8. The experimental characteristic has been obtained with the use of Agilent 35670A dynamic signals analyzer and compared with the simulation characteristic obtained in Matlab for the floating-point model

(Eq. 1). As we can see the magnitude plots coincide accurately. The experimental phase plot drops almost to -90^o for higher frequencies what means that there is some delay in the controller. This delay is caused by the low sampling frequency of the A/D converter. Nevertheless, the dynamic properties of the designed controller for the frequency range from 10 Hz to 1 kHz that is typical for AMB control, are very good.

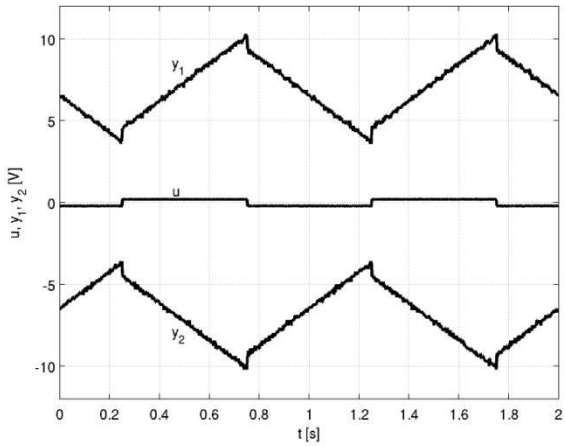

Fig. 6. Step responses y_1 and y_2 of the controller to the square input u of 1 Hz frequency and 50 mV amplitude

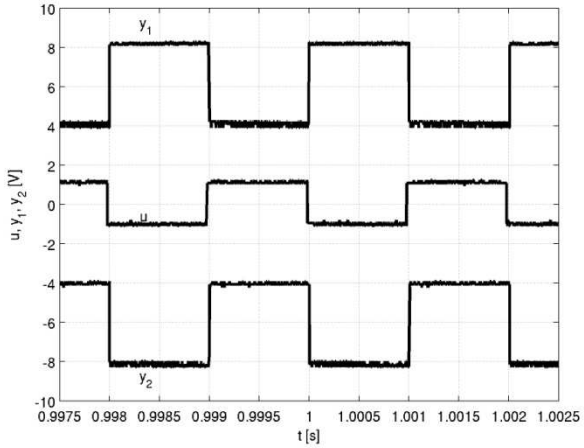

Fig. 7. Step responses y_1 and y_2 of the controller to the square input u OF 500 Hz frequency and 2 V amplitude

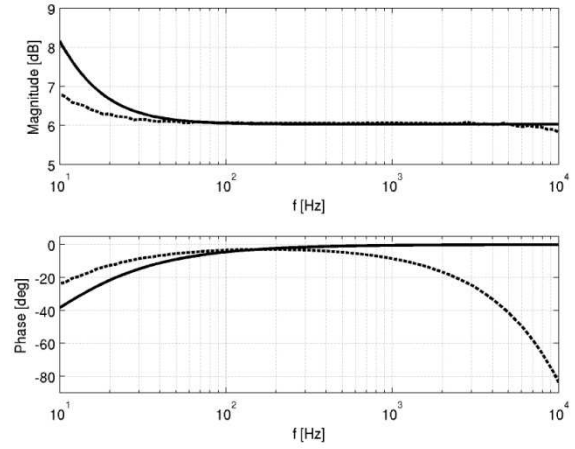

Fig. 8. Bode plots of the designed PID controller: simulation (continuous line) and experimental (dashed line)

The next step of the experimental investigations was to test the designed controller in the closed-loop AMB control system. Fig. 9 presents displacements x_l, y_l and Fig. 10 displacements x_r, y_r of the shaft in the left and the radial bearing at the moment of switching the controller on. The reference values for the displacements were as follows: $x_{lref} = -0{,}28\text{V}$, $y_{lref} = -0{,}25\text{V}$, $x_{rref} = -0{,}78\text{V}$, $y_{rref} = -0{,}39\text{V}$. As we can see, after a very short transient stage the controller levitates the shaft in bearings very well.

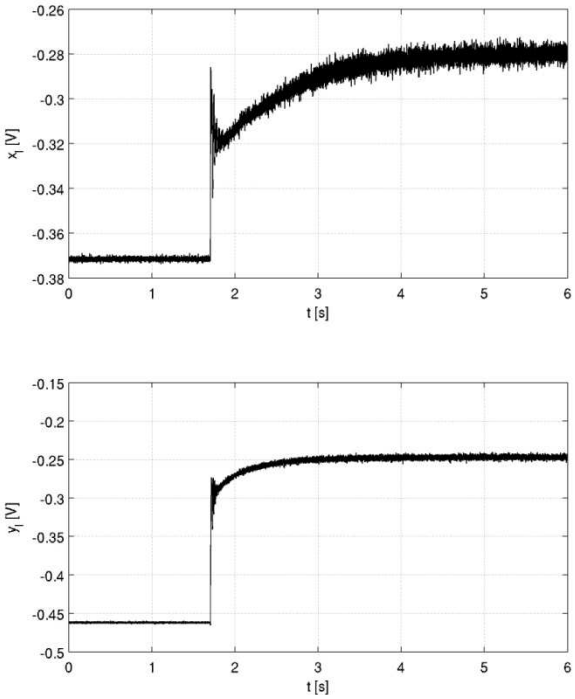

Fig. 9. Displacements x_l, y_l of the shaft in the left radial bearing

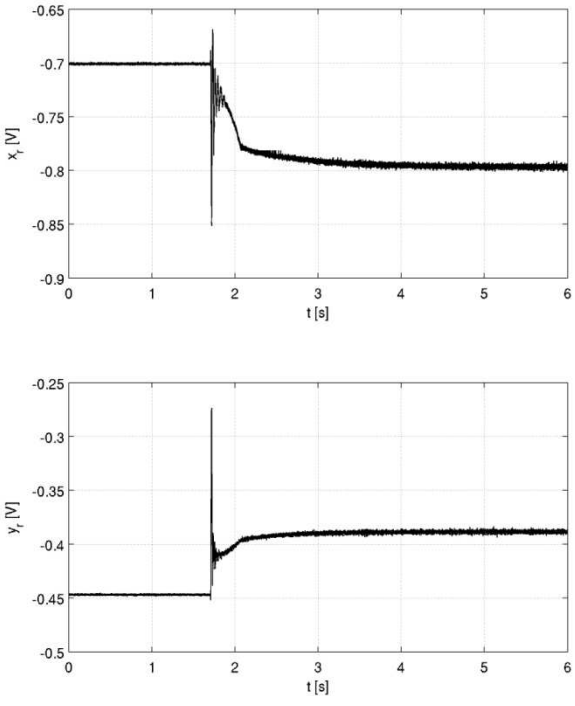

Fig. 10. Displacements x_r, y_r of the shaft in the right radial bearing

Fig. 12 presents displacements y_l and y_r of the shaft after summing output signals y_1, y_2 of the controller with a pulse-like disturbance signal y_d as it is shown in Fig. 11. We can see a good damping of the disturbances.

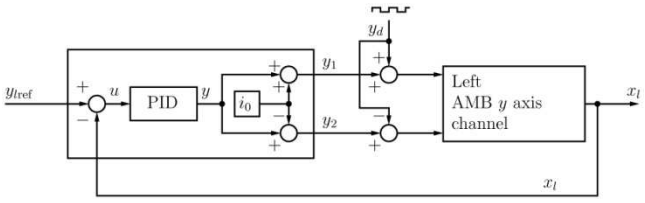

Fig. 11. Control loop of the left bearing y axis with disturbances

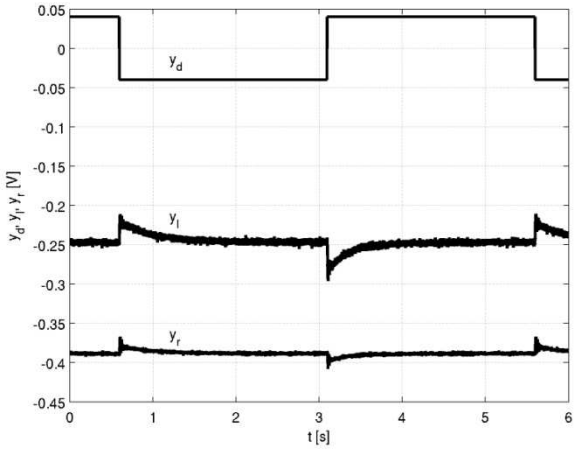

Fig. 12. Vertical displacements x_l, y_r of the shaft in both bearings with disturbance signal y_d

6. CONCLUSION

The designed hetero-polar AMB PID controller completely fulfills the preliminary requirements. It implements the PID control law in five separate control loops realized in two XC3S400 FPGAs. The FPGA resources are utilized in less than 50 percents. The dynamic performance of the controller is very good. The controller is about 20 times quicker when compared with the dSPACE controller that was used in the AMB system so far.

The main bottleneck of the controller is the low frequency of the A/D and D/A converters. The FPGA can be clocked with the very high frequency of 50 MHz and the output signal of the controllers can be calculated with this frequency too. Unfortunately this signal is updated with the frequency of 200 kHz only.

The controller can be improved by designing better A/D and D/A boards with quicker converters and by implementing better control laws.

REFERENCES

1. **16-Bit,** 100 kSPS/200 kSPS BiCMOS A/D Converters AD976/AD976A, (1999). Analog Devices technical data sheet.
2. **Chen J-S., Lin I-D.,** (2002), Toward the implementation of an ultrasonic motor servo drive using FPGA. *Mechatronics*, Vol. 12, 511-524.
3. **Chiba A., Fukao T., Ichikawa O., Oshima M., Takemoto M., Dorrel D.,** (2005), *Magnetic bearings and bearingless drives,* first ed., Newnes.
4. **Dual** Current Output, Parallel Input, 16-/14-Bit Multiplying DACs with 4-Quadrant Resistors AD6647/AD5557, (2004). Analog Devices technical data sheet.
5. **Gosiewski Z., Mystkowski A.,** (2008), Robust control of active magnetic suspension: analytical and experimental results. *Mechanical Systems and Signal Processing*, Vol. 22, No 6, 1297-1303.
6. **Hung J. Y., Albritton N. G., Xia F.,** (2003), Nonlinear control of a active magnetic bearing system. *Mechatronics*, Vol. 13, 621-637.
7. **Krach F., Frackelton B., Carletta J., Veilette R.,** (2003), *FPGA-based implementation of digital control for a magnetic bearing.* American Control Conference'2003; June 4-6, Vol. 2, 1080-1085.
8. **Memec** Spartan-3 LC User's Guide, (2004). Memec Design; June 14.
9. **Osornio-Rios R. A., Romero-Troncoso R. J., Herrera-Ruiz G., Castaneda-Miranda R.,** (2008), The application of reconfigurable logic to high speed CNC milling machines controllers. *Control Engineering Practice*, Vol. 16674-684.
10. **Spartan-3** FPGA Family, (2006): Complete Data Sheet. Xilinx technical data sheet; April.

This research was supported by the grant No PBZ-KBN-109/T-10/2004 from the Ministry of Science and Higher Education, Poland.

APPROXIMATION OF FRACTIONAL DIFFUSION-WAVE EQUATION

Wojciech MITKOWSKI*

*Department of Automatics, Faculty of Electrical Engineering, Automatics, Computer Science and Electronics, AGH University of Science and Technology, Al. Mickiewicza 30/B-1, 30-059 Kraków, Poland

wojciech.mitkowski@agh.edu.pl

Abstract: In this paper we consider the solution of the fractional differential equations. In particular, we consider the numerical solution of the fractional one dimensional diffusion-wave equation. Some improvements of computational algorithms are suggested. The considerations have been illustrated by examples.

1. INTRODUCTION

Development of fractional calculations have been done probably by Leibniz and Newton (in the years 1695-1822). Further mathematical fractional calculus and its applications have been formulated in the nineteenth century. Due to the development of IT tools in recent years, many authors come back to the problems of fractional dynamic systems (e.g. Lubich, 1986; Weilbeer 2005; Kilbas et. al., 2006; Sabatier et. al., 2007; Ostalczyk, 2008; Kaczorek, 2009, 2011a,b,c; Busłowicz, 2010). For instance, interesting results (important for applications) were obtained in Bialystok University of Technology (Busłowicz, 2008; Nartowicz, 2011; Ruszewski, 2009; Sobolewski and Ruszewski, 2011; also Kaczorek, 2011; Trzasko, 2011). Numerical methods for fractional systems were developed (e.g. Lubich, 1986; Podlubny et al., 1995; Podlubny, 2000; Agrawal, 2002; Diethelm and Walz, 1997; Diethelm et al., 2002; Weilbeer, 2005; Ciesielski and Leszczynski, 2006; Murillo and Yuste, 2009, 2011).

The paper is organized as follows. In the sections 2 and 3 we considered Caputo fractional differential equation and its approximation. Fractional diffusion-wave equation and its approximation is considered in the sections 4 and 5 respectively.

2. FRACTIONAL DIFFERENTIAL EQUATION

Fractional order differential equations are associated with the following operators (Weilbeer, 2005; Kaczorek, 2011): D^{α} – Riemann-Liouville operator (~1837), D_{GL}^{α} – Grünwald-Letnikov (~1867) operator and D_{*}^{α} – Caputo operator (1967).

Dynamical systems are generated by differential equations. For example consider the initial value problem (fractional differential equation of Caputo type):

$$D_{*}^{\alpha}u(t) = \lambda u(t), u(0) = 1, u^{(k)}(0) = 0, \quad (1)$$

$k = 1, 2, \dots, n-1$

where $\alpha > 0$, $\lambda \in R$, $n = [\alpha] = \min\{\xi \in N: \xi \geq \alpha\}$, N is a set of natural numbers and D_{*}^{α} is the Caputo fractional differential operator.

The solution of the initial value problem (1) is given by (Weilbeer, 2005)

$$u(t) = E_{\alpha}(\lambda t^{\alpha}),\ t \geq 0 \quad (2)$$

where

$$E_{\alpha}(z) = 1 + \frac{z}{\Gamma(1+\alpha)} + \frac{z^2}{\Gamma(1+2\alpha)} \dots = \sum_{k=0}^{kk=\infty} \frac{z^k}{\Gamma(1+k\alpha)} \quad (3)$$

is the Mittag-Leffler function with one parameter α. In eqaution (3) $\Gamma(\alpha)$ denote Euler's continuous gamma function

$$\Gamma(\alpha) = \int_0^{\infty} t^{\alpha-1}e^{-t}dt = \int_0^1 (ln\left(\frac{1}{t}\right))^{\alpha-1}dt. \quad (4)$$

General Euler's gamma function is defined in the whole complex plane except zero and negative integers (Weilbeer, 2005). Formula (4) is true for $\mathrm{Re}\alpha > 0$ and the following limit holds

$$\Gamma(\alpha) = \lim_{n\to\infty} \frac{n!n^{\alpha}}{\alpha(\alpha+1)(\alpha+2)\dots(\alpha+n)}. \quad (5)$$

For natural arguments and for half-integer arguments Euler's gamma function has the special form

$$\Gamma(n) = (n-1)!,\ \Gamma\left(\frac{n}{2}\right) = \frac{(n-2)!!\sqrt{n}}{2^{(n-1)/2}}, \lambda \in R \quad (6)$$

$n \in N = \{1, 2, 3, \dots\}$

where $n!!$ is the double factorial

$$n!! = \begin{cases} n \cdot (n-2) \dots 5 \cdot 3 \cdot 1 & n > 0\ odd \\ n \cdot (n-2) \dots 6 \cdot 4 \cdot 2 & n > 0\ even \\ 1 & n = 0, -1 \end{cases} \quad (7)$$

Example 1. Consider differential equation (1). From (1), (2) and (3), (6) for $\alpha = 1$ and $\alpha = 2$ we have respectively

$$E_1(\lambda t) = e^{\lambda t}, E_2(\lambda t^2) = \cos(\sqrt{|\lambda|}t), \lambda < 0. \quad (8)$$

3. CAPUTO FRACTIONAL DIFFERENTIAL EQUATION AND ITS APPROXIMATION

The Caputo fractional differential operator of order $\alpha > 1$ is defined by (e.g. Kaczorek 2011a, Weilbeer, 2005)

$$D_{*}^{\alpha}u(t) = \frac{1}{\Gamma(n-\alpha)}\int_0^t (t-s)^{n-\alpha-1}u^{(n)}(s)ds, \quad (9)$$

where $n = [\alpha] = \min\{\xi \in N: \xi \geq \alpha\}$.

Now we consider fractional differential equation of order $\alpha > 1$ of Caputo type

$$D_*^\alpha u(t) = f(u(t)), D^k u(0) = b_k, \quad (10)$$

$k = 0, 1, \dots, n-1$
where $b_k \in R$ are given. We are interested in a numerical solution $u(t)$ of equation (10) on a closed interval $[0, T]$ for some $T > 1$. Therefore, we assume that

$$t_m = m\tau, \tau > 0, m = 0, 1, 2, \dots, N$$
and $t_0 = 0$, $t_n = T$, $N = \frac{\tau}{T}$. (11)

Furthermore we denote by $u_m = u(t_m)$ and $f_m = f(u_m)$. Precisely u_m is the approximation of $u(t_m)$. From equality (10) for $t = t_m$ we obtain a discrete problem (Weilbeer, 2005; Murillo and Yuste, 2009, 2011)

$$\frac{1}{\tau^2}\Big[u_m - \sum_{k=1}^m \omega_k u(t_m - k\tau) + \Big(\frac{m^{-\alpha}}{\Gamma(m-\alpha)}\Big) u_0 - \sum_{k=0}^{n-1} \frac{b_k t_m^{k-\alpha}}{\Gamma(k+1-\alpha)}\Big] = f_m, \quad (12)$$

$m = 1, \dots, N$

Note that $t_m - k\tau = t_{m-k}$. Consistently with (12) we obtain

$$u_m = \sum_{k=1}^m \omega_k u_{m-k} - \Big(\frac{m^{-\alpha}}{\Gamma(m-\alpha)} - \sum_{j=0}^m \omega_j\Big)\, u_0 + \sum_{k=0}^{n-1} \frac{b_k t_m^{k-\alpha}}{\Gamma(k+1-\alpha)} + \tau^2 fm, \quad (13)$$

$\boldsymbol{m = 1, 2, \dots, N}$
where

$$\omega_k = (-1)^k \binom{\alpha}{k}, \quad (14)$$

$$\binom{\alpha}{k} = \frac{(-1)^{k-1}\Gamma(k-\alpha)}{\Gamma(1-\alpha)\Gamma(k+1)} = \frac{\alpha(\alpha-1)(\alpha-2)\dots(\alpha-k+1)}{k!}$$

$\alpha \in R$, $\alpha \in N_0 = \{0, 1, 2, \dots\}$.

Example 2. We consider equation (1) with $u(0) = u_0$. In this case $f_m = \lambda u_m$. Therefore from (13) we obtain the following discrete equation (numerical solution of equation (1))

$$u_m = \frac{1}{1-\lambda\tau^2}\Big\{\sum_{k=1}^m \omega_k u_{m-k} - \Big(\frac{m^{-\alpha}}{\Gamma(m-\alpha)} - \sum_{j=0}^m \omega_j\Big) u_0 + \frac{(m\tau)^{-\alpha}}{\Gamma(1-\alpha)} u_0\Big\} \quad (15)$$

$m = 1, 2, \dots, N$

In this case we can use the following formula for the $\Gamma(\alpha)$, $\alpha \in C\{0, -1, -2, \dots\}$, C is a set of complex numbers,

$$\frac{1}{\Gamma(\alpha)} = \alpha e^{\gamma\alpha} \prod_{n=1}^\infty (1 + \frac{\alpha}{n}) e^{-\alpha/n} \quad (16)$$

where γ is the Euler's constant (Weilbeer, 2005)

$$\gamma = \lim_{n\to\infty}(\sum_{k=1}^n \frac{1}{k} - \ln(n)) \approx 0{,}5772156649. \quad (17)$$

4. FRACTIONAL DIFFUSION-WAVE EQUATION

Let $u(x, t)$ be a function, $x \in [0, L]$ and $t \in [0, T]$. Denote by $D_{t,*}^\alpha$ the Caputo fractional differential operator at the variable t (see (9)). Consider the continuous-time fractional diffusion-wave system described by equation

$$D_*^\alpha u(x, t) = \frac{\partial^2}{\partial x^2} u(x, t) \quad (18)$$

with initial and boundary conditions

$$u(x, 0) = \varphi(x), u_t(x, 0) = 0 \quad (19)$$

$$u(0, t) = 0, u(L, t) = 0. \quad (20)$$

The solution of the homogeneous boundary problem (18), 19), (20) is given by (Weilbeer, 2005)

$$u(x, t) = \frac{2}{L}\sum_{k=1}^\infty c_k E_\alpha(-\frac{k^2\pi^2}{L^2} t^\alpha)\sin(\frac{k\pi}{L} x), \quad (21)$$

$$c_k = \int_0^L \varphi(x) sin(\frac{k\pi}{L} x) dx$$

Equation (18) for $\alpha = 1$ is the classical diffusion equation and for $\alpha = 2$ is the classical wave equation. Thus (18) for $\alpha \in (0, 2]$ is the diffusion-wave eqution. The fractional diffusion-wave equation plays an intermediate role between classical wave and diffusion equations (Weilbeer, 2005; Jafari and Momani, 2007; Povstenko, 2011; Murillo and Yuste, 2009, 2011).

Example 3. For $\alpha = 1$ and $\alpha = 2$ we obtain respectively

$$E_1\Big(-\frac{k^2\pi^2}{L^2} t\Big) = \exp(-\frac{k^2\pi^2}{L^2} t) \quad (22)$$
$$E_2\Big(-\frac{k^2\pi^2}{L^2} t\Big) = \cos(\frac{k\pi}{L} t)$$

Therefore using (22) from (21) for $\alpha = 1$ and $\alpha = 2$ we obtain the solution of classical diffusion equation and the solution of classical wave equation respectively.

5. APPROXIMATION OF FRACTIONAL DIFFUSION-WAVE EQUATION

Let $h = L/M$ and $\tau = T/N$ (see (19)) denote the step size of the discretization in the space and time axis respectively. Next let

$$\mathrm{x_i} = \mathrm{ih}, \mathrm{i} = 0, 1, \dots \mathrm{M} \quad (23)$$

and using the discretization on the space axis, the second derivative can be approximated by the central difference of second order

$$\frac{\partial^2}{\partial x^2} u(\mathrm{x_i}, t) \approx \frac{1}{h^2}[u(\mathrm{x_{i-1}}, t) - 2u(\mathrm{x_i}, t) + u(\mathrm{x_{i-1}}, t)] \quad (24)$$

$i = 1, 2, \dots, M-1$,
where from (20) $\mathrm{x_0} = \mathrm{x}_M = 0$. From (18) for $x = \mathrm{x_i}$ and (24) we have

$$D_{t,*}^\alpha u(\mathrm{x_i}, t) = \frac{1}{h^2}[u(\mathrm{x_{i-1}}, t) - 2u(\mathrm{x_i}, t) + u(\mathrm{x_{i-1}}, t)] \quad (25)$$

$i = 1, 2, \dots, M-1$

Let $t = t_m = m\tau$, $\tau > 0$, $m = 0, 1, 2, \dots, N$, where $N = \tau/T$. Thus from (25) and (13) we obtain

$$u_m(\mathrm{x_i}) - \frac{\tau^2}{h^2}[u_m(\mathrm{x_{i-1}}, t) - 2u_m(\mathrm{x_i}, t) + u_m(\mathrm{x_{i-1}}, t)] = z(u_{m-1}(\mathrm{x_i}) u_{m-2}(\mathrm{x_i}), \dots, u_0(x_i)),$$

$$z(u_{m-1}(\mathrm{x_i}) u_{m-2}(\mathrm{x_i}), \dots, u_0(x_i)) = \sum_{k=1}^m \omega_k u_{m-k}(\mathrm{x_i}) - \Big(\frac{m^{-\alpha}}{\Gamma(m-\alpha)} - \sum_{j=0}^m \omega_j\Big) u_0(x_i) + \sum_{k=0}^{n-1} \frac{b_k(\mathrm{x_i}) t_m^{k-\alpha}}{\Gamma(k+1-\alpha)} \quad (26)$$

$m = 1, 2, \dots, N$, $i = 1, 2, \dots, M-1$
where $u_m(x_i) = u(x_i, t_m)$. Let $Z = [z(x_i)]$ be vector $(M-1) \times 1$. Let $U_m = [u_m(x_i)]$ be vector $(M-1) \times 1$, $i = 1, 2, \dots, M-1$. Denote by $A = [\alpha_{ki}]$ tridiagonal matrix

$(M-1)\times(M-1)$ with $\alpha_{kk}=-2,\ \alpha_{k,k-1}=1, \alpha_{k,k+1}=1$. From (26) we have

$$U_m=\left[I-\frac{\tau^2}{h^2}A\right]^{-1}Z \tag{27}$$

At the time-step t_m, $m=1,2,\ldots,N$, the values for $u_m(x_i)=u(x_i,t_k)$, for $i=0,1,\ldots,M$ and $k=0,1,\ldots,m-1$ are known (in (27) Z is known).

6. NUMERICAL EXAMPLES

Example 4. A very simple approximation of the system (25) can be the equation (1) with suitably chosen parameter λ. For fixed $x=x_i$ the nature of the function $u(x_1,t)$ will be similar to the solution $u(t)$ of the system (1). Thus, in this paper we will present only the simulation of solutions of equation (1). In the calculations formula (3) and the Matlab Gamma function were used.

Let us consider the system (1). Let $kk=20$ (see (3)). In Fig. 1 trajectories $u(t)$ for $\lambda=-1$ and $\alpha=0{,}5$ (solid line), $\alpha=1$ (dotted line) are shown. In Fig. 2 trajectories $u(t)$ for $\lambda=-10$ and $\alpha=1{,}5$ (solid line), $\alpha=2$ (dotted line) are shown.

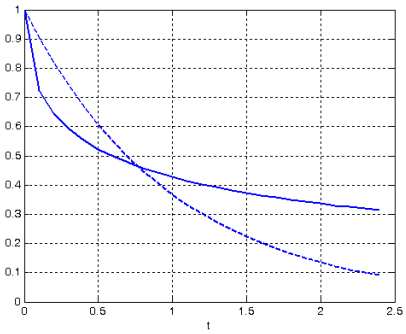

Fig. 1. Trajectories of the system (1) for $\alpha=0{,}5$ (solid line), $\alpha=1$ (dotted line)

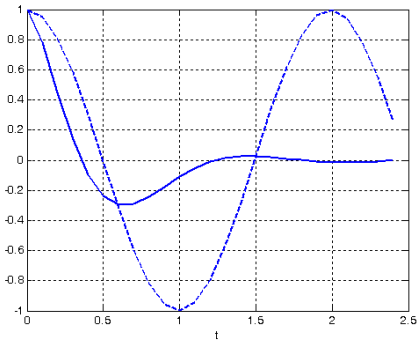

Fig. 2. Trajectories of the system (1) for $\alpha=1{,}5$ (solid line), $\alpha=1{,}2$ (dotted line)

Example 5. Consider the continuous-time fractional diffusion-wave system (18) with initial and boundary conditions (19), (20). The solution of the homogeneous boundary problem (18), (19), (20) is given by (21). In the calculations the Matlab Gamma function and the Matlab Mittag-Leffler function (Podlubny and Kacenak 2001) were used.

Let $L=\pi$ and $kk=40$, $\tau=0{,}1$; $h=0{,}0314$. Let $\varphi(x)=\sin(2x)$. Solutions of the boundary problem (18), (19), (20) with $\alpha=0{,}5;\ 1{,}0;\ 1{,}5;\ 1{,}8;\ 2{,}0$ are shown in Fig. 3, 4, 5, 6 and 7 respectively.

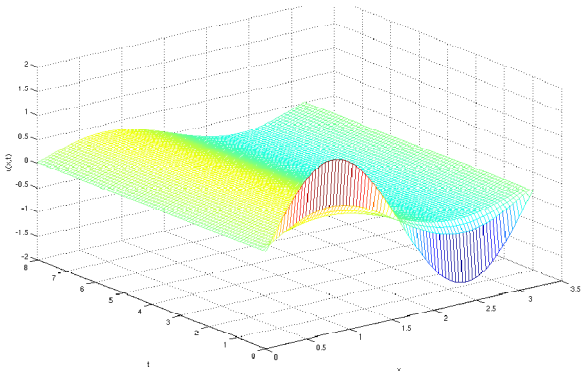

Fig. 3. Solution of the boundary problem (18)-(20) for $\alpha=0{,}5$

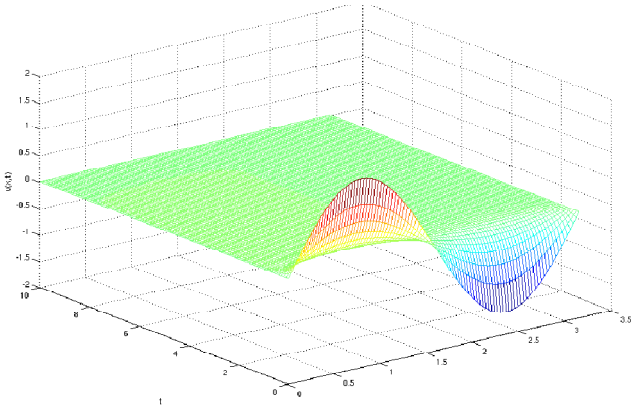

Fig. 4. Solution of the boundary problem (18)-(20) for $\alpha=1{,}0$

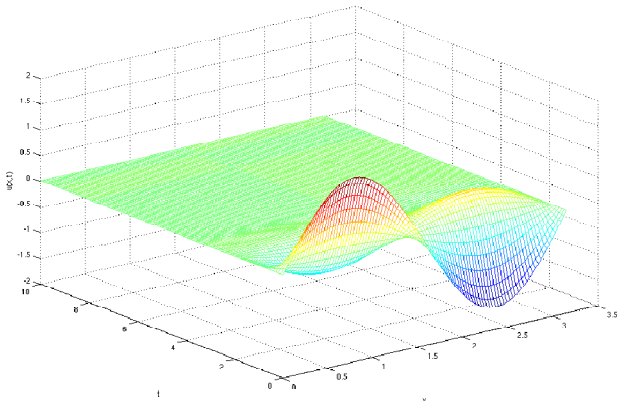

Fig. 5. Solution of the boundary problem (18)-(20) for $\alpha=1{,}5$

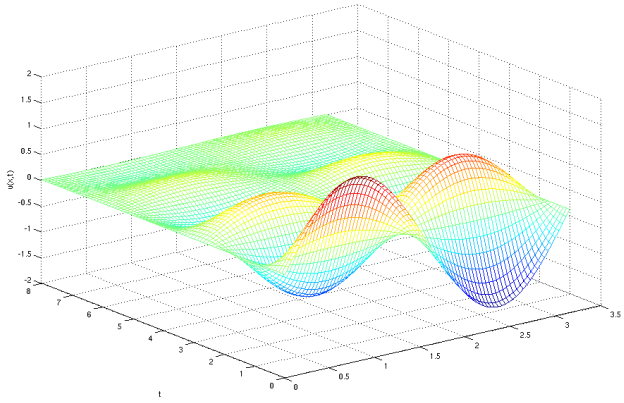

Fig. 6. Solution of the boundary problem (18)-(20) for $\alpha=1{,}8$

The calculations were performed on a computer with dual-core processor Intel Core 2 Duo (T7500) 2.2 GHz / core, 3.5 GB memory. It took approximately 1 hour to caluclate the data for each Figure.

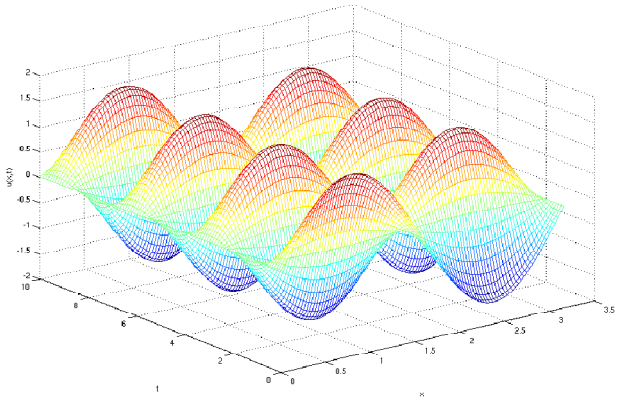

Fig. 7. Solution of the boundary problem (18)-(20) for $\alpha = 2{,}0$.

7. CONCLUDING REMARKS

In this paper we consider the selection of the fractional differential equations. The considerations have been illustrated by a numerical examples. The effectiveness of computational algorithms is dependent on the possibility of determining the Euler's continuous gamma function and depends on the possibility of calculating of the Mittag-Leffler function $E_\alpha(z)$. The function $E_\alpha(z)$ was first introduced in 1903 by Mittag-Leffler (Pillai, 1990).

Some recent interesting results in fractional systems theory and its applications in automatic control can be found in (Liang et al., 2004; Buslowicz, 2008; Ostalczyk, 2008; Ruszewski, 2009; Nartowicz, 2011; Sobolewski and Ruszewski, 2011).

REFERENCES

1. **Agrawal O. P.** (2002), Solution for a fractional diffusion-wave equation defined in a bounded domain, *Nonlinear Dynam.*, 29. No. 1-4,145-155.
2. **Busłowicz M.** (2008), Stability of linear continuous time fractional order systems with delay of the retarder type, *Bull. Pol. Acad. Sci. Tech.*, vol. 56, no. 4, 319-324.
3. **Busłowicz M.**(2010), Wybrane zagadnienia z zakresu liniowych ciągłych układów niecałkowitego rzędu, *Pomiary Automatyka Robotyka*, nr 2, 93-114.
4. **Ciesielski M**., **Leszczynski J.** (2006), Numerical Treatment of An Initial-Boundary Value Problem for Fractional Partial Differential Equations, *Signal Process.* 86, 2619.
5. **Diethelm K., Ford N. J., Freed A. D.** (2002), A predictor-corrector approach for the numerical solution of fractional differential equations, *Nonlinear Dynamicss*, 29, 3- 22.
6. **Diethelm K., Walz G.**(1997), Numerical solution of fractional order diferential equations by extrtapolation, *Numer. Algorithms*, 16, 231-253.
7. **Jafari H.**, **Momani S.** (2007), Solving fractional diffusion and wave equations by modified homotopy perturbation method, *Physics Letters A*, Elsevier, 370, 388–396.
8. **Kaczorek T.** (2009), *Wybrane zagadnienia teorii układów niecałkowitego rzędu*, Oficyna Wydawnicza Politechniki Białostockiej, Białystok.
9. **Kaczorek T.** (2011a), Positive fractional linear systems**.** *Pomiary Automatyka Robotyka*, No. 2, 91-112.
10. **Kaczorek T.** (2011b), Decomposition of the positive fractional discrete-time linear system, *Pomiary Automatyka Robotyka*, No. 2, 504-511.
11. **Kaczorek T.** (2011c), *Selected Problems of Fractional Systems Theory*, Springer, Berlin (in print).
12. **Kilbas A. A., Srivastava H. M. Trujillo J. J.** (2006), *Theory and Applications of Fractional Differential Equations*, Elsevier, Amsterdam.
13. **Liang J**., **Chen Y. Q**., **Meng Max Q.-H**., **Fullmer R.** (2004), Fractional-order Boundary Control of Fractional Wave Equation with Delayed Boundary Measurement Using Smith Predictor, *43rd IEEE Conference on Decision and Control*, Atlantis, Paradise Island, Bahamas, 5088-5093.
14. **Lubich C.** (1986), Discretized fractional calculus, *SIAM J. Math. Anal.*, 17, No. 3, 704.719.
15. **Murillo J. Q**., **Yuste S. B.** (2009), On three explicit difference schemes for fractional diffusion and diffusion-wave equations, *Physica Scripta*, T136, 014025 (6pp)**.**
16. **Murillo J. Q., Yuste S. B.**, (2011), An Explicit Difference Method for Solving Fractional Diffusion and Diffusion-Wave Equations in the Caputo Form, *Journal of Computational and Nonlinear Dynamics*, April 2011, Vol. 6, 021014-1-6.
17. **Nartowicz T.** (2011), Obszary stabilności układu regulacji z regulatorem ułamkowym dla niestabilnego obiektu pierwszego rzędu z opóźnieniem (Design of fractional order controller for a first order unstable plant with delay), *Pomiary Automatyka Robotyka*, No. 2, 595-602.
18. **Ostalczyk P.** (2008), *Zarys rachunku różniczkowo-całkowego ułamkowych rzędów. Teoria i zastosowania w automatyce (Epitome of the Fractional Calculus, Theory and its Applications in Automatics)*, Publishing Department of Technical University of Łódź, Łódź (in Polish).
19. **Pillai R. N.** (1990), On Mittag-Leffler functions and related distributions, *Ann. Inst. Statist. Math*. Vol. 42, No. 1, 157-161.
20. **Podlubny I.** (2000), Matrix approach to discrete fractional calculus, *Fract. Calc. Appl. Anal.*, 3, No. 4, 359-386.
21. **Podlubny I., Dorcak L., Misanek J.** (1995), Application of fractional-order derivatives to calculation of heat load intensity change in blast furnace walls, *Transactions of the Technical University of Kosice*, 5, 137-144.
22. **Podlubny I., Kacenak M.** (2001), http://www.mathworks.com/matlabcentral/fileexchange/8738
23. **Povstenko Y. Z.** (2011), Solutions to Time-Fractional Diffusion-Wave Equation in Cylindrical Coordinates, *Advances in Difference Equations*, Hindawi Publishing Corporation, Article ID 930297, Vol. 2011, Article ID 930297, 14 pages.
24. **Ruszewski A.** (2009), Stabilizacja układów inercyjnych ułamkowego rzędu z opóźnieniem za pomocą ułamkowego regulatora PID, *Pomiary Automatyka Robotyka*, No. 2, 406–414.
25. **Sabatier J., Agrawal O. P., Machado J. A. T.** (Eds) (2007), *Advances in Fractional Calculus, Theoretical Developments and Applications in Physics and Engineering*, Springer, London.
26. **Sobolewski A., Ruszewski A.** (2011), Realizacja praktyczna regulatora niecałkowitego rzędu (Practical realization of fractional-order controller), *Pomiary Automatyka Robotyka*, No. 2, 589-594
27. **Trzasko W.** (2011), Względna punktowa zupełność dodatnich układów ciągło-dyskretnych niecałkowitego rzędu (Relative pointwise completeness of positive continuous-discrete time fractional order systems), *Pomiary Automatyka Robotyka* , No. 2, 528-537.
28. **Weilbeer M.** (2005), Efficient Numerical Methods for Fractional Differential Equations and their Analytical, *Technischen Universität Braunschweig, Doktors Dissertation*, 1-224.

I thank Mrs. Anna Obraczka very much
for performing the calculations in Example 5.

LINEAR q-DIFFERENCE FRACTIONAL ORDER CONTROL SYSTEMS WITH FINITE MEMORY

Dorota MOZYRSKA[*], Ewa PAWŁUSZEWICZ[**]

[*]Faculty of Computer Science, Białystok University of Technology, 15-351 Białystok, Poland
[**]Faculty of Mechanical Engineering, Białystok University of Technology, 15-351 Białystok, Poland

d.mozyrska@pb.edu.pl, e.pawluszewicz@pb.edu.pl

Abstract: The formula for the solution to linear q-difference fractional-order control systems with finite memory is derived. New definitions of observability and controllability are proposed by using the concept of extended initial conditions. The rank condition for observability is established and the control law is stated.

1. INTRODUCTION

Recently the concept of fractional derivatives and differences is under strong consideration as a tool in descriptions of behaviors of real systems. In modeling the real phenomena authors emphatically use generalizations of n-th order differences to their fractional forms and consider the state-space equations of control systems in discrete-time, (e.g. Guermah, Djennoune and Bettayeb, 2008; Sierociuk and Dzieliński, 2006). Some problems and special attempt to the fractional q-calculus was provided and presented in Atici and Eloe (2007). The possible application of fractional q-difference was proposed by Ortigueira (2008).

In the generalization of classical discrete-case differences to fractional-order differences it is convenient to take finite summation (see: Kaczorek, 2007; Kaczorek, 2008; Guermah, Djennoune and Bettayeb, 2008; Sierociuk and Dzieliński, 2006). On the other hand there is no good reason for that. The way we use the fractional difference does not introduce any doubt on the initial condition problems for fractional linear systems in discrete-case. Moreover, what seems to be one of the greatest phenomena in using fractional derivatives and differences in systems modeling real behaviors is the initialization of systems. In fact the initial value problem is an important task in daily applications. Recently we can find papers dealing with the problem how to impose initial conditions for fractional-order dynamics, (e. g. Ortigueira and Coito, 2007; Lorenzo and Hartley, 2009; Atici and Eloe, 2009).

In this paper we deal with q-fractional difference control systems with the initialization by an additional function φ that vanishes on a time interval with infinitely many points. In that way we get only finite number of values of initializing function φ that can be nonzero. We call such set, stated as the extended vector, by l-memory. Hence a control system is defined together with initializing point of time and length of the memory.

We present the construction of the solution to l-memory initial value problem and discuss the observability and controllability in s-steps conditions for such system. Some results concerning the autonomous linear q-difference fractional-order system with l-memory were presented in Mozyrska and Pawłuszewicz (2010). Although we take as initial states the extended vectors for the initial memory, we restrict definition of indistinguishability relation and observability to those defined for s-steps, similarly as it is proposed in Mozyrska and Bartosiewicz (2010). We state the problem in the classical way, using the rank of observability matrix. For controllability we formulate the control law using recursively defined Gramian.

The paper is organized as follows. In Section 2 the foundation of fractional q-derivative is presented and it is showed that forward trajectory of linear q-difference fractional order control system with l-memory is uniquely defined. In Section 3 observability problem in finite memory domain is stated. Proposition 3.3 gives another, then in Mozyrska and Pawłuszewicz (2010), observability rank condition. Section 4 presents solution of controllability problem in finite memory domain.

2. FRACTIONAL q-DERIVATIVE AND q-DIFFERENCE SYSTEMS

Firstly we recall some basic facts connected with q-difference systems. Let $q \in (0,1)$. By q-difference of a function $f\colon \mathrm{R} \to \mathrm{R}$ we mean (see e.g. Jackson, 1910)

$$\Delta_q f(t) = \frac{f(qt) - f(t)}{qt - t},$$

where t is any nonzero real number.

Then $\Delta_q t^k = \frac{q^k - 1}{q-1} t^{k-1}$ and, if $p(t) = \sum_{k=0}^{n} a_k t^k$, then $\Delta_q p(t) = \sum_{k=0}^{n-1} a_{k+1} \frac{q^{k+1}-1}{q-1} t^k$. In the natural way this leads to the problem of solving q-difference equation in x with known function $f\colon \Delta_q x(t) = f(t)$. Detailing with this, last equation gives $x(t) = (1-q)t \sum_{i=0}^{\infty} q^i f(q^i t)$ under the assumption of the convergency of the series on the right side.

Let $q \in (0,1)$ and let α be any nonzero rational number. We need the following q-analogue of $n!$, introduced in Kac and Cheung (2001):

$$[n]! = \begin{cases} 1, & \text{if } n = 0, \\ [n]\cdot[n-1]\cdot\cdots\cdot[1], & \text{if } n = 1,2,\ldots \end{cases}$$

Hence $[n+1]! = [n]!\,[n+1]$ for each $n \in \mathrm{N}$. Also, following the notations in Kac and Cheung (2001), we write $[\alpha] = \frac{1-q^\alpha}{1-q}$ and for generalization of the q-binomial coefficients

$$\begin{bmatrix} \alpha \\ 0 \end{bmatrix} = 1, \begin{bmatrix} \alpha \\ j \end{bmatrix} = \frac{[\alpha][\alpha-1]\cdots[\alpha-j+1]}{[j]!},\ j \in N.$$

Note that:

1. $[1] = 1$ but $[n+1] = 1 + q + \cdots + q^n$ and $\lim_{n\to+\infty}[n] = \frac{1}{1-q}$;
2. For $n \in \mathrm{N}$: $\lim_{q\to 1}[n]! = n!$;
3. $\begin{bmatrix} \alpha \\ 1 \end{bmatrix} = [\alpha]$, $\begin{bmatrix} \alpha \\ 2 \end{bmatrix} = \frac{(1-q^{\alpha-1})(1-q^\alpha)}{(1-q^2)(1-q)}$

Example 2.1. Let $q = \alpha = 0.5$. Then the sequence $(\begin{bmatrix} \alpha \\ j \end{bmatrix}, j = 1..4) \approx (0.586, -0.324, 0.676, -3.358)$, according to computations in Maple package.

In Ortigueira (2008), the q-difference of fractional order is defined by

$$\Delta_q^\alpha x(t) := t^{-\alpha}\,\frac{\sum_{j=0}^{\infty}\begin{bmatrix} \alpha \\ j \end{bmatrix}(-1)^j q^{\frac{j(j+1)}{2}} q^{-j\alpha}}{(1-q)^\alpha}\, x(q^j t).$$

Let us denote $b_j = \begin{bmatrix} \alpha \\ j \end{bmatrix}(-1)^j q^{\frac{j(j+1)}{2}} q^{-j\alpha}$. Then

$$(1-q)^\alpha \Delta_q^\alpha x(t) = t^{-\alpha}\sum_{j=0}^{\infty} b_j x(q^j t). \tag{1}$$

It is easy to check that $b_0 = 1$. The series on the right side of (1) needs the infinite values of the function x(·). But if $x(\cdot)$ is such that it vanishes besides finite number of points, then summation is finite.

If s is a natural number or $s = 0$, and $t \in R_+$ then let $\boldsymbol{\Omega}_s(t_0) := \{q^k t_0 : k \in \mathrm{Z}, k \le s\}$.

Let $\alpha \in R_+$. By $u_\alpha : \mathrm{R} \to \{0,1\}$ we denote the Heaviside step function such that $u_\alpha(t) = 0$ for $t < \alpha$ and $u_\alpha(t) = 1$ for $t \ge \alpha$. Then we can easily deduce the following:

Proposition 2.2. Let $\alpha > 0$, $s \in \mathrm{Z}$. Let $\varphi : \mathrm{R} \to \mathrm{R}^n$ be any function and $x(t) = \varphi(t)u_\alpha(t)$. Then,

$$\Delta_q^\alpha x(t) = \begin{cases} 0 & \text{for } t < a, \\ t^{-\alpha}\sum_{j=0}^{N(t,a)} \frac{b_j}{(1-q)^\alpha} x(q^j t) & \text{for } t \ge a, \end{cases} \tag{2}$$

where $N(t,\alpha) = E[\frac{\ln\alpha - \ln t}{\ln q}]$ and $E[x]$ denotes the integer value of x.

Let $l \in \mathrm{N}\cup\{0\}$, $t_0 = q^{j_0}$, $\alpha = q^l t_0$, $\varphi : \mathrm{R} \to \mathrm{R}^n$. The vector

$$M(l,t_0,\varphi) := \begin{bmatrix} \varphi(t_0) \\ \varphi(qt_0) \\ \vdots \\ \varphi(q^l t_0) \end{bmatrix}$$ of ordered values of function φ on $\Omega_l(t_0)$, is called a finite l-memory at t_0. Observe that if $l \in \mathrm{N}\cup\{0\}$ and $s \in \mathrm{N}\cup\{0\}$, $\varphi : R \to R^n$, then

- $M(l,t_0,\varphi) \in R^{n+nl}$
- if $l_1, l_2 \in \mathrm{N}\cup\{0\}$, $l_2 \ge l_1$ and $t_0 > 0$, then $\Omega_{l_1}(t_0) \subset \Omega_{l_2}(t_0)$ and if I_{nl_1} is a matrix of the form
$$\begin{bmatrix} 1 & 0 & \ldots & 0 & 0 & \ldots & 0 \\ 0 & 1 & \ldots & 0 & 0 & \ldots & 0 \\ \vdots & \vdots & \ddots & \vdots & \vdots & \ddots & \vdots \\ 0 & 0 & \ldots & 1 & 0 & \ldots & 0 \end{bmatrix}$$
with the first block of the dimension $l_1 \times l_1$, then also $[I_{nl_1}, 0_{nl_1\times n(l_2-l_1)}]\cdot M(l_2,t_0,\varphi) = M(l_1,t_0,\varphi)$.

Definition 2.3. Let $l \in \mathrm{N}\cup\{0\}$ and $t_0 > 0$, $a = q^l t_0 \in \Omega_l(t_0)$, $\varphi : R \to R^n$. A linear q-difference fractional-order time-varying control system with l-memory is a system given by the following set of equations, denoted by $\Sigma_{(\varphi,l)}$:

$$\Delta_q^\alpha x(t) = A(qt)x(qt) + B(qt)u(qt), \quad t > t_0 \tag{3}$$

$$x(t) = (\varphi u_a)(t), \qquad t \le t_0 \tag{4}$$

$$y(t) = C(t)x(t), \tag{5}$$

where $A(\cdot) \in R^{n\times n}$, $B(\cdot) \in R^{m\times n}$, $C(\cdot) \in R^{p\times n}$ are matrices with elements depending on time, and $u : q^k \mapsto u(q^k) \in R^m$, $k \in \mathrm{Z}$, is any measurable function.

Remark 2.4. If $l \to +\infty$ then $q^l t_0 \to 0$ for any $t_0 > 0$ and the vector $M(l,t_0,\varphi)$ becomes infinite.

From equation (1) and (3) we have

$$x\left(\frac{t_0}{q}\right) = G\left(\frac{t_0}{q}\right)x(t_0) - \sum_{j=1}^{l} b_{j+1}x(q^j t_0) + f\left(\frac{t_0}{q}\right),$$

where $G(t) = (t(1-q))^\alpha A(qt) - b_1 I_n$, $f(t) = (t(1-q))^\alpha B(qt)u(qt)$.

Then,

$$G\left(\frac{t_0}{q^{k+1}}\right) = \left(\frac{t_0(1-q)}{q^{k+1}}\right)^\alpha A\left(\frac{t_0}{q^k}\right) - b_1 I_n$$

and $A_0 = \mathbf{0}_n$, while for $j > 0$: $A_j = -b_{j+1}I_n$, where I_n is the $n \times n$ – identity matrix. Moreover,

$$x\left(\frac{t_0}{q^{k+1}}\right) = G\left(\frac{t_0}{q^{k+1}}\right)x\left(\frac{t_0}{q^k}\right) + \sum_{j=1}^{k+l} A_j x\left(q^{k-j}t_0\right) + f\left(\frac{t_0}{q^{k+1}}\right).$$

The idea of the construction given in the next lines follows from Guermah, Djennoune and Bettayeb (2008). Here we extend the construction to q-difference with finite l-memory. Let us define the following sequence of matrices from $R^{n\times(nl+n)}$:

$$\tilde{\Phi}(t_0) = [I_n, \mathbf{0}_n, \ldots \mathbf{0}_n], \quad \tilde{\Phi}\left(\frac{t_0}{q}\right) = \left[G\left(\frac{t_0}{q}\right), A_1, \ldots A_l\right]$$

$$\tilde{\Phi}\left(\frac{t_0}{q^2}\right) = G\left(\frac{t_0}{q^2}\right)\tilde{\Phi}\left(\frac{t_0}{q}\right) + [A_1, \ldots, A_{l+1}] \tag{6}$$

and for $k \geq 2$:

$$\tilde{\Phi}\left(\frac{t_0}{q^{k+1}}\right) = G\left(\frac{t_0}{q^{k+1}}\right)\tilde{\Phi}\left(\frac{t_0}{q^k}\right) + \sum_{j=1}^{k-1} A_j \tilde{\Phi}\left(\frac{t_0}{q^{k-j}}\right) + [A_k, A_{k+1}, \ldots, A_{k+l}].$$

With the sequence $\left\{\tilde{\Phi}(\frac{t_0}{q^k})\right\}_{k\in N\cup\{0\}}$ we connect the sequence $\left\{\Phi(\frac{t_0}{q^k})\right\}_{k\in N\cup\{0\}}$ of their sub-matrices in $R^{n\times n}$ that we subtract from $\left\{\tilde{\Phi}(\frac{t_0}{q^k})\right\}_{k\in N\cup\{0\}}$ by the following operation

$$\Phi\left(\frac{t_0}{q^k}\right) = \tilde{\Phi}\left(\frac{t_0}{q^k}\right) \cdot \begin{bmatrix} I_n \\ \mathbf{0}_{n\times(nl)} \end{bmatrix}. \tag{7}$$

Theorem 2.5. Let $l \in N \cup \{0\}$ and $t_0 > 0$; $a = q^l t_0 \in \Omega_l(t_0)$, $\varphi: R \to R^n$. The solution of the system $\Sigma_{(\varphi,l)}$ stated in Definition 2.3, corresponding to control u and a memory function φ is given by values for $t \geq t_0$:

$$x\left(\frac{t_0}{q^k}\right) = \tilde{\Phi}\left(\frac{t_0}{q^k}\right)\tilde{x}(t_0) + F\left(\frac{t_0}{q^k}\right), \tag{8}$$

where $\tilde{x}(t_0) = M(l, t_0, \varphi)$ and for $k > 2$

$$F\left(\frac{t_0}{q^k}\right) = G\left(\frac{t_0}{q^k}\right)F\left(\frac{t_0}{q^{k-1}}\right) + \sum_{j=1}^{k-2} A_j F\left(\frac{t_0}{q^{k-j-1}}\right) + f\left(\frac{t_0}{q^k}\right),$$

while $F\left(\frac{t_0}{q}\right) = f\left(\frac{t_0}{q}\right)$ and

$$F\left(\frac{t_0}{q^2}\right) = G\left(\frac{t_0}{q^2}\right)f\left(\frac{t_0}{q}\right) + f\left(\frac{t_0}{q^2}\right).$$

Proof. For the proof we use the mathematical induction with respect to $k \in N \cup \{0\}$, where $t = t_0/q^k$. First we check steps for $k \in \{1,2\}$. For $k = 1$:

$$\tilde{\Phi}\left(\frac{t_0}{q}\right)\tilde{x}(t_0) = G\left(\frac{t_0}{q}\right)\varphi(t_0) + [A_1, \ldots, A_l] \cdot \begin{bmatrix} \varphi(qt_0) \\ \vdots \\ \varphi(q^l t_0) \end{bmatrix}$$

and then:

$$x\left(\frac{t_0}{q}\right) = G\left(\frac{t_0}{q}\right)\varphi(t_0) + \sum_{j=1}^{l} A_j \varphi(q^j t_0) + f\left(\frac{t_0}{q}\right)$$

$$= \tilde{\Phi}\left(\frac{t_0}{q}\right)\tilde{x}(t_0) + f\left(\frac{t_0}{q}\right).$$

Similarly for $k = 1$ holds

$$x\left(\frac{t_0}{q^2}\right) = G\left(\frac{t_0}{q^2}\right)x\left(\frac{t_0}{q}\right) + A_1\varphi(t_0) + \sum_{j=1}^{l} A_{j+1}\varphi(q^j t_0) + f\left(\frac{t_0}{q^2}\right)$$

Using the formula for $x(t_0/q)$ we get

$$x\left(\frac{t_0}{q^2}\right) = G\left(\frac{t_0}{q^2}\right)G\left(\frac{t_0}{q}\right)\varphi(t_0) + A_1\varphi(t_0)$$

$$+ G\left(\frac{t_0}{q^2}\right)\left(\sum_{j=1}^{l} A_j \varphi(q^j t_0) + f\left(\frac{t_0}{q}\right)\right) + \sum_{j=1}^{l} A_{j+1}\varphi(q^j t_0)$$

$$+ f\left(\frac{t_0}{q^2}\right) = \Phi\left(\frac{t_0}{q^2}\right)\varphi(t_0) + \sum_{j=1}^{l}\left(G\left(\frac{t_0}{q^2}\right)A_j + A_{j+1}\right)\varphi(q^j t_0)$$

$$+ F\left(\frac{t_0}{q^2}\right) = \tilde{\Phi}\left(\frac{t_0}{q^2}\right)\tilde{x}(t_0) + F\left(\frac{t_0}{q^2}\right)$$

Now let us assume that the solution formula holds for all $t \in \Omega_k(t_0)$, $k \in Z_-$. Let us take now $t = t_0/q^{k+1}$. Hence

$$x(t) = G(t)x(qt) + \sum_{j=1}^{k+l} A_j x\left(\frac{t_0}{q^{k-j}}\right) + f(t).$$

Using the inductive assumption we get

$$x(t) = G(t)\tilde{\Phi}\left(\frac{t_0}{q^k}\right)\tilde{x}(t_0) + A_1 x\left(\frac{t_0}{q^{k-1}}\right) + \cdots + A_{k-1}x\left(\frac{t_0}{q}\right) + A_k\varphi(t_0)$$

$$+ A_{k+1}\varphi(qt_0) + \cdots + A_{k+l}\varphi\left(q^l t_0\right) + G(t)F\left(\frac{t_0}{q^k}\right) + f\left(\frac{t_0}{q^{k+1}}\right).$$

We can also use again inductive assumption for each of $x(t_0/q^j), j = 1, \ldots, k-1$:

$$x\left(\frac{t_0}{q^j}\right) = \tilde{\Phi}\left(\frac{t_0}{q^j}\right)\tilde{x}(t_0) + F\left(\frac{t_0}{q^j}\right)$$

and

$$A_1 x\left(\frac{t_0}{q^{k-1}}\right) + \cdots + A_{k-1}x\left(\frac{t_0}{q}\right) = \sum_{j=1}^{k-1} A_j \tilde{\Phi}\left(\frac{t_0}{q^{k-j}}\right)\tilde{x}(t_0) + \sum_{j=1}^{k-1} A_j F\left(\frac{t_0}{q^{k-j}}\right).$$

In the consequence

$$x(t) = G(t)\tilde{\Phi}\left(\frac{t_0}{q^k}\right) + \sum_{j=1}^{k-1} A_j \tilde{\Phi}\left(\frac{t_0}{q^{k-j}}\right) + [A_k, \ldots, A_{k+l}]\ \tilde{x}(t_0)$$

$$+ G\left(\frac{t_0}{q^{k+1}}\right)F\left(\frac{t_0}{q^k}\right) + \sum_{j=1}^{k-1} A_j F\left(\frac{t_0}{q^{k-j}}\right) + f\left(\frac{t_0}{q^{k+1}}\right)$$

$$= \tilde{\Phi}\left(\frac{t_0}{q^{k+1}}\right)\tilde{x}(t_0) + F\left(\frac{t_0}{q^{k+1}}\right).$$

Hence from the mathematical induction the formula for solution holds for all $k \in N \cup \{0\}$.

Example 2.6. Let $t_0 = 1$, $l = 1$, $q = \alpha = 0{,}5$ and $A = \begin{bmatrix} 0 & -1 \\ 1 & 0 \end{bmatrix}$, $B = \begin{bmatrix} 1 \\ 0 \end{bmatrix}$ Let us take also the control $u(t) \equiv 1$. Then using Maple and formula given in Theorem 2.5 we can do calculations recursively. In this case we get:

$$\tilde{\Phi}(t_0/q) \approx \begin{bmatrix} 0.414 & -1 & 0.081 & 0 \\ 1 & 0.414 & 0 & 0.081 \end{bmatrix},$$

$$\tilde{\Phi}(t_0/q^2) \approx \begin{bmatrix} -1.162 & -1 & 0.062 & -0.114 \\ 1 & -1.162 & 0.114 & 0.063 \end{bmatrix}.$$

Moreover, as we take $l = 1$ we need to start memory in four dimensional space for $\tilde{x}(t_0)$. Let us take $\tilde{x}(t_0) = \begin{bmatrix} 0 \\ 0 \\ 1 \\ 1 \end{bmatrix}$. Hence the initial state is in the origin, while from the memory we have (1,1). Then $x(2) = \begin{bmatrix} 1{,}081 \\ 0{,}081 \end{bmatrix}$, $x(4) = \begin{bmatrix} 1{,}777 \\ 1{,}592 \end{bmatrix}$, $x(8) = \begin{bmatrix} -0{,}347 \\ 4{,}234 \end{bmatrix}$, $x(16) = \begin{bmatrix} -9{,}109 \\ 0{,}0909 \end{bmatrix}$, $x(32) = \begin{bmatrix} -3{,}367 \\ -35{,}612 \end{bmatrix}$, $x(64) = \begin{bmatrix} 205{,}288 \\ -33{,}612 \end{bmatrix}$.

3. OBSERVABILITY IN FINITE MEMORY DOMAIN

In this section we recall some facts related to the concept of the observability of linear q-difference fractional system with l-memory given by Definition 2.3. The standard definition of observability says that a system is observable on time-interval if from the knowledge of the output of a given system we can reconstruct uniquely the initial condition. As we consider here systems together with the extended initial conditions, called l-memory, we want to determine the extended initial condition $\tilde{x}(t_0)$ from the knowledge of $\mathbf{Y} := \{y(t_0/q^k), k = 0, \dots, s\}$. Hence we need to distinguish in our definitions the starting point t_0, it is the similar situation as for time-varying systems (discrete or continuous). For that we use the definition of an l-event as a pair $(t, \tilde{x}) \in \{q^k : k \in Z\} \times R^{n+nl}$, as the idea comes from Sontag (1990).

Let us consider the linear q-difference fractional-order system $\Sigma_{(\varphi,l)}$.

Definition 3.1. Let l, s be any natural number, $t_0 = q^{j_0} \in \{q^k : k \in Z\}$ and let $\varphi_{1,2}$ be maps from the set $\{q^k : k \in Z\} \cup \{0\}$ into R^n. We say that two l-events $(t_0, \tilde{x}_1)$, $(t_0, \tilde{x}_2)$, where $\tilde{x}_1 = M(l, t_0, \varphi_1)$, $\tilde{x}_2 = M(l, t_0, \varphi_2)$, are indistinguishable with respect to $\Sigma_{(\varphi,l)}$ in s-steps if and only if there is a control u such that for all $t \in \Omega_s(t_0)$, $s \in Z_-$,

$$C(t)x_1(t) = C(t)x_2(t), \tag{9}$$

where functions $x_1(\cdot)$, $x_2(\cdot)$ are given by (8) and correspond respectively to φ_1, φ_2. Otherwise, the l-events $(t_0, \tilde{x}_1)$, $(t_0, \tilde{x}_2)$ are distinguishable with respect to $\Sigma_{(\varphi,l)}$ in s-steps.

Definition 3.2. Let $l, s \in N \cup \{0\}$, $\varphi_{1,2} : R \to R^n$. We say that the system $\Sigma_{(\varphi,l)}$ is observable at t_0 in s-steps if any two l-events $(t_0, \tilde{x}_1)$, $(t_0, \tilde{x}_2)$, $\tilde{x}_1 = M(l, t_0, \varphi_1)$, $\tilde{x}_2 = M(l, t_0, \varphi_2)$, are distinguishable with respect to $\Sigma_{(\varphi,l)}$ in s-steps.

Directly from Definition 3.2 follows that the system $\Sigma_{(\varphi,l)}$ is observable at t_0 in l-memory domain in s-steps if and only if the initial extended state $\tilde{x}(t_0) = M(l, t_0, \varphi)$ can be uniquely determined from the knowledge of $\mathbf{Y} := \{y(t_0/q^k), k = 0, \dots, s\}$.

Proposition 3.3. Let $l, s \in N \cup \{0\}$. The system $\Sigma_{(\varphi,l)}$ is observable at t_0 in s-steps if and only if one of the following conditions holds

1. the $n \times n$ real matrix:
$$W(s, t_0) = \sum_{k=0}^{s} \Phi^T\left(\frac{t_0}{q^k}\right) C^T C \Phi\left(\frac{t_0}{q^k}\right) \text{ is nonsingular;}$$
2. the matrix $\Phi(t_0/q^k)$ has linearly independent columns for all k $\in \{0, \dots, s\}$;
3. $$rank\, \mathrm{O}(s) = rank \begin{bmatrix} C\Phi(t_0) \\ C\Phi\left(\frac{t_0}{q}\right) \\ \vdots \\ C\Phi\left(\frac{t_0}{q^s}\right) \end{bmatrix} = n\,.$$

Proof. Proof goes in the same manner as in the classical linear control theory, see for example Kaczorek (2007).

Example 3.4. For the system in Example 2.6 we have $W(1, t_0) = \begin{bmatrix} 0 & 0{,}414 \\ 0{,}414 & 1{,}172 \end{bmatrix}$. Hence system $\Sigma_{(\varphi,l=1)}$ is observable in $s = 1$ steps, because rank $W(1, t_0) = 2$.

4. CONTROLLABILITY LAW

In the literature one can find many various concepts of controllability. In our case is that we start our system at $t_0 \in R_+$, not exactly at a point from the set $\{q^k : k \in Z\}$.

Definition 4.1. The system $\Sigma_{(\varphi,l)}$ is said to be completely l-memory controllable from $t_0 \in R_+$ in s-steps, if for any $\varphi = \varphi(t)$, $t \in \Omega_l(t_0)$, and any final value $x_f \in R^n$ there is a control $u = u(t)$, $t \in \Omega_{-s}(t_0)$, such that $x(t_0/q^s) = x_f$.

Definition 4.2. Let $t_0 \in R_+$ and $s \in N$. The (l, φ) – memory controllability Gramian for the system $\Sigma_{(\varphi,l)}$ on $\Omega_{-s}(t_0)$ we define recursively in the sequel

$$W\left(\frac{t_0}{q}\right) = \left(\frac{t_0(1-q)}{q}\right)^{-\alpha} B^T(t_0) B(t_0),$$

$$W\left(\frac{t_0}{q^2}\right) = \left(\frac{t_0(1-q)}{q}\right)^{-\alpha} G\left(\frac{t_0}{q^2}\right) B^T(t_0) B(t_0) + \left(\frac{t_0(1-q)}{q^2}\right)^{-\alpha} B^T\left(\frac{t_0}{q}\right) B\left(\frac{t_0}{q}\right)$$

and for $k \geq 3$:

$$W\left(\frac{t_0}{q^k}\right) = G\left(\frac{t_0}{q^k}\right) W\left(\frac{t_0}{q^{k-1}}\right) + \sum_{j=1}^{k-2} A_j W\left(\frac{t_0}{q^{k-j-1}}\right) + \left(\frac{t_0(1-q)}{q^k}\right)^{-\alpha} B^T\left(\frac{t_0}{q^{k-1}}\right) B\left(\frac{t_0}{q^{k-1}}\right).$$

Theorem 4.3. Let $t_0 \in R_+$ and $s \in N$. If the matrix $W(t_0/q^s)$ is nonsingular, then the control function given for $k \in \{1, \dots, s\}$

$$\bar{u}\left(\frac{t_0}{q^k}\right) = -\left(\frac{t_0(1-q)}{q^{k+1}}\right)^{-\alpha} B^T\left(\frac{t_0}{q^k}\right) W^{-1}\left(\frac{t_0}{q^s}\right)\left(x_f - \tilde{\Phi}\left(\frac{t_0}{q^s}\right)\tilde{x}(t_0)\right)$$

transfers $x(t_0) = \varphi(t_0)$ to $x_f = x\left(\frac{t_0}{q^s}\right)$.

Proof. If $W(t_0/q^s)$ is nonsingular, then the proof is by direct substitution the form of control $\bar{u}(t_0/q^k)$ for $k \in \{1, \ldots, s\}$ to the formula of solution $x(t_0/q^s)$.

REFERENCES

1. A**tici F. M., Eloe P. W.** (2007), Fractional q-calculus on a time scale, *Journal of Nonlinear Mathematical Physics*, Vol.14, No 3, 333-344.
2. **Atici F. M., Eloe P.W.** (2009), Initial value problems in discrete fractional calculus, *Proc. AMS*, No. 13, 7981-989.
3. **Guermah S., Djennoune S.**, **Bettayeb M.** (2008), Controllability and the observability of linear discrete-time fractional-order systems, *Int. J. Appl. Math. Comput. Sci.*, Vol. 18, No 2, 213-222.
4. **Jackson H. F.** (1910), q-Difference equations, *Am. J. Math.*, No 32, 305-314.
5. **Kac V., Cheung P.** (2001), *Quantum calculus*, New York Berlin Heidelberg.
6. **Kaczorek T.** (2007), Reachability and controllability to zero of positive fractional discrete--time systems, *Proceedings of European Control Conference ECC'07*, Kos, Greece.
7. **Kaczorek T**. (2008), Reachability of fractional positive continuous--time linear systems and their reachability, *Int. J. Appl. Math. Comput. Sci*, Vol. 18, No 2, 223-228.
8. **Lorenzo C. F., Hartley T. T.** (2009), On self-consistent operators with application to operators of fractional order, *Proceedings of the ASME 2009 International Design Engineering technical Conferences & Computers and Information in Engineering Conference IDETC/CIE 2009*, San Diego, California, USA.
9. **Mozyrska D., Bartosiewicz Z.** (2010), On observability concepts for nonlinear discrete--time fractional order control systems, *New Trends in Nanotechnology and Fractional Calculus Applications*, 305-312.
10. **Mozyrska D., Pawłuszewicz E**. (2010), Observability of linear q-difference fractional-order systems with finite initial memory, *Bull. Pol. Acad. Sci. Tech. Sci.*, Vol. 58, No 4, 601-605.
11. **Ortigueira M. D.** (2008), The fractional quantum derivative and the generalised Euler-Cauchy equation, *J. Inequal. Appl*. 956-962.
12. **Ortigueira M. D., Coito F. J.** (2007), Revisiting the Initial Conditions Problem in Fractional Linear Systems, *Symposium on Applied Fractional Calculus SAFC07*, University of Extremadura, Badajoz, Spain.
13. **Sierociuk D., Dzieliński A.** (2006), Fractional Kalman filter algorithn for the states, parameters and order of fractonal system estimation, *Int. J. Appl. Math. Comput. Sci.*, Vol. 16, No 1, 129-140.
14. **Sontag E.** (1990), *Mathematical Control Theory*, Springer – Verlag.

The work was partially presented at the 4th IFAC Workshop on Fractional Differentials and its Application FDA10., Badajoz, Spain, 2010.

The first author is supported by Białystok University of Technology grant No S/WI/02/11, the second – by Białystok University of Technology grant No S/WM/02/08.

MICROSTRUCTURAL CHANGES OF ODS FERRITIC STEEL POWDERS DURING MECHANICAL ALLOYING

Zbigniew OKSIUTA*

*Zakład Inżynierii Materiałowej i Biomedycznej, Wydział Mechaniczny, Politechnika Białostocka,
ul. Wiejska 45 C, 15-351 Białystok

oksiuta@pb.edu.pl

Abstract: The ODS ferritic steel powder with chemical composition of Fe-14Cr-2W-0.3Ti-0.3Y2O3 was mechanically alloyed (MA) either from elemental or pre-alloyed powders in a planetary ball mill. Different milling parameters have been used to investigate their influence on the morphology and microstructure of the ODS ferritic steel powder. The time of MA was optimized by studying the structural evolution of the powder by means of X-ray diffractometry and TEM. In the case of elemental powder very small, about 10 µm in diameter, spherical particles with a large surface area have been obtained. Flakey-like particles with an average size of about 45 µm were obtained in the case of the pre-alloyed powder. The lattice strain calculated from XRD spectra of the elemental and pre-alloyed powders exhibits a value of about 0.51 % and 0.67, respectively. The pre-alloyed powder after consolidation process showed the highest density and microhardness value.

1. INTRODUCTION

30 years have passed since Benjamin (1970) used a mechanical alloying (MA) technique for the first time to synthesize different kinds of materials. The structural and chemical changes during MA in a solid state powder are so complex that it is difficult to predict particular reaction or time needed to obtain final product properties. The MA process is commonly used to obtain intermetallic powders starting from elemental powder particles and it is one of the most popular methods for the production of oxide dispersion strengthening (ODS) ferritic steel reinforced with yttrium oxide (Y_2O_3). ODS ferritic steel is candidate material for structural applications in future fusion reactors, due to their excellent high temperature properties, thermal stability and irradiation resistance. Such material can be produced using various initial powders, e.g., elemental and/or pre-alloyed powders as well as milling devices and MA parameters (Suryanarayana, 2001).

The physical and chemical features of the mechanically alloyed powders depend on the MA parameters, such as: type of ball milling device, linear velocity, type, size and number of the balls, the balls-to-powder weight ratio (BPR), the milling atmosphere, a process control agent (PCA), process temperature and many others (Suryanarayana, 2001; Mukhopadhyay et al., 1998; Cayron et al., 2004; Chul-Jin, 2000; Ohtsuka et al., 2005; Patil et al., 2005). In spite of plenty of published articles there is still a lack of systematic studies comparing morphology, size distribution and other characteristics of ODS ferritic steel powders produced by ball milling method.

In this paper the microstructural evolution of elemental and pre-alloyed ODS ferritic steel powders during MA in a planetary ball mill has been studied to obtain the desired solid solution properties. Different ball milling conditions were investigated to establish their influence on the morphology and microstructural changes of the ODS ferritic steel powders.

2. EXPERIMENTAL PROCEDURE

Selection of MA methods and conditions was done on the basis of a literature survey (Suryanarayana, 2001; Mukhopadhyay et al., 1998; Cayron et al., 2004). Commercially pure elemental Fe, Cr, W, Ti and Y_2O_3 powders (more than 99.8% of purity) for the ODS ferritic steel with the composition of Fe-14Cr-2W-0.3Ti-0.3Y_2O_3 (in wt.%) were mechanically alloyed in a planetary ball mill equipped with stainless steel vials and balls, performed under argon or hydrogen atmosphere. Two different BPR's of: 10:1 and 20:1 (100 and 200 stainless steel balls with a diameter of 10 mm) and two different rotation speeds (RS) of 250 rpm and 350 rpm were used. At selected times a small amount of as-milled powder was taken out from the milling jar for further morphology and microstructure analyses. To minimize air contamination of the powder loading and unloading of the powder was performed in an argon glove box. The time of MA was optimized by studying the structural evolution of the powder by means of X-ray diffractometry (XRD), in a Siemens D5000 device, using the Cu-Kα radiation (λ=0.15406 nm). The crystallite mean size and lattice strain were determined by the Williamson-Hall method ($B_s \cos\theta = 2(\varepsilon)\sin\theta + k\lambda/D$) [8], where B_s is the full-width at half-maximum of the diffraction peak (FWHM), θ is the Bragg angle, ε is the internal lattice strain λ is the wavelength of the X-ray, D is the crystallite size and k is constant (k=0.9). B_s can be calculated from; $B^2_s = B^2_m - B^2_c$, where B_s is the peak broadening due to instrumental effect measured using crystallized LaB_6 standard and B_m is the eva-

luated width. MA process was conducted until the solute elements peaks in X-ray diffraction patterns disappeared.

The powders morphology and microstructure were studied using scanning electron microscopy (SEM) and transmission electron microscopy (TEM). The etched microstructure of the powder was observed by means of optical microscopy (OM). Chemical analysis of the powders was performed using wavelength dispersive X-ray fluorescence spectroscopy (WD-XRF) as well as LECO TC-436 and LECO IR-412 analysers for measurements of O, N and C contents, respectively.

After MA the ODS powders were submitted to hot isostatic pressing (HIP) at the temperature of 1150º C and pressure 200 MPa for 4 hours. Density of the specimens after compaction was measured by means of Archimedes method. Microhardness measurements were performed by using a Vickers diamond pyramid and applying a load of 0.98N for 15s. Each result is the average of at least 10 measurements.

3. RESULTS AND DISCUSSION

3.1. Morphology and microstructure of the ODS powders after MA

The particles of the as-received elemental ODS ferritic steel powders appear mostly round in shape, with an average size of about 10 µm (see Fig. 1a). SEM micrographs of the particles after MA for 50 h in a planetary ball mill with a BPR of 10:1 and RS of 250 rpm are shown in Fig. 1a. Fig 2 shows changes of the particles size during MA. At the early stage of ball milling fast increase in the particle size up to 150 µm were observed (see Fig. 2). Further milling, up to 8 h, leads to a significant decrease in the particle size and uniform size distribution. In prolonging the time of MA up to 12 h agglomeration process takes place again increasing the size of the particles from 10 to 80 µm. However, further prolongation of the milling time resulted in the hardening and fracturing of the particles due to fatigue failure mechanism. This trend, gradual refining of the powder, was observed up to 40 h of MA. From 40 to 50 h of MA a small variation of particle size can be observed probably due to the equilibrium state between fracturing and welding of the particles. Finally, after 50 h of MA, about 10 µm in diameter and homogenous particles were obtained.

It was also observed that by increasing the rotation speed from 250 to 350 rpm the milling time was reduced from 50 up to 42 h. When a BPR of 20:1 and a RS 350 rpm were applied the time of formation of a solid solution decreases up to 22 h. SEM observations of the elemental ODS powders (see Fig. 1) revealed that varying the milling parameters: BPR, RS or milling atmosphere (argon or hydrogen), no significant changes in the morphology of the ODS powders were achieved and about 10 µm in diameter particles were produced. However, a higher C content (about 20%) was detected in the powder using higher BPR of 20:1 and about 20% of oxygen content was reduced after using hydrogen atmosphere (see Table 1).

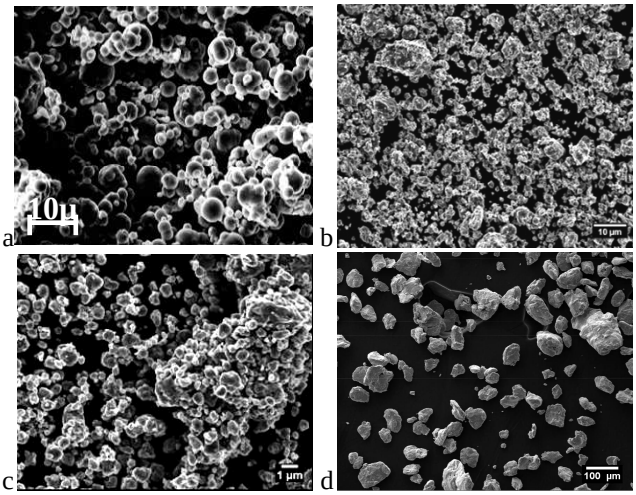

Fig. 1. Morphology of the ODS powder particles: a) as-received elemental powder, b) elemental powder MA for 50 h in argon, BPR 10:1, c) elemental powder MA for 22 h in argon, BPR 20:1, and d) pre-alloyed powder MA for 20 h in hydrogen, BPR 10:1

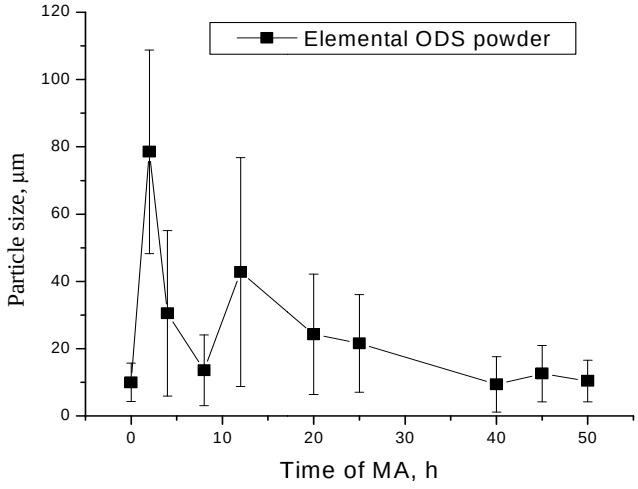

Fig. 2. Particle size distribution of the elemental ODS powder during MA in the planetary ball mill for 50 h in argon

Table 1. Chemical composition (in wt.%) of the ODS Fe-14Cr-2W-0.3Ti-0.3Y_2O_3 elemental and pre-alloyed powders after MA in the planetary ball mill

Chemical content, wt.%						
Conditions	C	Cr	W	Ti	Y	O
As-received	0.078	14.1	1.96	0.31	0.23	0.338
Elemental, MA in Ar for 50 h	0.088	13.7	1.84	0.26	0.21	0.482
Elemental, MA in H_2 for 42 h	0.067	13.7	1.80	0.25	0.28	0.372
Pre-alloyed, H_2, 20 h	0.043	13.5	1.92	0.33	0.25	0.175

It is well known that the MA technique yields contamination of the milled powder, which substantially alters the nature of the particles and therefore changes the final

properties of a bulk material (Mukhopadhyay et al., 1998; Ohtsuka et al., 2005). The data in Table 1 shown that the un-milled ODS powder contains a high oxygen content (0.338 wt.%) and after MA in a high purity argon atmosphere (99.9999 wt.%) an oxygen content of 0.482 wt.% was measured. The amounts of such elements as C, N, Mn and Si also increased due to the contamination coming from the grinding media.

To reduce oxygen and carbon content MA, a process with application of a pre-alloyed, gas-atomised Fe-14Cr-2W powder with 0.3%Y_2O_3 and 0.3%Ti was performed. The MA process was carried out up to 20 h under pure hydrogen atmosphere using BPR 10:1 and rotation speed 350 rpm. Fig. 1d shows SEM image of the pre-alloyed ODS powder after ball milling. According to the SEM observations the pre-alloyed powder, in comparison with the elemental one, exhibits more than 4 times larger particles with an average size of about 45µm, however, C and O content is significantly lower.

Optical micrographs of the etched elemental powder after MA for different milling times revealed that during the initial stage of milling (up to 10 hrs) a typical lamellar microstructure was observed (Fig 3a). Prolongation of the MA time caused refinement of the lamellas. Featureless contrasts as well as cracks that initiate break down of the particles are observed. After MA (Fig. 3b), the powder consists of a huge number of an agglomerated particles which form featureless image what may suggest that the particles exhibit nano-sized grains.

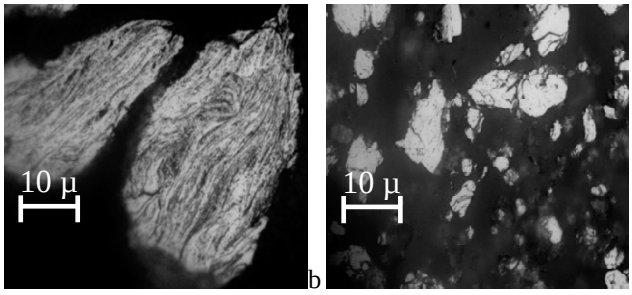

a b

Fig. 3. Microstructure of the elemental powder MA in argon for: a) 10 h and b) 50 h

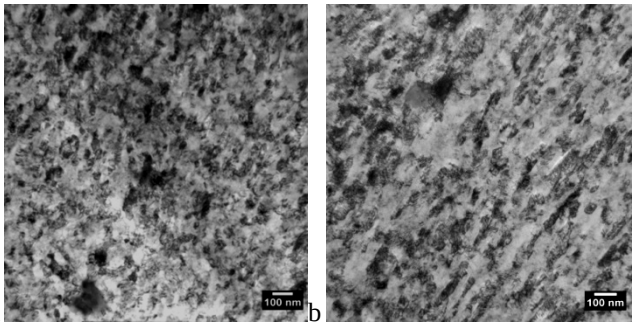

a b

Fig. 4. Bright-field TEM images of: a) elemental ODS powder MA in argon, and b) pre-alloyed ODS powder MA in hydrogen

Figs. 4a and 4b show TEM images of elemental and pre-alloyed ODS powders after mechanical alloying under argon and hydrogen atmosphere and using the same milling conditions (BPR=10:1, RS=350 rpm). TEM observations indicate that both powders have a strongly deformed and nano-sized microstructure and no yttria particles. However, some differences of the microstructure are also observed. The elemental powder has equiaxed nano-sized grains whereas elongated (textured) in the direction parallel to the surface of the particle grains are observed in the case of pre-alloyed powder. It can also be noticed that it was difficult to estimate the nano-grain size, due to the lack of clearly visible grain boundaries. Thus, results of the X-ray diffraction tests of the powders will be presented in the next section 3.2.

3.2. XRD analysis of the ODS powders

X-ray diffraction patterns of the ODS elemental and pre-alloyed powders MA in the planetary ball mill are shown in Figs. 5 and 6, respectively**.** After very short time of MA (2 h), in the case of elemental powder, the peaks of Y_2O_3 and the other solute elements disappeared completely and XRD pattern exhibits major α-Fe and W peaks (see Fig. 5). With increasing the milling time the intensity of Fe and W peaks decreases and its width increases due to a reduction of the crystallite size and increase in the deformation level of the particles. After 50 h of ball milling of the W peak disappears completely suggesting that MA process is accomplished.

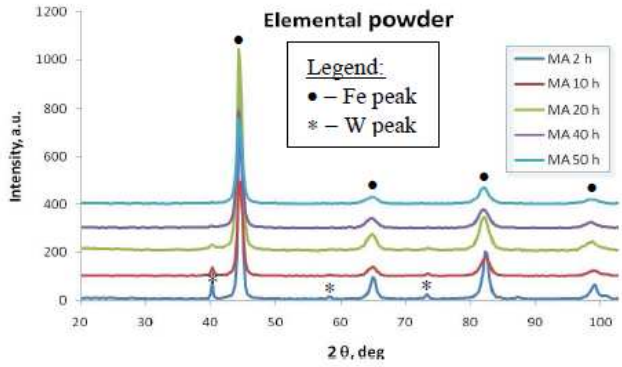

Fig. 5. XRD plots of the elemental powder MA in the planetary ball mill up to 50 h in argon

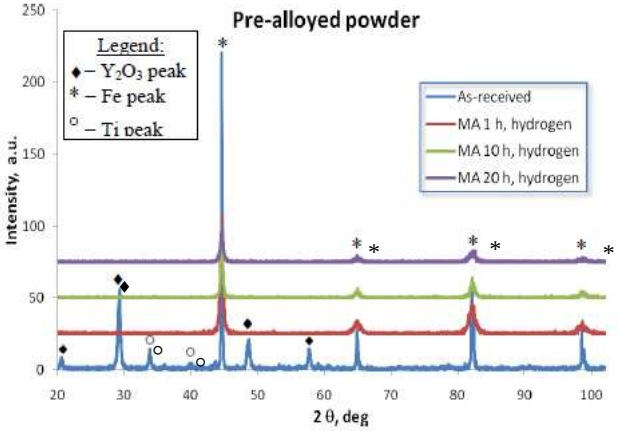

Fig. 6. XRD plots of the pre-alloyed powder MA in planetary ball mill up to 20 h in hydrogen

Also XRD examinations of the pre-alloyed powder (see Fig. 6) revealed that after 1 h of MA the peaks of Y_2O_3 and Ti disappeared what suggests that Y_2O_3 particles were completely dissolved in the ODS steel matrix. It seems highly probable, however, that yttria could still remain as a small particles incorporated deeper into the steel matrix, and as a consequence, could give a weaker X-ray signal than from the yttria particles lying on the surface of the ODS powder. This is due to the limited penetration depth of the X-rays into the material described in literature (Cullity, 1965). Hence, MA process of the pre-alloyed powder was continued up to 20 h to ensure homogenous incorporation of the Y_2O_3 particles in the ODS steel powder.

Detailed analysis of the XRD spectra indicates that during MA the main [110] α-Fe peak is gradually broadened and shifted towards lower 2θ angle values. This indicates an increase in solid solubility of the solute elements in the α-Fe matrix, an increase in the lattice strain as well as the gradual reduction of the crystallite size as it was confirmed in Figs. 7 and 8. In the early stage of MA a rapid decrease in the crystallite size to about 40 nm was observed (Fig. 7). Further ball milling proceeds relatively slowly and finally elemental and pre-alloyed powders reach an average crystallite size about 35 and 32 nm, respectively. These results are not consistent with TEM observations presented in Fig. 4. However, it is well known (Suryanarayana, 2001) that TEM reveals grain size images, whereas the X-ray technique gives information about an average crystallite size defined as coherently diffracted domain.

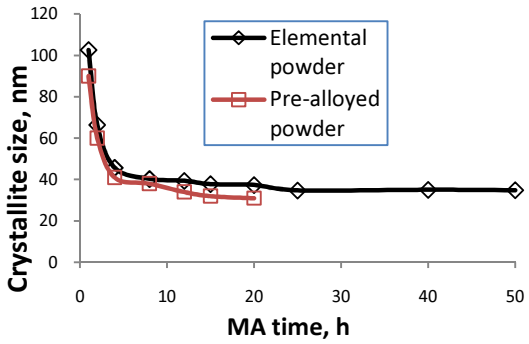

Fig. 7. Crystallite size plotted as a function of the milling time

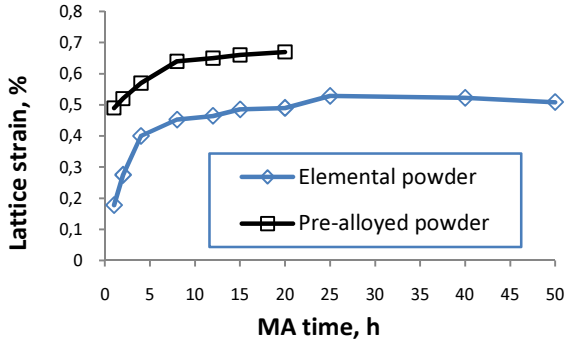

Fig. 8. Lattice strain vs. MA time of elemental and pre-alloyed powders

Fig. 8 shows the lattice strain value of the ODS powders, calculated from XRD data, and both milled using the same milling conditions. These results indicate that a higher about 30% lattice strain exhibits pre-alloyed powder.

This is probably due to an initial solid solution strengthening effect of the pre-alloyed powder. On the contrary, smaller and more reactive elemental powder particles may undergo faster recovery process, and as a consequence, a lower internal strain can be measured (Hwang, 2001). Nevertheless, both powders demonstrate similar trends, the lattice strain increase and crystallite size decrease with the milling time prolonging and after a certain period of milling a steady state is reached.

3.3. HIPping of the ODS powders

Following MA, the consolidation process was carried out under a pressure of 200 MPa at a temperature of 1150° C for 4 h. The results of microhardness and apparent density of the specimens after HIPping are summarized in Tab. 2.

The obtained in Table 2 results indicate that the highest density and microhardness value has the pre-alloyed powder mechanically alloyed in hydrogen. On the contrary, the lowest density has the material consolidated from elemental powder MA in argon. This is a consequence of the highest impurities content measured in the elemental powder after milling which can not be reduced during further degassing and HIPping process.

Tab. 2. Microhardness and density results of the ODS ferritic steel specimens after MA in different atmospheres and HIPped under a pressure of 200 MPa at 1150° C for 4 h

As-HIPped	Elemental, MA 42 h, argon	Elemental, MA 42 h, H_2	Pre-alloyed, MA 20 h, H_2
$\mu HV_{0.1}$	410±21	345±14	425±17
Apparent density, %	99.20*	99.52*	99.78*

** Apparent density=specimen density/theoretical density of an ODS ferritic steel (theoretical density=7.84 g/cm^3)*

These results also reveal that the parameters of HIPping process were suitable to produce almost fully dense ODS ferritic steel material.

4. CONCLUSIONS

On the basis of the results the following conclusions can be drawn:

1. There are significant differences in the morphology of the elemental and pre-alloyed powders after MA. About four times smaller particle were obtained after ball milling of the elemental powder whereas, larger and flakey-like particles were observed in the case of pre-alloyed powder.
2. An increase in the parameters of MA process yields a decrease in the time of milling, however, no significant changes in the morphology of particles have been observed.
3. The average crystallite size of about 35 nm, estimated from XRD spectra, was found comparable for both powders. However, in the case of pre-alloyed powder

TEM observations revealed elongated up to 100 nm nano-grains what is not in a good accordance with XRD results.

4. MA under argon atmosphere resulted in an increase of the O content which had detrimental influence on the density of the bulk material after HIPping.
5. It was found that the highest density and microhardness value was achieved when pre-alloyed powder was consolidated.

REFERENCES

1. **Benjamin J. S.** (1976), Mechanical Alloying, *Scientific American, 234, 40-8*.
2. **Cayron C. et al.** (2004), Microstructural evolution of Y_2O_3 and $MgAl_2O_4$ ODS EUROFER steels during their elaboration by mechanical milling and hot isostatic pressing, *Journal of Nuclear Material*, Vol. 335, 83-102.
3. **Chul-Jin Choi** (2000), Preparation of ultrafine TiC–Ni cermet powders by mechanical alloying, *Journal of Materials Processing Technology*, Vol. 104, 127-132.
4. **Cullity B. D.** (1965), *Elements of X-ray Diffraction*, *Addison-Wesley Publishing Company*, INC. London, England.
5. **Hwang S., Nishimura C., McCormick P. G.** (2001), Mechanical Milling of Magnesium Powder, *Material Science and Engineering*, Vol. A318, 22-33.
6. **Mukhopadhyay D. K., Froes F. H., Gelles D.S.** (1998), Development of oxide dispersion strengthened ferritic steels for fusion, *Journal of Nuclear Materials*, Vol. 258-263, 1209-1215.
7. **Ohtsuka S., et al.** (2005), Nano-structure control in ODS martensitic steels by means of selecting titanium and oxygen contents, *Journal of Physics and Chemistry of Solids*, Vol. 66, 571-575.
8. **Patil U., et al.** (2005), An unusual phase transformation during mechanical alloying of an Fe-based bulk metallic, *Journal of Alloy and Compounds*, Vol. 389, 121-126.
9. **Suryanarayana C.** (2001), Mechanical alloying and milling, *Progress in Mat. Science*, Vol. 46, 1-184.
10. **Williamson G .K., Hall W. H.** (1953), X-ray line broadening from filed aluminum and wolfram, *Acta Metall.*, Vol.1, p. 22.

This work was supported by Bialystok Technical University, a grant no. W/WM/21/10.

NUMERICAL EVALUATION OF FRACTIONAL DIFFER-INTEGRAL OF SOME ELEMENTARY FUNCTIONS VIA INVERSE TRANSFORMATION

Piotr OSTALCZYK[*], Dariusz BRZEZIŃSKI[*]

[*]Faculty of Electrical, Electronic, Computer and Control Engineering, Department of Computer Engineering, Technical University of Lodz, ul. Stefanowskiego 18/22 , 90-537 Łódź

piotr.ostalczyk@p.lodz.pl, dbrzezin@kis.p.lodz.pl

Abstract: This paper presents methods of calculating fractional differ-integrals numerically. We discuss extensively the pros and cons of applying the Riemann-Liouville formula, as well as direct approach in form of The Grünwald-Letnikov method. We take closer look at the singularity, which appears when using classical form of Riemann-Liouville formula. To calculate Riemann-Liouville differ-integral we use very well-known techniques like The Newton-Cotes Midpoint Rule. We also use two Gauss formulas. By implementing transformation of the core integrand of Riemann-Liouville formula (we called it "the inverse transformation"), we would like to point the possible way of reducing errors when calculating it. The core of this paper is the subject of reducing the absolute error when calculating Riemann-Liouville differ-integrals of some elementary functions; we use our own C++ programs to calculate them and compare obtained results of all methods with, where possible, exact values, where not – with values obtained using excellent method of integration incorporated in Mathematica. We will not discuss complexity of numerical calculations. We will focus solely on minimization of the absolute errors.

1. INTRODUCTION

Fractional calculus is playing recently a major role in many scientific areas. The fractional-order derivative (FOD) or integral (FOI) are natural extensions of the well-known derivatives and integrals. This generalisation enables better physical phenomena identification (Oustaloup et al., 2005; Sabatier et al., 2007), analysis (Carpinteri and Mainardi, 1997; Chen et al., 2004; Kilbas et al., 2006; Michalski, 1993; Miller and Ross, 1993; Nishimoto, 1984, 1989, 1991, 1996; Oldham and Spanier, 1974; Oustaloup, 1995; Samko et al., 1993) and control (Machado, 2001, Ostalczyk, 2000, 2003a, b; Oustaloup, 1984). But there are still problems in numerical evaluation of the fractional-order derivatives or integrals (Deng, 2007; Diethelm, 1997; Gorenflo, 2001; Lubich, 1986; Mayoral, 2006; Podlubny, 1999; Schmidt and Amsler, 1999; Tuan and Gorenflo, 1995). In this paper several numerical methods applied to FOD/FOI calculation are compared, due to its accuracy. Appropriate conclusions and remarks are derived.

The paper is organised as follows. Firstly basic definitions of FOD and FOI are given. In Section 3 short review of numerical methods used in calculation of the improper integrals is given. Section 4 presents functions subjected to the fractional differentiation and integration. In Section 5 main results are presented. Finally, the conclusions are given.

2. MATHEMATICAL PRELIMINARIES

There are several formulas, which can be used to calculate differ-integrals numerically. One of them is Grünwald-Letnikov and second one Riemann-Liouville, formula (Ostalczyk, 2000; Podlubny, 1999; Samko et al., 1993). They distinct from each other in one main way: Grünwald-Letnikov formula derives from differential quotient and Riemann-Liouville from multiple integrals.

This paper shows the pros and cons of applying the Riemann-Liouville formula. Also, the ideas how to reduce absolute errors when calculating it numerically. The Grünwald-Letnikov formula is used for comparing purposes only. The accuracy reached by this method as reference.

2.1. The Grünwald-Letnikov formula of a fractional-order differ-integral (GrLet)

The derivative of a real order $v > 0$ (for the integral we use order $-v < 0$) of a continuous bounded function $f(t)$ is defined as follows

$$ {}_{t_0}D_t^{v} f(t) = \lim_{\substack{h\to 0 \\ t-t_0 = kh}} \frac{\sum_{i=0}^{\frac{t-t_0}{h}} a_i^{(v)} f(t-hi)}{h^{v}} \tag{1} $$

where

$$ a_i^{(v)} = \begin{cases} 1 \quad \text{for} \quad i = 0 \\ a_{i-1}^{(v)}\left(1-\dfrac{1+v}{i}\right) \end{cases} \quad \text{for} \quad i = 1,2,3,\ldots \tag{2} $$

2.2. The Riemann-Liouville formula of a fractional-order differ-integral (RL)

The definite Riemann-Liouville integral of the real function $f(t)$ of the $v > 0$ order is defined as follows:

$$ {}_{t_0}I_t^{\nu} f(t) = \frac{1}{\Gamma(\nu)} \int_{t_0}^{t} (t-\tau)^{\nu-1} f(\tau) d\tau. \tag{3} $$

where: t_0, t – integration range, which comply with the condition $-\infty < t_0 < t < \infty$, $\Gamma(\nu)$ – Euler's Gamma function.

Before we define the Riemann-Liouville derivative, we have to describe natural number n, which comply with the condition:

$$ n = [\nu] + 1. \tag{4} $$

n also denotes an order of classical derivative.

The Riemann-Liouville derivative of the real function $f(t)$ of the $\nu > 0$ order is defined as follows:

$$ {}_{t_0}D_t^{\nu} f(t) = \sum_{i=0}^{n-1} \frac{(t-t_0)^{i-\nu} f^{(i)}(t_0)}{\Gamma(i+1-\nu)} + \frac{1}{\Gamma(n-\nu)} \int_{t_0}^{t} (t-\tau)^{n-\nu-1} f^{(n)}(\tau) d\tau \tag{5} $$

3. SHORT REVIEW OF FUNDAMENTAL METHODS OF NUMERICAL INTEGRATION AND TESTED FUNCTIONS

In the process of calculating differ-integrals it is necessary to calculate a value of the definite integral over the range $[t_0, t]$. Usually it is interpolated with the following formula

$$ \int_{t_0}^{t} f(t) dt = \sum_{k=0}^{L} A_k f(t_k) + R. \tag{6} $$

The right side of the equation is called quadrature, in which t_k – denotes quadrature nodes, A_k – quadrature coefficients (weights), L – number of intervals in interpolation and R – the remainder.

The above formula is shared by all quadratures. The difference lies in the algorithms of calculating their nodes and coefficients.

We used following formulas to calculate differ-integrals:

- Riemann-Liouville differ-integral (RL);
- Modified Riemann-Liouville differ-integral via mentioned at the beginning – inverse transformation (mRL).

Additionally we use Grünwald-Letnikov differ-integral formula (GrLET).

Our C++ programs which were developed especially for the purpose of this experiment used following methods of numerical integration while applying formulas (RL, mRL):

- Newton-Cotes quadrature, Midpoint Rule (NCM);
- Gauss-Legendre quadrature (GaLEG);
- Gauss-Laguerre quadrature (GaLAG).

We have chosen three basic functions

$$ f(t) = t^p 1(t), t \in (0;1) \text{ for } p = 0,1,2 \tag{7} $$

where

$$ 1(t) = \begin{cases} 0 & \text{for } t < 0 \\ 1 & \text{for } t \geq 0 \end{cases} \tag{8} $$

is the Heaviside function. For functions (7) we calculate two types of expressions: ${}_{t_0}D_t^{\nu} f(t)$ and ${}_{t_0}I_t^{\nu} f(t)$. In Tab. 1 different methods specifications are collected.

Tab. 1. Important parameters used in integration rules

Method /weight function	h / A_k	t_k	$R \leq$
NCM	$h = \frac{t-t_0}{L}$	$t_k = t_0 + (k+1/2)h$	$\frac{h^3}{24} \left| f^{(II)}(\zeta) \right|$, $\zeta \in [t_0, t]$
GaLEG $p(x)=1$	$A_k = \frac{2}{(1-t_k^2)[P_n'(t_k)]^2}$	Abscissas of the Legendre polynomial $P_n(x)$ of desired grade x_k. $t_k = \frac{t-t_0}{2} x_k + \frac{t-t_0}{2}$	$\frac{t-t_0}{2016000} f^{(VI)}(\zeta)$, $\zeta \in [t_0, t]$
GaLAG $p(x) = e^{-x}$	$A_k = \frac{(n!)^2}{x_k [L_n'(x_k)]^2}$	Abscissas of the Laguerre polynomial $L_n(x)$ of desired grade x_k.	$\frac{(n!)^2}{(2n)!} f^{(2n)}(\zeta)$ $\zeta \in \langle 0; +\infty)$

Our goal was to figure out how the methods will perform when using the smallest, arbitral chosen, number of sample points:

For the method GrLET and NCM we used L=4,8,16,24,32,100,300 and 600 intervals.

For both Gauss methods – L=4,8,16,24 and 32 intervals only.

It is widely known, that number of L greater than 30-40 for the Gauss methods often causes the error rise rapidly. Sometimes 100% and more! That's why you will encounter empty fields in all tables with results for these methods.

4. THE INVERSE TRANSFORMATION (mRL) EXPLAINED

As we remember the Riemann-Liouville differ-integral formula includes improper integral which has singularity at end of the integration range. For example for t=1: $\int_0^1 (1-x)^{\nu-1} f(x) dx$. The variable changes $1 - x = 1/t^{\alpha}$, $\alpha = 1, 2, 3, \ldots$ and $t - 1 = u$ convert the improper integral into one, that, after extracting weight function $p(x) = e^{-x}$ can then be calculated by the Gauss-Laguerre quadrature formula $\int_0^{\infty} e^{-x} f(t) dx$, which were developed to deal with such problems.

Yet more: with the parameter α we can control the convergence of the integrand, which plays major role when obtaining best results while the order of differ-integral changes. As you will notice further, there exists very close

relation between order of differ-integral and the value of parameter α. We will use it to our advantage.

5. THE TEST RESULTS

First ${}_{t_0}I_t^{\nu} f(t)$ of function $f(t) = t^0 1(t) = 1(t)$, for $t \in (1,1)$, $\nu = 0.2, 0.5, 0.8$ using modified Riemann-Liouville differ-integral formula via mRL

$$ {}_{t_0}I_t^{\nu} f(t) = \frac{1}{\Gamma(\nu)} \int_0^{\infty} e^t \frac{\alpha}{\left(\frac{1}{(1+t)^{\alpha}}\right)^{\nu-1} (1+t)^{\alpha+1}} dt \qquad (9) $$

was evaluated. The results are presented in Tab. 2a – 2c. Related absolute errors are plotted in Figs. 1a – 1c

Tab. 2a. Obtained values of absolute error for $\nu = 0.2$

L	RL NCM	RL GaLEG	GrLET	mRL GaLAG
4	5.427e-01	4.587e-01	2.206e-02	4.822e-02
8	4.725e-01	3.557e-01	1.097e-02	4.529e-03
16	4.114e-01	2.729e-01	5.465e-03	1.297e-04
24	3.794e-01	2.330e-01	3.639e-03	1.417e-05
32	3.582e-01	**2.081e-01**	2.728e-03	**1.076e-10**
100	2.852e-01	-	8.718e-03	-
300	2.289e-01	-	2.905e-04	-
600	**1.993e-01**	-	**1.452e-04**	-

Tab. 2b. Obtained values of absolute error for $\nu = 0.5$

L	RL NCM	RL GaLEG	GrLET	mRL GaLAG
4	1.699e-01	1.039e-01	3.463e-02	6.951e-02
8	1.205e-01	5.781e-02	1.748e-02	7.111e-03
16	8.527e-02	2.977e-02	8.780e-03	1.909e-04
24	6.964e-02	2.005e-02	5.861e-03	1.096e-05
32	6.032e-02	**1.511e-02**	4.399e-03	**9.725e-10**
100	3.413e-02	-	1.410e-03	-
300	1.970e-02	-	4.701e-04	-
600	**1.393e02**	-	**2.351e-04**	-

Tab. 2c. Obtained values of absolute error for ν=0.8

L	RL NCM	RL GaLEG	GrLET	mRL GaLAG
4	3.048e-02	1.439e-02	2.070e-02	6.501e-02
8	1.765e-02	5.183e-03	1.055e-02	6.162e-03
16	1.017e-02	1.792e-03	5.321e-03	1.771e-04
24	7.362e-03	9.516e-04	3.558e-03	1.033e-05
32	5.852e-03	**6.054e-04**	2.672e-03	**2.545e-10**
100	2.354e-03	-	8.577e-03	-
300	9.777e-04	-	2.862e-04	-
600	**5.615e-04**	-	**1.431e-04**	-

In Tab. 3 optimal values of α as functions of orders are presented. Convergence of modified integrands – Fig. 2.

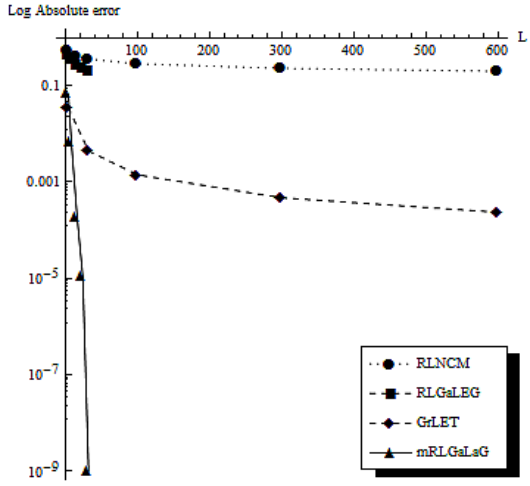

Fig. 1a. Values of absolute error for $\nu = 0.2$

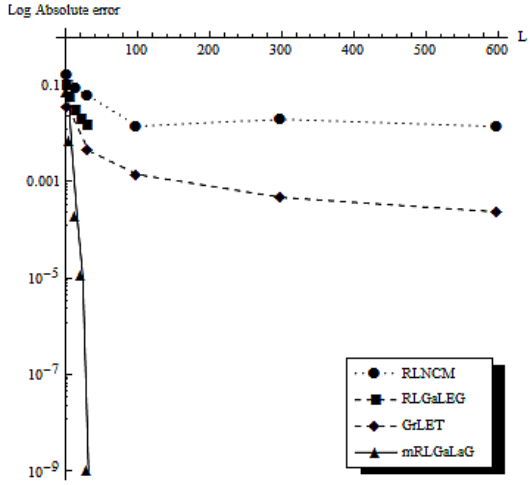

Fig. 1b. Values of absolute error for $\nu = 0.5$

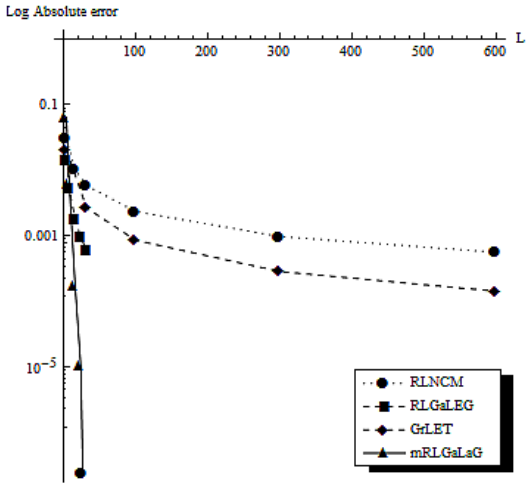

Fig. 1c. Values of absolute error for ν=0.8

Tab. 3. Lowest values of absolute error obtained for optimal values of α depending on ν (mRL GaLAG)

α	$\nu = 0.2$	$\nu = 0.5$	ν=0.8
12.95	**1.076e-08**	4.591e-05	6.842e-04
5.97	3.171e-03	**9.725e-10**	7.705e-06
3.71	2.975e-02	1.020e-04	**2.545e-09**

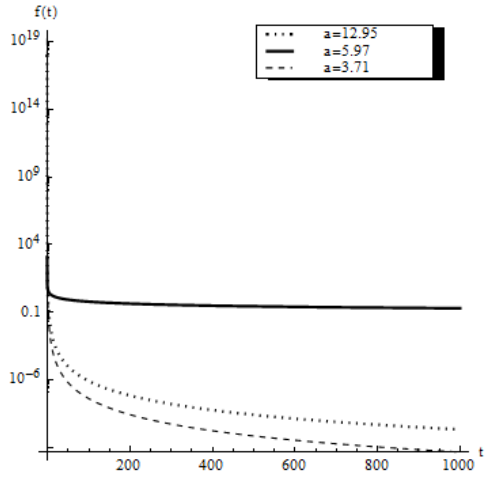

Fig. 2. Convergence of integrand (9) for optimal values of α depending on v (mRL GaLAG)

Next similar integrals are obtained for function $f(t) = t^1 1(t)$ for $t \in (0,1)$, $v = 0.2, 0.5, 0.8$. This time a modified Riemann-Liouville differ-integral formula via mRL assumes the form

$$ {}_{t_0}I_t^v f(t) = \frac{1}{\Gamma(v)} \int_0^\infty e^t \frac{\alpha\left(1-\frac{1}{(1+t)\alpha}\right)}{\left(\frac{1}{(1+t)^\alpha}\right)^{v-1}} \frac{}{(1+t)^{\alpha+1}} dt \qquad (10) $$

The results are presented in Tabs. 4a – 4c and related plots are included in Figs. 3a – 3c.

Tab. 4a. Obtained values of absolute error for $v = 0.2$

L	RL NCM	RL GaLEG	GrLET	mRL GaLAG
4	5.442e-01	4.592e-01	2.608e-02	6.521e-02
8	7.339e-01	3.558e-01	1.332e-02	1.380e-02
16	4.118e-01	2.729e-01	6.734e-02	6.505e-04
24	3.796e-01	2.330e-01	4.505e-02	2.389e-05
32	3.583e-01	**2.081e-01**	3.385e-03	**9.019e-07**
100	2.852e-01	-	1.087e-03	-
300	2.289e-01	-	3.628e-04	-
600	**1.993e-01**	-	**1.815e-04**	-

Tab. 4b. Obtained values of absolute error for $v = 0.5$

L	RL NCM	RL GaLEG	GrLET	mRL GaLAG
4	1.735e-01	6.806e-02	6.806e-02	8.860e-02
8	1.218e-01	5.790e-02	3.463e-02	2.299e-03
16	8.576e-01	2.972e-02	1.747e-02	1.406e-03
24	6.991e-01	2.005e-02	1.168e-02	7.497e-04
32	6.050e-01	**1.512e-02**	8.775e-03	**8.816e-07**
100	3.416e-01	-	2.816e-03	-
300	1.971e-01	-	9.399e-04	-
600	**1.393e-01**	-	**4.700e-04**	-

Tab. 4c. Obtained values of absolute error for $v = 0.8$

L	RL NCM	RL GaLEG	GrLET	mRL GaLAG
4	3.237e-02	1.459e-02	1.055e-01	9.402e-02
8	1.826e-02	5.203e-03	5.320e-02	4.341e-02
16	1.036e-02	1.793e-03	1.036e-02	5.540e-03
24	7.459e-03	9.521e-04	1.784e-02	5.880e-04
32	5.911e-03	**6.056e-04**	1.339e-02	**1.202e-06**
100	2.362e-03	-	4.292e-03	-
300	9.789e-04	-	1.431e-03	-
600	**5.619e-04**	-	**7.157e-04**	-

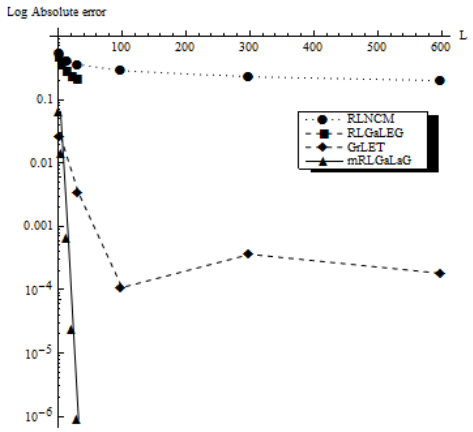

Fig. 3a. Values of absolute error for $v = 0.2$

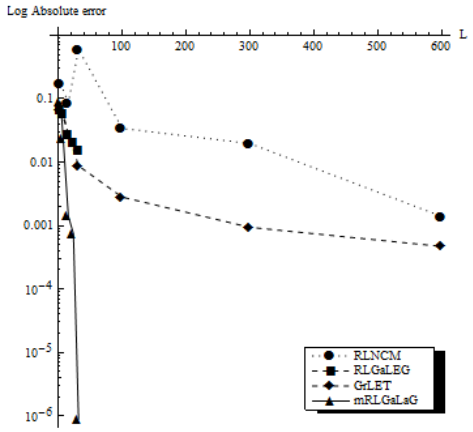

Fig. 3b. Values of absolute error for $v = 0.5$

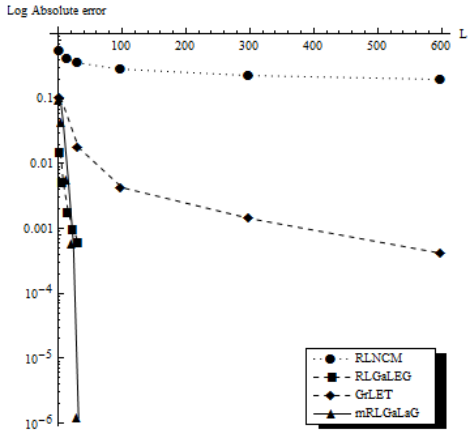

Fig. 3c. Values of absolute error for $v = 0.8$

In Tab. 5 optimal values of α as functions of orders are presented. Convergence of modified integrands – Fig. 4.

Tab. 5. Lowest values of absolute error obtained for optimal values of α depending on ν (mRL GaLAG)

α	$\nu = 0.2$	$\nu = 0.5$	$\nu = 0.8$
9.090	**1.202e-06**	1.112e-03	3.591e-03
4.341	1.604e-02	**8.816e-07**	5.725e-05
2.900	6.567e-02	8.919e-04	**9.019e-07**

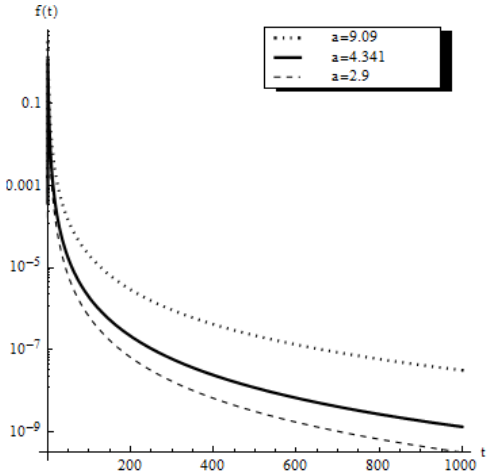

Fig. 4. Convergence of integrand (10) for optimal values of α depending on ν (mRL GaLAG)

Tab. 6a. Obtained values of absolute error for $\nu = 0.2$

L	RL NCM	RL GaLEG	GrLET	mRL GaLAG
4	5.463e-01	4.579e-01	4.493e-02	8.935e-02
8	4.742e-01	5.222e-01	2.258e-02	5.645e-03
16	4.121e-01	1.795e-01	1.132e-02	9.926e-03
24	3.798e-01	9.529e-01	7.551e-03	3.905e-03
32	3.585e-01	**6.057e-01**	1.088e-03	**1.330e-03**
100	2.853e-01	-	1.814e-03	-
300	2.290e-01	-	6.050e-04	-
600	**1.993e-01**	-	**3.025e-04**	-

Tab. 6b. Obtained values of absolute error for $\nu = 0.5$

L	RL NCM	RL GaLEG	GrLET	mRL GaLAG
4	1.789e-01	1.106e-01	9.550e-02	9.566e-02
8	1.236e-01	5.800e-02	4.740e-02	3.233e-03
16	8.638e-01	2.980e-02	2.360e-02	6.917e-03
24	7.024e-01	2.006e-02	1.571e-02	1.623e-03
32	6.071e-01	**1.512e-02**	1.178e-02	**3.450e-04**
100	3.420e-01	-	3.764e-03	-
300	1.972e-01	-	1.254e-03	-
600	**1.394e-01**	-	**6.269e-04**	-

Finally we calculate ${}_{t_0}I_t^{\nu} f(t)$ of function $f(t) = t^2 1(t)$ for $t \in (0,1)$, $\nu = 0.2, 0.5, 0.8$. The modified Riemann-Liouville differ-integral formula via mRL assumes the form

$$ {}_{t_0}I_t^{\nu} f(t) = \frac{1}{\Gamma(\nu)} \int_0^{\infty} e^{t} \frac{\alpha\left(1-\frac{1}{(1+t)\alpha}\right)^2}{\left(\frac{1}{(1+t)^{\alpha}}\right)^{\nu-1} (1+t)^{\alpha+1}} dt \qquad (11) $$

The results are presented in Tab. 6a – 6c and related plots are included in Figs. 5a – 5c. In Tab. 7 optimal values of α as functions of orders are presented. Convergence of modified integrands – Fig. 10.

Tab. 6c. Obtained values of absolute error for $\nu = 0.8$

L	RL NCM	RL GaLEG	GrLET	mRL GaLAG
4	3.819e-02	1.480e-02	1.255e-01	2.393e-02
8	1.986e-02	5.222e-03	6.121e-02	8.463e-03
16	1.081e-02	1.795e-03	3.021e-02	1.875e-03
24	7.667e-03	9.529e-04	2.006e-02	2.769e-04
32	6.033e-03	**6.057e-04**	1.501e-02	**4.059e-05**
100	2.377e-03	-	4.782e-03	-
300	9.808e-04	-	1.592e-03	-
600	**5.624e-04**	-	**7.956e-04**	-

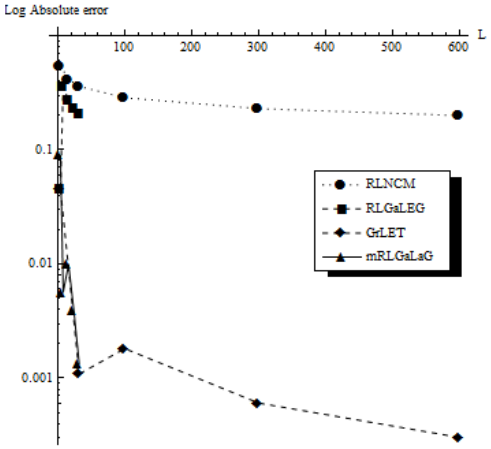

Fig. 5a. Values of absolute error for $\nu = 0.2$

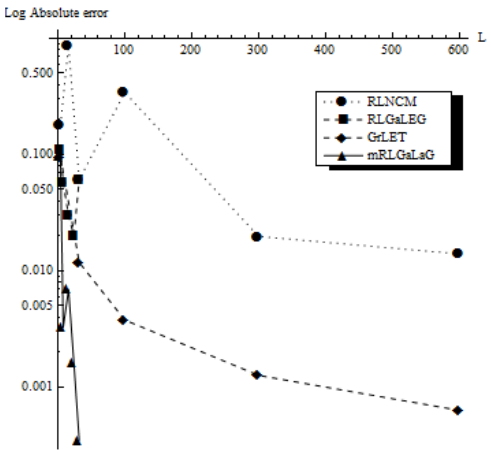

Fig. 5b. Values of absolute error for $\nu = 0.5$

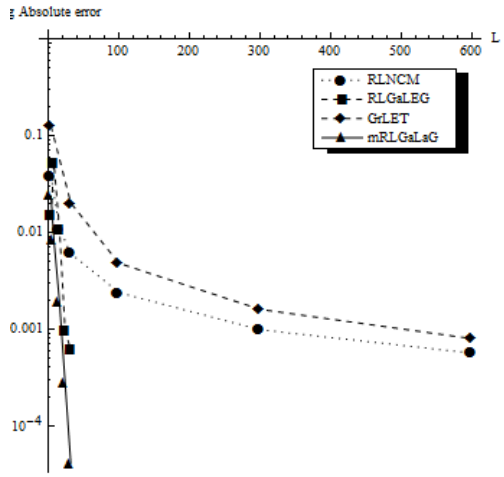

Fig. 5c. Values of absolute error for $v = 0.8$

Tab. 7. Lowest values of absolute error obtained for optimal values of α depending on v(mRL GaLAG)

α / v	0.2	0.5	0.8
7.91	**1.330e-03**	3.238e-03	6.127e-03
5.05	8.027e-03	**3.640e-04**	8.272e-04
2.90	6.564e-02	9.081e-04	**4.059e-05**

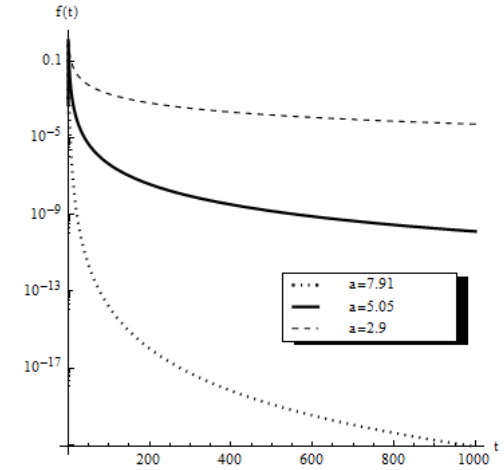

Fig. 6. Convergence of integrand (11) for optimal values of α depending on v (mRL GaLAG)

Now a problem of the fractional derivative ${}_{t_0}D_t^v f(t)$ of function $f(t) = t^0 1(t)$ for $t \in (0,1)$, $v = 0.2, 0.5, 0.8$ is considered. We assume $f(0) = 1$ and calculate

$$\lceil n \rceil = v + 1 \tag{12}$$

Then the modified Riemann-Liouville differ-integral formula via mRL takes the form

$${}_{t_0}D_t^v f(t) = \tag{13}$$

$$= \frac{f(0)}{\Gamma(1-v)} + \frac{1}{\Gamma(n-v)} \int_0^{\infty} e^t \frac{\overbrace{\alpha \cdot 0}^{=0}}{\left(\frac{1}{(1+t)^{\alpha}}\right)^{n-v-1} (1+t)^{\alpha+1}} dt$$

One can realize that the above value depends, in this case solely on accuracy of the inverse gamma function. The obtained results are presented in Tabs. 8a – 8c and related plots are included in Figs. 7a – 7c.

Tab. 8a. Obtained values of absolute error for $v = 0.2$

L	RL NCM	RL GaLEG	GrLET	mRL GaLAG
4	**0.0**	**0.0**	2.777e-02	**0.0**
8	**0.0**	**0.0**	1.377e-02	**0.0**
16	**0.0**	**0.0**	6.562e-03	**0.0**
24	**0.0**	**0.0**	4.348e-03	**0.0**
32	**0.0**	**0.0**	3.251e-03	**0.0**
100	**0.0**	-	1.034e-03	-
300	**0.0**	-	3.439e-04	-
600	**0.0**	-	**1.718e-04**	-

Tab. 8b. Obtained values of absolute error for $v = 0.5$

L	RL NCM	RL GaLEG	GrLET	mRL GaLAG
4	**0.0**	**0.0**	6.081e-02	**0.0**
8	**0.0**	**0.0**	2.829e-02	**0.0**
16	**0.0**	**0.0**	1.376e-02	**0.0**
24	**0.0**	**0.0**	9.011e-03	**0.0**
32	**0.0**	**0.0**	6.721e-03	**0.0**
100	**0.0**	-	2.127e-03	-
300	**0.0**	-	7.065e-04	-
600	**0.0**	-	**3.529e-04**	-

Tab. 8c. Obtained values of absolute error for $v = 0.8$

L	RL NCM	RL GaLEG	GrLET	mRL GaLAG
4	**0.0**	**0.0**	4.894e-02	**0.0**
8	**0.0**	**0.0**	2.177e-02	**0.0**
16	**0.0**	**0.0**	1.031e-02	**0.0**
24	**0.0**	**0.0**	6.758e-03	**0.0**
32	**0.0**	**0.0**	5.026e-03	**0.0**
100	**0.0**	-	1.581e-03	-
300	**0.0**	-	5.242e-04	-
600	**0.0**	-	**2.617e-04**	-

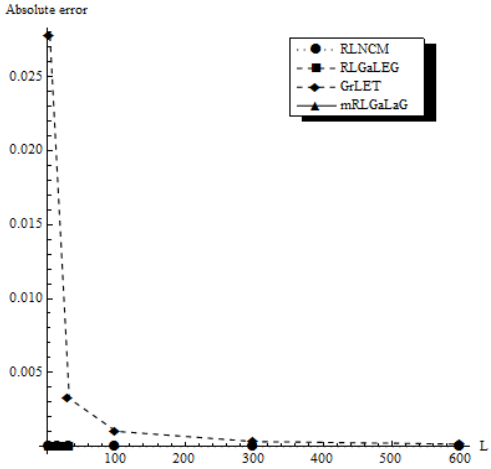

Fig. 7a. Values of absolute error for $v = 0.2$

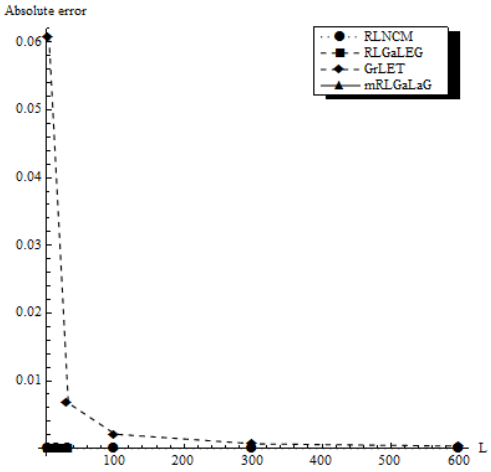

Fig. 7b. Values of absolute error for $v = 0.5$

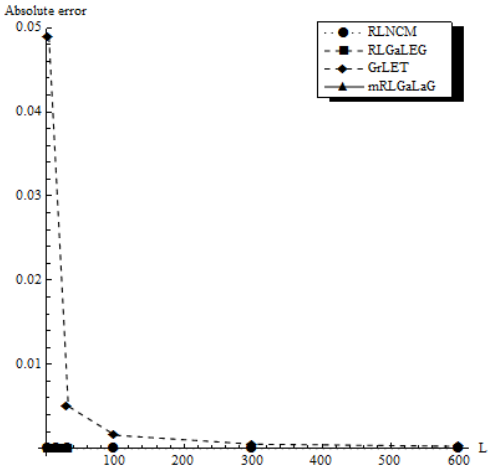

Fig. 7c. Values of absolute error for $v = 0.8$

Tab. 9a. Obtained values of absolute error for $v = 0.2$

L	RL NCM	RL GaLEG	GrLET	mRL GaLAG
4	3.048e-02	1.439e-02	2.070e-02	6.501e-02
8	1.765e-02	5.183e-03	1.055e-02	6.616e-03
16	1.017e-02	1.792e-03	5.321e-03	1.771e-04
24	7.362e-03	9.516e-04	3.558e-03	1.033e-05
32	5.852e-03	**6.054e-04**	2.672e-03	**2.545e-09**
100	2.354e-03	-	8.577e-04	-
300	9.776e-04	-	2.862e-04	-
600	**5.615e-04**	-	**1.431e-04**	-

Tab. 9b. Obtained values of absolute error for $v = 0.5$

L	RL NCM	RL GaLEG	GrLET	mRL GaLAG
4	1.699e-01	1.093e-02	3.463e-02	7.006e-02
8	1.205e-01	5.781e-02	1.748e-02	7.148e-03
16	8.527e-02	2.977e-02	8.780e-03	1.932e-04
24	6.964e-02	2.005e-02	5.861e-03	1.103e-05
32	6.032e-02	**1.511e-02**	4.399e-03	**3.353e-08**
100	3.413e-02	-	1.410e-03	-
300	1.970e-02	-	4.700e-04	-
600	**1.393e-02**	-	**2.350e-04**	-

Tab. 9c. Obtained values of absolute error for $v = 0.8$

L	RL NCM	RL GaLEG	GrLET	mRL GaLAG
4	5.424e-01	4.587e-01	2.206e-02	4.781e-02
8	4.725e-01	3.557e-01	1.097e-02	4.483e-03
16	4.114e-01	2.729e-01	5.465e-03	1.293e-04
24	3.794e-01	2.330e-01	3.639e-03	1.452e-05
32	3.582e-01	**2.081e-01**	2.728e-03	**4.105e-08**
100	2.852e-01	-	8.718e-04	-
300	2.289e-01	-	2.905e-04	-
600	**1.993e-01**	-	**1.452e-04**	-

Next similar derivative is obtained for function $f(t) = t^1 1(t)$ for $t \in (0,1)$, $v = 0.2, 0.5, 0.8$. Under a condition (12) modified Riemann-Liouville differ-integral formula via mRL assumes the form

$$ {}_{t_0}D_t^{v} f(t) = \tag{14}$$

$$= \frac{1}{\Gamma(n-v)} \int_0^{\infty} e^t \frac{\alpha}{\left(\frac{1}{(1+t)^{\alpha}}\right)^{n-v-1} (1+t)^{\alpha+1}} dt$$

The obtained results are presented in Tabs. 9a – 9c and related plots are included in Figs. 8a – 8c. In table 10 optimal values of α as functions of orders are presented. Convergence of modified integrands – Fig. 9.

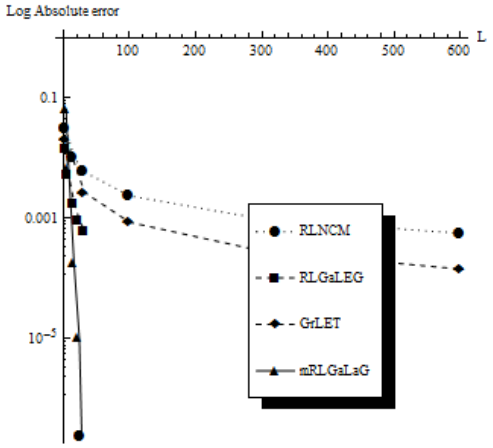

Fig. 8a. Values of absolute error for $v = 0.2$

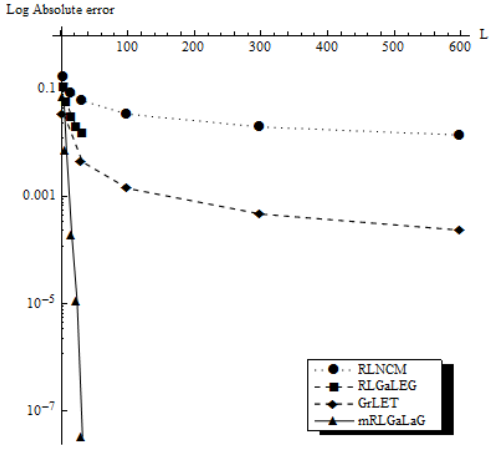

Fig. 8b. Values of absolute error for $v = 0.5$

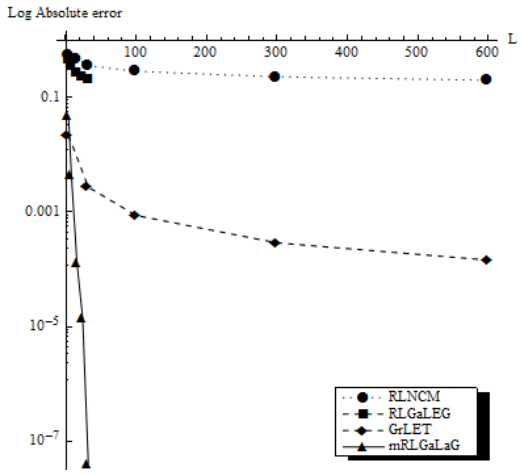

Fig. 8c. Values of absolute error for $v = 0.8$

Tab. 10. Lowest values of absolute error obtained for optimal values of α depending on v (mRL GaLAG)

α	$v = 0.2$	$v = 0.5$	$v = 0.8$
12.90	6.691e-04	4.489e-05	**4.101e-08**
6.000	7.922e-06	**3.353e-08**	3.077e-03
3.710	**2.545e-09**	1.020e-04	2.975e-02

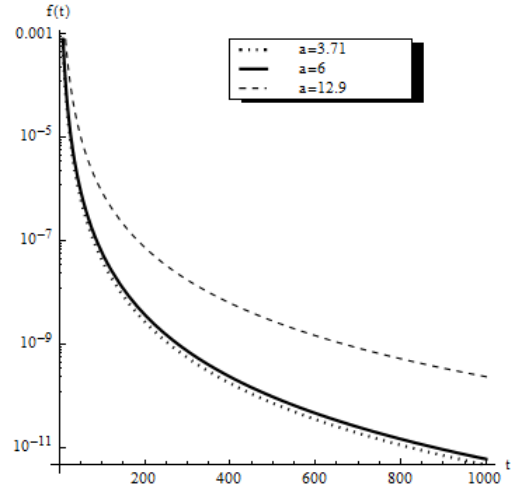

Fig. 9. Convergence of integrand (14) for optimal values of α depending on v (mRL GaLAG)

Finally we calculate ${}_{t_0}D_t^v f(t)$ of function $f(t) = t^2 1(t)$ for $t \in (0,1)$, $v = 0.2, 0.5, 0.8$. Then under the condition (12) modified Riemann-Liouville differ-integral formula via mRL assumes the form

$$ {}_{t_0}D_t^{\nu} f(t) = \tag{15}$$

$$= \frac{1}{\Gamma(n-\nu)} \int_0^{\infty} e^t \frac{2\alpha\left(1-\frac{1}{(1+t)^{\alpha}}\right)}{\left(\frac{1}{(1+t)^{\alpha}}\right)^{n-\nu-1}} \frac{dt}{(1+t)^{\alpha+1}}$$

The obtained results are presented in Tabs. 11a – 11c and related plots are included in Figs. 10a – 10c. In Tab. 12 optimal values of α as functions of orders are presented.

Convergence of modified integrands – Fig. 11.

Tab. 11a. Obtained values of absolute error for $v = 0.2$

L	RL NCM	RL GaLEG	GrLET	mRL GaLAG
4	6.473e-02	2.918e-02	5.225e-02	1.804e-01
8	3.651e-02	1.041e-02	2.648e-02	2.759e-02
16	2.073e-02	3.587e-03	1.133e-02	1.031e-03
24	1.492e-02	1.094e-03	8.907e-03	4.778e-05
32	1.182e-02	**1.211e-03**	6.688e-03	**1.844e-06**
100	4.724e-03	-	2.145e-03	-
300	1.958e-03	-	7.155e-04	-
600	**1.124e-03**	-	**3.578e-04**	-

Tab. 11b. Obtained values of absolute error for $v = 0.5$

L	RL NCM	RL GaLEG	GrLET	mRL GaLAG
4	3.469e-01	2.198e-01	1.373e-01	1.772e-01
8	2.436e-01	1.158e-02	6.960e-02	4.600e-02
16	1.715e-01	5.957e-02	3.503e-02	2.813e-03
24	1.398e-01	4.011e-02	2.341e-02	1.502e-04
32	1.210e-01	**3.023e-02**	1.757e-02	**1.736e-06**
100	6.832e-02	-	5.363e-03	-
300	3.942e-02	-	1.880e-03	-
600	**2.787e-02**	-	**9.402e-04**	-

Tab. 11c. Obtained values of absolute error for $v = 0.8$

L	RL NCM	RL GaLEG	GrLET	mRL GaLAG
4	1.880e-00	9.183e-01	2.146e-01	1.833e-01
8	9.466e-01	7.117e-01	1.081e-01	8.234e-02
16	8.235e-01	5.458e-01	5.426e-02	1.002e-02
24	7.592e-01	4.659e-01	3.622e-02	9.573e-04
32	7.166e-01	**4.161e-01**	2.718e-02	**1.573e-06**
100	5.704e-01	-	8.708e-03	-
300	4.579e-01	-	2.904e-03	-
600	**3.968e-01**	-	**1.453e-03**	-

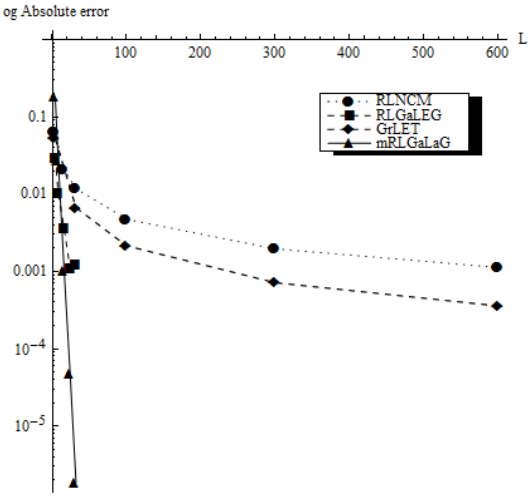

Fig. 10a. Values of absolute error for $v = 0.2$

Tab. 12. Lowest values of absolute error obtained for optimal values of α depending on ν (mRL GaLAG)

α	$\nu = 0.2$	$\nu = 0.5$	$\nu = 0.8$
8.905	6.643e-03	2.044e-03	**1.573e-06**
4.341	1.145e-04	**1.763e-06**	3.201e-02
2.900	**1.804e-06**	1.784e-03	1.313e-01

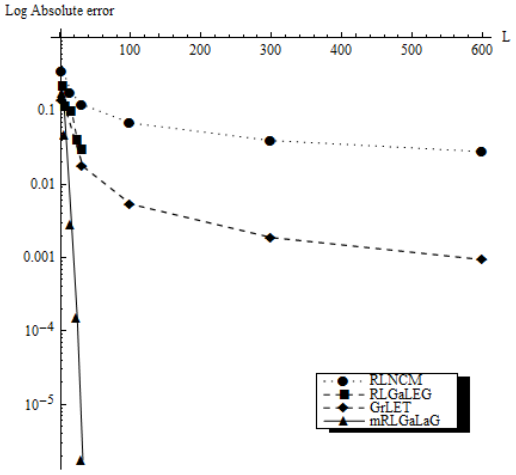

Fig. 10b. Values of absolute error for $\nu = 0.5$

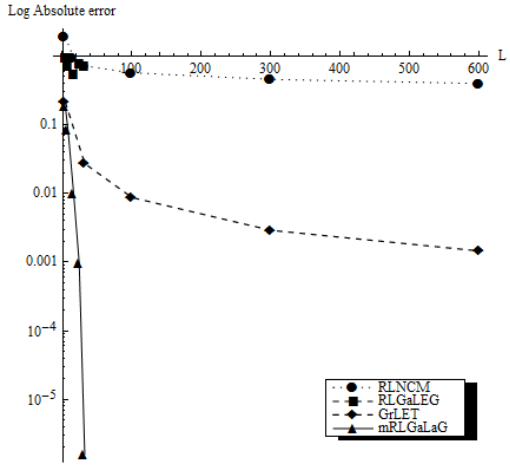

Fig. 10c. Values of absolute error for $\nu = 0.8$

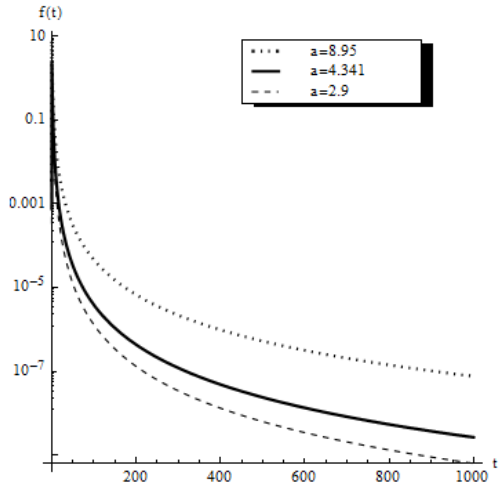

Fig. 11. Convergence of integrand (15) for optimal values of α depending on ν (mRL GaLAG)

6. FINAL CONCLUSIONS

The results presented in Section 5 enable us to formulate the following conclusions:

1. The shape of the integrand does not influence accuracy of the calculations when using Grünwald-Letnikov method. The number of coefficients used – does. Using maximum number of 600 of coefficients we were able to obtain values with maximum $10e-04$ accuracy.
2. The shape of integrand does influence accuracy of the calculations when applying advanced methods of integration to calculate differ-integrals using Riemann-Liouville formula.
3. The values of the integrand obtained using "pure" Riemann-Liouville formula are charged with great absolute error. This makes the formula often unsuitable in practical, technical applications.
4. This level of errors appeared because off the fact that the "core" integrand of the formula has "fast-changing" character and singularity at the end point of the integration range.
5. Applying inverse transformation of the integrand to "smash" the singularity allowed not only obtain much better results than by using Grünwald-Letnikov method, but often using radical reduced number of sampling points. This lowers the level of calculation complexity.
6. Applied transformation of variables and special substitute expression mentioned earlier to the "core" integrand allowed to lower the values of absolute errors about 2-6 times.
7. The values of absolute errors increased proportionally to the order of "complexity" (parameter p) of the function tested: for increasing values of p, absolute errors also increased proportionally.
8. Heaviside function – due to its character is the "domain" of Grünwald-Letnikov formula, but as the "complexity" of the function (other two functions tested) rises, if the integrand is modified, Newton-Cotes and Gauss-Laguerre rules seems to be appropriate to apply.
9. The Newton-Cotes Midpoint Rule is universal tool. Not only it does not depend so strongly as the Gauss-Legendre rule, on shape and changeability of the integrand, but also can be applied to integrands which have singularities at the both and/or end of the integration range.
10. Gauss-Laguerre rule, when applied to transformed integrand, seems to be the better way, not only because of the low values of absolute error, but also because of the fact, that these low values are obtained with only 5% sample points used by Grünwald-Letnikov method and Newton-Cotes Rule. This can dramatically reduce the complexity of the calculations.
11. Manipulation of the α variable in the inverse transformation allows to speed up the convergence of the integrand and lower the absolute error (notice figures: Convergence of integrand for optimal values of α depending on ν (mRL GaLAG)). We noticed close relation between the values of α and ν, when minimising the absolute error in calculations: for integrals – α should be reduced when ν increases; for the derivatives – the other way round.

12. The logic of our programs needed only the degree of the desired polynomial as a input data. All other data were calculated "on the fly" (the polynomial itself, its derivative, abscissas and weights). In practical applications we can and should use tabulated values of abscissas and weights which were the subject of standardization all over the world. This can reduce more the complexity of calculations which then can make the method become yet more suitable in practical applications.

REFERENCES

1. **Burden R. L., Faires J. D.** (2003), *Numerical Analysis*, 5th. Ed., Brooks/Cole Cengage Learning, Boston.
2. Carpinteri, F., A. Mainardi [ed.] (1997), *Fractals and Fractional Calculus in Continuum Mechanics*, Springer Verlag, Wien and New York.
3. **Chen Y. Q, Vinagre B. M., Podlubny I**. (2004), *Continued Fraction Expansion Approaches to Discretizing Fractional Order Derivatives – an Expository Review*, Nonlinear Dynamics 38, Kluwer Academic Publishers, 155-170.
4. **Deng W.** (2007), Short memory principle and a predictor-corrector approach for fractional differential equations. *Journal of Computational and Applied Mathematics* 206, 174-188.
5. **Diethelm K.** (1997), An algorithm for the numerical solution of differential equations of fractional order, *Electronic Transactions on Numerical Analysis*, Vol. 5, 1-6.
6. **Gorenflo R.** (2001), Fractional Calculus: Some Numerical Methods, *CISM Courses and Lectures*, Vol. 378, 277 – 290.
7. **Kilbas A. A., Srivastava H. M., Trujillo J. J.** (2006), *Theory and Applications of Fractional Differential Equations*, North-Holland Mathematics Studies 204, Elsevier.
8. **Krommer R. A., Ueberhuber Ch. W.** (1986), *Computational Integration*, SIAM, Philadelphia.
9. **Kythe P. K., Schäferkotter M. R.** (2005), *Handbook of Computational Methods For Integration*, Chapman & Hall/CRC.
10. **Lubich, C. H.** (1986), Discretized fractional calculus, *SIAM Journal of Mathematica1 Analysis*, Vol. 17, 704-719.
11. **Machado, J. A. T.** (2001), Discrete-time fractional-order controllers, *FCAA Journal*, Vol. 1, 47-66.
12. **Mayoral L.** (2006), *Testing for fractional integration versus short memory with trends and structural breaks*, Dept. of Economics and Business, Universidad Pompeu Fabra.
13. **Michalski M. W.** (1993), *Derivatives of noninteger order and their applications*, Dissertationes Mathematicae, CCC XXVIII, Inst. Math. Polish Acad. Sci., Warsaw.
14. **Miller, K. S., Ross B.** (1993), *An Introduction to the Fractional Calculus and Fractional Differential Equations*, John Wiley & Sons Inc., New York, USA.
15. **Nishimoto K.** (1984, 1989, 1991, 1996), *Fractional Calculus. Integration and Differentiation of Arbitrary Order*, tom I – IV, Descartes Press, Koriyama.
16. **Oldham K. B., Spanier J.** (1974), *The Fractional Calculus*, Academic Press, New York.
17. **Ooura T.** (2008), An IMT-type quadrature formula with the same asymptotic performance as the DE formula, *Journal of Computational and Applied Mathematics* 213, Elsevier ScienceDirect, 1-8.
18. **Ostalczyk P.** (2000), The non-integer difference of the discrete-time function and its application to the control system synthesis, *International Journal of System Science*, Vol. 31, no. 12, 1551-1561.
19. **Ostalczyk P.** (2001), *Discrete-Variable Functions*, A Series of Monographs No 1018, Technical University of Łódź, Poland.
20. **Ostalczyk P.** (2003a), The linear fractional-order discrete-time system description", *Proceedings of the 9th IEEE International Conference on Methods and Models in Automation and Robotics*, MMAR 2002, Międzyzdroje, T.I, 429 – 434.
21. **Ostalczyk P.** (2003b), The time-varying fractional order difference equations", Proceedings of DETC'03, *ASME 2003 Design Engineering Technical Conference & Computers and Information in Engineering Conference*, Chicago, USA, 1-9.
22. **Oustaloup A.** (1984), *Systèmes Asservis Linéaries d'Ordre Fractionnaire*, Masson, Paris.
23. **Oustaloup A., Cois O., Lelay L.** (2005), *Représentation et identification par modèle non entire*, Hermes.
24. **Oustaloup, A.** (1995), *La dèrivation non entière*, Éditions Hermès, Paris, France.
25. **Podlubny, I.** (1999), *Fractional differential equations*, Academic Press, San Diego, USA.
26. **Sabatier J., Agrawal O. P., Machado T. J. A.** [ed.] (2007), *Advances in Fractional Calculus. Theoretical Developments and Applications in Physics and Engeneering*, Springer Verlag.
27. **Samko S., Kilbas A., Marichev O.** (1993), *Fractional Integrals and derivatives: Theory and Applications*, Gordon and Breach, London.
28. **Schmidt P., Amsler C.** (1999), *Test of short memory with trick tailed errors*, Michigan State University.
29. **Stroud A. H., Secrest D.** (1966), *Gaussian Quadrature Formulas*, Prentice-Hall, Englewood Cliffs, NJ.
30. **Taylor J. R.** (1996), *An Introduction to Error Analysis. The Study of Uncertainties in Physical Measurements*, 2nd. Ed., University Science Books.
31. **Tuan V. K., Gorenflo R.** (1995), Extrapolation to the limit for numerical fractional differentiation, *Zeitschrift Angew. Math. Mech.*, 75, no. 8, 646-648.

VARIABLE-, FRACTIONAL-ORDERS CLOSED-LOOP SYSTEMS DESCRIPTION

Piotr OSTALCZYK*

*Katedra Informatyki Stosowanej, Politechnika Łódzka, ul. Stefanowskiego 18/22, 90-924 Łódź

piotr.ostalczyk@p.lodz.pl

Abstract: In this paper we explore the linear difference equations with fractional orders, which are functions of time. A description of closed-loop dynamical systems described by such equations is proposed. In a numerical example a simple control strategy based on time-varying fractional orders is presented.

1. INTRODUCTION

Over the last few decades a growing interest in a fractional calculus (Carpinteri and Mainardi, 1997; Lubich, 1986; Miller and Ross, 1993; Oustaloup, 1995; Podlubny, 1999) has been observed. Its technical application effected in new fractional-order models of physical processes and materials behaviour (Oustaloup, 1995; Podlubny, 1999). Extensive possibilities of modern digital processors to analyse, modify or extract information from measured signals require describing signals by discrete-time functions (Ostalczyk, 2001). In practical applications the use of a backward difference is necessary.

A variable- (V), fractional order (FO) backward difference (BD) of a discrete-time bounded function f_k is defined as follows (Ostalczyk, 2000, 2003, Ostalczyk and Derkacz, 2003).

$$ {}_0\Delta_{\infty}^{(n_j)} f_k = \sum_{i=0}^{\infty} b_i^{(n_j)} f_{k-i} = $$

$$ \begin{bmatrix} b_0^{(n_j)} & b_1^{(n_j)} & \cdots & b_k^{(n_j)} & b_{k+1}^{(n_j)} & b_{k+2}^{(n_j)} & \cdots \end{bmatrix} \begin{bmatrix} f_k \\ f_{k-1} \\ \vdots \\ f_1 \\ f_0 \\ f_{-1} \\ \vdots \end{bmatrix}, \tag{1} $$

where a difference order $n_j \in \mathbf{R}$ and discrete time instants $k \in \mathbf{N} \cup \{0\}$ ($\mathbf{R}$ and $\mathbf{N}$ denote sets of real and natural numbers, respectively). Coefficients $b_i^{(n_j)}$ are defined below

$$ b_i^{(n_j)} = \begin{cases} 1 & \text{for} \quad i = 0 \\ \dfrac{n_j(n_j-1)\cdots(n_j-i+1)}{i!} & \text{for} \quad i = 1,2,3\cdots \end{cases}. \tag{2} $$

For discrete-time functions f_k satisfying $f_k = 0$ for k<0 we can write

$$ {}_0\Delta_k^{(n_j)} f_k = \begin{bmatrix} b_0^{(n_j)} & b_1^{(n_j)} & \cdots & b_{k-1}^{(n_j)} & b_k^{(n_j)} \end{bmatrix} \begin{bmatrix} f_k \\ f_{k-1} \\ \vdots \\ f_1 \\ f_0 \end{bmatrix}. \tag{3} $$

Realize that in the formula given above the constant order n_j is independent of the time-variable k. Next we define a discrete variable function

$$ \mathbf{N} \cup \{0\} \ni j \to n_j \in \mathbf{R}. \tag{4} $$

The VFOBD defined by formula (3) is a function of two discrete variables k and j

$$ \mathbf{N} \cup \{0\} \ni k \to g_{k,j} = {}_0\Delta_k^{(n_j)} f_k \in \mathbf{R}. \tag{5} $$

For a special assignment of n_j and k we define a new one discrete variable function

$$ \mathbf{N} \cup \{0\} \ni k \to h_k = {}_0\Delta_k^{(n_k)} f_k \in \mathbf{R}, \tag{6} $$

defined as

$$ h_k = {}_0\Delta_{\infty}^{(n_k)} f_k = \sum_{i=0}^{\infty} b_i^{(n_k)} f_{k-i} = $$

$$ \begin{bmatrix} b_0^{(n_k)} & b_1^{(n_k)} & \cdots & b_k^{(n_k)} & b_{k+1}^{(n_k)} & b_{k+2}^{(n_k)} & \cdots \end{bmatrix} \begin{bmatrix} f_k \\ f_{k-1} \\ \vdots \\ f_1 \\ f_0 \\ f_{-1} \\ \vdots \end{bmatrix} \tag{7} $$

with

$$ b_i^{(n_k)} = \begin{cases} 1 & \text{for} \quad i = 0 \\ \dfrac{n_k(n_k-1)\cdots(n_k-i+1)}{i!} & \text{for} \quad i = 1,2,3\cdots \end{cases}. \tag{8} $$

For $f_k = 0$ for $k < 0$ we obtain

$$ {}_0\Delta_k^{(n_k)} f_k = \sum_{i=0}^{k} b_i^{(n_k)} f_{k-i}. \tag{9} $$

It should be noted that the VFOBD is related to a variable-order fractional operator defined as (Coimbra, 2003; Lorenzo and Hartley, 2002)

$$ {}_0d_t^{n(t)}y(t)=\int_0^t \frac{(t-\tau)^{-n(t)-1}}{\Gamma(-n(t))}y(\tau)d\tau . \tag{10}$$

It can be proved (Oustaloup, 1995) that for every $t \geq 0$ the formula given above is equivalent to the following limit

$$ {}_0d_t^{n(t)}y(t)=\lim_{h\to 0}\frac{\sum_{i=0}^{\left[\frac{t}{h}\right]} b_i^{(n(t))}y(t-ih)}{h^{n(t)}} . \tag{11}$$

where [.] denotes a function rounding towards the nearest integer, $h>0$ is an integration step. Substituting $t=kh$ with $h=1$ we immediately obtain a VFOBD defined by formula (9)

In this paper we focus our attention on linear systems described by VFOBD equations with time-invariant coefficients. Next we explore an adequate description of a closed-loop system with a controller and plant modelled by a FO difference equation. In the second numerical example we show that even though the physical processes described by VFOBD equations are yet unknown, they are useful in a control strategies design.

2. LINEAR VFO DISCRETE-TIME SYSTEMS

Now we consider a linear VFO difference equation (DE)

$$ \sum_{i=0}^{r} A_i\, {}_0\Delta_\infty^{(n_{i,k})}y_k = \sum_{j=0}^{s} B_j\, {}_0\Delta_\infty^{(m_{j,k})}u_k , \tag{12}$$

where

$$ A_r\neq 0 ,\ A_i, B_j \in \mathbf{R} ,\ i=0,1,2,\cdots,r ,\ j=0,1,2,\cdots,s , \tag{13}$$

$$ n_{rk}, n_{r-1,k},\cdots,n_{1,k},n_{0,k}\in\mathbf{R} \tag{14}$$

$$ m_{s,k}, m_{s-1,k},\cdots,m_{1,k},m_{0,k}\in\mathbf{R}$$

Here we admit a case when some $n_{i,k}=n_{j,k}$, $m_{i,k}=m_{j,k}$ or even $n_{i,k}=n_{j,k}=0$ for $i\neq j$ (a subscript k denotes an appropriate discrete time instant).

From this point on we will make use of a permanent assumption that $u_k=0$ for $k<0$. Hence difference Equation (12) can be expressed in the following form

$$ \begin{bmatrix} A_r & A_{r-1} & \cdots & A_1 & A_0 \end{bmatrix} \begin{bmatrix} {}_0\Delta_\infty^{(n_{r,k})}y_k \\ {}_0\Delta_\infty^{(n_{r-1,k})}y_k \\ \vdots \\ {}_0\Delta_\infty^{(n_{1,k})}y_k \\ {}_0\Delta_\infty^{(n_{0,k})}y_k \end{bmatrix} = \tag{15}$$

$$ = \begin{bmatrix} B_s & B_{s-1} & \cdots & B_1 & B_0 \end{bmatrix} \begin{bmatrix} {}_0\Delta_k^{(m_{s,k})}u_k \\ {}_0\Delta_k^{(m_{s-1,k})}u_k \\ \vdots \\ {}_0\Delta_k^{(m_{1,k})}u_k \\ {}_0\Delta_k^{(m_{0,k})}u_k \end{bmatrix} .$$

Substituting the column vectors in difference equation (15) by formulae (1) and (3) yields

$$ \begin{bmatrix} A_r & A_{r-1} & \cdots & A_1 & A_0 \end{bmatrix} \times \tag{16}$$

$$ \times \begin{bmatrix} b_0^{(n_{r,k})} & b_1^{(n_{r,k})} & \cdots & b_k^{(n_{r,k})} & \cdots \\ b_0^{(n_{r-1,k})} & b_1^{(n_{r-1,k})} & \cdots & b_k^{(n_{r-1,k})} & \cdots \\ \vdots & \vdots & & \vdots & \\ b_0^{(n_{1,k})} & b_1^{(n_{1,k})} & \cdots & b_k^{(n_{1,k})} & \cdots \\ b_0^{(n_{0,k})} & b_1^{(n_{0,k})} & \cdots & b_k^{(n_{0,k})} & \cdots \end{bmatrix} \begin{bmatrix} y_k \\ y_{k-1} \\ \vdots \\ y_0 \\ \vdots \end{bmatrix} =$$

$$ = \begin{bmatrix} B_s & B_{s-1} & \cdots & B_1 & B_0 \end{bmatrix} \times$$

$$ \times \begin{bmatrix} b_0^{(m_{s,k})} & b_1^{(m_{s,k})} & \cdots & b_{k-1}^{(m_{s,k})} & b_k^{(m_{s,k})} \\ b_0^{(m_{s-1,k})} & b_1^{(m_{s-1,k})} & \cdots & b_{k-1}^{(m_{s-1,k})} & b_k^{(m_{s-1,k})} \\ \vdots & \vdots & & \vdots & \vdots \\ b_0^{(m_{1,k})} & b_1^{(m_{1,k})} & \cdots & b_{k-1}^{(m_{1,k})} & b_k^{(m_{1,k})} \\ b_0^{(m_{0,k})} & b_1^{(m_{0,k})} & \cdots & b_{k-1}^{(m_{0,k})} & b_k^{(m_{0,k})} \end{bmatrix} \begin{bmatrix} u_k \\ u_{k-1} \\ \vdots \\ u_1 \\ u_0 \end{bmatrix} .$$

Multiplications of the row-vectors by appropriate matrices in Equation (16) yield

$$ \begin{bmatrix} a_{0,k} & a_{1,k} & \cdots & a_{k,k} & \cdots \end{bmatrix} \begin{bmatrix} y_k \\ y_{k-1} \\ \vdots \\ y_0 \\ \vdots \end{bmatrix} = \begin{bmatrix} b_{0,k} & \cdots & b_{k,k} \end{bmatrix} \begin{bmatrix} u_k \\ \vdots \\ u_0 \end{bmatrix} , \tag{17}$$

where

$$ a_{i,k} = \begin{bmatrix} A_r & A_{r-1} & \cdots & A_1 & A_0 \end{bmatrix} \begin{bmatrix} b_i^{(n_{r,k})} \\ b_i^{(n_{r-1,k})} \\ \vdots \\ b_i^{(n_{1,k})} \\ b_i^{(n_{0,k})} \end{bmatrix} ,\ i=0,1,2,\cdots, \tag{18}$$

and

$$ b_{j,k} = \begin{bmatrix} B_s & B_{s-1} & \cdots & B_1 & B_0 \end{bmatrix} \begin{bmatrix} b_j^{(m_{s,k})} \\ b_j^{(m_{s-1,k})} \\ \vdots \\ b_j^{(m_{1,k})} \\ b_j^{(m_{0,k})} \end{bmatrix} ,\ j=0,1,,\cdots,k .$$

Further we assume that $a_{0,k}\neq 0$ for all k. It should be noted that practical realisations of the discrete-time systems impose an additional condition $\max\{n_{r,k},\ldots,n_{0,k}\}\geq \max\{m_{s,k},\ldots,m_{0,k}\}$ on all non-negative k. Equation (17) is valid for every positive integer. Thus for $k-1$ we have

$$\begin{bmatrix} a_{0,k} & a_{1,k} & \cdots & a_{k,k} & \cdots \end{bmatrix} \begin{bmatrix} y_k \\ y_{k-1} \\ \vdots \\ y_0 \\ \vdots \end{bmatrix} = \begin{bmatrix} b_{0,k} & \cdots & b_{k,k} \end{bmatrix} \begin{bmatrix} u_k \\ \vdots \\ u_0 \end{bmatrix}, \tag{19}$$

while

$$\begin{bmatrix} a_{0,k-1} & a_{1,k-1} & \cdots & a_{k-1,k-1} & \cdots \end{bmatrix} \begin{bmatrix} y_{k-1} \\ y_{k-2} \\ \vdots \\ y_0 \\ \vdots \end{bmatrix} = \begin{bmatrix} b_{0,k-1} & \cdots & b_{k-1,k-1} \end{bmatrix} \begin{bmatrix} u_{k-1} \\ \vdots \\ u_0 \end{bmatrix} \tag{20}$$

This can be further transformed into an equivalent form

$$\begin{bmatrix} 0 & a_{0,k-1} & \cdots & a_{k-1,k-1} \end{bmatrix} \begin{bmatrix} y_k \\ y_{k-1} \\ \vdots \\ y_0 \end{bmatrix} + \begin{bmatrix} a_{k,k-1} & a_{k+1,k-1} & \cdots \end{bmatrix} \begin{bmatrix} y_{-1} \\ y_{-2} \\ y_{-3} \\ \vdots \end{bmatrix} =$$

$$= \begin{bmatrix} 0 & b_{0,k-1} & \cdots & b_{k-2,k-1} & b_{k-1,k-1} \end{bmatrix} \begin{bmatrix} u_k \\ u_{k-1} \\ \vdots \\ u_1 \\ u_0 \end{bmatrix}. \tag{21}$$

Repeating this notation for $k-1, k-2, \ldots, 1, 0$ and putting them together in the matrix-vector form we get

$$\begin{bmatrix} a_{0,k} & a_{1,k} & \cdots & a_{k-1,k} & a_{k,k} \\ 0 & a_{0,k-1} & \cdots & a_{k-2,k-1} & a_{k-1,k-1} \\ \vdots & \vdots & & \vdots & \vdots \\ 0 & 0 & \cdots & a_{0,1} & a_{1,1} \\ 0 & 0 & \cdots & 0 & a_{0,0} \end{bmatrix} \begin{bmatrix} y_k \\ y_{k-1} \\ \vdots \\ y_1 \\ y_0 \end{bmatrix} +$$

$$+ \begin{bmatrix} a_{k+1,k} & a_{k+2,k} & a_{k+3,k} & \cdots \\ a_{k,k-1} & a_{k+1,k-1} & a_{k+2,k-1} & \cdots \\ \vdots & \vdots & \vdots & \\ a_{1,0} & a_{2,0} & a_{3,0} & \cdots \end{bmatrix} \begin{bmatrix} y_{-1} \\ y_{-2} \\ y_{-3} \\ \vdots \end{bmatrix} = \tag{22}$$

$$= \begin{bmatrix} b_{0,k} & b_{1,0} & \cdots & b_{k-1,k} & b_{k,k} \\ 0 & b_{0,k-1} & \cdots & b_{k-2,k-1} & b_{k-1,k-1} \\ \vdots & \vdots & & \vdots & \vdots \\ 0 & 0 & \cdots & b_{0,1} & b_{1,1} \\ 0 & 0 & \cdots & 0 & b_{0,0} \end{bmatrix} \begin{bmatrix} u_k \\ u_{k-1} \\ \vdots \\ u_1 \\ u_0 \end{bmatrix}$$

or

$$\mathbf{D}_k \mathbf{y}_k + \mathbf{I}_k \mathbf{y}_I = \mathbf{N}_k \mathbf{u}_k, \tag{23}$$

where

$$\mathbf{D}_k = \begin{bmatrix} a_{0,k} & a_{1,k} & \cdots & a_{k-1,k} & a_{k,k} \\ 0 & a_{0,k-1} & \cdots & a_{k-2,k-1} & a_{k-1,k-1} \\ \vdots & \vdots & & \vdots & \vdots \\ 0 & 0 & \cdots & a_{0,1} & a_{1,1} \\ 0 & 0 & \cdots & 0 & a_{0,0} \end{bmatrix}, \tag{24}$$

is $(k+1)\times(k+1)$ output matrix,

$$\mathbf{I}_k = \begin{bmatrix} a_{k+1,k} & a_{k+2,k} & a_{k+3,k} & \cdots \\ a_{k,k-1} & a_{k+1,k-1} & a_{k+2,k-1} & \cdots \\ \vdots & \vdots & \vdots & \\ a_{1,0} & a_{2,0} & a_{3,0} & \cdots \end{bmatrix}, \tag{25}$$

is $(k+1)\times(\infty)$ initial conditions matrix,

$$\mathbf{N}_k = \begin{bmatrix} b_{0,k} & b_{1,0} & \cdots & b_{k-1,k} & b_{k,k} \\ 0 & b_{0,k-1} & \cdots & b_{k-2,k-1} & b_{k-1,k-1} \\ \vdots & \vdots & & \vdots & \vdots \\ 0 & 0 & \cdots & b_{0,1} & b_{1,1} \\ 0 & 0 & \cdots & 0 & b_{0,0} \end{bmatrix}, \tag{26}$$

is $(k+1)\times(k+1)$ input matrix,

$$\mathbf{y}_k = \begin{bmatrix} y_k \\ y_{k-1} \\ \vdots \\ y_1 \\ y_0 \end{bmatrix}, \mathbf{y}_I = \begin{bmatrix} y_{-1} \\ y_{-2} \\ y_{-3} \\ \vdots \end{bmatrix}, \mathbf{u}_k = \begin{bmatrix} u_k \\ u_{k-1} \\ \vdots \\ u_1 \\ u_0 \end{bmatrix}, \tag{27}$$

are $(k+1)\times 1$ output, $\infty \times 1$ initial conditions, and $(k+1)\times 1$ input vectors, respectively. Square matrix (24) is always non-singular. Hence Equation (23) can be always rearranged into the form

$$\mathbf{y}_k = \mathbf{D}_k^{-1}\mathbf{N}_k\mathbf{u}_k - \mathbf{D}_k^{-1}\mathbf{I}_k\mathbf{y}_I, \tag{28}$$

where the first right-hand side term denotes a forced part of the response, the second a homogenous one. The above investigations are illustrated by following numerical example.

2.1. Numerical example

Consider the VFODE of the form

$${}_0\Delta_{\infty}^{(n_{1,k})} y_k + \frac{1}{2} y_k = \frac{1}{2} u_k, \tag{29}$$

For a given external function $u_k = 1_{k-1}$ (discrete unit step function) and the assumed zero initial conditions $0 = y_{-1}, y_{-2}, y_{-3} = \cdots$ one should find an order function $n_{1,k}$ for which the solution has the form

$$y_k = \begin{cases} \alpha k & \text{for} \quad 0 \le k \le k_s \\ 1 & \text{for} \quad k_s < k \end{cases}, \tag{30}$$

where α and k_s mean undetermined yet: the response slope

parameter and the switch time instant, respectively. Substituting (3) into (29) we get (15) and further (17). For $k-1, k-2, \ldots, 1, 0$ we obtain (23) with

$$\mathbf{y}_k = \begin{bmatrix} y_k \\ y_{k-1} \\ \vdots \\ y_1 \\ y_0 \end{bmatrix}, \mathbf{y}_I = \begin{bmatrix} 0 \\ 0 \\ 0 \\ \vdots \end{bmatrix}, \mathbf{u}_k = \begin{bmatrix} 1 \\ 1 \\ \vdots \\ 1 \\ 1 \end{bmatrix}, \tag{31}$$

$$\mathbf{D}_k = \begin{bmatrix} 1.5 & b_1^{(n_{1,k})} & \cdots & b_{k-1}^{(n_{1,k})} & b_k^{(n_{1,k})} \\ 0 & 1.5 & \cdots & b_{k-2}^{(n_{1,k-1})} & b_{k-1}^{(n_{1,k-1})} \\ \vdots & \vdots & & \vdots & \vdots \\ 0 & 0 & \cdots & 1.5 & b_1^{(n_{1,1})} \\ 0 & 0 & \cdots & 0 & 1.5 \end{bmatrix}, \tag{32}$$

$$\mathbf{I}_k = \begin{bmatrix} b_{k+1}^{(n_{1,k})} & b_{k+2}^{(n_{1,k})} & b_{k+3}^{(n_{1,k})} & \cdots \\ b_{k+1}^{(n_{1,k-1})} & b_{k+2}^{(n_{1,k-1})} & b_{k+3}^{(n_{1,k-1})} & \cdots \\ \vdots & \vdots & \vdots & \\ b_1^{(n_{1,0})} & b_2^{(n_{1,0})} & b_3^{(n_{1,0})} & \cdots \end{bmatrix}, \tag{33}$$

$$\mathbf{N}_k = \begin{bmatrix} 0 & 0.5 & 0 & \cdots & 0 \\ 0 & 0 & 0.5 & \cdots & 0 \\ 0 & 0 & 0 & \cdots & 0 \\ \vdots & \vdots & \vdots & & \vdots \\ 0 & 0 & \cdots & 0 & 0 \end{bmatrix}, \tag{34}$$

Now we evaluate the consecutive values of an order function $n_{1,k}$. For $k = 0$ and any $n_{1,0}$ the unique solution of equation (29) is $y_0 = 0$. For $k = 1$ and any $n_{1,1}$ one possible solution is $y_1 = 1/3$. Hence we must put $\alpha = 1/3$. This implies that $y_2 = 2/3$ and $y_i = 1$ for $i = 3, 4, \cdots$. Further, for $k = 2$, from formulae (28) and (31) – (36) we obtain

$$1.5y_2 - n_{1,2}y_1 + 0.5n_{1,2}(n_{1,2} - 1)y_0 = 0.5, \tag{35}$$

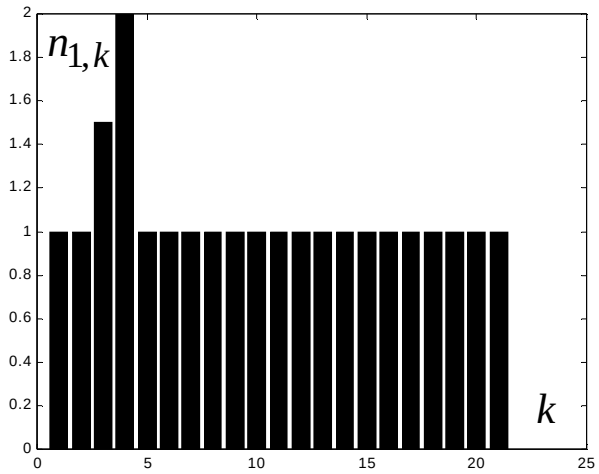

Fig. 1. Plot of an order function $n_{1,k}$

Substituting appropriate values, after elementary operations, we get $n_{1,2} = 1{,}5$. For $k = 3$ we get equation

$$1.5y_3 - n_{1,3}y_2 + \frac{n_{1,3}(n_{1,3}-1)}{2}y_1 + \frac{n_{1,3}(n_{1,3}-1)(n_{1,3}-2)}{6}y_0 = 0.5, \tag{36}$$

From two possible solutions $n_{1,3} = 2$ and $n_{1,3} = 3$ we take the first one. Continuing this procedure as an order function we take

$$n_{1,k} = \begin{cases} 1\,(\text{any}) & \text{for} \quad k = 0,1 \\ 1.5 & \text{for} \quad k = 2 \\ 2 & \text{for} \quad k = 3 \\ 1 & \text{for} \quad k \geq 4 \end{cases}, \tag{37}$$

Its plot is presented in Fig. 1 .

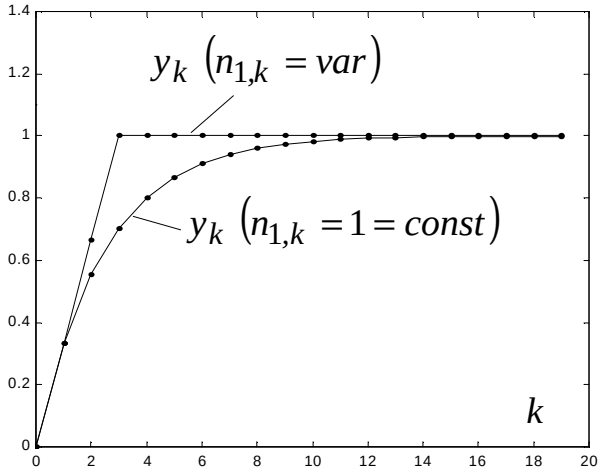

Fig. 2. Plot of the VFODE and classical first-order DE solutions

The solution to difference equation (29) with order function (37) is plotted in Fig. 2. Here, for the sake of comparison, the solution to a classical fist-order difference equation ($n_{1,k} = 1 = \text{const}$) is also plotted.

The numerical example considered above shows that it is possible to reshape the solution to a VFODE. It should be noted that although y_0, y_1 do not depend on $n_{1,0}, n_{1,1}$ for $k \geq 2$ we have

$$\begin{matrix} y_2(n_{1,2}) \\ y_3(n_{1,2}, n_{1,3}) \\ y_4(n_{1,2}, n_{1,3}, n_{1,4}) \\ \vdots \end{matrix}, \tag{38}$$

3. DESCRIPTION OF A CLOSED - LOOP DYNAMICAL SYSTEM

Next we consider a unity-feedback system with a linear discrete-time plant and a discrete-time controller. In general, we assume that a time-invariant coefficients plant is described by the (time-invariant or time-variant) fractional order difference equation. A block diagram of a closed-loop system is presented in Fig. 3.

A plant is described by an equation similar to Equation (28)

$$\mathbf{p}_k = \mathbf{D}_{P,k}^{-1}\mathbf{N}_{P,k}\mathbf{u}_k - \mathbf{D}_{P,k}^{-1}\mathbf{I}_{P,k}\mathbf{p}_I \tag{39}$$

where $\mathbf{u}_k, \mathbf{p}_k$ are the plant input and output signals, respectively. The vectors $\mathbf{p}_I$ and $\mathbf{v}_I$ denote the plant and regulator initial conditions, respectively. The plant is controlled by the controller output signal $\mathbf{v}_k$ and subjected to a plant disturbance signal $\mathbf{d}_{i,k}$ vector. A controller algorithm is described by VFODE (12) or equivalently by the matrix-vector Eq. (28)

$$\mathbf{v}_k = \mathbf{D}_{R,k}^{-1}\mathbf{N}_{R,k}\mathbf{e}_k - \mathbf{D}_{R,k}^{-1}\mathbf{I}_{R,k}\mathbf{v}_I \tag{40}$$

where $\mathbf{e}_k$ denotes the controller input (a closed-loop system error). Column vectors $\mathbf{r}_k, \mathbf{d}_k, \mathbf{n}_k$ denote: a system command, a plant output disturbance and the sensor noise signals, respectively. The vector $\mathbf{y}_k$ is a system output signal. Additional four equations describe the closed-loop system

$$\begin{aligned} &\mathbf{e}_k = \mathbf{r}_k - \mathbf{w}_k,\ \mathbf{w}_k = \mathbf{y}_k + \mathbf{n}_k, \\ &\mathbf{y}_k = \mathbf{p}_k + \mathbf{d}_k, \mathbf{u}_k = \mathbf{v}_k + \mathbf{d}_{ik}. \end{aligned} \tag{41}$$

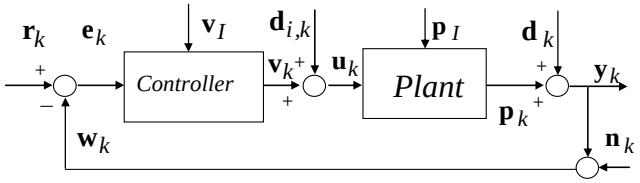

Fig. 3. Block diagram of the closed-loop system

Combining Equations (39)-(41) we get an input/output description of the closed-loop system

$$\begin{aligned} \mathbf{y}_k = &\left(\mathbf{1}_k + \mathbf{G}_{O,k}\right)^{-1}\left(\mathbf{G}_{O,k}\mathbf{r}_k - \mathbf{G}_{O,k}\mathbf{n}_k + \mathbf{d}_k\right) + \\ &+ \left(\mathbf{1}_k + \mathbf{G}_{O,k}\right)^{-1}\mathbf{D}_{P,k}^{-1}\mathbf{N}_{P,k}\mathbf{d}_{i,k} - \\ &- \left(\mathbf{1}_k + \mathbf{G}_{O,k}\right)^{-1}\mathbf{D}_{P,k}^{-1}\left[\mathbf{N}_{P,k}\mathbf{D}_{R,k}^{-1}\mathbf{I}_{R,k} \quad \mathbf{I}_{P,k}\right]\begin{bmatrix}\mathbf{v}_I \\ \mathbf{p}_I\end{bmatrix} \end{aligned} \tag{42}$$

where $\mathbf{G}_{O,k} = \mathbf{D}_{P,k}^{-1}\mathbf{N}_{P,k}\mathbf{D}_{R,k}^{-1}\mathbf{N}_{R,k}$ is an open loop system description, the matrix $\mathbf{1}_k$ is $(k+1)\times(k+1)$ unit matrix.

4. VFOs $\mathrm{PI}^{(\mathbf{m_{1,k}})}\mathrm{D}^{(\mathbf{m_{2,k}})}$ CONTROLLER DESCRIPTION

Linear control strategies in the form of PID algorithms are still basic in digital control since they give satisfactory solutions to different control problems. In such controllers control strategies are implemented by software thus a realisation may be restricted mainly by a micro-controller memory and speed.

The constant fractional-order discrete-time PID controllers have been the subject of investigations for many years (Machado, 2001; Podlubny, 1999). Here we define a VFOs discrete-time $\mathrm{PI}^{(m_{1,k})}\mathrm{D}^{(m_{2,k})}$ controller. Its algorithm is described by a special case of Equation (12) where we put

$$r = 0, n_{0,k} = 0,\ s = 2, m_{2,k}, m_{1,k}, m_{0,k} \in \mathbf{R} \tag{43}$$

In general, to preserve the PID strategy, in general, we assume that $m_{0,k} = 0$ and $m_{1,k} > 0, m_{2,k} > 0$. According to Fig.3, the controller input is denoted by e_k and the output by v_k. Hence the $\mathrm{PI}^{(m_{1,k})}\mathrm{D}^{(m_{2,k})}$ controller is described by the following difference equation

$$v_k = \sum_{j=0}^{2} B_j\, {}_0\Delta_\infty^{(m_{j,k})} e_k = \begin{bmatrix}K_P & K_I & K_D\end{bmatrix}\begin{bmatrix} e_k \\ {}_0\Delta_\infty^{(m_{1,k})} e_k \\ {}_0\Delta_\infty^{(m_{2,k})} e_k \end{bmatrix} \tag{44}$$

where $B_0 = K_p$, $B_1 = K_I$, $B_2 = K_D$ denote proportional, integral and derivative gain, respectively. It is assumed that $K_p + K_I + K_D \neq 0$. Equation (44) implies that $\mathbf{D}_{R,k} = \mathbf{I}_k$, hence from (40) we get

$$\mathbf{v}_k = \mathbf{N}_{R,k}\mathbf{e}_k - \mathbf{I}_{R,k}\mathbf{v}_I, \tag{45}$$

where the matrix $\mathbf{N}_{R,k}$ is defined by equation (26) with

$$b_{j,k} = \begin{bmatrix}K_P & K_I & K_D\end{bmatrix}\begin{bmatrix} b_j^{(m_{0,k})} \\ b_j^{(m_{1,k})} \\ b_j^{(m_{2,k})} \end{bmatrix},\ j = 0,1,2,\cdots,k-1,k. \tag{46}$$

The possible use of such a controller will be presented in the following numerical example.

4.1. Closed-loop system with VFO PID controller transient response numerical evaluation

Consider a closed-loop system with a plant described by difference Equation (12) with the following coefficients (Günther, 1986)

$$\begin{aligned} &A_2 = 1, A_1 = 1.9397, A_0 = 0.3804, B_2 = 0.0191, \\ &B_1 = -0.0666, B_0 = 0.0475, n_2 = m_2 = 2, \\ &n_1 = m_1 = 1, n_0 = m_0 = 0 \end{aligned} \tag{47}$$

The controller is described by a VFODE of the form

$$v_k = K_P e_k + K_I\, {}_0\Delta_k^{(m_{1,k})} e_k + K_D\, {}_0\Delta_k^{(m_{2,k})} e_k. \tag{48}$$

We assume that the following constraint

$$-20 \le |v_k| \le 20, \tag{49}$$

is imposed on the controlling signal.

To preserve the maximum value of the controlling signal for $k = 0$, the coefficients K_p, K_I, K_D must satisfy the equality $K_p + K_I + K_D = 20$ The controller gains chosen are $K_p = 16{,}375$, $K_I = 3{,}125$ and $K_D = 0{,}5$ and the orders $m_{1,0} = -1$ and $m_{2,0} = 1$ can be chosen freely. The VFOs are selected and plotted in Fig.4

$$m_{1,k} = \begin{cases} -1\,(\text{arbitrary}) & \text{for} \quad k = 0 \\ -1.2505 & \text{for} \quad k = 1 \\ -1 + 0.8e^{-(k-1)} & \text{for} \quad 2 \le k \le 9 \\ -1 & \text{for} \quad k \ge 10 \end{cases}, \tag{50}$$

$$m_{2,k} = \begin{cases} 1\,(\text{arbitrary}) & \text{for} \quad \mathrm{k} = 0 \\ 0.9596 & \text{for} \quad \mathrm{k} = 1 \\ 1 + 6.034e^{-0.05(k-1)} & \text{for} \quad 2 \le k \le 9 \\ 1 & \text{for} \quad k \ge 10 \end{cases}, \tag{51}$$

It should observed that the exponential order functions in formulae (50) and (51) are non-unique. There is a wide choice of other functions. It seems important to preserve the condition $m_{1,k} = -1$ and $m_{2,k} = 1$ for all $k \geq k_I$ (when the system achieves its steady-state). Over mentioned interval the closed-loop system can be described by classical (integer order) DE. This requirement eliminates real-time calculation problems.

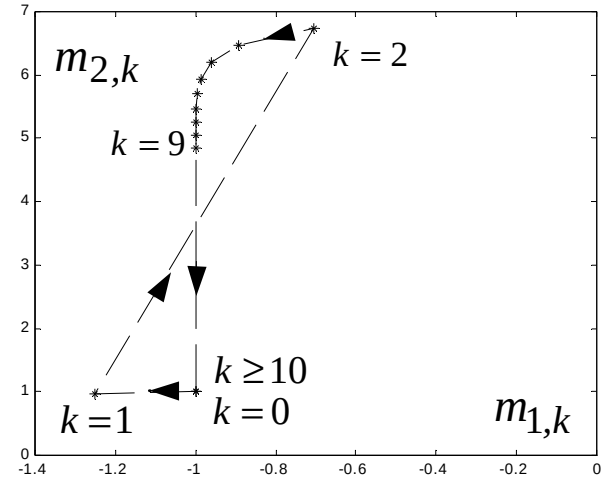

Fig. 4. VFOs $m_{1k} - m_{2k}$ trajectory

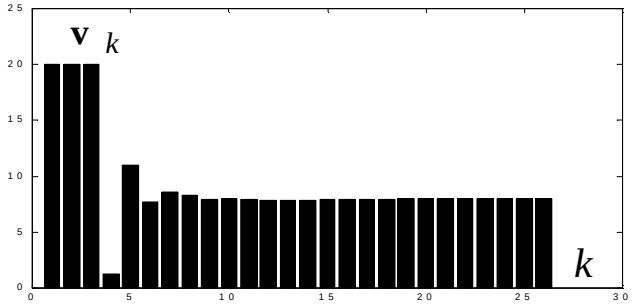

Fig. 5. The closed-loop system-controlling signal $\mathbf{v}_k$

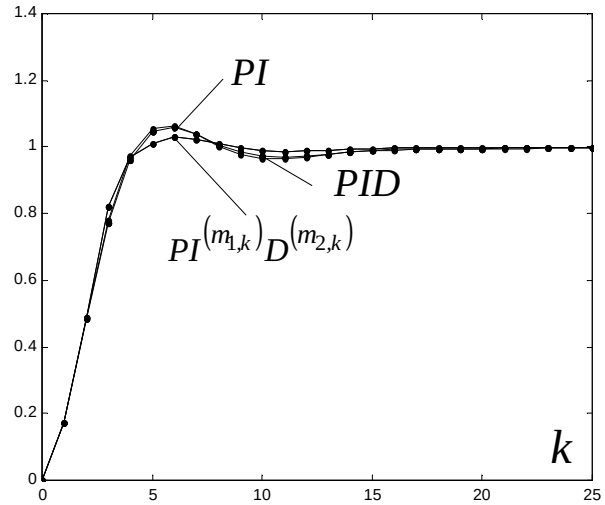

Fig. 6. The closed-loop system outputs with different controllers

In Fig. 3 the VFO satisfying Equations (50) and (51) are presented in orders plane $m_1 m_2$. It should be noted that after a finite number of time instants, the VFODE based control algorithm becomes a simple integer-order one, and as a result, a linear increase of samples considered in a calculation process (growing "calculation tail" or "finite memory problem") can be avoided. Thus, it is not necessary to simplify an algorithm by cutting the "calculation tail".

The control algorithm has PID controller properties (Günther, 1986; Ifeachor and Jervis, 1993; Isermann, 1988; Ogata, 1987). To avoid a growing number of samples (so called "calculation tail" (Podlubny, 1999)), after a finite number of a control algorithm steps the orders m_{1k} and m_{2k} become integers. Thus, the "calculation tail" has automatically been cut off. This should be achieved in a quasi-steady-state of the closed-loop system response. We assume zero initial conditions of the plant and the controller. In Fig. 5 we show the controlling signal $\mathbf{v}_k$.

Fig. 6 presents the plant output $\mathbf{y}_k(.)$ for the case when $\mathbf{d}_k = \mathbf{d}_{ik} = \mathbf{n}_k = 0$ and the reference signal is the unit discrete-time step function $\mathbf{r}_k = \mathbf{1}_k = [1 \;\; 1 \;\; 1 \;\; \cdots \;\; 1]^{\mathrm{T}}_{(k+1)\times 1}$. In the same Figure we also show the system responses with classical PI and PID controllers (Günther, 1986; Ifeachor and Jervis, 1993; Isermann, 1988) described by the discrete transfer functions

$$R_{PI}(z) = \frac{r_0 + r_1 z^{-1}}{1 + p_1 z^{-1}}, \tag{52}$$

where: $r_0 = 20$, $r_1 = -17$, $p_1 = -1$ and

$$R_{PID}(z) = \frac{q_0 + q_1 z^{-1} + q_2 z^{-2}}{1 + p_1 z^{-1}}, \tag{53}$$

where: $q_0 = 20$, $q_1 = -16.572$, $q_2 = -0.4337$, $p_1 = -1$.

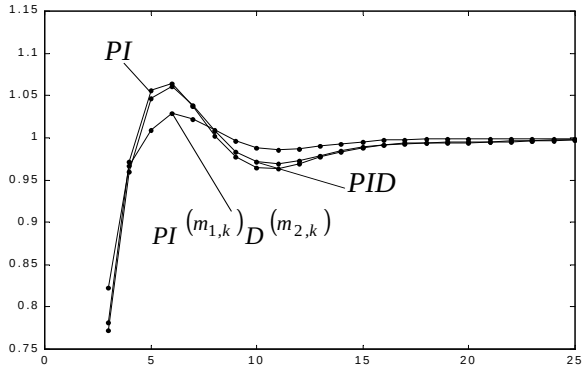

Fig. 7. The closed-loop system outputs with different controllers restricted to k ∈ [3 25]

The PI and PID controller parameters were obtained to preserve the minimum value of the performance criterion on the assumption of a bounded controlling signal (49).

$$I_{k_{\min},k_{\max}} = \min_{|u_k| \leq 20} \sum_{i=k_{\min}}^{k_{\max}} e_k^2, \; k_{\min} = 0, \; k_{\max} = 50, \tag{54}$$

Assumption (49), required by practical applications, is so strong that for PI, PID and proposed $\mathrm{PI}^{(m_{1,k})}\mathrm{D}^{(m_{2,k})}$ control

strategy, $v_0 = v_1 = 20$. This causes that the closed-loop system responses for $k = 0, 1, 2$ to be the same for all strategies. Owing to this, the PI and PID controllers produce very similar responses.

In Fig. 7 the same responses are presented over the time interval $k \in [3,\ 25]$.

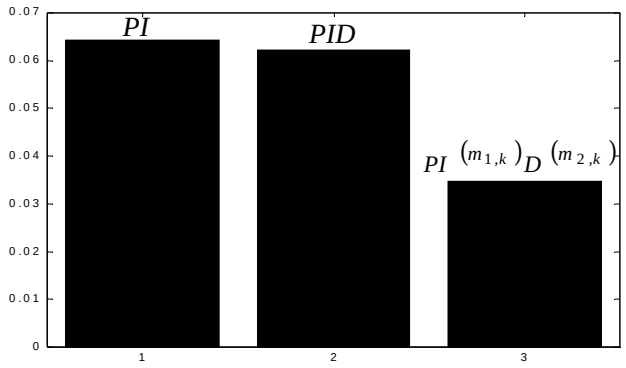

Fig. 8. $I_{PI^{(m1,k)}D^{(m2,k)}}$, $I_{PID,3,50}$, $I_{PI^{(m1,k)}D^{(m2,k)}I_{PI,3,50}}$ values performance criteria

The differences between $\mathbf{y}_{PI,k}$, $\mathbf{y}_{PID,k}$ and $\mathbf{y}_{PI^{(m1,k)}D^{(m2,k)},k}$ become significant when the following performance criteria are evaluated

$$I_{PI^{(m1,k)}D^{(m2,k}} = \min_{|u_k|\le 20} \sum_{i=3}^{50} e^2_{PI^{(m1,k)}D^{(m2,k)},k}$$

$$I_{PID,3,50} \min_{|u_k|\le 20} \sum_{i=3}^{50} e^2_{PID,k} \quad , \tag{55}$$

$$I_{PI^{(m1,k)}D^{(m2,k}I_{PI,3,50} = \min_{|u_k|\le 20} \sum_{i=3}^{50} e^2_{PI,k}$$

Its values are presented in Fig. 8.

5. FINAL CONCLUSIONS

The notion of the linear, time-invariant (with respect to coefficients), VFOs difference equations is applied to the discrete-time closed-loop system synthesis. A new description of linear time-invariant fractional-order closed-loop dynamical systems is investigated. As a practical application, a simple control strategy has been applied to a linear plant. It is non-unique. It appears that a large variety of advanced control strategies may effectively be applied in a real-time control. An open problem is how to design the VFOs depending on the closed-loop system error $m_{1,k}(\mathbf{e}_k)$ and $m_{2,k}(\mathbf{e}_k)$. An appropriate choice of order functions seems to be a fruitful task in further investigations in the case of plant parameters variations or uncertainties.

It is important to point out that applying fractional-order control strategies a linearly growing number of samples should be taken into calculations (linearly growing "calculation tail"). This can be avoided by introducing an assumption that for a quasi steady-state, the control strategy is described by an integer-orders difference equation.

REFERENCES

1. **Carpinteri F., Mainardi A.** [ed.] (1997) *Fractals and Fractional Calculus in Continuum Mechanics*, Springer Verlag, Wien and New York.
2. **Coimbra C. F. M.** (2003), Mechanics with Variable Order Diferential Operators, *Annalen der Physik*, Vol. 12, no. 11-12, 692 – 703.
3. **Günther M.** (1986), *Zeitdiskrete Steuerungssysteme*, VEB Verlag Technik, Berlin, Germany.
4. **Ifeachor E. C., Jervis B. W.** (1993), *Digital Signal processing, A Practical Approach*, Addison Wesley Longman Limited, Edinburg Gate, England.
5. **Isermann R.** (1998), *Digitale Regelsysteme*, Springer-Verlag, Berlin, Germany.
6. **Lorenzo C. F., Hartley T. T.** (2002), Variable Order and Distributed Order Fractional Operators, *Journal of Nonlinear Dynamics*, Vol. 20, no. 1-4, 201-233.
7. **Lubich C. H.** (1986), Discretized fractional calculus, *SIAM Journal of Mathematica1 Analysis*, Vol. 17, 704-719.
8. **Machado J. A. T.** (2001), Discrete-time fractional-order controllers", *FCAA Journal*, Vol. 1, 47-66.
9. **Miller K. S., Ross B.** (1993), *An Introduction to the Fractional Calculus and Fractional Differential Equations*, John Wiley & Sons Inc., New York, USA.
10. **Ogata K.** (1987), *Discrete-time Control Systems*, Prentice-Hall International Editions, Englewood-Cliffs, USA.
11. **Ostalczyk P.** (2000), The non-integer difference of the discrete-time function and its application to the control system synthesis, *International Journal of System Science*, Vol. 31, no. 12, 1551-1561.
12. **Ostalczyk P.** (2001), *Discrete-Variable Functions*, A Series of Monographs No 1018, Technical University of Łódź.
13. **Ostalczyk P.** (2003), The linear fractional-order discrete-time system description, *Proceedings of the 9th IEEE International Conference on Methods and Models in Automation and Robotics, MMAR 2002, Międzyzdroje*, T.I, 429 – 434.
14. **Ostalczyk P.** (2003), The time-varying fractional order difference equations, *Proceedings of DETC'03, ASME 2003 Design Engineering Technical Conference & Computers and Information in Engineering Conference*, Chicago, USA, 1-9.
15. **Ostalczyk P., Derkacz M.** (2003), Minimal realisation of a linear fractional-order discrete-time system, *Proceedings of the 9th IEEE International Conference on Methods and Models in Automation and Robotics, MMAR 2002, Międzyzdroje*, T.I, 461 – 464.
16. **Oustaloup A.** (1995), *La dèrivation non entière*, Éditions Hermès, Paris, France.
17. **Podlubny I.** (1999), *Fractional differential equations*, Academic Press, San Diego, USA.
18. **Zhou K., Doyle J. C., Glover K.** (1995), *Robust and optimal control*, Prentice Hall, New Jersey, USA.

CONTROL OF FRACTIONAL-ORDER NONLINEAR SYSTEMS: A REVIEW

Ivo PETRÁŠ*, Dagmar BEDNÁROVÁ*

* Faculty of BERG, Technical University of Košice, ul. B. Němcovej 3, 042 00 Košice, Slovakia

ivo.petras@tuke.sk, dagmar.bednarova@tuke.sk

Abstract: This paper deals with the control of the fractional-order nonlinear systems. A list of the control strategies as well as synchronization of the chaotic systems is presented. An illustrative example of sliding mode control (SMC) of the fractional-order (commensurate and incommensurate) financial system is described and commented together with the simulation results.

1. INTRODUCTION

Control of nonlinear systems, especially *chaotic systems*, was the subject of intensive studies in the last few decades. As noted (Andrievskii and Fradkov, 2003, 2004), several thousand publications have appeared over the recent decade. It is due to the fact that chaotic behavior was discovered in numerous systems in mechanics, laser and radio physics, hydrodynamics, chemistry, biology and medicine, electronic circuits, economical systems, etc. (see (Petráš, 2011)). For this reason a natural question arises: "*How can we control chaotic systems*?"

The first important thing is that we need the mathematical formulation of chaotic processes by the basic models of the chaotic systems that are used. The most popular mathematical models used in the literature on control of chaos are represented by the systems of ordinary differential equations. In some works we can also find discrete models defined by difference state equations. The second important thing is the formulation of the problems of control of chaotic processes. An important type of problems of control of chaotic processes is represented by the modification of the attractors, for example, transformation of chaotic oscillations into periodic and so on.

2. FRACTIONAL-ORDER NONLINEAR SYSTEMS

In this paper, we will consider the general incommensurate fractional-order nonlinear system represented as follows:

$$\begin{aligned} {}_0D_t^{q_i} x_i(t) &= f_i(x_1(t), x_2(t), \ldots, x_n(t), t) \\ x_i(0) &= c_i, \quad i = 1, 2, \ldots, n, \end{aligned} \tag{1}$$

where c_i are initial conditions. The vector form of (1) is:

$$D^q x = f(x), \tag{2}$$

where $q = [q_1, q_2, \ldots, q_n]^{\mathrm{T}}$ for $0 < q_i < 2$, $(i = 1, 2, \ldots, n)$ and $x \in R^n$, and where ${}_0D_t^q$ is the Caputo's derivative.

The Caputo's definition of fractional derivatives can be written as (Podlubny, 1999):

$${}_aD_t^q f(t) = \frac{1}{\Gamma(m-q)} \int_a^t \frac{f^{(m)}(\tau)}{(t-\tau)^{q-m+1}} d\tau, \quad (m-1 < q < m) \tag{3}$$

In Eq. (3) we assume boundary $a = 0$. Other definitions of the fractional derivative can be found in (Podlubny, 1999).

3. SYNCHRONIZATION OF CHAOTIC SYSTEMS

The important class of the control objectives corresponds to the problems of synchronization or, more precisely, controllable synchronization as opposed to the autosynchronization. Numerous publications on control of synchronization of chaotic processes and its application in the data transmission systems appeared in the 1990's. In the general case, by the synchronization is meant the coordinated variation of the states of two or more systems or, possibly, coordinated variation of some of their characteristics such as oscillation frequencies.

Let us take a look at the synchronization more closely. Several methods can be used for synchronization of chaotic systems. In this paragraph we will mention three well-known methods. If chaos synchronization is achieved by drive-response systems, the instability measure is negative. That means the system is not chaotic.

The first method is the Master-Slave (or drive-response) configuration scheme of two autonomous-dimensional fractional-order chaotic systems (Lu, 2005; Peng, 2007):

$$\begin{cases} M: & \dfrac{d^\alpha x}{dt^\alpha} = f(x), \\ S: & \dfrac{d^\alpha \tilde{x}}{dt^\alpha} = f(\tilde{x}) + C(x - \tilde{x}), \end{cases} \tag{4}$$

where $\alpha = (\alpha_1, \alpha_2, \ldots, \alpha_n) \in R^n$, $\alpha_i > 0$, is the fractional order and the systems are chaotic. C is a coupling matrix. For simplicity, let C have the form: $C = diag(d_1, d_2, \ldots, d_n)$, where $d_i \geq 0$. The error is $e = x - \tilde{x}$ and the aim of the synchroniziation is to design the coupling matrix such that $\| e(t) \| \to 0$ as $t \to +\infty$.

The second method is the method for constructing the drive-response configuration, which was introduced by Pecora and Carroll in 1990, known as a (PC). Let us build a PC drive-response configuration in which a drive system is given by the fractional-order system (with three state variables: *x, y, z*) and a response system is given by the subspace containing the (*x, y*) variables. Then we can use the chaotic signal *z* to drive the response subsystem.

The third method is the synchronization via active-passive decomposition method (APD). Let us build an APD drive-response configuration with a drive system given by the chaotic system and with a response system given by its replica. Then we can take *s*(*t*) as a drive signal (Li et al., 2006).

Chaos synchronization and its potential application to secure communications have attracted much attention from various disciplines in science and engineering since the pioneering work of (Pecora and Carroll, 1990). In this section, we briefly discuss the chaos synchronization methods between the chaotic fractional-order systems and we can also mention method via master-slave configuration with linear coupling (Zhu et al., 2009).

4. CONTROL OF CHAOTIC SYSTEMS

In (Andrievskii and Fradkov, 2003, 2004) were collected and presented several methods used for the control of chaotic processes. The authors considered the classical integer-order chaotic systems but in general we can use those methods for the fractional-order chaotic systems as well. In addition some other methods have been proposed for control of such systems and they can be summarized as follows (Petráš, 2011):

1. Open loop (feed-forward) control is based on varying behavior of the nonlinear system under the action of predetermined external input. This approach is simple because it does without any measurements or sensors. This is especially important for the control of superfast processes.
2. Linear and nonlinear (feed-back) control deals with the possibilities of using the traditional approaches, and methods of automatic control to the problems of chaos control are discussed in numerous papers. The desired aim can be reached sometimes even by means of the simple proportional law of control and feedback. The potentialities of the dynamic feedbacks can be better realized by using the observers. Other methods of the modern theory of nonlinear control such as the theory of center manifold, sliding mode control, the backstepping procedure, the reset control, the H∞-optimal design and so on can be used to solve the problems of stabilization about the given state.
3. Adaptive control assumes the possibility of applying the methods of adaptation to the control of chaotic processes, where the parameters of the controlled plant are unknown and the information about the model structure more often than not is incomplete. A number of the existing methods of adaptation such as the methods of gradient and speed gradient, least squares, maximum likelihood, and so on can be used to develop algorithms of adaptive control and parametric identification. A controller is usually designed using the reference model or the methods of linearization by feedback.
4. Linearization of the Poincaré map method can be formulated by the following two key ideas: (i) designing controller by the discrete system model based on linearization of the Poincaré map and (ii) using the property of recurrence of the chaotic trajectories and applying the control action only at the instants when the trajectory returns to some neighborhood of the desired state or given orbit.
5. Time-delayed feedback method considers the problem of stabilizing an unstable periodic orbit of a nonlinear system by a simple feedback law with time delay. Sensitivity to the parameter, especially to the delay time, is a disadvantage of the control law.
6. Neural network-based control deals with the ability of neural networks to control and predict behavior of nonlinear systems. The various structures of neural networks for control and prediction of the processes in nonlinear chaotic systems can be found in literature.
7. Fuzzy control uses a description of system indeterminacy in terms of fuzzy models, provides specific versions of the control algorithms, which consists of four blocks: knowledge base, fuzzification, inference and defuzzification.

5. NEW CHAOS CONTROL STRATEGY

The fractional calculus techniques as for example a fractional differentiator based controller of a fractional integrator based controller can also be used (Tavazoei et al., 2009). Both of them are particular cases of the fractional-order controllers described as (Podlubny, 1999):

$$u(t) = K_p e(t) + T_{i\,0}D_t^{-\lambda} e(t) + T_{d\,0}D_t^{\delta} e(t), \quad (\lambda, \delta > 0), \qquad (5)$$

where K_p is the proportional constant, T_i is the integration constant and T_d is the differentiation constant. Controller (5) is more flexible than classical one and gives better results of the control performances (Monje et al., 2010).

6. EXAMPLE: SLIDING MODE CONTROL OF THE FRACTIONAL-ORDER ECONOMICAL SYSTEM

A sliding model control (SMC) strategy is also applicable for the fractional-order chaotic systems. It is a form of variable structure control method that alters the dynamics of a nonlinear system by application of a high-frequency switching control. The state feedback control law is not a continuous function of time. It switches from one conti-

nuous structure to another based on the current position in the state space. Trajectories always move toward a switching condition. The motion of the system as it slides along these boundaries is called a sliding mode. The sliding mode control scheme involves: (i) selection of the sliding surface that represents a desirable system dynamic behavior, (ii) finding a switching control law that a sliding mode exists on every point of the sliding surface.

Consider the following general structure of the fractional-order nonlinear system under control

$$ {}_0D_t^q x(t) = f(x(t)) + Bu(t), \tag{6}$$

where $u(t) = [u_1(t)u_2(t)...u_m(t)]^T$ is an m-dimensional input vector that will be used and the following control structure will be considered for state feedback:

$$ u(t) = u_{eq}(t) + u_{sw}(t), \tag{7}$$

where $u_{eq}(t)$ is the equivalent control and $u_{sw}(t)$ is the switching control of the system (6). A common task is to design a state feedback control law to stabilize the dynamical system (6) around the origin $x(t) = [0, 0, \ldots, 0]^T$. In the sliding mode, the sliding surface and its derivative must satisfy $\sigma(t) = 0$ and $\dot{\sigma}(t) = 0$.

Let us use the controlled fractional-order financial system in the form (Dadras and Momeni, 2010):

$$\begin{aligned} {}_0D_t^{q_1} x_1(t) &= x_3(t) + (x_2(t) - a)x_1(t), \\ {}_0D_t^{q_2} x_2(t) &= 1 - bx_2(t) - x_1^2(t) + u(t), \\ {}_0D_t^{q_3} x_3(t) &= -x_1(t) - cx_3(t), \end{aligned} \tag{8}$$

where a is the saving amount, b is the cost per investment, and c is the elasticity of demand of commercial market, $(a,b,c) \in R$ and $(a,b,c) > 0$. The state variables $x_1(t)$, $x_2(t)$, and $x_3(t)$ are the interest rate, the investment demand, and the price index, respectively.

The proposed fractional sliding surface is defined as

$$ \sigma(t) = \int_0^t (x_1^2(\tau) + Kx_2(\tau))d\tau + {}_0D_t^{q_2-1} x_2(t), \tag{9}$$

where K is a positive constant, in addition $K = K_{eq}$. The equivalent control $u_{eq}(t)$ is obtained by setting the derivative of sliding surface to zero and then solving the second equation of (8) for $u(t)$. We obtain

$$ {}_0D_t^{q_2} x_2(t) = -(x_1^2(t) + Kx_2(t)) $$

and then we get the relation

$$\begin{aligned} u_{eq}(t) &= {}_0D_t^{q_2} x_2(t) - 1 + bx_2(t) + x_1^2(t) \\ &= -(x_1^2(t) + K_{eq}x_2(t) - 1 + bx_2(t) + x_1^2(t) \\ &= (b - K_{eq})x_2(t) - 1, \end{aligned} \tag{10}$$

where K_{eq} is the constant of the controller.

The switching control $u_{sw}(t)$ law is chosen in order to satisfy the sliding condition

$$ u_{sw}(t) = K_{sw} sign(\sigma), \tag{11}$$

where

$$ sign(\sigma) = \begin{cases} +1 & : \sigma > 0, \\ 0 & : \sigma = 0, \\ -1 & : \sigma < 0, \end{cases} $$

and K_{sw} is the gain of the controller ($K_{sw} < 0$). Finally, the total control law is defined as follows:

$$ u(t) = u_{eq}(t) + u_{sw}(t) = (b - K_{eq})x_2(t) - 1 + K_{sw} sign(\sigma). \tag{12}$$

We assume the following parameters of the chaotic system (8): $a = 1$, $b = 0.1$, $c = 1$, and the controller (12) parameters, experimentally found: $K_{eq} = 1.5$ and $K_{sw} = -3.5$. The controller will be applied at $t = 30$ *s*. In the first case we use a commensurate order of derivatives $q_1 = q_2 = q_3 = 0.9$ and in the second case we use an incommensurate order of the derivatives $q_1 = 1.0$, $q_2 = 0.95$, and $q_3 = 0.99$ of the fractional-order chaotic system (8). The initial conditions for both cases are $(x_1(0), x_2(0), x_3(0)) = (2, -1, 1)$.

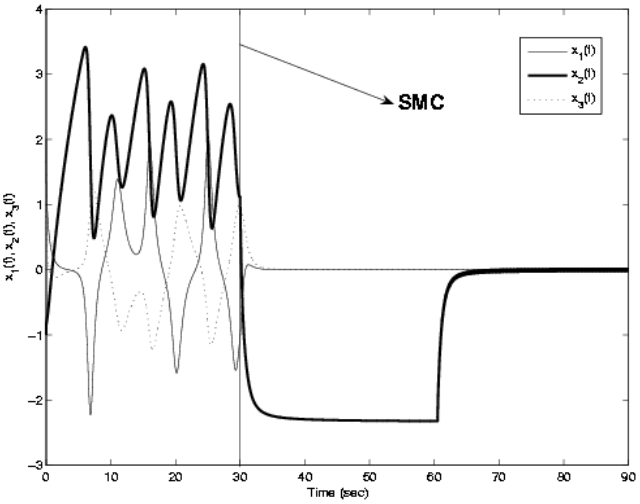

Fig. 1. Controlled state variables $x_1(t)$, $x_2(t)$, and $x_3(t)$ of commensurate fractional-order financial system, where the SMC was activated at 30 *s*

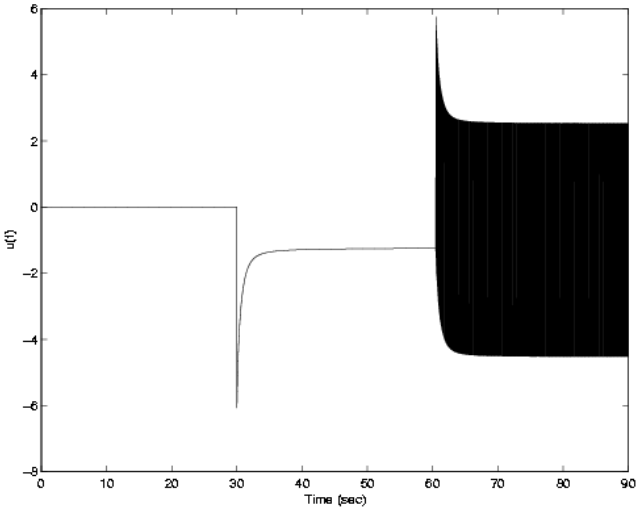

Fig. 2. Time response of control law $u(t)$ for commensurate fractional-order system

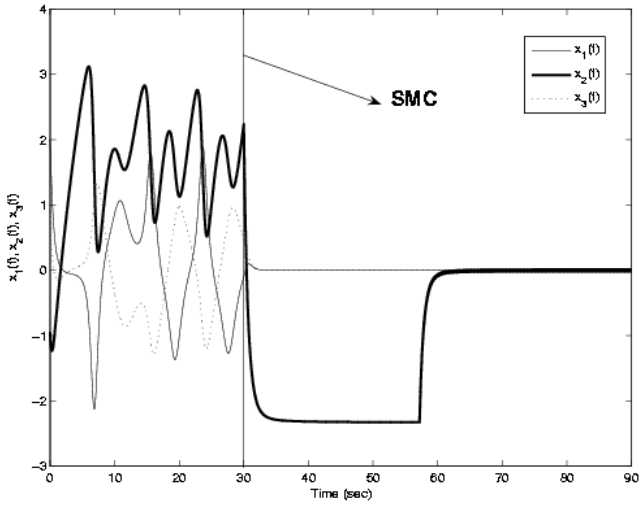

Fig. 3. Controlled state variables $x_1(t)$, $x_2(t)$, and $x_3(t)$ of incommensurate fractional-order financial system, where the SMC was activated at 30 *s*

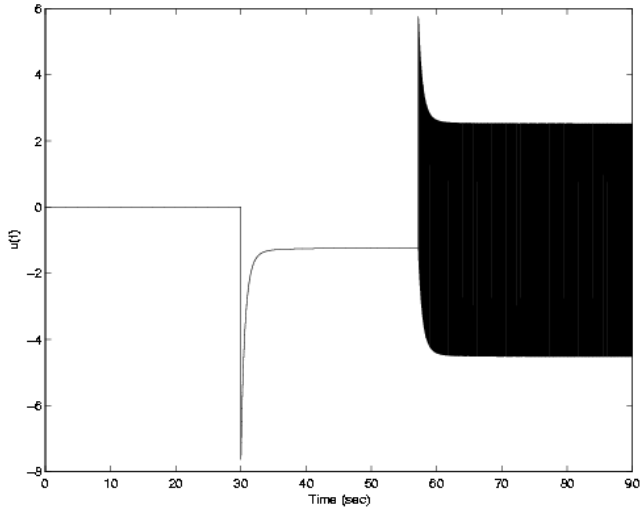

Fig. 4. Time response of control law $u(t)$ for incommensurate fractional-order system

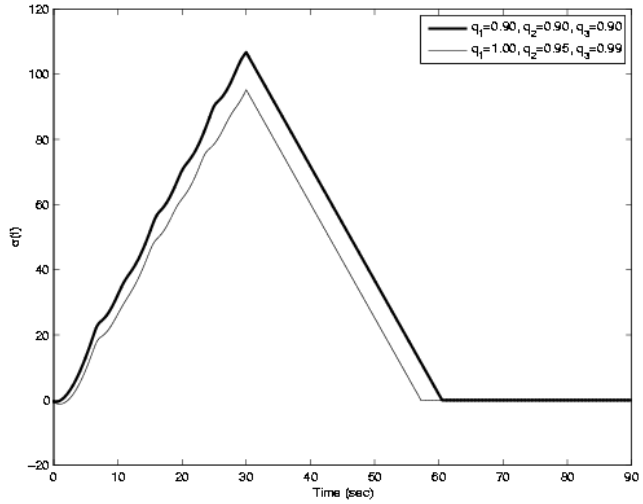

Fig. 5. Time responses of sliding surfaces $\sigma(t)$

In Fig. 1 are depicted the controlled state variables of the commensurate fractional-order financial systems (8) with the parameters: a = 1, b = 0.1, c = 1, orders $q_1 = q_2 = q_3$ = 0.9, controller (12) parameters: K_{eq} = 1.5 and K_{sw} = -3.5, initial conditions: ($x_1(0)$, $x_2(0)$, $x_3(0)$) = (2, -1, 1) for simulation time T_{sim} = 90 *s* and time step h = 0.005.

In Fig. 2 is shown the control law of commensurate fractional-order financial system which drives the system states to the sliding surface. We can observe chattering in the sliding mode.

In Fig. 3 are depicted the controlled state variables of the incommensurate fractional-order financial systems (8) with the parameters: a = 1, b = 0.1, c = 1, orders q_1 = 1.0, q_2 = 0.95, and q_3 = 0.99, controller (12) parameters: K_{eq} = 1.5 and K_{sw} = -3.5, initial conditions: ($x_1(0)$, $x_2(0)$, $x_3(0)$) = (2, -1, 1) for simulation time T_{sim} = 90 *s* and time step h = 0.005.

In Fig. 4 is shown the control law of incommensurate fractional-order financial system which drives the system states to the sliding surface. We can again observe chattering in the sliding mode.

In Fig. 5 are depicted the time responses of the sliding surface. We can observe that the controller kept the system states on the sliding surface for all subsequent time.

Performed simulations show that system responses after applying the control law (12) are satisfactory for both cases. The results confirm that obtained control strategy is efficient for controlling the fractional-order financial system (8) for various parameters (Petráš and Bednárová, 2010).

7. CONCLUSIONS

In this article is presented a review of the control strategies for the fractional-order nonlinear systems. On illustrative example is shown the SMC control method. This control method is simple and control law achieved asymptotically stabilized system if the controller is applied to the investment demand in order to control the whole economical system. This approach is applicable for different types of the fractional-order chaotic systems as well as the other control strategies (Monje et al., 2010).

REFERENCES

1. **Andrievskii B. R., Fradkov A. L.** (2003). Control of Chaos: Methods and Applications. I. Methods, *Automation and Remote Control*, Vol. 64, 673-713.
2. **Andrievskii B. R., Fradkov A. L.** (2004). Control of Chaos: Methods and Applications. II. Applications, *Automation and Remote Control*, Vol. 65, 505-533.
3. **Dadras S., Momeni H. R.** (2010). Control of a fractional-order economical system via sliding mode, *Physica A*, Vol. 389, 2434-2442.
4. **Li C. P., Deng W. H., Xu D.** (2006). Chaos synchronization of the Chua system with a fractional order, *Physica A*, Vol. 360, 171-185.
5. **Lu J. G.** (2005). Chaotic dynamics and synchronization of fractional-order Chua's circuits with a piecewise-linear nonlinearity, *Int. J. Mod. Phys. B*, Vol. 19, 3249-3259.

6. **Monje C. A., Chen Y. Q., Vinagre B. M., Xue D., Feliu V.** (2010). *Fractional Order Systems and Control - Fundamentals and Applications*, Advanced Industrial Control Series, London: Springer.
7. **Pecora L. M., Carroll T. L.** (1990). Synchronization in chaotic systems, *Phys. Rev. Lett.*, Vol. 64, 821-824.
8. **Peng G.** (2007). Synchronization of fractional order chaotic systems, *Physics Letters A*, Vol. 363, 426-432.
9. **Petráš I.** (2011). *Fractional - Order Nonlinear Systems*: *Modeling, Analysis and Simulation*, HEP, Springer, Series: Nonlinear Physical Science.
10. **Petráš I., Bednárová D.** (2010). Control of fractional-order chaotic systems: A survey of control strategies, Proc. of the of the 4th IFAC Workshop on Fractional Differentiation and Its Applications – FDA'10, University of Extremadura, Badajoz, Spain, October 18-20.
11. **Podlubny I.** (1999). *Fractional Differential Equations*, Academic Press, San Diego.
12. **Tavazoei M. S., Haeri M., Bolouki S., Siami M.** (2009). Using fractional-order integrator to control chaos in single-input chaotic systems, *Nonlinear Dyn*., Vol. 55, 179-190.
13. **Zhu H, Zhou S., He Z.** (2009). Chaos synchronization of the fractional-order Chen's system, *Chaos, Solitons and Fractals*, Vol. 41, 2733-2740.

Acknowledgments: This work is partially supported by grants VEGA: 1/0390/10, 1/0497/11, and 1/0746/11, grants APVV-0040-07, and SK-PL-0052-09.

The most parts of this article have been presented at the FDA'10, 4th IFAC Workshop on Fractional Differentiation and Its Applications, which was held at the University of Extremadura, Badajoz, Spain, October 18-20, 2010. The IFAC copyright for the FDA'10 version of this article has been released on January 21, 2011.

INVESTIGATION OF FIXED-POINT COMPUTATION INFLUENCE ON NUMERICAL SOLUTIONS OF FRACTIONAL DIFFERENTIAL EQUATIONS

Paweł PIĄTEK*, Jerzy BARANOWSKI*

*AGH University of Science and Technology, The Faculty of Electrical Engineering, Automatics, Computer Science and Electronics, Department of Automatics, Al. Mickiewicza 30/B1, 30-059 Kraków

ppi@agh.edu.pl, jb@agh.edu.pl

Abstract: In this paper the problem of the influence of fixed point computation on numerical solutions of linear differential equations of fractional order is considered. It is a practically important problem, because of potential possibilities of using dynamical systems of fractional order in the tasks of control and filtering. Discussion includes numerical method is based on the Grünwald-Letnikov fractional derivative and how the application of fixed-point architecture influences its operation. Conclusions are illustrated with results of floating-point arithmetic with double precision and fixed point arithmetic with different word lengths.

1. INTRODUCTION

Dynamical system described by fractional differential equations take an increasing role in technical sciences. The initial concept dating to private correspondence of Leibnitz and L'Hospital from 1695, was systematically developed however outside the main stream. Currently we can say, that mathematical side of the problem is well rounded, what can be observed by presence of multiple monographs such as Miller and Ross (1993); Oldham and Spanier (1974); Podlubny (1999); Samko et al. (1993).

In recent years especially interesting is the aspect of applications. They are found in modelling of supercapacitors, distributed parameter systems, problems of variational calculus or modelling of very complicated phenomena such as flame spreading Lederman et al. (2002); Weilbeer (2005). Besides modelling also fractional systems are used to influence reality as controllers Ortigueira (2008); Ruszewski (2008) or filters Magin et al. (2011). In the context of fractional order systems also problems such as state estimation (Dzieliński and Sierociuk (2008)), controllability (Klamka (2009)) or stability (Kaczorek (2008a); Busłowicz (2008); Kalinowski and Busłowicz (2011)) are considered. A comprehensive survey of theory and applications of fractional calculus in control engineering can be found in Ostalczyk (2008).

In this paper authors focus on the problem of actual implementation of fractional order systems. Many works are devoted to the concept of approximation of fractional order systems with integer order systems (see for example Djouambi et al. (2007); Sobolewski and Ruszewski (2011)). This paper analyses the application of numerical methods for solving fractional order differential equations. Because the focus of this research is the implementation of fractional controllers and filters on commercially available hardware platforms special emphasis is placed on influence of fixed point computation. In the following parts of the paper considered class of systems is described, solution of differential equations on dedicated hardware platforms with individual section on problems quantisation. Then discretisation of fractional differential equations is analysed. Finally numerical experiments are conducted in both floating and fixed point arithmetic.

2. CONSIDERED SYSTEMS

In this paper linear fractional order dynamical system described by a following system of fractional order equations

$$\begin{aligned} &\frac{\mathrm{d}^{\alpha}}{\mathrm{d}t^{\alpha}}\mathbf{x}(t) = \mathbf{A}\mathbf{x}(t) + \mathbf{B}\mathbf{u}(t), \quad 0 < \alpha \le 1 \\ &\mathbf{x}(0) = \mathbf{x}_0 \end{aligned} \tag{1}$$

where: $\mathbf{x}(t) \in R^n$, $\mathbf{u}(t) \in R^r$ and $\mathbf{A}$, $\mathbf{B}$ are constant matrices of appropriate dimensions. Fractional differentiation operation of order α is given by Caputo definition (see for example Kaczorek (2008b)).

$$\frac{\mathrm{d}^{\alpha}}{\mathrm{d}t^{\alpha}}x(t) = \frac{1}{\Gamma(n-\alpha)}\int_0^t \frac{x^{(n)}(\tau)}{(t-\tau)^{\alpha+1-n}}\mathrm{d}\tau, \quad n = \lceil \alpha \rceil \tag{2}$$

where: Γ function is given by

$$\Gamma(z) = \int_0^{\infty} t^{z-1}e^{-t}\mathrm{d}t$$

Important fact is that in analogue to integer order equations one can express solution of (1) by variation of constants, that is

$$\mathbf{x}(t) = \mathbf{\Phi}_0(t)\mathbf{x}_0 + \int_0^t \mathbf{\Phi}(t-\tau)\mathbf{B}\mathbf{u}(\tau)\mathrm{d}\tau \tag{3}$$

$$\mathbf{\Phi}_0(t) = \mathbf{E}_{\alpha}(\mathbf{A}t^{\alpha}) \tag{4}$$

$$\mathbf{\Phi}(t) = t^{\alpha-1}\mathbf{E}_{\alpha,\alpha}(\mathbf{A}t^{\alpha}) \tag{5}$$

where: **E** is the Mittag-Leffler function (see for example Weilbeer (2006)) given by:

$$\mathbf{E}_{\alpha,\beta}(\mathbf{z}) = \sum_{k=0}^{\infty} \frac{\mathbf{z}^k}{\Gamma(\alpha k + \beta)}, \quad \alpha > 0, \beta > 0 \tag{6}$$

$$\mathbf{E}_{\alpha}(\mathbf{z}) = \mathbf{E}_{\alpha,1}(\mathbf{z}), \quad \alpha > 0 \tag{7}$$

It should be noted that Mittag-Leffler function is the generalisation of e^z and for $\alpha = 1$ the following equality occurs

$$\mathbf{E}_1(\mathbf{z}) = e^{\mathbf{z}} \tag{8}$$

In this paper only initial conditions equal to zero will be considered. It is justified by the fact that the main goal is to devise methods of effective filter and controller implementation. Moreover one can transform a fractional system into one with zero initial conditions through addition of additional inhomogeneity (see for example Podlubny (2000)).

3. SOLVING DIFFERENTIAL EQUATIONS WITH DEDICATED CONTROL SYSTEMS

In classical control systems that is those, which model of controller or system is described by integer order differential equations the following hardware platforms are used:

- universal platforms:
  - classical computer systems,
  - industrial PLC controllers,
  - universal microprocessor controllers,
- dedicated platforms:
  - using general purpose processors,
  - using digital signal processors (DSP),
  - using FPGA circuits.

In case of fractional order differential equations this division stays correct. Because of possibility of obtaining very short computation times - dedicated systems are very promising. Among those especially systems using FPGA circuits raise interest.

Using a dedicated control system for computation of both ordinary and fractional differential equations carries many consequences. Substantial benefits are that one can achieve substantial increase in computation speed and keep the regimes of real time processing. On the other hand use of dedicated systems introduces multiple constraints associated with their construction and type of operation. The most serious limit introduced by dedicated control systems is lack of support for floating-point arithmetic. Most microcontrollers designed for control systems do not have an integrated floating-point coprocessor. Similar situation occurs for DSPs. One can of course show solutions supporting floating-point formats but that is not the norm. Different case is for implementation of such formats in FPGA circuits. These circuits are rather freely configurable. One can also implement the support for writing of the floating-point data format. However because of needed amount of circuit's hardware resources it is not always possible or economically feasible.

In this paper control systems with fixed-point data formats are considered. In case of the FPGA circuits these formats are supported by hardware description languages (e.g. VHDL) or are relatively easy to implement. The most substantial merit of using the fixed-point arithmetic is the possibility of construction of parallel data processing structures, which can significantly accelerate computation (see Wiatr (2003)). Other important merit is the possibility of using computation words of desired length (see Piątek (2007)). When programming microcontrollers or DSP the programmer can use the data types available in the microprocessor architecture. Using of non standard data types is associated with need for additional operations, which can increase the computation time.

When solving systems of differential equations in computer systems, so also in the control systems we have to deal with quantisation of signals and parameters in time (discretisation) and in values (quantisation) caused by digital character of computation. Both these operations have their properties and can disrupt the results of computation - that is the solution of the system of differential equations.

4. QUANTISATION

Application of digital systems, especially those which use a fixed-point data format causes introduction of numerical errors to the computation. Sources of these errors are (see Gevers and Li (1993); Świder (2003, 2002)):

- quantisation of analogue signals – for example by A/D converters in control systems;
- computation result overflow errors caused by too short data word length;
- round-off errors of arithmetic operations – multiplication, addition;
- quantisation errors of model coefficients resulting from writing them on words with finite length.

Converter quantisation errors are determined by resolution of used A/D converter system. In the case of modelling the converter model by stochastic methods it is assumed that the converter model consists of a sampling system and a quantiser. Quantiser is modelled as a summation node introducing a random error to the signal. It is assumed that this error is a discrete white noise not correlated with the sampled signal and its variance is dependent on the number of converter bits (see Świder (2003)). Quantisation noise created in the process of analogue-digital conversion can be filtered in the control system by the usage of appropriate digital filters.

Overflow errors are practically present only in the systems performing computations using fixed point arithmetic. They occur in the situations, when the result of arithmetic operation requires writing in the registry of larger number of bits than it is available in the computation system. In some situations (e.g. using notation in the two's complement code) it causes large relative errors (see Gevers and Li (1993)). Elimination of overflow errors relies on appropriate scaling of signals and coefficients of the model. Such operations unfortunately introduce

additional round-off errors associated with changing the signals and model coefficients ranges. In computation systems using floating-point arithmetic overflow errors are not present or occur rarely, because of the large ranges of such data storage.

Other two kinds of errors - round off errors of arithmetic operations and parameter quantisation errors are always present during digital realisation of control algorithms and it is not possible to completely eliminate their influence on the result of computation (see Gevers and Li (1993)). Arithmetic operation round off errors are introduced during the computations connected to determination of system response and their level is dependent on the structure of algorithm and the data word length. Model coefficient quantisation errors are introduced by the finite data word length. Ideal values of parameters are rounded to the values that can be stored. Similar to the arithmetic operation errors, coefficient quantisation errors are dependent on the structure of algorithm and the data word length. Effects connected with these two kinds of errors are called FWL (Finite Word Length) effects (see Gevers and Li (1993)). They can be limited by increasing the length of data words and by changing model structure. Length modification is not always possible. Usually in computer systems only two or three word lengths are available, and in simple microprocessor system even only one. Relatively simple increase of precision is possible only in the range of data types supported by the architecture and additional improvements (above the machine command precision) has a cost of a substantial increase in the number of commands required for determination of system response. In case of realisation of control system with dedicated architecture for example with FPGA circuits, word length can be adjusted at will. Too long word lengths however cause substantial increase in the hardware resources usage, which can be interpreted as the increase in the computation cost.

5. DISCRETISATION OF FRACTIONAL ORDER DIFFERENTIAL EQUATIONS

There are different classes of numerical methods for solving fractional differential equations (see Weilbeer (2005)). One of them are linear multistep methods. Their construction relies on transformation of fractional differential equation to the equivalent Volterra integral equation and solving it through quadratures. It is similar to Adams methods for ODE (see Hairer et al. (2000)). Another group considers equivalent Abel-Volterra equation and solves it via power series - these are generalised Taylor expansion and Adomian decomposition method. One more group are collocation methods also popular for integral equations. For applications in the context of filter and controller implementations the most practical seem to be backward difference methods. This class includes Diethelm method and quadrature based Lubich method.

In this paper third backward difference method is considered – that is the method based on the Grünwald-Letnikov fractional derivative. By this definition the fractional derivative takes form of a limit of fractional difference quotients

$$\frac{\mathrm{d}^{\alpha}}{\mathrm{d}t^{\alpha}}x(t) = \lim_{h\to 0}\frac{(\Delta_h^{\alpha}x)(t)}{h^{\alpha}} \tag{9}$$

where:

$$(\Delta_h^{\alpha}x)(t) = \sum_{k=0}^{m}(-1)^k\binom{\alpha}{k}x(t-kh)\Big|_{h=t/m} \tag{10}$$

Generalised Newton symbol is given by

$$\binom{\alpha}{k} = \frac{\Gamma(k-\alpha)}{\Gamma(-\alpha)\Gamma(k+1)} = \tag{11}$$

$$= \begin{cases} \dfrac{\alpha(\alpha-1)\cdot\ldots\cdot(\alpha-j+1)}{j!} & \text{for} \quad j\in N \\ 1 & \text{for} \quad j=0 \end{cases} \tag{12}$$

Fractional derivative takes form

$$\frac{\mathrm{d}^{\alpha}}{\mathrm{d}t^{\alpha}}x(t) = \lim_{\substack{h\to 0 \\ h=t/m}}\frac{1}{h^{\alpha}}\sum_{k=0}^{m}(-1)^k\binom{\alpha}{k}x(t-kh) \tag{13}$$

It should be noted that definitions of Grünwald-Letnikov and Caputo are not fully equivalent. It is especially important in the context of fractional differential equations, where initial conditions influence the solution in different way (see Weilbeer (2005)). If initial conditions are zero, as in the considered case the solutions are however equal.

As it can be seen in the fractional difference when h decreases m increases, so in the limit sum is infinite. The idea of numerical solution on the interval $t\in[0,T]$ relies on determining finite m and omitting the limit. In that way differential equation (1) becomes

$$\frac{1}{h^{\alpha}}\sum_{k=0}^{m}(-1)^k\binom{\alpha}{k}\mathbf{x}(t-kh) = \mathbf{A}\mathbf{x}(t)+\mathbf{B}\mathbf{u}(t), \tag{14}$$
$$t\in[0,T],\ h = T/m$$

or equivalently

$$\frac{\mathbf{x}(t)}{h^{\alpha}}+\frac{1}{h^{\alpha}}\sum_{k=1}^{p}(-1)^k\binom{\alpha}{k}\mathbf{x}(t-kh) = \mathbf{A}\mathbf{x}(t)+\mathbf{B}\mathbf{u}(t) \tag{15}$$
$$h = T/m,\ t = ph,\ p = 0,1,\ldots,m$$

It should be noted that $\mathbf{x}(t)$ is present on both sides of equality. In case of nonlinear systems it would require iterational procedures, however because the considered system is linear so

$$\mathbf{x}(t) = (\mathbf{I}-h^{\alpha}\mathbf{A})^{-1}\left(h^{\alpha}\mathbf{B}\mathbf{u}(t)-\sum_{k=1}^{p}c_k\mathbf{x}(t-kh)\right) \tag{16}$$

$$h = T/m,\ t = ph,\ p = 0,1,\ldots,m \tag{17}$$

$$c_k = (-1)^k\binom{\alpha}{k},\quad k = 1,2,\ldots,m \tag{18}$$

Different approach can be seen in the work of Podlubny (2000). Method presented there formulates the problem of numerical solution as a system of linear algebraic equations solving the fractional differential equations in all points of the interval simultaneously. That approach has many benefits, but is not adequate for series signal processing.

As it can be seen, when changing m also h is changed which can cause FWL effects. In the next section the behaviour of numerical solution of fractional differential equation obtained with (16) behaves when changing parameters.

6. FLOATING-POINT ARCHITECTURE SIMULATIONS

In order to perform simulational analysis of the solution of fractional differential equation the following example needs to be considered.

Example 1. (Kaczorek (2008b)) The unit step response of the following system is considered

$$\begin{aligned} &\frac{\mathrm{d}^{\alpha}}{\mathrm{d}t^{\alpha}} x(t) = -x(t) + u(t) \\ &x(0) = 0 \in R \\ &u(t) = 1(t) \end{aligned} \tag{19}$$

From (3) the solution is

$$\begin{aligned} x(t) = & \int_0^t (t-\tau)^{\alpha-1} E_{\alpha,\alpha}(-(t-\tau)^{\alpha})\mathrm{d}\tau = \\ = & \int_0^t s^{\alpha-1} E_{\alpha,\alpha}(-s^{\alpha})\mathrm{d}s = \\ = & \int_0^t \sum_{k=0}^{\infty} \frac{(-1)^k s^{\alpha k+\alpha-1}}{\Gamma(\alpha(k+1))}\mathrm{d}s = \\ = & \sum_{k=0}^{\infty} \frac{(-1)^k}{\Gamma(\alpha(k+1))} \int_0^t s^{\alpha k+\alpha-1}\mathrm{d}s = \\ = & \sum_{k=0}^{\infty} \frac{(-1)^k}{\Gamma(\alpha(k+1))} \frac{t^{\alpha(k+1)}}{\alpha(k+1)} = t^{\alpha} E_{\alpha,\alpha+1}(-t^{\alpha}) \end{aligned} \tag{20}$$

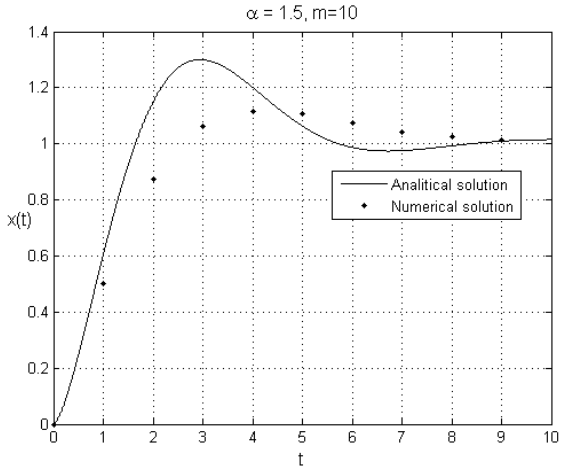

Fig. 1. Comparison of analytical and numerical solution of fractional differential equation (19) with α=3/2 for m=10

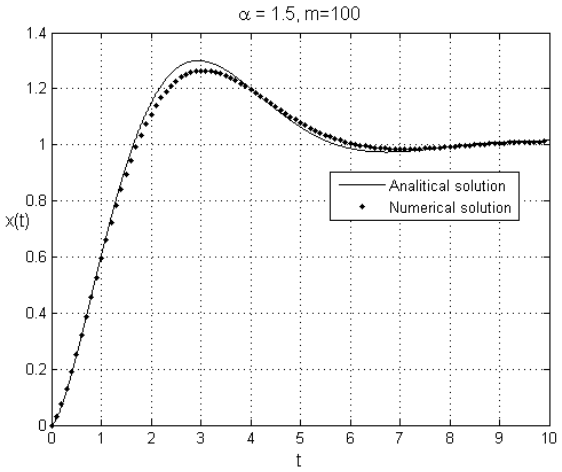

Fig. 2. Comparison of analytical and numerical solution of fractional differential equation (19) with α=3/2 for m=100

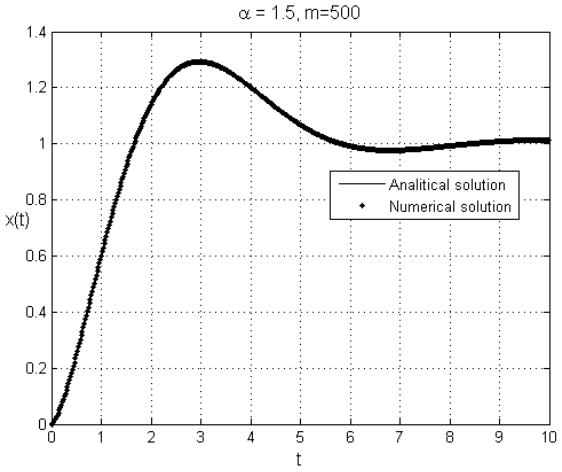

Fig. 3. Comparison of analytical and numerical solution of fractional differential equation (19) with α=3/2 for m=500

The step response was expressed by Mittag-Leffler function (6) It should be noted that for $\alpha > 1$ initial conditions for all $n < \alpha$ need to be specified.

Obtained analytical solution can be used for verification of correctness of (16). System with $\alpha = 3/2$ is considered. Comparisons are made for different m. Computations were performed in Matlab in double precision. Analytical solution consisted of 100 first expression of power series form of Mittag-Leffler function (6). The analysis was performed on interval $t \in [0, 10]$.

It should be noted that for $\alpha > 1$ solutions have oscillatory character. Solution consisting of 10 points (Fig. 1) represents the oscillations but it happens in different moment and with much smaller amplitude. Increasing precision to 100 points the solution improves (Fig. 2), and for 500 points (Fig. 3) numerical solution becomes truly close to an analytical one. It should be noted that increasing number of points in the interval the requirements toward solutions increase, as in every step of computation all the earlier ones are necessary.

7. FIXED POINT ARCHITECTURE SIMULATIONS

For numerical experiments Matlab environment was used with the Fixed-Point Toolbox. With this software one can create and use variables with desired word lengths in bits. These simulations were performed for step response of system (19). Numerical method (16) was used and number of steps per interval was set to $m = 100$. Compared are:

- analytical solution;
- numerical solution using method (16) operating with floating-point arithmetic;
- numerical solution using method (16) operating with fixed-point arithmetic.

In the last case a fixed point notation allowing operation on numbers with nonzero fractional part. These numbers are coded with use of two's complement code (see Biernat(2001); Pochopień(2004)). Thanks to using it scaling could be avoided. Figure 4 presents the format of this fixed-point notation.

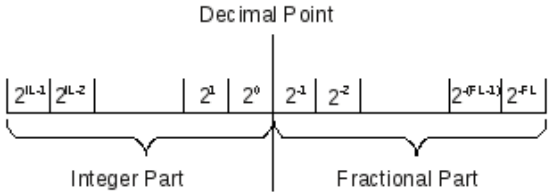

Fig. 4. Fixed point notation during the experiments

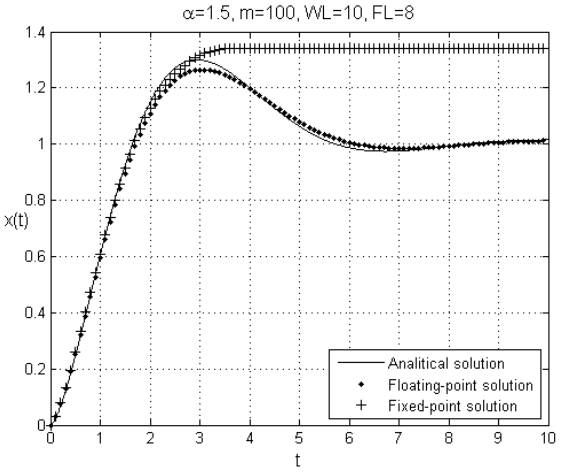

Fig. 5. System unit step response (FL=8)

Corresponding to the Fig. 4 following quantities were introduced:

- FL denotes number of bits devoted to the fractional part,
- IL denotes number of bits devoted to the integer part,
- total number of bits in the data word was WL = IL + FL .

It was decided to use a single word length for all elements of the algorithm. That means that both system coefficients, constants associated with α and number of steps and system state were denoted in variables with the same word length and the same lengths of fractional and integer parts. Nine numerical experiments were performed, in which step response of system (19) was computed. In every experiment the word length for the fractional part was increased by one from 8 to 16 bits. The most representative were the results obtained for fractional parts of 8, 9, 10, 12 and 16 bits. For all the experiments IL=2 was set.

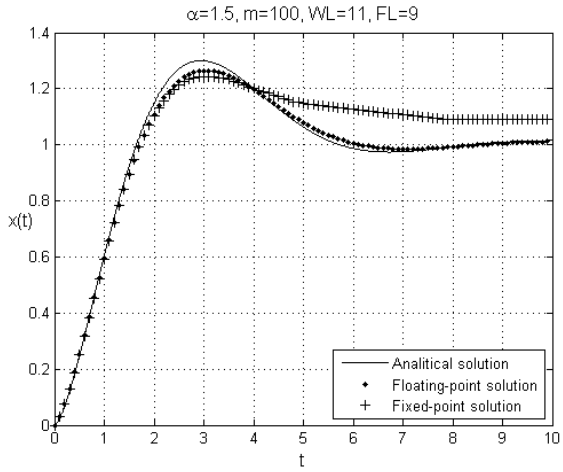

Fig. 6. System unit step response (FL=9)

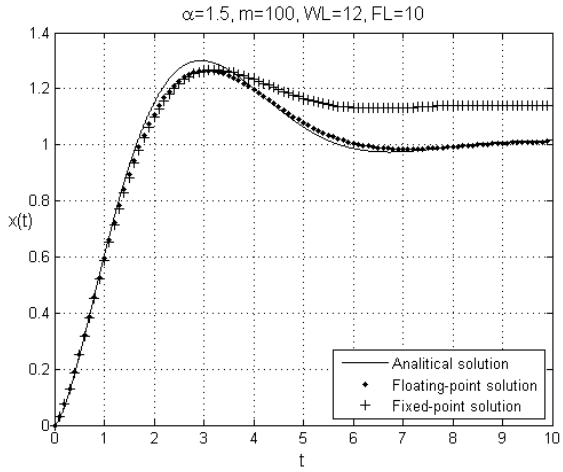

Fig. 7. System unit step response (FL=10)

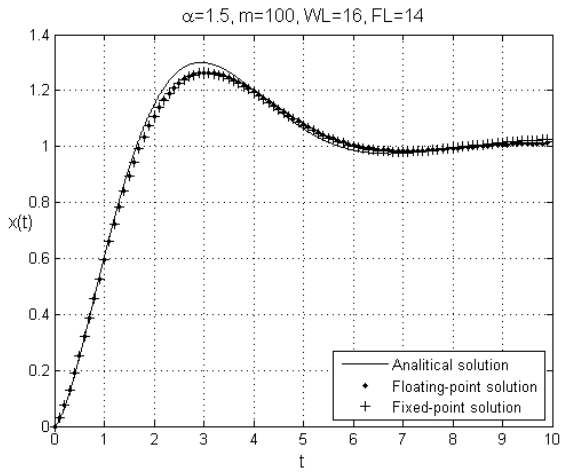

Fig. 8. System unit step response (FL=14)

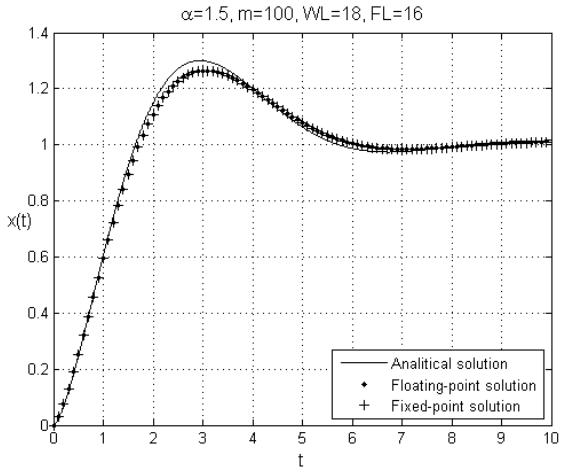

Fig. 9. System unit step response (FL=16)

Results of simulations are presented in Figs. 5, 6, 7, 8 and 9. In the figures three responses are presented: analytical, computed numerically with floating-point and computed numerically with fixed point.

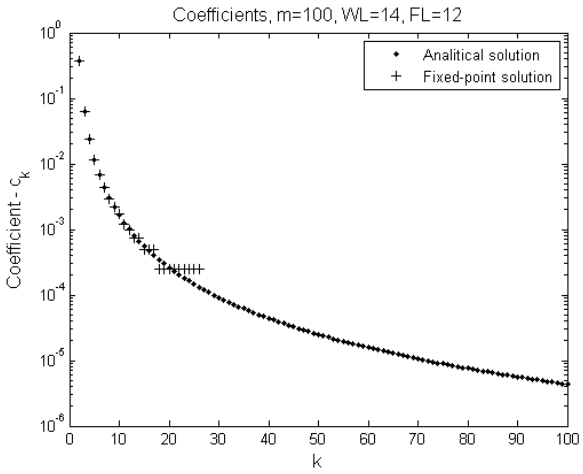

Fig. 10. Coefficient values for WL=14

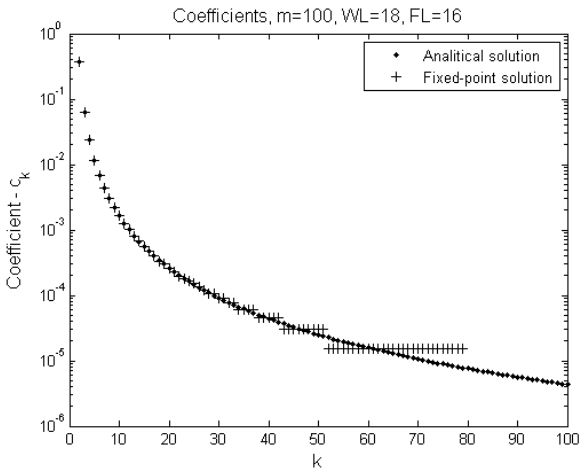

Fig. 11. Coefficient values for WL=18

Analysis of the figures, allows to observe, that reduction of fractional part word length increases the numerical error of such computed fractional part. For FL=8 (Fig. 5) the response differs so much that it loses its original character.

Further study allowed to find one of the reasons for substantial differences between analytical, floating-point and fixed-point solutions. It appears that it has a strong connection to the coefficients c_k (18). In Fig. 10 and 11 values of coefficients c_k computed analytically and numerically with application of fixed point arithmetic with different word lengths. Vertical axes in those figures are in the logarithmic scale for easier observation of the effects.

For word length WL=14 the effect of quantisation is evidently visible for coefficients with index greater than 13. Moreover coefficients with index greater than 27 they become equivalent to zero, regardless that analytically they are different from zero. For word length WL=18 the similar effect is visible, however quantisation is visible for indices greater than 34 and they become zero for indices greater than 80. Coefficients equal to zero are not visible in the plot, as 0 does not belong to the domain of algorithm.

It should be noted, that this effect causes qualitative change in the system character. From the system with potentially infinite memory it becomes a system with finite memory. It should be compared with practically stable discrete fractional systems (see for example Kaczorek(2011)).

8. CONCLUSIONS

After analysis of results of numerical experiments it can be concluded, that main reasons for errors occurring when using fixed-point arithmetic are the quantisation and rounding of coefficients (18). In figures it can be observed, that for analysed systems these coefficients are reduced along with index. For small values this effect is especially visible. Below certain value (certain index) quantisation reduces them to zero. Simulations illustrated, that the errors caused by using fixed-point arithmetic can significantly change the response of analysed system. Word length should be then chosen very carefully. In further works the possibility of using different word lengths for coefficients and state. Additional modification of numerical method should be considered in order to increase robustness to these errors.

It should be also noted, that zeroing of coefficients due to fixed-point computation leads to system with finite memory. It is very similar to practically stable discrete fractional systems. It is interesting how other properties of these systems transfer to analysed systems.

REFERENCES

1. **Biernat J.** (2001), *Metody i układy arytmetyki komputerowej*, Oficyna Wydawnicza Politechniki Wrocławskiej, Wrocław.
2. **Busłowicz M.** (2008), *Frequency domain method for stability analysis of linear continuous-time fractional systems*, In Malinowski K. and Rutkowski L. editors, Recent advances in control and automation, chapter 2, pages 83-92, Akademicka Oficyna Wydawnicza EXIT, Warszawa.

3. **Djouambi A. B., Charef A. F., Besançon A. V.** (2007), Optimal approximation, simulation and analog realization of the fundamental fractional order transfer function, *Int. J. Appl. Math. Comput. Sci.*, 17(4):455-462.
4. **Dzieliński A., Sierociuk D.** (2008), Obserwator zredukowany dla dyskretnych układów ułamkowego rzędu, In Malinowski K. and Rutkowski L., editors, Sterowanie i Automatyzacja: Aktualne problemy i ich rozwiązania, chapter 2, pages 66-75. Akademicka Oficyna Wydawnicza EXIT.
5. **Gevers M., Li G.** (1993), *Parametrizations in Control, Estimation, and Filtering Problems: Accuracy Aspects*, Springer-Verlag, London.
6. **Hairer E., Nørsett S. P., Wanner G.** (2000), *Solving Ordinary Differential Equations: I Nonstiff problems*, Springer..
7. **Kaczorek T.** (2008a), Practical stability of positive fractional discrete-time linear systems, *Bulletin of the Polish Academy of Sciences Technical Sciences*, 56(4):313-317.
8. **Kaczorek T.** (2008b), Fractional positive linear systems and electrical circuits, *Materiały XXXI Międzynarodowej konferencji z podstaw elektrotechniki i teorii obwodów IC-SPETO*, 3-4, Ustroń , 28-31.05.2008.
9. **Kaczorek T.** (2011), *Positive fractional linear systems*, Pomiary Automatyka Robotyka, 2:91--112.
10. **Kalinowski T., Busłowicz M.** (2011), Odporna stabilność rodziny wielomianów niecałkowitego stopnia o współczynnikach wieloliniowo zależnych od niepewnych parametrów, *Pomiary Automatyka Robotyka*, 2:576-585.
11. **Klamka J.** (2009), Controllability and minimum energy control problem of infinite dimensional fractional discrete-time systems with delays, *Proceedings of 2009 First Asian Conference on Intelligent Information and Database Systems*, 398-403.
12. **Lederman C., Roquejoffre J. M., Wolanski N.** (2002), Mathematical justification of a nonlinear integro-differential equation for the propagation of spherical flames, *C. R. Math. Acad. Sci. Paris*, 334(7):569—574.
13. **Magin R., Ortigueira M. D., Podlubny I., Trujillo J.** (2011), On the fractional signals and systems. Signal Processing, *Advances in Fractional Signals and Systems*, 91(3):350 - 371.
14. **Miller K. S., Ross B.** (1993), *An introduction to the fractional calculus and fractional differential equations*, John Wiley & Sons Inc., New York.
15. **Oldham K. B., Spanier J.** (1974), *The fractional calculus*, Academic Press [A subsidiary of Harcourt Brace Jovanovich, Publishers], New York-London.
16. **Ortigueira M. D.** (2008), An Introduction to the Fractional Continuous-Time Linear Systems: The 21st Century Systems, *IEEE Circuits and Systems Magazine*, 8(3):19-26.
17. **Ostalczyk P.** (2008), *Zarys rachunku różniczkowo-całkowego ułamkowych rzędów. Teoria i zastosowania w automatyce*, Wydawnictwo Politechniki Łódzkiej.
18. **Piątek P.** (2007), *Wykorzystanie specjalizowanych architektur sprzętowych do realizacji krytycznych czasowo zadań sterowania, Application of Specialized Hardware Architectures for Realization of Time-critical Control Tasks*, Rozprawa doktorska, Promotor: W. Grega, Akademia Górniczo-Hutnicza im. Stanisława Staszica, Wydział Elektrotechniki, Automatyki, Informatyki i Elektroniki, Kraków.
19. **Pochopień B.** (2004), *Arytmetyka w systemach cyfrowych*, Akademicka Oficyna Wydawnicza EXIT, Warszawa.
20. **Podlubny I.** (1999), Fractional differential equations. An introduction to fractional derivatives, fractional differential equations, to methods of their solution and some of their applications, volume 198 of *Mathematics in Science and Engineering*, Academic Press Inc., San Diego, California.
21. **Podlubny I.** (2000), *Matrix approach to discrete fractional calculus*, Fractional Calculus and Applied Analysis, 3(4):359--386.
22. **Ruszewski A.** (2008), *Stabilization of Fractional-order Strejc's process model with time delay using fractional-order PI controller*, In Malinowski, K. and Rutkowski, L., editors, Recent advances in control and automation, chapter 2, pages 103-113. Akademicka Oficyna Wydawnicza EXIT, Warszawa, 2008.
23. **Samko S., Kilbas A., Marichev O.** (1993*), Fractional Integrals and derivatives: Theory and Applications*, Gordon and Breach Science Publishers.
24. **Sobolewski A., Ruszewski A.** (2011), Realizacja praktyczna regulatora niecałkowitego rzędu, *Pomiary Automatyka Robotyka*, 2:586-594.
25. **Świder Z.** (2002), Redukcja błędów zaokrągleń w układzie sterowania niewrażliwym na zakłócenie periodyczne, *Materiały XIV Krajowej Konferencji Automatyki*, Zielona Góra, 537-542.
26. **Świder Z**. (2003), *Realizacje cyfrowe algorytmów sterowania i filtracji*, Oficyna Wydawnicza Politechniki Rzeszowskiej, Rzeszów, 2003.
27. **Weilbeer M.** (2005), *Efficient Numerical Methods for Fractional Differential Equations and their Analytical Background*, PhD thesis, Technischen Universität Braunschweig.
28. **Wiatr K.** (2003), *Akceleracja obliczeń w systemach wizyjnych*, WNT, Warszawa.

Work partially financed by National Centre of Science funds for 2011-2013 as a research project. Contract no. N N514 644440.

SOLUTIONS TO TIME-FRACTIONAL DIFFUSION-WAVE EQUATION IN SPHERICAL COORDINATES

Yuriy POVSTENKO[*,**]

[*]Institute of Mathematics and Computer Science, Jan Długosz University in Częstochowa,
al. Armii Krajowej 13/15, 42-200, Częstochowa, Poland
[**]Department of Computer Science, European University of Informatics and Economics (EWSIE) in Warsaw,
ul. Białostocka 22, 03-741Warsaw, Poland

j.povstenko@ajd.czest.pl

Abstract: Solutions to time-fractional diffusion-wave equation with a source term in spherical coordinates are obtained for an infinite medium. The solutions are found using the Laplace transform with respect to time t, the finite Fourier transform with respect to the angular coordinate $\boldsymbol{\varphi}$, the Legendre transform with respect to the spatial coordinate $\boldsymbol{\mu}$, and the Hankel transform of the order n+1/2 with respect to the radial coordinate $\boldsymbol{r}$. In the central symmetric case with one spatial coordinate $\boldsymbol{r}$ the obtained results coincide with those studied earlier.

1. INTRODUCTION

The time-fractional diffusion-wave equation

$$\frac{\partial^\alpha c}{\partial t^\alpha} = a\Delta c \tag{1}$$

is a mathematical model of important physical phenomena ranging from amorphous, colloid, glassy and porous materials through fractals, percolation clusters, random and disordered media to comb structures, dielectrics and semiconductors, polymers and biological systems (see Metzler and Klafter, 2000, 2004; Povstenko, 2005; Magin, 2006; Uchaikin, 2008, among many others, and references therein).

The fundamental solution for the time-fractional diffusion-wave equation in one Cartesian space-dimension was obtained by Mainardi (1996). Wyss (1986) obtained the solutions to the Cauchy problem in terms of *H*-functions using the Mellin transform. Schneider and Wyss (1989) converted the diffusion-wave equation with appropriate initial conditions into the integrodifferential equation and found the corresponding Green functions in terms of Fox functions. Fujita (1990) treated integrodifferential equation which interpolates the heat conduction equation and the wave equation.

Previously, in studies concerning this equation in spherical coordinates only central symmetric case has been investigated (Povstenko, 2008a, 2008b, 2008c; Lenci et al., 2009, Qi and Liu, 2010). In this paper we investigate solutions to time-fractional diffusion-wave equation in an infinite medium in spherical coordinate system in the case of three spatial coordinates r, θ, and φ.

Consider the time-fractional diffusion-wave equation with a source term

$$\frac{\partial^\alpha c}{\partial t^\alpha} = a\left[\frac{\partial^2 c}{\partial r^2} + \frac{2}{r}\frac{\partial c}{\partial r} + \frac{1}{r^2\sin\theta}\frac{\partial}{\partial\theta}\left(\sin\theta\frac{\partial c}{\partial\theta}\right) + \frac{1}{r^2\sin^2\theta}\frac{\partial^2 c}{\partial\varphi^2}\right] + Q(r,\theta,\varphi,t), \tag{2}$$

$0 \le r < \infty$, $0 \le \theta \le \pi$, $0 \le \varphi \le 2\pi$, $0 < t < \infty$, $0 < \alpha \le 2$.

Here we use the Caputo fractional derivative (see Gorenflo and Mainardi, 1997; Kilbas et al., 2006; Klimek, 2009)

$$\frac{d^\alpha c(t)}{dt^\alpha} = \begin{cases} \dfrac{1}{\Gamma(n-\alpha)}\displaystyle\int_0^t (t-\tau)^{n-\alpha-1}\frac{d^n c(\tau)}{dt^n}d\tau, \\ \qquad\qquad n-1<\alpha<n, \\ \dfrac{d^n c(t)}{dt^n}, \qquad\qquad \alpha = n, \end{cases} \tag{3}$$

where $\Gamma(\alpha)$ is the gamma function.

For its Laplace transform rule the Caputo fractional derivative requires the knowledge of the initial values of the function $c(t)$ and its integer derivatives of the order $k = 1,2,...,n-1$:

$$L\left\{\frac{d^\alpha c(t)}{dt^\alpha}\right\} = s^\alpha L\{c(t)\} - \sum_{k=0}^{n-1} c^{(k)}(0^+)s^{\alpha-1-k}, \tag{4}$$

$n-1<\alpha<n$,

where s is the transform variable.

Change of variable $\mu = cos\theta$ in (2) leads to the following equation

$$\frac{\partial^\alpha c}{\partial t^\alpha} = a\left[\frac{\partial^2 c}{\partial r^2} + \frac{2}{r}\frac{\partial c}{\partial r} + \frac{1}{r^2}\frac{\partial}{\partial\mu}\left(\left(1-\mu^2\right)\frac{\partial c}{\partial\mu}\right) + \frac{1}{r^2\left(1-\mu^2\right)}\frac{\partial^2 c}{\partial\varphi^2}\right] + Q(r,\mu,\varphi,t), \tag{5}$$

$0 \le r < \infty$, $-1 \le \mu \le 1$, $0 \le \varphi \le 2\pi$, $0 < t < \infty$, $0 < \alpha \le 2$.

For simplicity, we have not introduced different letters for $Q(r,\theta,\varphi,t)$ and $Q(r,\mu,\varphi,t)$. For equation (5) the initial conditions are prescribed:

$$t=0: \quad c=f(r,\mu,\varphi),\ 0<\alpha\le 2, \tag{6}$$

$$t=0: \quad \frac{\partial c}{\partial t}=F(r,\mu,\varphi),\ 1<\alpha\le 2. \tag{7}$$

The solution to the initial value problem (5)-(7) can be written in the following form

$$c=\int_0^{2\pi}\int_{-1}^{1}\int_0^{\infty} f(\rho,\zeta,\phi)G_f(r,\mu,\varphi,\rho,\zeta,\phi,t)\rho^2 d\rho\, d\zeta\, d\phi$$

$$+\int_0^{2\pi}\int_{-1}^{1}\int_0^{\infty} F(\rho,\zeta,\phi)G_F(r,\mu,\varphi,\rho,\zeta,\phi,t)\rho^2 d\rho\, d\zeta\, d\phi$$

$$+\int_0^{t}\int_0^{2\pi}\int_{-1}^{1}\int_0^{\infty} Q(\rho,\zeta,\phi,\tau)$$

$$\times G_Q(r,\mu,\varphi,\rho,\zeta,\phi,t-\tau)\rho^2 d\rho\, d\zeta\, d\phi\, d\tau. \tag{8}$$

In the subsequent text, we investigate the fundamental solutions for the first Cauchy problem $G_f(r,\mu,\varphi,\rho,\xi,\phi,t)$, to the second Cauchy problem $G_F(r,\mu,\varphi,\rho,\xi,\phi,t)$, and for the source problem $G_Q(r,\mu,\varphi,\rho,\xi,\phi,t)$.

2. FUNDAMENTAL SOLUTION TO THE FIRST CAUCHY PROBLEM

Let us examine the time-fractional diffusion-wave equation

$$\frac{\partial^\alpha G_f}{\partial t^\alpha}=a\left[\frac{\partial^2 G_f}{\partial r^2}+\frac{2}{r}\frac{\partial G_f}{\partial r}+\frac{1}{r^2}\frac{\partial}{\partial\mu}\left(\left(1-\mu^2\right)\frac{\partial G_f}{\partial\mu}\right)\right.$$

$$\left.+\frac{1}{r^2\left(1-\mu^2\right)}\frac{\partial^2 G_f}{\partial\varphi^2}\right], \tag{9}$$

$0\le r<\infty,\ -1\le\mu\le 1,\ 0\le\varphi\le 2\pi,\ 0<t<\infty,\ 0<\alpha\le 2,$

with the prescribed initial value of a function

$$t=0: \quad G_f=\frac{1}{r^2}\,\delta(r-\rho)\,\delta(\mu-\zeta)\,\delta(\varphi-\phi), \tag{10}$$

$0<\alpha\le 2,$

$$t=0: \quad \frac{\partial G_f}{\partial t}=0,\ 1<\alpha\le 2. \tag{11}$$

The three-dimensional Dirac delta function $\delta(x)\delta(y)\delta(z)$ after passing to the spherical coordinates takes the form $\frac{1}{\pi r^2}\delta_+(r)$, but for the sake of simplicity we have omitted the factor 4π in the solution (8) as well as the factor $(4\pi)^{-1}$ in the initial condition (10).

Now we introduce the new looked-for function $v=\sqrt{r}c$ and use the Laplace transform with respect to time t, the finite Fourier transform with respect to the angular coordinate φ, the Legendre transform with respect to the coordinate μ, and the Hankel transform of the order $n+1/2$ with respect to the radial coordinate r. The details of application the integral transform technique to the Laplace operator in spherical coordinates can be found in the book of Özişik (1980). In the transforms domain we obtain

$$v^*(\xi,m,n,\varphi,\rho,\zeta,\phi,s)=\frac{1}{\sqrt{\rho}}J_{n+1/2}(\rho\xi)P_n^m(\zeta)$$

$$\times\cos[m(\varphi-\phi)]\,\frac{s^{\alpha-1}}{s^\alpha+a\xi^2}, \tag{12}$$

where the asterisk indicates the transforms, $J_{n+1/2}(r)$ is the Bessel function of the first kind of order $n+1/2$, $P_n^m(\xi)$ are the associated Legendre polynomials of degree n and order m, s is the Laplace transform variable, ξ is the Hankel transform variable, the integer m is the Fourier transform variable, and the integers n and m are the Legendre transform variables.

To invert the Laplace transform we use the following result (Gorenflo and Mainardi, 1997; Kilbas et al. , 2006)

$$L^{-1}\left\{\frac{s^{\alpha-1}}{s^\alpha+a\xi^2}\right\}=E_\alpha\left(-a\xi^2 t^\alpha\right), \tag{13}$$

where $E_\alpha(z)$ is the Mittag-Leffler function

$$E_\alpha(z)=\sum_{n=0}^{\infty}\frac{z^n}{\Gamma(\alpha n+1)},\ \alpha>0,\ z\in C. \tag{14}$$

For large values of argument the Mittag-Leffler function is represented as

$$E_\alpha\left(-a\xi^2 t^\alpha\right)\approx\frac{1}{\Gamma(1-\alpha)}\frac{1}{a\xi^2 t^\alpha}. \tag{15}$$

Inversion of all the integral transforms gives:

$$G_f(r,\mu,\varphi,\rho,\zeta,\phi,t)=\frac{1}{\pi\sqrt{r\rho}}\sum_{n=0}^{\infty}{\sum_{m=0}^{n}}'\frac{2n+1}{2}$$

$$\times\frac{(n-m)!}{(n+m)!}P_n^m(\mu)P_n^m(\zeta)\cos[m(\varphi-\phi)] \tag{16}$$

$$\times\int_0^{\infty}E_\alpha\left(-a\xi^2 t^\alpha\right)J_{n+1/2}(r\xi)J_{n+1/2}(\rho\xi)\xi\, d\xi,$$

where the prime near the summation symbol denotes that the term corresponding to $m=0$ in the sum should be multiplied by the factor $1/2$.

In the central symmetric case ($m=0,\ n=0$), taking into account that the Bessel functions of the first kind of the order one half can be represented as

$$J_{1/2}(r)=\sqrt{\frac{2r}{\pi}}\frac{\sin r}{r}, \tag{17}$$

from (16) we get

$$G_f(r,\rho,t)=\frac{1}{2\pi^2 r\rho}\int_0^{\infty}E_\alpha\left(-a\xi^2 t^\alpha\right)$$

$$\times\sin(r\xi)\sin(\rho\xi)d\xi. \tag{18}$$

Solution (18) was obtained earlier by Povstenko (2008c) using sin-Fourier transform with respect to the radial coordinate r. The limiting case of (18) under $\rho\to 0$,

$$G_f(r,\rho,t)=\frac{1}{2\pi^2 r}\int_0^\infty E_\alpha\left(-a\xi^2 t^\alpha\right)\sin(r\xi)\xi\, d\xi\ , \qquad (19)$$

was also investigated earlier (Povstenko, 2008b).

Asymptotic behavior of Mettag-Leffler function $E_\alpha(-\alpha\xi^2 t^\alpha)$ (15) is responsible for appearance of singularity of the solution (16) at the point of applying the delta pulse: $r=\rho,\ \mu=\xi,\ \varphi=\phi$ also for $t>0$. The sign of the singularity depends on α: plus for $0<\alpha<1$ and minus for $1<\alpha<2$. Only the solution to the classical diffusion equation ($\alpha=1$ and $E_1(-\alpha\xi^2 t^\alpha)=\exp(-\alpha\xi^2 t^\alpha)$) has no singularity.

3. FUNDAMENTAL SOLUTION TO THE SECOND CAUCHY PROBLEM

In the case of the second Cauchy problem, which is considered for the order of time derivative $1<\alpha\le 2$, the initial value of the time derivative of the sought-for function is prescribed, and for the corresponding fundamental solution we have

$$\frac{\partial^\alpha G_F}{\partial t^\alpha}=a\left[\frac{\partial^2 G_F}{\partial r^2}+\frac{2}{r}\frac{\partial G_F}{\partial r}+\frac{1}{r^2}\frac{\partial}{\partial\mu}\left(\left(1-\mu^2\right)\frac{\partial G_F}{\partial\mu}\right)\right.$$

$$\left.+\frac{1}{r^2\left(1-\mu^2\right)}\frac{\partial^2 G_F}{\partial\varphi^2}\right], \qquad (20)$$

$0\le r<\infty,\ -1\le\mu\le 1,\ 0\le\varphi\le 2\pi,\ 0<t<\infty,\ 1<\alpha\le 2,$

with the following initial conditions:

$$t=0:\quad G_F=0,\ 1<\alpha\le 2\ , \qquad (21)$$

$$t=0:\quad \frac{\partial G_F}{\partial t}=\frac{1}{r^2}\,\delta(r-\rho)\,\delta(\mu-\zeta)\,\delta(\varphi-\phi),$$

$$1<\alpha\le 2\,. \qquad (22)$$

The integral transform technique allows us to remove the partial derivatives and to get the expression for the auxiliary function v in the transforms domain

$$v^*(\xi,m,n,\varphi,\rho,\zeta,\phi,s)=\frac{1}{\sqrt{\rho}}J_{n+1/2}(\rho\xi)P_n^m(\zeta)$$

$$\times\cos[m(\varphi-\phi)]\,\frac{s^{\alpha-2}}{s^\alpha+a\xi^2}\,. \qquad (23)$$

After inversion of integral transforms we gain

$$G_F(r,\mu,\varphi,\rho,\zeta,\phi,t)=\frac{1}{\pi\sqrt{r\rho}}\sum_{n=0}^{\infty}{\sum_{m=0}^{n}}'\frac{2n+1}{2}$$

$$\times\frac{(n-m)!}{(n+m)!}P_n^m(\mu)P_n^m(\zeta)\cos[m(\varphi-\phi)] \qquad (24)$$

$$\times\int_0^\infty t\,E_{\alpha,2}\left(-a\xi^2 t^\alpha\right)J_{n+1/2}(r\xi)J_{n+1/2}(\rho\xi)\xi\,d\xi\,,$$

where $E_{\alpha,\beta}(z)$ is the generalized Mittag-Leffler function in two parameters α and β (Gorenflo and Mainardi, 1997; Kilbas et al., 2006)

$$E_{\alpha,\beta}(z)=\sum_{n=0}^{\infty}\frac{z^n}{\Gamma(\alpha n+\beta)}, \qquad (25)$$

$\alpha>0\quad,\ \beta>0,\ z\in C\,.$

We have used the following formula for the inverse Laplace transform

$$L^{-1}\left\{\frac{s^{\alpha-\beta}}{s^\alpha+a\xi^2}\right\}=t^{\beta-1}E_{\alpha,\beta}\left(-a\xi^2 t^\alpha\right). \qquad (26)$$

In the central symmetric case we have (Povstenko, 2008c)

$$G_F(r,\rho,t)=\frac{1}{2\pi^2 r\rho}\int_0^\infty t\,E_{\alpha,2}\left(-a\xi^2 t^\alpha\right)$$

$$\times\sin(r\xi)\sin(\rho\xi)d\xi\,. \qquad (27)$$

It should be noted that due to the behavior of the Mittag-Leffler function $E_{\alpha,2}(-\alpha\xi^2 t^\alpha)$ for large values of argument

$$E_{\alpha,2}\left(-a\xi^2 t^\alpha\right)\approx\frac{1}{\Gamma(2-\alpha)}\frac{1}{a\xi^2 t^\alpha},\ 1<\alpha<2\,, \qquad (28)$$

the fundamental solution (24) has the singularity with the positive sign at the point of applying the delta pulse for $t>0$ and all values of $1<\alpha<2$.

4. FUNDAMENTAL SOLUTION TO THE SOURCE PROBLEM

Consider the time-fractional diffusion equation with a source term being the time and space delta pulse applied at point with the spatial coordinates ρ,ξ and ϕ.

$$\frac{\partial^\alpha G_Q}{\partial t^\alpha}=a\left[\frac{\partial^2 G_Q}{\partial r^2}+\frac{2}{r}\frac{\partial G_Q}{\partial r}+\frac{1}{r^2}\frac{\partial}{\partial\mu}\left(\left(1-\mu^2\right)\frac{\partial G_Q}{\partial\mu}\right)\right.$$

$$\left.+\frac{1}{r^2\left(1-\mu^2\right)}\frac{\partial^2 G_Q}{\partial\varphi^2}\right]$$

$$+\frac{1}{r^2}\,\delta(r-\rho)\,\delta(\mu-\zeta)\,\delta(\varphi-\phi)\,\delta_+(t), \qquad (29)$$

$0\le r<\infty,\ -1\le\mu\le 1,\ 0\le\varphi\le 2\pi,\ 0<t<\infty,\ 0<\alpha\le 2,$

under zero initial conditions

$$t=0:\quad G_Q=0,\ 0<\alpha\le 2\,, \qquad (30)$$

$$t=0:\quad \frac{\partial G_Q}{\partial t}=0,\ 1<\alpha\le 2\,. \qquad (31)$$

Using integral transform, we arrive at

$$v^*=\frac{1}{\sqrt{\rho}}J_{n+1/2}(\rho\xi)P_n^m(\zeta)\cos[m(\varphi-\phi)]\,\frac{1}{s^\alpha+a\xi^2}\,, \qquad (32)$$

and after inversion of integral transforms

$$G_Q(r,\mu,\varphi,\rho,\zeta,\phi,t)=\frac{1}{\pi\sqrt{r\rho}}\sum_{n=0}^{\infty}{\sum_{m=0}^{n}}'\frac{2n+1}{2}$$

$$\times\frac{(n-m)!}{(n+m)!}P_n^m(\mu)P_n^m(\zeta)\cos[m(\varphi-\phi)] \qquad (33)$$

$$\times\int_0^{\infty}t^{\alpha-1}E_{\alpha,\alpha}\left(-a\xi^2t^{\alpha}\right)J_{n+1/2}(r\xi)J_{n+1/2}(\rho\xi)\,\xi\,d\xi\,.$$

In the central symmetric case we have (Povstenko, 2008c)

$$G_Q(r,\rho,t)=\frac{1}{2\pi^2r\rho}\int_0^{\infty}t^{\alpha-1}E_{\alpha,\alpha}\left(-a\xi^2t^{\alpha}\right)$$

$$\times\sin(r\xi)\sin(\rho\xi)d\xi\,. \qquad (34)$$

Due to the behavior of the Mittag-Leffler function $E_{\alpha,\alpha}(-\alpha\xi^2t^{\alpha})$ for large values of argument

$$E_{\alpha,\alpha}\left(-a\xi^2t^{\alpha}\right)\approx-\frac{1}{\Gamma(-\alpha)}\frac{1}{a^2\xi^4t^{2\alpha}} \qquad (35)$$

the solution (33) has no singularity at the point of applying the delta pulse for $t>0$.

5. CONCLUSIONS

The new solutions to the Cauchy and source problems for time-fractional diffusive-wave equation have been obtained for an infinite medium referred to spherical coordinate system r,θ,φ. For the first time, the non-central-symmetric case has been considered. The found solutions satisfy the appropriate initial conditions and reduce to the solutions of classical diffusion equation in the limit $\alpha=1$ and of the standard wave equation in the case of ballistic diffusion ($\alpha=2$). Our results provide a new analytical tool for studying anomalous diffusion.

REFERENCES

1. **Fujita Y.** (1990), Integrodifferential equation which interpolates the heat equation and the wave equation, *Osaka Journal of Mathematics*, Vol. 27, No. 2, 309-321.
2. **Goreflo R., Mainardi F.** (1997), *Fractional calculus: Integral and differential equations of fractional order*, In: Fractals and Fractional Calculus in Continuum Mechanics, A. Carpinteri and F. Mainardi (eds.), 223-276, Springer, Wien.
3. **Kilbas A., Srivastava H. M., Trujillo J. J.** (2006), *Theory and Applications of Fractional Differential Equations*, Elsevier, Amsterdam.
4. **Klimek M.** (2009), *On Solutions of Linear Fractional Differential Equations of a Variational Type*, The Publishing Office of Częstochowa University of Technology, Częstochowa.
5. **Lenzi E. K., da Silva L. R., Silva A. T., Evangelista L. R, Lenzi M. K.** (2009), Some results for a fractional diffusion equation with radial symmetry in a confined region, *Physica A*, Vol. 388, No. 4, 806-810.
6. **Magin R. L.** (2006), *Fractional Calculus in Bioengineering*, Begell House Publishers, Inc, Connecticut.
7. **Mainardi F.** (1996), The fundamental solutions for the fractional diffusion-wave equation, *Applied Mathematics Letters*, Vol. 9, No. 6, 23-28.
8. **Metzler R., Klafter J.** (2000), The random walk's guide to anomalous diffusion: a fractional dynamics approach, *Physics Reports*, Vol. 339, No. 1, 1-77.
9. **Metzler R., Klafter J.** (2004), The restaurant at the end of the random walk: recent developments in the description of anomalous transport by fractional dynamics, *Journal of Physics A: Mathematical and General*, Vol. 37, No. 31, R161-R208,.
10. **Özişik M. N.** (1980), *Heat Conduction*, John Wiley and Sons, New York.
11. **Povstenko Y. Z.** (2005), Fractional heat conduction equation and associated thermal stress, *Journal of Thermal Stresses*, Vol. 28, No. 1, 83-102.
12. **Povstenko Y. Z.** (2008a), Time-fractional radial diffusion in a sphere, *Nonlinear Dynamics*, Vol. 53, No. 1, 55-65.
13. **Povstenko Y. Z.** (2008b), Fundamental solutions to three-dimensional diffusion-wave equation and associated diffusive stresses, *Chaos Solitons and Fractals*, Vol. 36, No. 4, 961-972.
14. **Povstenko Y. Z.** (2008c), Fundamental solutions to central symmetric problems for fractional heat conduction equation and associated thermal stresses, *Journal of Thermal Stresses*, Vol. 31, No. 2, 127-148.
15. **Qi H., Liu J.** (2010), Time-fractional radial diffusion in hollow geometries, *Meccanica*, Vol. 45, No. 4, 577-583.
16. **Schneider W.R., Wyss W.** (1989), Fractional diffusion and wave equations, *Journal of Mathematical Physics*, Vol. 30, No. 1, 134-144.
17. **Uchaikin V.V.** (2008), *Method of Fractional Derivatives*, Artishock,Ulyanovsk. (In Russian).
18. **Wyss W.** (1986), The fractional diffusion equation, *Journal of Mathematical Physics*, Vol. 27, No. 11, 2782-2785.

GENERAL RESPONSE FORMULA FOR FRACTIONAL 2D CONTINUOUS-TIME LINEAR SYSTEMS DESCRIBED BY THE ROESSER MODEL

Krzysztof ROGOWSKI*

*Phd student, Faculty of Electrical Engineering, Białystok University of Technology, Wiejska 45 D, 15-351 Białystok

k.rogowski@doktoranci.pb.edu.pl

Abstract: A new class of fractional two-dimensional (2D) continuous-time linear systems is introduced. The general response formula for the system is derived using a 2D Laplace transform. It is shown that the classical Cayley-Hamilton theorem is valid for such class of systems. Usefulness of the general response formula to obtain a solution of the system is discussed and illustrated by a numerical example.

1. INTRODUCTION

The most popular models of two-dimensional (2D) linear system are the ones introduced by Roesser (1975), Fornasini and Marchesini (1976, 1978) and Kurek (1985). An overview of 2D linear systems theory is given in (Bose, 1982, 1985; Kaczorek, 1985, 2001; Gałkowski, 2001, Farina and Rinaldi, 2000).

Mathematical fundamentals of fractional calculus and its applications are given in the monographs (Oldham and Spanier, 1974; Nashimoto, 1984; Miller and Ross, 1993; Podlubny, 1999, Ostalczyk, 2008).

The notion of fractional 2D discrete-time linear systems was introduced by Kaczorek (2008a) and extended in (Kaczorek, 2008b, 2009, Kaczorek and Rogowski, 2010, Rogowski, 2011). An overview in state of the art in 1D and 2D fractional systems is given in the monograph (Kaczorek, 2011).

In this paper a new 2D continuous-time fractional Roesser type model will be introduced. The general response formula for the system will be derived using the 2D Laplace transform method (Section 2). Moreover the classical Cayley-Hamilton theorem will be extended to fractional 2D continuous-time systems in Section 3. In Section 4 usefulness of the general response formula to obtaining the solution of the system will be discussed and illustrated by a numerical example. Concluding remarks are given in Section 5.

To the best knowledge of the author 2D continuous-time fractional linear systems have not been considered yet.

2. FRACTIONAL 2D STATE EQUATIONS AND THEIR SOLUTION

Let $R^{n\times m}$ be the set of $n\times m$ real matrices and $R^n := R^{n\times 1}$. The set of nonnegative integers will be denoted by Z_+ and the $n\times n$ identity matrix will be denoted by I_n.

We introduce the following definition of fractional partial derivative of a 2D continuous function $f(t_1,t_2)$ of two independent variables $t_1, t_2 \geq 0$.

Definition 1. The α_i order partial derivative of a 2D continuous function $f(t_1,t_2)$ is given by the formula

$$D_{t_i}^{\alpha_i} f(t_1,t_2) = \frac{\partial^{\alpha_i}}{\partial t_i^{\alpha_i}} f(t_1,t_2) = \frac{1}{\Gamma(N_i-\alpha_i)} \int_0^{t_i} \frac{f_{t_i}^{(N_i)}(\tau_i)}{(t_i-\tau_i)^{\alpha_i-N_i+1}} d\tau_i, \tag{1}$$

where $i = 1,2$; $N_i - 1 < \alpha_i < N_i \in N = \{1,2,\ldots\}$, $\alpha_i \in R$ is the order of fractional partial derivative,

$$\Gamma(x) = \int_0^{\infty} e^{-t} t^{x-1} dt \tag{2}$$

for $x \geq 0$ is the gamma function and

$$f_{t_i}^{(N_i)}(\tau_i) = \begin{cases} \dfrac{\partial^{N_1} f(\tau_1,t_2)}{\partial \tau_1^{N_1}} & \text{for} \quad i=1 \\ \dfrac{\partial^{N_2} f(t_1,\tau_2)}{\partial \tau_2^{N_2}} & \text{for} \quad i=2. \end{cases} \tag{3}$$

Consider the fractional 2D continuous-time system described by the state equations

$$\begin{bmatrix} D_{t_1}^{\alpha_1} x^h(t_1,t_2) \\ D_{t_2}^{\alpha_2} x^v(t_1,t_2) \end{bmatrix} = \begin{bmatrix} A_{11} & A_{12} \\ A_{21} & A_{22} \end{bmatrix} \begin{bmatrix} x^h(t_1,t_2) \\ x^v(t_1,t_2) \end{bmatrix} + \begin{bmatrix} B_1 \\ B_2 \end{bmatrix} u(t_1,t_2), \tag{4a}$$

$$y(t_1,t_2) = C \begin{bmatrix} x^h(t_1,t_2) \\ x^v(t_1,t_2) \end{bmatrix} + Du(t_1,t_2), \tag{4b}$$

where $x^h(t_1,t_2) \in R^{n_1}$, $x^v(t_1,t_2) \in R^{n_2}$ $(n = n_1 + n_2)$ are the horizontal and vertical state vectors, respectively, $u(t_1,t_2) \in R^m$ is the input vector, $y(t_1,t_2) \in R^p$ is the output vector and $A_{kl} \in R^{n_k\times l}$, $B_k \in R^{n_k\times m}$ for $k,l = 1,2$; $C \in R^{p\times n}$; $D \in R^{p\times m}$.

The boundary conditions for (4) are given in the form

$$x_{t_1}^{h(k)}(0,t_2)=\left[\frac{\partial^k x^h(t_1,t_2)}{\partial t_1^k}\right]_{t_1=0} \tag{5a}$$

for $k=0,1,\ldots,N_1-1$ and $t_2\geq 0$,

$$x_{t_2}^{v(l)}(t_1,0)=\left[\frac{\partial^l x^v(t_1,t_2)}{\partial t_2^l}\right]_{t_2=0} \tag{5b}$$

for $l=0,1,\ldots,N_2-1$ and $t_1\geq 0$.

In the following theorem the Riemman-Liouville formula of fractional integration of a function $f(t)$ will be used (Podlubny, 1999)

$$I_t^{\alpha} f(t)=\frac{1}{\Gamma(\alpha)}\int_0^t f(\tau)(t-\tau)^{\alpha-1}\,d\tau, \tag{6}$$

where $\alpha>0$ is the fractional (real) order of the integration. Similarly, we may define the 2D fractional integral of function $f(t_1,t_2)$

$$\begin{aligned} I_{t_1,t_2}^{\alpha,\beta} f(t_1,t_2) &= I_{t_1}^{\alpha}\left[I_{t_2}^{\beta} f(t_1,t_2)\right]=I_{t_2}^{\beta}\left[I_{t_1}^{\alpha} f(t_1,t_2)\right] \\ &=\frac{1}{\Gamma(\alpha)\Gamma(\beta)}\times \\ &\int_0^{t_1}\int_0^{t_2}(t_1-\tau_1)^{\alpha-1}(t_2-\tau_2)^{\beta-1} f(\tau_1,\tau_2)\,d\tau_2 d\tau_1, \end{aligned} \tag{7}$$

where $\alpha,\beta>0$.

Theorem 1. The solution to the equation (4a) with the boundary conditions (5) is given by

$$\begin{aligned} \begin{bmatrix} x^h(t_1,t_2)\\ x^v(t_1,t_2)\end{bmatrix} &= \sum_{i=0}^{\infty}\sum_{j=1}^{\infty} T_{ij}\left\{\sum_{k=1}^{N_1}\frac{t_1^{k+i\alpha_1-1}}{\Gamma(k+i\alpha_1)} I_{t_2}^{j\alpha_2}\begin{bmatrix} x_{t_1}^{h(k-1)}(0,t_2)\\ 0\end{bmatrix}\right. \\ &\left.+\begin{bmatrix} B_1\\ 0\end{bmatrix} I_{t_1,t_2}^{(i+1)\alpha_1,\,j\alpha_2} u(t_1,t_2)\right\} \\ &+\sum_{i=0}^{\infty} T_{i0}\left\{\sum_{k=1}^{N_1}\frac{t_1^{k+i\alpha_1-1}}{\Gamma(k+i\alpha_1)}\begin{bmatrix} x_{t_1}^{h(k-1)}(0,t_2)\\ 0\end{bmatrix}\right. \\ &\left.+\begin{bmatrix} B_1\\ 0\end{bmatrix} I_{t_1}^{(i+1)\alpha_1} u(t_1,t_2)\right\} \\ &+\sum_{i=0}^{\infty}\sum_{j=0}^{\infty} T_{ij}\left\{\sum_{l=1}^{N_2}\frac{t_2^{l+j\alpha_2-1}}{\Gamma(l+j\alpha_2)} I_{t_1}^{i\alpha_1}\begin{bmatrix} 0\\ x_{t_2}^{v(l-1)}(t_1,0)\end{bmatrix}\right. \\ &\left.+\begin{bmatrix} 0\\ B_2\end{bmatrix} I_{t_1,t_2}^{i\alpha_1,\,(j+1)\alpha_2} u(t_1,t_2)\right\} \\ &+\sum_{j=0}^{\infty} T_{0j}\left\{\sum_{l=1}^{N_2}\frac{t_2^{l+j\alpha_2-1}}{\Gamma(l+j\alpha_2)}\begin{bmatrix} 0\\ x_{t_2}^{v(l-1)}(t_1,0)\end{bmatrix}\right. \\ &\left.+\begin{bmatrix} 0\\ B_2\end{bmatrix} I_{t_2}^{(j+1)\alpha_2} u(t_1,t_2)\right\}, \end{aligned} \tag{8}$$

where

$$T_{ij}=\begin{cases} I_n & \text{for } i=0,\ j=0\\ T_{10}T_{i-1,j}+T_{01}T_{i,j-1} & \text{for } i+j>0,(i,j\in Z_+)\\ 0 \text{ (zero matrix)} & \text{for } i<0 \text{ and/or } j<0\end{cases} \tag{9}$$

and

$$T_{10}=\begin{bmatrix} A_{11} & A_{12}\\ 0 & 0\end{bmatrix},\quad T_{01}=\begin{bmatrix} 0 & 0\\ A_{21} & A_{22}\end{bmatrix}. \tag{10}$$

Proof. Let $F(p,t_2)$ $(F(t_1,s))$ be the Laplace transform of a 2D continuous function $f(t_1,t_2)$ with respect to t_1 (t_2) defined by

$$\begin{aligned} &F(p,t_2)=\mathcal{L}_{t_1}\left[f(t_1,t_2)\right]=\int_0^{\infty} f(t_1,t_2)e^{-pt_1}dt_1 \\ &\left(F(t_1,s)=\mathcal{L}_{t_2}\left[f(t_1,t_2)\right]=\int_0^{\infty} f(t_1,t_2)e^{-st_2}dt_2\right). \end{aligned} \tag{11}$$

The 2D Laplace transform of $f(t_1,t_2)$ will be denoted by $F(p,s)$ and defined by

$$\begin{aligned} F(p,s)&=\mathcal{L}_{t_1}\left\{\mathcal{L}_{t_2}\left[f(t_1,t_2)\right]\right\}=\mathcal{L}_{t_2}\left\{\mathcal{L}_{t_1}\left[f(t_1,t_2)\right]\right\} \\ &=\mathcal{L}_{t_1,t_2}\left[f(t_1,t_2)\right] \\ &=\int_0^{\infty}\int_0^{\infty} f(t_1,t_2)e^{-pt_1-st_2}dt_1dt_2. \end{aligned} \tag{12}$$

Applying (12) to (1) for $i=1$ and taking into account that (Kaczorek, 2011)

$$\mathcal{L}_{t_1}\left[t_1^{\alpha}\right]=\frac{\Gamma(\alpha+1)}{p^{\alpha+1}} \tag{13}$$

and

$$\mathcal{L}_{t_1}\left[f_{t_1}^{(N)}(t_1)\right]=p^N F(p,t_2)-\sum_{k=1}^{N} p^{N-k} f_{t_1}^{(k-1)}(0,t_2) \tag{14}$$

for $N=0,1,\ldots$; we obtain

$$\begin{aligned} \mathcal{L}_{t_1,t_2}\left[D_{t_1}^{\alpha_1} f(t_1,t_2)\right] &= \mathcal{L}_{t_2}\left\{\mathcal{L}_{t_1}\left[D_{t_1}^{\alpha_1} f(t_1,t_2)\right]\right\} \\ &=\frac{1}{\Gamma(N_1-\alpha_1)}\mathcal{L}_{t_2}\left\{\mathcal{L}_{t_1}\left[\int_0^{t_1}\frac{f_{t_1}^{(N_1)}(\tau_1)}{(t_1-\tau_1)^{\alpha_1-N_1+1}}d\tau_1\right]\right\} \\ &=\frac{1}{\Gamma(N_1-\alpha_1)}\mathcal{L}_{t_2}\left\{\mathcal{L}_{t_1}\left[t_1^{N_1-\alpha_1-1}\right]\mathcal{L}_{t_1}\left[f_{t_1}^{(N_1)}(\tau_1)\right]\right\} \\ &=p^{\alpha_1}F(p,s)-\sum_{k=1}^{N_1} p^{\alpha_1-k}F_{t_1}^{(k-1)}(0,s), \end{aligned} \tag{15}$$

where

$$F_{t_1}^{(k)}(0,s)=\mathcal{L}_{t_2}\left\{\left[\frac{\partial^k f(t_1,t_2)}{\partial t_1^k}\right]_{t_1=0}\right\} \tag{16}$$

for $k=0,1,\ldots$.

Similarly, for $i=2$ in (1) we have

$$\mathcal{L}_{t_1,t_2}\left[D_{t_2}^{\alpha_2} f(t_1,t_2)\right] = s^{\alpha_2} F(p,s) - \sum_{l=1}^{N_2} s^{\alpha_2-l} F_{t_2}^{(l-1)}(p,0), \tag{17}$$

where

$$F_{t_2}^{(l)}(p,0) = \mathcal{L}_{t_1}\left\{\left[\frac{\partial^l f(t_1,t_2)}{\partial t_2^l}\right]_{t_2=0}\right\} \tag{18}$$

for $l = 0, 1, ...$

Taking into account (15) and (17) we obtain the 2D Laplace transform of the state equation (4a)

$$\begin{bmatrix} p^{\alpha_1} X^h(p,s) - \sum_{k=1}^{N_1} p^{\alpha_1-k} X_{t_1}^{h(k-1)}(0,s) \\ s^{\alpha_2} X^v(p,s) - \sum_{l=1}^{N_2} s^{\alpha_2-l} X_{t_2}^{v(l-1)}(p,0) \end{bmatrix} = \begin{bmatrix} A_{11} & A_{12} \\ A_{21} & A_{22} \end{bmatrix} \begin{bmatrix} X^h(p,s) \\ X^v(p,s) \end{bmatrix} + \begin{bmatrix} B_1 \\ B_2 \end{bmatrix} U(p,s). \tag{19}$$

Premultiplying (19) by the matrix

$$\text{blockdiag}\left[p^{-\alpha_1} I_{n_1}, s^{-\alpha_2} I_{n_2}\right]$$

we obtain

$$\begin{bmatrix} X^h(p,s) \\ X^v(p,s) \end{bmatrix} = G^{-1}(p,s) \times \left\{ \begin{bmatrix} \sum_{k=1}^{N_1} p^{-k} X_{t_1}^{h(k-1)}(0,s) \\ \sum_{l=1}^{N_2} s^{-l} X_{t_2}^{v(l-1)}(p,0) \end{bmatrix} + \begin{bmatrix} p^{-\alpha_1} B_1 \\ s^{-\alpha_2} B_2 \end{bmatrix} U(p,s) \right\}, \tag{20}$$

where

$$G(p,s) = \begin{bmatrix} I_{n_1} - p^{-\alpha_1} A_{11} & -p^{-\alpha_1} A_{12} \\ -s^{\alpha_2} A_{21} & I_{n_2} - s^{\alpha_2} A_{22} \end{bmatrix}. \tag{21}$$

Let

$$G^{-1}(p,s) = \sum_{i=0}^{\infty}\sum_{j=0}^{\infty} T_{ij} p^{-i\alpha_1} s^{-j\alpha_2}. \tag{22}$$

From

$$G^{-1}(p,s) G(p,s) = G(p,s) G^{-1}(p,s) = I_n,$$

using (21) and (22), it follows that

$$\sum_{i=0}^{\infty}\sum_{j=0}^{\infty} \left\{T_{ij} - T_{10} T_{i-1,j} - T_{01} T_{i,j-1}\right\} p^{-i\alpha_1} s^{-j\alpha_2} = I_n \tag{23}$$

where T_{10} and T_{01} are defined by (10).

Comparing the coefficients at the same powers of p and s we obtain (9).

Substituting the expansion (22) into (20) we obtain

$$\begin{bmatrix} X^h(p,s) \\ X^v(p,s) \end{bmatrix} = \sum_{i=0}^{\infty}\sum_{j=0}^{\infty} T_{ij} \left\{ \begin{bmatrix} p^{-(i+1)\alpha_1} s^{-j\alpha_2} B_1 \\ p^{-i\alpha_1} s^{-(j+1)\alpha_2} B_2 \end{bmatrix} U(p,s) + \begin{bmatrix} \sum_{k=1}^{N_1} p^{-k-i\alpha_1} s^{-j\alpha_2} X_{t_1}^{h(k-1)}(0,s) \\ \sum_{l=1}^{N_2} p^{-i\alpha_1} s^{-l-j\alpha_2} X_{t_2}^{v(l-1)}(p,0) \end{bmatrix} \right\}, \tag{24}$$

Taking into account (Kaczorek, 2011)

$$\mathcal{L}^{-1}\left[p^{-\alpha} F(p)\right] = I_t^{\alpha} f(t), \tag{25}$$

where $\alpha > 0$ and $\mathcal{L}^{-1}$ denotes the inverse Laplace transform, it is easy to show that

$$\mathcal{L}_{t_1,t_2}^{-1}\left[p^{-\alpha_1} s^{-\alpha_2} F(p,s)\right] = I_{t_1,t_2}^{\alpha_1,\alpha_2} f(t_1,t_2), \tag{26}$$

where $\alpha_1, \alpha_2 > 0$.

Applying the inverse 2D Laplace transform to (24) and taking into account (26) we obtain the formula (8).

3. EXTENSION OF CAYLEY-HAMILTON THEOREM

Theorem 2. Let

$$\det G(p,s) = \begin{vmatrix} I_{n_1} - p^{-\alpha_1} A_{11} & -p^{-\alpha_1} A_{12} \\ -s^{\alpha_2} A_{21} & I_{n_2} - s^{\alpha_2} A_{22} \end{vmatrix} = \sum_{k=0}^{n_1}\sum_{l=0}^{n_2} a_{n_1-k,n_2-l} p^{-k\alpha_1} s^{-l\alpha_2} \tag{27}$$

be the characteristic polynomial of the system (4). Then the transition matrices T_{ij} satisfy the equality

$$\sum_{k=0}^{n_1}\sum_{l=0}^{n_2} a_{k,l} T_{k+m_1,l+m_2} = 0, \tag{28}$$

where $m_1, m_2 = 0, 1, ...$

Proof. From the definition of the inverse matrix, as well as (22) and (27), we have

$$\text{Adj}G(p,s) = \left(\sum_{k=0}^{n_1}\sum_{l=0}^{n_2} a_{n_1-k,n_2-l} p^{-k\alpha_1} s^{-l\alpha_2}\right) \times \left(\sum_{i=0}^{\infty}\sum_{j=0}^{\infty} T_{ij} p^{-i\alpha_1} s^{-j\alpha_2}\right) = \sum_{k=0}^{n_1}\sum_{l=0}^{n_2}\sum_{i=-k}^{\infty}\sum_{j=-l}^{\infty} a_{kl} T_{i+k,j+l} p^{-(i+n_1)\alpha_1} s^{-(j+n_2)\alpha_2}, \tag{29}$$

where $\mathrm{Adj}G(p,s)$ denotes the adjoint matrix of $G(p,s)$.

Comparing the coefficients at the same powers of p and s for $i \geq 0$ and $j \geq 0$we obtain (28) since $AdjG(p,s)$ is a polynomial matrix of the form

$$\mathrm{Adj}G(p,s) = \sum_{\substack{i=0 \\ i,j\neq n_1,n_2}}^{n_1} \sum_{j=0}^{n_2} D_{ij}\, p^{-i\alpha_1} s^{-j\alpha_2}, \tag{30}$$

where $D_{ij} \in R^{n\times n}$ are some real matrices.

Theorem 2 is an extension of the well-known classical Cayley-Hamilton theorem to fractional 2D continuous-time systems.

4. NUMERICAL EXAMPLE

Example 1. Consider fractional 2D system (4) with $\alpha_1 = 0{,}7$, $\alpha_2 = 0{,}9$ and matrices

$$\begin{bmatrix} A_{11} & A_{12} \\ A_{21} & A_{22} \end{bmatrix} = \begin{bmatrix} -0.9 & 0.7 \\ 0 & -0.3 \end{bmatrix}, \quad \begin{bmatrix} B_1 \\ B_2 \end{bmatrix} = \begin{bmatrix} 1 \\ 1 \end{bmatrix}, \quad C = \begin{bmatrix} 1 & 0 \\ 0 & 1 \end{bmatrix}, \quad D = [0]. \tag{31}$$

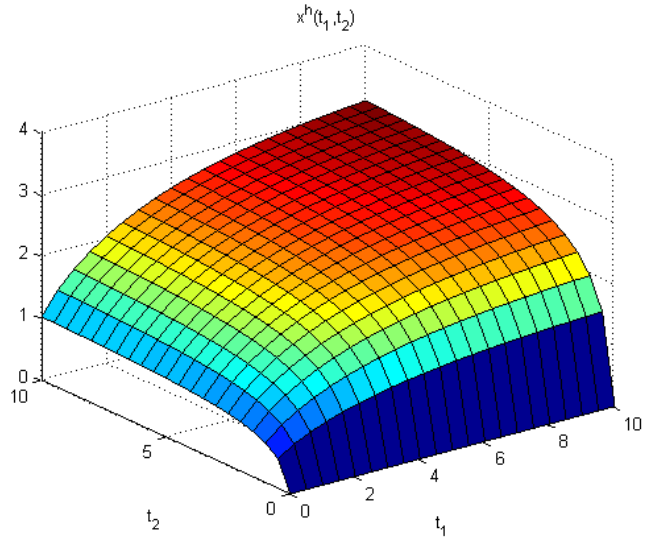

Fig. 1. State variable $x^h(t_1,t_2)$ of the system

Find a step response of the system (4) with the matrices (31), i.e. $y(t_1,t_2)$ for $t_1,t_2 \geq 0$ and

$$u(t_1,t_2) = H(t_1,t_2) = \begin{cases} 0 & for \quad t_1 < 0 \quad and/or \quad t_2 < 0 \\ 1 & for \quad t_1,t_2 \geq 0 \end{cases} \tag{32}$$

and zero boundary conditions

$$x^h(0,t_2) = 0, \qquad x^v(t_1,0) = 0. \tag{33}$$

Note that in this case from (31) and (4) it follows that

$$y(t_1,t_2) = \begin{bmatrix} x^h(t_1,t_2) \\ x^v(t_1,t_2) \end{bmatrix}.$$

It is well-known that (Podlubny, 1999)

$$I_t^{\alpha} H(t) = \frac{t^{\alpha}}{\Gamma(1+\alpha)}. \tag{34}$$

From (34) and (7) it is easy to show that

$$I_{t_1,t_2}^{\alpha_1,\alpha_2} u(t_1,t_2) = I_{t_1,t_2}^{\alpha_1,\alpha_2} H(t_1,t_2) = \frac{t_1^{\alpha_1} t_2^{\alpha_2}}{\Gamma(1+\alpha_1)\Gamma(1+\alpha_2)}. \tag{35}$$

Using (8) for $N_1, N_2 = 1$ and taking into account (31), (32) (33) and (35) we obtain

$$\begin{aligned} \begin{bmatrix} x^h(t_1,t_2) \\ x^v(t_1,t_2) \end{bmatrix} &= \sum_{i=0}^{\infty}\sum_{j=1}^{\infty} T_{ij} \begin{bmatrix} 1 \\ 0 \end{bmatrix} \frac{t_1^{(i+1)\alpha_1} t_2^{j\alpha_2}}{\Gamma[1+(i+1)\alpha_1]\Gamma(1+j\alpha_2)} \\ &+ \sum_{i=0}^{\infty} T_{i0} \begin{bmatrix} 1 \\ 0 \end{bmatrix} \frac{t_1^{(i+1)\alpha_1}}{\Gamma[1+(i+1)\alpha_1]} \\ &+ \sum_{i=1}^{\infty}\sum_{j=0}^{\infty} T_{ij} \begin{bmatrix} 0 \\ 1 \end{bmatrix} \frac{t_1^{i\alpha_1} t_2^{(j+1)\alpha_2}}{\Gamma[1+i\alpha_1]\Gamma[1+(j+1)\alpha_2]} \\ &+ \sum_{j=0}^{\infty} T_{0j} \begin{bmatrix} 0 \\ 1 \end{bmatrix} \frac{t_2^{(j+1)\alpha_2}}{\Gamma[1+(j+1)\alpha_2]}, \end{aligned} \tag{36}$$

where transition matrices T_{ij} are given by (9).

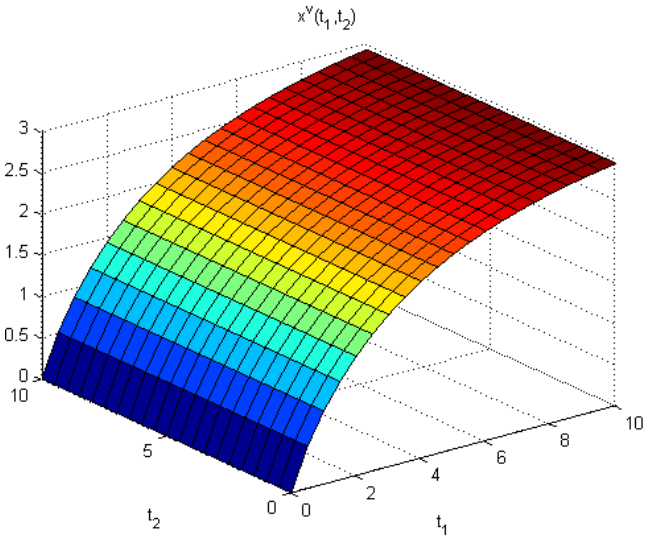

Fig. 2. State variable $x^v(t_1,t_2)$ of the system

Formula (36) describes the step response of the system (4) with the matrices (31). It is easy to show that the coefficients $1/\Gamma(.)$ strongly decrease when i and j increase. Therefore, in numerical analysis we may assume that i and j are bounded by some natural numbers L_1 and L_2.

The plots of the step response (36) where $L_1 = 50$ and $L_2 = 50$ are shown on Fig. 1 and 2.

5. CONCLUDING REMARKS

A new class of fractional 2D continuous-time linear systems described by the Roesser model has been introduced. The general response formula for such systems has been derived (Theorem 1) using the 2D Laplace transform. The classical Cayley-Hamilton theorem has been extended to fractional 2D continuous-time systems (Theorem 2). It has been shown that using the general response formula we are able to obtain the step response of the fractional 2D continuous-time system. The considerations have been illustrated by a numerical example.

The above considerations can be extended for general 2D model (Kurek, 1985). An open problems are the positivity and stability of fractional 2D continuous-time systems.

REFERENCES

1. **Bose N. K.** (1982), *Applied Multidimensional Systems Theory*, Van Nonstrand Reinhold Co., New York.
2. **Bose N. K.** (1985), *Multidimensional Systems Theory Progress, Directions and Open Problems*, D. Reidel Publish. Co., Dodrecht.
3. **Farina L., Rinaldi S.** (2000), *Positive linear systems: theory and applications*, J. Wiley, New York.
4. **Fornasini E., Marchesini G.** (1976), State-space realization theory of two-dimensional filters, *IEEE Trans. Automat. Contr.*, Vol. AC-21, No. 4, 484-491.
5. **Fornasini E., Marchesini G.** (1978), Double indexed dynamical systems, *Math. Sys. Theory*, Vol. 12, No. 1, 59-72.
6. **Gałkowski K.** (2001), *State-space Realizations of Linear 2-D Systems with Extensions to the General nD ($n > 2$) Case*, Springer-Verlag, London.
7. **Kaczorek T.** (1985), *Two-Dimensional Linear Systems*, Springer-Verlag, London.
8. **Kaczorek T.** (2001), *Positive 1D and 2D Systems*, Springer-Verlag, London.
9. **Kaczorek T.** (2008a), Fractional 2D linear systems, *Automation , Mobile Robotics and Intelligent systems*, Vol. 2, No. 2, 5-9.
10. **Kaczorek. T.** (2008b), Positive different orders fractional 2D linear systems, *Acta Mechanica et Automatica*, Vol. 2, No. 2, 51-58.
11. **Kaczorek T.** (2009), Positive 2D fractional linear systems, COMPEL, Vol. 28, No. 2, 341-352.
12. **Kaczorek T.** (2011), *Selected Problems in Fractional Systems Theory*, Springer-Verlag.
13. **Kaczorek T., Rogowski K.** (2010), Positivity and stabilization of fractional 2D linear systems described by the Roesser model, *Int. J. Appl. Math. Comput. Sci.*, Vol. 20, No. 1, 85-92.
14. **Kurek J.** (1985), The general state-space model for two-dimensional linear digital systems, *IEEE Trans. Automat. Contr.*, Vol. AC-30, No. 2, 600-602.
15. **Miller K. S., Ross B.** (1993), *An Introduction to the Fractional Calculus and Fractional Differential Equations*, J. Willey, New York.
16. **Nashimoto K**. (1984), *Fractional Calculus*, Descartes Press, Kariyama.
17. **Oldham K. B., Spanier J.** (1974), *The Fractional Calculus*, Academic Press, New York.
18. **Ostalczyk P.** (2008), *Epitome of the Fractional Calculus: Theory and its Applications in Automatics*, Wydawnictwo Politechniki Łódzkiej, Łódź (in polish).
19. **Podlubny I.** (1999), *Fractional Differential Equations*, Academic Press, San Diego.
20. **Roesser R.** (1975), A discrete state-space model for linear image processing, *IEEE Trans. Automat. Contr., vol. AC-20, No. 1, 1-10.*
21. **Rogowski K.** (2011), Positivity and stability of fractional 2D Lyapunov systems described by the Roesser model, *Bull. Pol. Acad. Sci. Techn.*, (in press).

STABILIZATION OF INERTIAL PLANT WITH TIME DELAY USING FRACTIONAL ORDER CONTROLLER

Andrzej RUSZEWSKI[*], Tomasz NARTOWICZ[**]

[*]Białystok University of Technology, Faculty of Electrical Engineering, Wiejska 45 D, 15-351 Białystok
[**]PhD Student, Białystok University of Technology, Faculty of Electrical Engineering, Wiejska 45 D, 15-351 Białystok

andrusz@pb.edu.pl, tomek.nartowicz@gmail.com

Abstract: The paper presents the problem of designing of a fractional order controller satisfying the conditions of gain and phase margins of the closed-loop system with time-delay inertial plant. The transfer function of the controller follows directly from the use of Bode's ideal transfer function as a reference transfer function for the open loop system. Using the classical D-partition method and the gain-phase margin tester, a simple computational method for determining stability regions in the controller parameters plane is given. An efficient analytical procedure to obtain controller parameter values for specified gain and phase margin requirements is also given. The considerations are illustrated by numerical examples computed in MATLAB/Simulink.

1. INTRODUCTION

In recent years considerable attention has been paid to fractional calculus and its application in many areas in science and engineering (see, e.g. (Das, 2008; Kaczorek, 2011; Kilbas et al., 2006; Ostalczyk, 2008)).

In control system fractional order controllers are used to improve the performance of the feedback control loop. One of the most developed approaches to design robust and fractional order controllers is CRONE control methodology, French acronym of "Commande Robuste d'Ordre Non Entier" (non-integer order robust control) (Oustaloup 1991, 1995, 1999).

The fractional PID controllers, namely $PI^{\lambda}D^{\mu}$ controllers, including an integrator of λ order and a differentiator of μ order were proposed in (Podlubny, 1994, 1999). Several design methods of tuning the $PI^{\lambda}D^{\mu}$ controllers were presented in (Monje et al., 2004; Valerio, 2005; Valerio and Costa, 2006). These methods are based on the mathematical description of the process. The first order-plant with time delay is the most frequently used model for tuning fractional and integral controllers (O'Dwyer, 2003).

The asymptotic stability is the basic requirement of a closed-loop system. Some methods for determining the asymptotic stability regions in the controller parameter space were proposed in (Hamamci, 2007; Ruszewski, 2008). Gain and phase margins are measures of relative stability for a feedback system, therefore the synthesis of control systems is very often based on them. In typical control systems the phase margin is from 30° to 60° whereas the gain margin is from 5dB to 10dB. In paper (Ruszewski, 2010) a simple method of determining the stability region (satisfying the conditions of gain and phase margins) in the parameter space of a fractional-order inertial plant with time delay and a fractional-order PI controller was given.

In this paper the methods for tuning a fractional order controller satisfying the conditions of gain and phase margins are given. The transfer function of the controller follows from the use of Bode's ideal transfer function as a reference transfer function for the open loop system (Barbosa et al., 2004; Boudjehem et al., 2008; Busłowicz and Nartowicz, 2009; Skogestad, 2001; Nartowicz, 2010). Using the D-partition method a simple and efficient computational method for determining stability regions in the controller parameters space is given. Moreover analytical forms directly expressing the controller parameters for specified gain and phase margin requirements are determined.

2. PROBLEM FORMULATION

Consider the feedback control system shown in Fig. 1. The main path of the control system includes the gain-phase margin tester $A\exp(-j\phi)$, where A and ϕ are gain margin and phase margin respectively. This tester does not exist in the real control system, it is only used for tuning the controller.

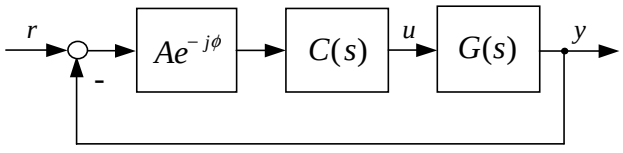

Fig. 1. Feedback control system structure

The process to be controlled is described by an inertial plant with time delay

$$G(s) = \frac{k}{1+sT} e^{-sh}, \tag{1}$$

where k, T, h are positive real numbers.

The transfer function of controller $C(s)$ directly follows from the use of Bode's ideal transfer function

$$K(s) = \left(\frac{\omega_c}{s}\right)^{\beta}, \tag{2}$$

as a reference transfer function of the open loop system, where ω_c is the gain crossover frequency ($|K(j\omega_c)| = 1$) and β is the fractional order. Transfer function (2) describes the fractional derivative plant for $\beta < 0$ and the fractional integral plant for $\beta > 0$. The open loop system with transfer function (2) has a constant phase margin of the value $\phi_m = (1 - 0.5\beta)\pi$. Hence, such a system is insensitive to gain variation in the open loop system. Detailed analysis (including time domain) of the system considered is presented, for instance, in (Barbosa et al., 2004).

In order to obtain the transfer function of the open loop system in the form of transfer function (2), with expected time delay, we simplify the plant transfer function

$$G(s) = \frac{k}{1+sT}e^{-sh} \approx \frac{k}{sT}e^{-sh}. \tag{3}$$

Then the transfer function of the controller must have the form

$$C(s) = k_c s^{1-\alpha}, \tag{4}$$

where α is a positive real number. We will assume $\alpha > 1$.

The characteristic function of the closed-loop system with simplified transfer function (3), transfer function of controller (4) and gain-phase tester is given by

$$w(s) = Akk_c s^{1-\alpha}e^{-j\phi}e^{-sh} + sT. \tag{5}$$

The closed-loop system in Fig. 1 is said to be bounded-input bounded-output stable if and only if all the zeros o characteristic function (5) have negative real parts. It is noted that (5) is the fractional order quasi-polynomial which has an infinite number of zeros. This makes the problem of analysing the stability of the closed-loop system difficult. There is no general algebraic methods available in the literature for the stability test of fractional order quasi-polynomials. The next problem of closed-loop system synthesis is how to choose such a fractional order α of the controller that the closed-loop system will be stable and characterized by specified gain and phase margins.

The aim of the paper is to propose tuning methods based on gain and phase margin specifications. The first one is to give the method for determining the stability region in the parameter plane (α, k_c). The second is to give a simple analytical formula to obtain the controller parameter values for specified gain and phase margin requirements.

3. MAIN RESULT

By using the D-partition method (Gryazina, 2004) the stability region in the parameter plane (α, k_c) can be determined and the parameters can be specified. The plane (α, k_c) is decomposed by the boundaries of the D-partition into finite number regions $D(k)$. Any point in $D(k)$ corresponds to such values of k_c and α that quasi-polynomial (5) has exactly k zeros with positive real parts. The region $D(0)$, if it exists, is the stability region of quasi-polynomial (5). The D-partition boundaries are curves on which each point corresponds to quasi-polynomial (5) having zeros on the imaginary axis. It may be the real zero boundary or the complex zero boundary. It is easy to see that quasi-polynomial (5) has zero $s = 0$ if $k_c = 0$ (the real zero boundary). The complex zero boundary corresponds to the pure imaginary zeros of (5). We obtain this boundary by solving the equation

$$w(j\omega) = Akk_c(j\omega)^{1-\alpha}e^{-j\phi}e^{-j\omega h} + j\omega T = 0, \tag{6}$$

which we obtain by substituting $s = j\omega$ in quasi-polynomial (5) and equating to 0. The term of j^{α} which is required for equation (6) can be expressed by

$$j^{\alpha} = \cos\left(\alpha\frac{\pi}{2}\right) + j\sin\left(\alpha\frac{\pi}{2}\right). \tag{7}$$

Using (7) equation (6) takes the form

$$\begin{aligned} &Akk_c\omega^{1-\alpha}\cos\left(\frac{\pi}{2}(\alpha-1)\right) - \omega T\sin(\omega h+\phi) + \\ &- jAkk_c\omega^{1-\alpha}\sin\left(\frac{\pi}{2}(\alpha-1)\right) + j\omega T\cos(\omega h+\phi) = 0. \end{aligned} \tag{8}$$

Complex equation (8) can be rewritten as a set of real equations in the form

$$Akk_c\omega^{1-\alpha}\cos\left(\frac{\pi}{2}(\alpha-1)\right) - \omega T\sin(\omega h+\phi) = 0, \tag{9}$$

$$-Akk_c\omega^{1-\alpha}\sin\left(\frac{\pi}{2}(\alpha-1)\right) + \omega T\cos(\omega h+\phi) = 0. \tag{10}$$

Finally, by solving equations (9) and (10) we get

$$\alpha = \frac{2(\pi - \omega h - \phi)}{\pi}, \tag{11}$$

$$k_c = \frac{T}{Ak}\omega^{\frac{2(\pi-\omega h-\phi)}{\pi}}. \tag{12}$$

Equations (11) and (12) determine the complex zero boundary as a function of ω. The real zero boundary and the complex zero boundary for $\omega \geq 0$ decompose plane (α, k_c) into regions $D(k)$. The stability region $D(0)$ is chosen by testing an arbitrary point from each region and checking the stability of quasi-polynomial (5) using the methods proposed in (Busłowicz, 2008). In this paper only the stability region $D(0)$ in the parameter plane of quasi-polynomial (5) is presented.

For $A = 1$ and $\phi = 0$ in (11) and (12) the stability boundaries are calculated. To determine the complex zero boundary for a given value of gain margin A of the control system we should set $\phi = 0$ in (11) and (12). On the other hand by setting $A = 1$ in (12), we can obtain the boundary for a given phase margin ϕ.

The complex zero boundary (11) and (12) is determined

for parameter $\omega \geq 0$. The complex zero boundary for a given value of gain margin A begins at the point $\alpha = 2$, $k_c = 0$ which we obtain by substituting $\omega = 0$ in (11) and (12). However, the complex zero boundary for the given phase margin ϕ starts at the point $\alpha = 2(\pi - \phi)/\pi$, $k_c = 0$. If $\omega \to \infty$ plot of the complex zero boundary tends towards k_c -axis.

Example 1. Consider the feedback control system shown in Fig. 1. in which the process to be controlled is described by transfer function

$$G(s) = \frac{0.55}{1+62s} e^{-10s}. \tag{13}$$

On computing by the proposed method complex zero boundaries (11) and (12) we obtain the stability regions in controller parameter plane (α, k_c).

Fig. 2 shows boundaries in controller parameter plane (α, k_c) for gain margin $A = 1$ and a few values of phase margin ϕ. The stability regions lie between line $k_c = 0$ (the real zero boundary) and the curve assigned to specified phase margin ϕ (the complex zero boundary).

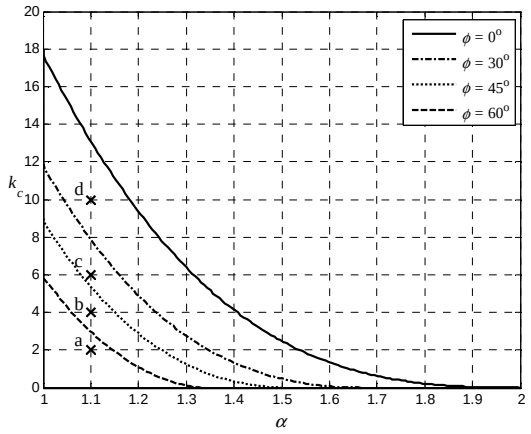

Fig. 2. Stability regions of quasi-polynomial (5) for $A = 1$ and different values of ϕ

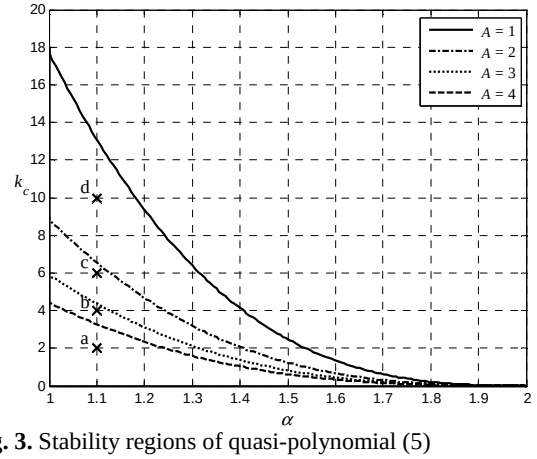

Fig. 3. Stability regions of quasi-polynomial (5) for $\phi = 0$ and different values of A

On choosing any point from the stability region we obtain the controller parameter values provided the phase margin of this system not less than specified for drawing the complex boundary. For example, any point from the region limited by the line $k_c = 0$ and the curve corresponding to $\phi = 60°$ provides a phase margin of this system not less than 60°. From Fig.2 we see that the increasing value of ϕ results in the disappearance of the stability region.

The stability regions of quasi-polynomial (5) for phase margin $\phi = 0$ and a few values of gain margin A are shown in Fig.3. We see that increasing value of A results in the disappearance of the stability region. On choosing any point from the stability region we obtain the controller parameter values provided that the gain margin of this system is not less than specified for drawing the complex boundary. For example a choosing point between $k_c = 0$ and the complex boundary for $A = 4$ we obtain the controller parameters satisfying a gain margin of not less than 4.

The controller parameters and stability margins of the control system for all points marked in Fig. 2 and Fig. 3 are listed in Tab. 1. It is shown that the stability margin values are larger than specified for drawing the complex boundaries of the stability regions. Gain and phase margins of the control system are calculated for transfer function (1).

Tab. 1. Gain and phase margins

Point	Controller parameters	Gain margin		Phase margin
a	$\alpha = 1.1,\ k_c = 2$	7.13	17.06 dB	107.36°
b	$\alpha = 1.1,\ k_c = 4$	3.56	11.64 dB	74.38°
c	$\alpha = 1.1,\ k_c = 6$	2.38	7.52 dB	55.51°
d	$\alpha = 1.1,\ k_c = 10$	1.43	3.08 dB	26.64°

Tab. 1 confirms the results received on the basis of the D-partition method showing that the points from the stability regions satisfy the gain and phase margin requirements.

The step responses of the control system are presented in Fig. 4. It can be seen that the increasing value of ϕ results in smaller oscillations.

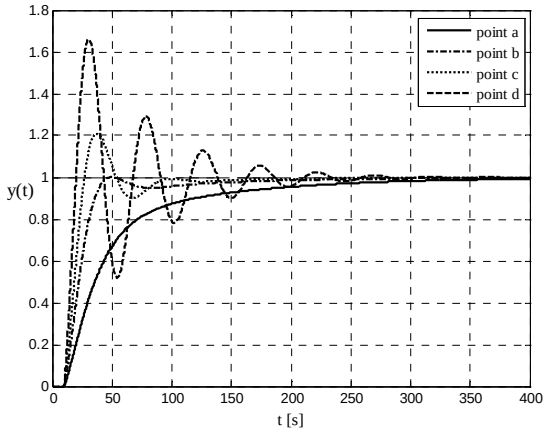

Fig. 4. Step responses of control system

By using the stability regions we can obtain the controller parameter values for specified gain and phase margins requirements simultaneously. For this purpose we draw in one plot the complex zero boundary for specified phase margin ϕ with $A = 1$ and the complex zero boundary for specified gain margin A with $\phi = 0$. Intersection point of the complex zero boundaries determines the controller parameter values.

Example 2. Consider the feedback control system as in Example 1. Calculate the controller parameter values so that the control system has the gain margin $A = 4$ (about 12 dB) and the phase margin $\phi = 55°$.

On computing the complex zero boundaries (11) and (12) for specified gain margin $A = 4$ with $\phi = 0$ and for specified phase margin $\phi = 55°$ with $A = 1$ we obtain the stability regions which are shown in Fig. 5. The intersection point of the complex zero boundaries is marked on Fig. 5 and has coordinates $\alpha = 1.1339$, $k_c = 2.9358$. On calculating the stability margins of control system for simplified transfer function (3) we obtain $A = 4$ and $\phi = 55°$. Whereas stability margins for model plant (1) are $A = 4.4$ and $\phi = 80°$ because of simplification (3). Fig. 6 shows the Bode plot with the gain and phase margins marked for controller parameters $\alpha = 1.1339$, $k_c = 2.9358$.

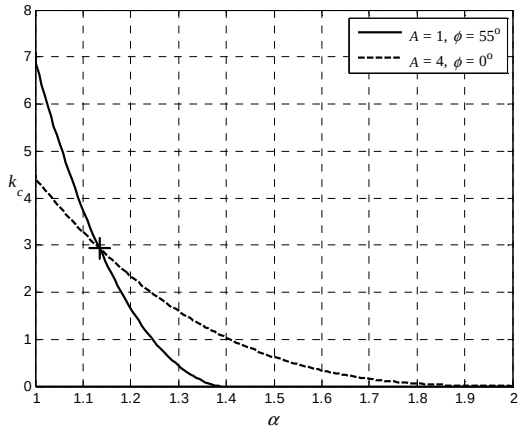

Fig. 5. Stability regions of quasi-polynomial (5) for $A = 1$, $\phi = 55°$ and $A = 4$, $\phi = 0$

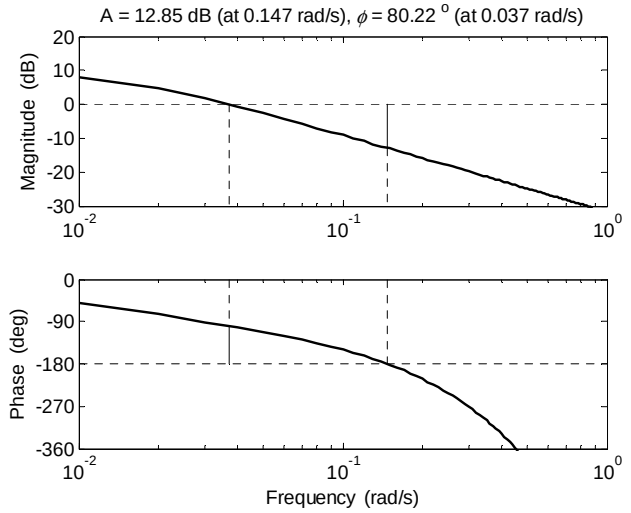

Fig. 6. Bode plot with gain and phase margins

By using expressions of the stability boundaries (11) and (12) we can determine analytical description for direct calculations of the controller parameter values for specified gain and phase margins requirements without drawing the stability region.

To determine the complex zero boundary for a given value of gain margin A of the control system we set $\phi = 0$ in (11) and (12). On solving system of equations (11) and (12) for the unknown quantities of ω and k_c with $\phi = 0$ we obtain

$$\omega = \frac{\pi(2-\alpha)}{2h}, \tag{14}$$

$$k_c = \frac{T}{Ak}\left(\frac{\pi(2-\alpha)}{2h}\right)^{\alpha}. \tag{15}$$

Expression (15) gives the relationship between k_c and α for specified gain margin A.

Similarly to determine the complex zero boundary for a given phase margin ϕ of the control system we set $A = 1$ in (12). On solving system of equations (11) and (12) for the unknown quantities of ω and k_c with $A = 1$ we obtain

$$\omega = \frac{\pi(2-\alpha)-2\phi}{2h}, \tag{16}$$

$$k_c = \frac{T}{k}\left(\frac{\pi(2-\alpha)-2\phi}{2h}\right)^{\alpha}. \tag{17}$$

Expression (17) gives the relationship between k_c and α for specified phase margin ϕ.

Note from Fig.5 that for fixed value of α which guarantees gain and phase margins requirements simultaneously the values of k_c in the two complex boundaries are the same (the intersection point). Therefore the value of α which ensures gain and phase margins requirements can be calculated by solving following nonlinear equation

$$\frac{T}{Ak}\left(\frac{\pi(2-\alpha)}{2h}\right)^{\alpha} = \frac{T}{k}\left(\frac{\pi(2-\alpha)-2\phi}{2h}\right)^{\alpha}. \tag{18}$$

After simplifications equation (18) can be rewritten in the form

$$A = \left(\frac{\pi(2-\alpha)}{\pi(2-\alpha)-2\phi}\right)^{\alpha}. \tag{19}$$

If we get the value of α from (19) we can calculate controller gain k_c from expression (15) or (17).

From the above it can be seen that the procedure for calculating parameters of controller (4) for specified gain and phase margins requirements is as follows:

1. Solve the nonlinear equation (19) and determine α.
2. Calculate controller gain k_c from expression (15) or (17).

Note that in the procedure proposed the calculation of the gain crossover frequency or the phase crossover frequency is not necessary in contrast to methods presented in (Boudjehem et al., 2008; Busłowicz and Nartowicz, 2009; Nartowicz, 2010). The advantage of the procedure proposed is that the controller settings are easily calculated.

Example 3. Consider the feedback control system as in Example 2. Using the procedure presented calculate the controller parameters values so that the control system has gain margin $A = 4$ (about 12 dB) and phase margin $\phi = 55°$.

On solving nonlinear equation (19) we have $\alpha = 1.1339$. From (15) or (17) we calculate controller gain $k_c = 2.9358$. Note that we obtain the same values of the controller parameter as in Example 2.

Gain and phase margins are measures of relative stability for a feedback system. Although the phase margin is used more frequently than both margins. The phase margin is closely related to transient response i.e. overshoot.

From the above it can be seen that the procedure for calculating parameters of controller (4) for specified phase margin requirement is as follows:

1. Calculate the start point of the complex zero boundary $\alpha = 2(\pi - \phi)/\pi$.
2. Choose any positive value smaller than determined α.
3. Calculate controller gain k_c from expression (17).

In the above procedure solving nonlinear equation is not necessary.

4. CONCLUSION

In this paper the stability problem of control systems composed of the fractional-order controller and the inertial plant with time delay is examined. On the basis of the D-partition method analytical forms expressing the boundaries of stability regions in the parameter space for specified gain and phase margin requirements were determined. When the the stability regions are known the tuning of the fractional controller can be carried out. Simple analytical formulas for obtaining the controller parameter values for specified gain and phase margins requirements were also given. In the method proposed the controller settings are easily calculated.

The calculations and simulations were made using the Matlab/Simulink programme.

REFERENCES

1. **Barbosa R. S., Machado J. A., Ferreira I. M.** (2004), Tuning of PID controllers based on Bode's ideal transfer function, *Nonliner Dynamics*, Vol. 38, 305-321.
2. **Boudjehem B., Boudjehem D., Tebbikh H.** (2008), Simple analytical design method for fractional-order controller, *Proc. 3-rd IFAC Workshop on Fractional Differentiation and its Applications*, Ankara, Turkey, (CD-ROM).
3. **Busłowicz M.** (2008), Frequency domain method for stability analysis of linear continuous-time fractional systems. In: **Malinowski K.** and **Rutkowski L.** (Eds.), *Recent Advances in Control and Automation*, Academic Publishing House EXIT, Warsaw, 83-92.
4. **Busłowicz M., Nartowicz T.** (2009), Design of fractional order controller for a class of plants with delay, *Measurement Automation and Robotics*, No. 2, 398-405 (in Polish).
5. **Das. S.** (2008), *Functional Fractional Calculus for System Identification and Controls*, Springer, Berlin.
6. **Gryazina E. N.** (2004), The D-Decomposition Theory, *Automation and Remote Control*, Vol. 65, No. 12, 1872-1884.
7. **Hamamci S. E.** (2007), An Algorithm for Stabilization of Fractional-Order Time Delay Systems Using Fractional-Order PID Controllers, *IEEE Trans. on Automatic Control*, Vol. 52, 1964-1969.
8. **Kaczorek T.** (2011), *Selected Problems of Fractional Systems Theory*, Springer, Berlin, (in print).
9. **Kilbas A. A., Srivastava H. M., Trujillo J. J.** (2006), *Theory and Applications of Fractional Differential Equations*, Elsevier, Amsterdam.
10. **Monje C. A., Calderon A. J., Vinagre B. M., Chen Y., Feliu V.** (2004), On fractional PI controllers: some tuning rules for robustness to plant uncertainties, *Nonlinear Dynamics*, Vol. 38, 369-381.
11. **Ostalczyk P.** (2008), *Epitome of the Fractional Calculus, Theory and its Applications in Automatics*, Publishing Department of Technical University of Łódź, (in Polish).
12. **Oustaloup A.** (1991), *La commande CRONE*, Editions Hermes, Paris.
13. **Oustaloup A.** (1995), *La derivation non entiere – theorie, syntheses at applications*, Editions Hermes, Paris.
14. **Oustaloup A.** (1999), La commande crone: du scalaire au multivariable, Editions Hermes, Paris.
15. **Podlubny I.** (1999), *Fractional Differential Equations*, Academic Press, San Diego.
16. **Podlubny I.** (1999), Fractional-order systems and PID-controllers, *IEEE Trans. on Automatic Control*, Vol. 44, No.1, 208-214.
17. **Skogestad, S.** (2001), Probably the best simple PID tuning rules in the world, *AIChE Annual Meeting*, Reno, Nevada.
18. **Valerio D., da Costa J. S.** (2006), Tuning of fractional PID controllers with Ziegler-Nichols type rules, *Signal Processing*, Vol. 86, 2771-2784.
19. **Valerio D.** (2005), *Fractional Robust Systems Control*. PhD Dissertation, Technical University of Lisbona.
20. **Nartowicz T.** (2010), Design of fractional order controller satisfying gain and phase margin of the closed loop system with time delay inertial plant with integral term, *Measurement Automation and Robotics*, No. 2, 443-452 (in Polish).
21. **O'Dwyer A.** (2003), *PI and PID Controller Tuning Rules*, Imperial College Press/Word Scientific, London, 2003.
22. **Ruszewski A.** (2008), Stability regions of closed loop system with time delay inertial plant of fractional order and fractional order PI controller, *Bull. Pol. Ac.: Sci. Tech.* Vol. 56, No. 4, 329–332.
23. **Ruszewski A.** (2010), Stabilization of inertial processes with time delay using fractional order PI controller, *Measurement Automation and Monitoring*, No. 2, 160-162.

Acknowledgments: The work was supported by the Ministry of Science and High Education of Poland under grant No. N N514 638940.

POSITIVE REALIZATION OF SISO 2D DIFFERENT ORDERS FRACTIONAL DISCRETE-TIME LINEAR SYSTEMS

Łukasz SAJEWSKI*

*Faculty of Electrical Engineering, Białystok University of Technology, ul. Wiejska 45D, 15-351 Białystok

l.sajewski@pb.edu.pl

Abstract: The realization problem for single-input single-output 2D positive fractional systems with different orders is formulated and a method based on the state variable diagram for finding a positive realization of a given proper transfer function is proposed. Sufficient conditions for the existence of a positive realization of this class of 2D linear systems are established. A procedure for computation of a positive realization is proposed and illustrated by a numerical example.

1. INTRODUCTION

In positive systems inputs, state variables and outputs take only non-negative values. Examples of positive systems are industrial processes involving chemical reactors, heat exchangers and distillation columns, storage systems, compartmental systems, water and atmospheric pollution models. A variety of models having positive linear systems behavior can be found in engineering, management science, economics, social sciences, biology and medicine, etc.

Positive linear systems are defined on cones and not on linear spaces. Therefore, the theory of positive systems is more complicated and less advanced. An overview of state of art in positive systems theory is given in the monographs (Farina and Rinaldi, 2000; Kaczorek, 2002). The realization problem for positive discrete-time and continuous-time systems without and with delays was considered in Benvenuti and Farina (2004), Farina and Rinaldi (2000) and Kaczorek (2006a, 2006b, 2004, 2005). A new class of positive 2D hybrid linear system has been introduced in Kaczorek (2007), and the realization problem for this class of systems has been considered in Kaczorek (2008c).

The first definition of the fractional derivative was introduced by Liouville and Riemann at the end of the 19th century (Nishimoto, 1984; Oldham and Spanier, 1974). This idea has been used by engineers for modeling different process (Engheta, 1997; Ferreira and Machado, 2003; Klamka, 2005; Ostalczyk, 2000; Oustaloup, 1993). Mathematical fundamentals of fractional calculus are given in the monographs (Miller and Ross, 1993; Nishimoto, 1984; Oldham and Spanier, 1974; Ortigueira, 1997; Podlubny, 1999). The fractional order controllers have been developed in (Ostalczyk, 2000; Podlubny et al., 1997). A generalization of the Kalman filter for fractional order systems has been proposed in Zaborowsky and Meylaov (2001). A new class of positive fractional 2D hybrid linear system has been introduced in Kaczorek (2008e) and positive fractional 2D linear systems described by the Roesser model in Rogowski and Kaczorek (2010). The realization problem for positive fractional systems was considered in Kaczorek (2008b, 2008d, 2011) and Sajewski (2010).

The main purpose of this paper is to present a method for computation of a positive realization of SISO 2D different orders fractional systems with given proper transfer function using the state variable diagram method. Sufficient conditions for the existence of a positive realization of this class of systems will be established and a procedure for computation of a positive realization will be proposed.

The paper is organized as follows. In section 2 basic definition and theorem concerning positive 2D different orders fractional systems are recalled. Also in this section using the zet transform the transfer matrix (function) of the different orders fractional systems is derived and the positive realization problem is formulated. Main result is given in section 3 where solution to the realization problem for given transfer function of the 2D different orders fractional discrete-time linear systems is given. In the same section the sufficient conditions for the positive realization are derived and the procedure for computation of the positive realization is proposed. Concluding remarks are given in section 4.

The following notation will be used: $\Re$ – the set of real numbers, $\Re^{n\times m}$ – the set of $n \times m$ real matrices, $\Re_+^{n\times m}$ – the set of $n \times m$ matrices with nonnegative entries and $\Re_+^n = \Re_+^{n\times 1}$, I_n – the $n \times n$ identity matrix, $z[f(k)]$ – zet transform of the discrete-time function $f(k)$.

2. PRELIMINARIES AND PROBLEM FORMULATION

Consider a 2D system with different fractional orders described by the equations

$$\Delta^{\alpha} x_1(k+1) = A_{11}x_1(k) + A_{12}x_2(k) + B_1u(k) \tag{2.1a}$$

$$\Delta^{\beta} x_2(k+1) = A_{21}x_1(k) + A_{22}x_2(k) + B_2u(k) \tag{2.1b}$$

$$y(k) = C_1x_1(k) + C_2x_2(k) + Du(k),\ k \in Z_+ \tag{2.1c}$$

where $x_1(k) \in \Re^{n_1}$, $x_2(k) \in \Re^{n_2}$ are state vectors and $u(k) \in \Re^m$ is input vector $y(k) \in \Re^P$ is output vector and $A_{ij} \in \Re^{n_i\times n_j}$, $B_i \in \Re^{n_i\times m}$, $C_i \in \Re^{p\times n_i}$, $i,j = 1,2$; $D \in \Re^{P\times m}$.

The fractional difference of $\alpha \in \Re$ order is defined by

$$\Delta^{\alpha} x(k) = \sum_{j=0}^{k} (-1)^j \binom{\alpha}{j} x(k-j) \tag{2.2a}$$

and

$$\binom{\alpha}{j} = \begin{cases} 1 & \text{for} \quad j = 0 \\ \dfrac{\alpha(\alpha-1)...(\alpha-j+1)}{j!} & \text{for} \quad j = 1,2,... \end{cases} \tag{2.2b}$$

Using (2.2a) we can write the equation (2.1a) and (2.1b) in the following form

$$\begin{aligned} x_1(k+1) &= A_{1\alpha} x_1(k) + A_{12} x_2(k) \\ &\quad - \sum_{j=2}^{k+1} (-1)^j \binom{\alpha}{j} x_1(k-j+1) + B_1 u(k) \\ x_2(k+1) &= A_{21} x_1(k) + A_{2\beta} x_2(k) \\ &\quad - \sum_{j=2}^{k+1} (-1)^j \binom{\beta}{j} x_2(k-j+1) + B_2 u(k) \end{aligned} \tag{2.3}$$

where

$$\begin{aligned} A_{1\alpha} &= A_{11} + \alpha I_{n_1} \\ A_{1\beta} &= A_{22} + \beta I_{n_2} \end{aligned} \tag{2.4}$$

Definition 2.1. The fractional system (2.1) is called positive if and only if $x_1(k) \in \Re^{n_1}$, $x_2(k) \in \Re^{n_2}$ and $y(k) \in \Re_+^p$, $k \in Z_+$ for any initial conditions $x_1(0) = x_{10} \in \Re_+^{n_1}$, $x_2(0) = x_{20} \in \Re_+^{n_2}$, and all input sequences $u(k) \in \Re^m$, $k \in Z_+ = \{0, 1, ...\}$.

Theorem 2.1. (Kaczorek, 2011) The fractional discrete-time linear system (2.1) with $0 < \alpha < 1$, $0 < \beta < 1$ is positive if and only if

$$A = \begin{bmatrix} A_{1\alpha} & A_{12} \\ A_{21} & A_{2\beta} \end{bmatrix} \in \Re_+^{n \times n}, \; B = \begin{bmatrix} B_1 \\ B_2 \end{bmatrix} \in \Re_+^{n \times m},$$

$$[C_1 \quad C_2] \in \Re_+^{p \times n}, \; D \in \Re_+^{p \times m}. \tag{2.5}$$

Proof is given in Kaczorek (2011).

Substituting (2.2a) into (2.1a) and (2.1b) we obtain

$$\begin{aligned} x_1(k+1) + \sum_{j=1}^{k+1} (-1)^j \binom{\alpha}{j} x(k-j+1) &= A_{11} x_1(k) + A_{12} x_2(k) + B_1 u(k) \\ x_2(k+1) + \sum_{j=1}^{k+1} (-1)^j \binom{\beta}{j} x(k-j+1) &= A_{21} x_1(k) + A_{22} x_2(k) + B_2 u(k) \\ y(k) &= C_1 x_1(k) + C_2 x_2(k) + D u(k) \end{aligned} \tag{2.6a}$$

Performing the zet transform with zero initial conditions we have

$$\begin{aligned} z X_1(z) + \sum_{j=1}^{k+1} (-1)^j \binom{\alpha}{j} z^{1-j} X_1(z) &= A_{11} X_1(z) + A_{12} X_2(z) + B_1 U(z) \\ z X_2(z) + \sum_{j=1}^{k+1} (-1)^j \binom{\beta}{j} z^{1-j} X_2(z) &= A_{21} X_1(z) + A_{22} X_2(z) + B_2 U(z) \\ Y(z) &= C_1 X_1(z) + C_2 X_2(z) + D U(z) \end{aligned} \tag{2.7}$$

where $X(z) = Z[x(k)]$, $U(z) = z[u(k)]$, $Y(z) = z[y(k)]$.

The equations (2.7) can be written in the matrix form

$$\begin{aligned} \begin{bmatrix} X_1(z) \\ X_2(z) \end{bmatrix} &= \begin{bmatrix} I_{n_1}(z - c_\alpha) - A_{11} & -A_{12} \\ -A_{21} & I_{n_2}(z - c_\beta) - A_{22} \end{bmatrix}^{-1} \begin{bmatrix} B_1 \\ B_2 \end{bmatrix} U(z) \\ Y(z) &= \begin{bmatrix} C_1 & C_2 \end{bmatrix} \begin{bmatrix} X_1(z) \\ X_2(z) \end{bmatrix} + D U(z) \end{aligned} \tag{2.8}$$

where

$$\begin{aligned} c_\alpha &= c_\alpha(k, z) = \sum_{j=1}^{k+1} (-1)^{j-1} \binom{\alpha}{j} z^{1-j} \\ c_\beta &= c_\beta(k, z) = \sum_{j=1}^{k+1} (-1)^{j-1} \binom{\beta}{j} z^{1-j} \end{aligned} \tag{2.9}$$

The transfer matrix of the system (2.1) is given by

$$T(z) = \begin{bmatrix} C_1 & C_2 \end{bmatrix} \begin{bmatrix} I_{n_1}(z - c_\alpha) - A_{11} & -A_{12} \\ -A_{21} & I_{n_2}(z - c_\beta) - A_{22} \end{bmatrix}^{-1} \begin{bmatrix} B_1 \\ B_2 \end{bmatrix} + D \tag{2.10}$$

In this case the transfer matrix is the function of the operators $w_\alpha = z - c_\alpha$, $w_\beta = z - c_\beta$ and for single-input single-output (shortly SISO) systems it has the following form

$$T(w_\alpha, w_\beta) = \frac{\sum_{i=0}^{n_1} \sum_{j=0}^{n_2} b_{i,j} {w_\alpha}^i {w_\beta}^j}{{w_\alpha}^{n_1} {w_\beta}^{n_2} - \sum_{\substack{i=0 \\ i+j \neq n_1+n_2}}^{n_1} \sum_{j=0}^{n_2} b_{i,j} {w_\alpha}^i {w_\beta}^j} \tag{2.11}$$

for known α, β.

Definition 2.2. The matrices (2.5) are called the positive realization of the transfer matrix $T(z)$ if they satisfy the equality (2.10).

The realization problem can be stated as follows.

Given a proper rational matrix $T(w_{\alpha,} w_\beta) \in \Re^{p \times m}(w_{\alpha,} w_\beta)$ and fractional orders α, β, find its positive realization (2.5), where $\Re^{p \times m}(w_{\alpha,} w_\beta)$ is the set of $p \times m$ rational matrices in w_α and w_β.

3. PROBLEM SOLUTION FOR SISO SYSTEMS

The essence of proposed method for solving of the realization problem for positive linear systems with different fractional orders will be presented on single-input single-output system. It will be shown that state variable diagram method previously used for standard discrete-time systems and 2D hybrid systems (Kaczorek, 2002, 2008c) is also valid for fractional order discrete-time systems.

In standard (nonfractional) discrete-time systems it is well-known that

$$z[x(k+1)] = z \cdot z[x(k)] = zX(z) \tag{3.1a}$$

and

$$z[x(k)] = \frac{1}{z} \cdot z[x(k+1)] \tag{3.1b}$$

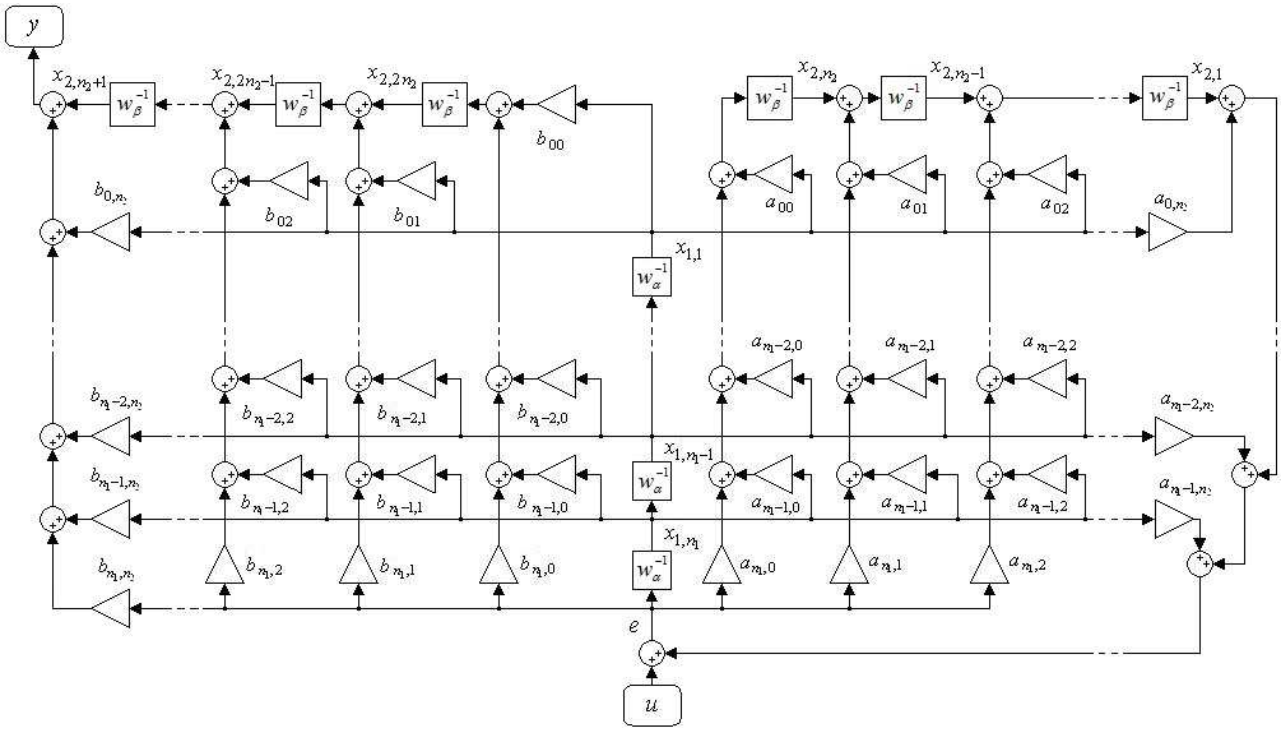

Fig. 3.1. State variable diagram for 2D fractional different orders system

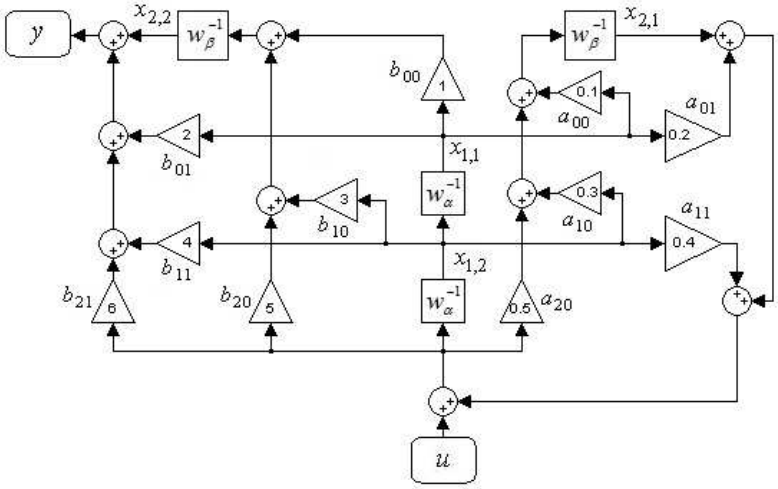

Fig. 3.2. State variable diagram for 2D fractional different orders transfer function (3.14)

Therefore, to draw the state variable diagram for standard discrete-time linear systems (Kaczorek, 2002) we use the of delay element $1/z$.

By similarity, for the fractional discrete-time linear systems we have

$$z[\Delta^{\alpha} x_1(k+1)] = z\left[x_1(k+1) + \sum_{j=1}^{k+1} (-1)^j \binom{\alpha}{j} x_1(k-j+1) \right]$$

$$= \left(z - \sum_{j=1}^{k+1} (-1)^{j-1} \binom{\alpha}{j} z^{1-j} \right) X_1(z) = (z - c_{\alpha}) X_1(z) = w_{\alpha} X_1(z),$$

$$z[\Delta^{\beta} x_2(k+1)] = (z - c_{\beta}) X_2(z) = w_{\beta} X_1(z) \tag{3.2}$$

and to draw the state variable diagram we have to use the fractional of delay elements $\frac{1}{w_{\alpha}} = w_{\alpha}^{-1}$ and $\frac{1}{w_{\beta}} = w_{\beta}^{-1}$.

Consider a 2D different orders fractional discrete-time linear system described by the transfer function (2.11). Multiplying the numerator and denominator of transfer function (2.11) by $w_{\alpha}^{-n_1} w_{\beta}^{-n_2}$ we obtain

$$T(w_{\alpha}, w_{\beta}) = \frac{Y}{U}$$

$$= \frac{b_{n_1,n_2} + b_{n_1,n_2-1} w_{\beta}^{-1} + b_{n_1-1,n_2} w_{\alpha}^{-1} + \ldots + b_{00} w_{\alpha}^{-n_1} w_{\beta}^{-n_2}}{1 - a_{n_1,n_2-1} w_{\beta}^{-1} - a_{n_1-1,n_2} w_{\alpha}^{-1} - \ldots - a_{00} w_{\alpha}^{-n_1} w_{\beta}^{-n_2}} \tag{3.3}$$

Following Kaczorek (2002, 2008c) we define

$$E=\frac{U}{1-a_{n_1,n_2-1}w_\beta^{-1}-a_{n_1-1,n_2}w_\alpha^{-1}-\ldots-a_{00}w_\alpha^{-n_1}w_\beta^{-n_2}} \tag{3.4}$$

and from (3.3) we have

$$E=U+(a_{n_1,n_2-1}w_\beta^{-1}+a_{n_1-1,n_2}w_\alpha^{-1}+\ldots+a_{00}w_\alpha^{-n_1}w_\beta^{-n_2})E$$
$$Y=(b_{n_1,n_2}+b_{n_1,n_2-1}w_\beta^{-1}+b_{n_1-1,n_2}w_\alpha^{-1}+\ldots+b_{00}w_\alpha^{-n_1}w_\beta^{-n_2})E \tag{3.5}$$

Using (3.5) we may draw the state variable diagram shown in Fig. 3.1.

As a state variable we choose the outputs of fractional (order α) of delay elements $(x_{1,1}(k), x_{1,2}(k), \ldots, x_{1,n_1}(k))$ and fractional (order β) of delay elements $(x_{2,1}(k), x_{2,2}(k), \ldots, x_{2,2n_2}(k))$. Using state variable diagram (Fig. 3.1) we can write the following discrete-time different orders fractional equations

$$\begin{aligned}
&\Delta^\alpha x_{1,1}(k+1)=x_{1,2}(k)\\
&\Delta^\alpha x_{1,2}(k+1)=x_{1,3}(k)\\
&\vdots\\
&\Delta^\alpha x_{1,n_1-1}(k+1)=x_{1,n_1}(k)\\
&\Delta^\alpha x_{1,n_1}(k+1)=e(k)\\
&\Delta^\beta x_{2,1}(k+1)=a_{0,n_2-1}x_{1,1}(k)+a_{1,n_2-1}x_{1,2}(k)\\
&\qquad+\ldots+a_{n-1,n_2-1}x_{1,n_1}(k)+x_{2,2}(k)+a_{n_1,n_2-1}e(k)\\
&\Delta^\beta x_{2,2}(k+1)=a_{0,n_2-2}x_{1,1}(k)+a_{1,n_2-2}x_{1,2}(k)\\
&\qquad+\ldots+a_{n-1,n_2-2}x_{1,n_1}(k)+x_{2,3}(k)+a_{n_1,n_2-2}e(k)\\
&\vdots\\
&\Delta^\beta x_{2,n_2-1}(k+1)=a_{0,1}x_{1,1}(k)+a_{1,1}x_{1,2}(k)\\
&\qquad+\ldots+a_{n_1-1,1}x_{1,n_1}(k)+x_{2,n_2}(k)+a_{n_1,1}e(k)\\
&\Delta^\beta x_{2,n_2}(k+1)=a_{00}x_{1,1}(k)+a_{10}x_{1,2}(k)\\
&\qquad+\ldots+a_{n_1-1,0}x_{1,n_1}(k)+a_{n_1,0}e(k)\\
&\Delta^\beta x_{2,n_2+1}(k+1)=b_{0,n_2-1}x_{1,1}(k)+b_{1,n_2-1}x_{1,2}(k)\\
&\qquad+\ldots+b_{n_1-1,n_2-1}x_{1,n_1}(k)+x_{2,n_2+2}(k)+b_{n_1,n_2-1}e(k)\\
&\Delta^\beta x_{2,n_2+2}(k+1)=b_{0,n_2-2}x_{1,1}(k)+b_{1,n_2-2}x_{1,2}(k)\\
&\qquad+\ldots+b_{n_1-1,n_2-2}x_{1,n_1}(k)+x_{2,n_2+3}(k)+b_{n_1,n_2-2}e(k)\\
&\vdots\\
&\Delta^\beta x_{2,2n_2-1}(k+1)=b_{0,1}x_{1,1}(k)+b_{1,1}x_{1,2}(k)\\
&\qquad+\ldots+b_{n_1-1,1}x_{1,n_1}(k)+x_{2,2n_2}(k)+b_{n_1,1}e(k)\\
&\Delta^\beta x_{2,2n_2}(k+1)=b_{00}x_{1,1}(k)+b_{10}x_{1,2}(k)\\
&\qquad+\ldots+b_{n_1-1,0}x_{1,n_1}(k)+b_{n_1,0}e(k)\\
&y(k)=b_{0,n_2}x_{1,1}(k)+b_{1,n_2}x_{1,2}(k)+\ldots+b_{n_1-1,n_2}x_{1,n_1}(k)\\
&\qquad+x_{2,n_2+1}(k)+b_{n_1,n_2}e(k)
\end{aligned} \tag{3.6}$$

where

$$\begin{aligned}
e(k)&=a_{0,n_2}x_{1,1}(k)+a_{1,n_2}x_{1,2}(k)\\
&\quad+\ldots+a_{n_1-1,n_2}x_{1,n_1}(k)+x_{2,1}(k)+u(k)
\end{aligned} \tag{3.7}$$

Defining

$$x_1(k)=\begin{bmatrix}x_{1,1}(k)\\ \vdots\\ x_{1,n_1}(k)\end{bmatrix},\quad x_2(k)=\begin{bmatrix}x_{2,1}(k)\\ \vdots\\ x_{2,2n_2}(k)\end{bmatrix} \tag{3.8}$$

and substituting (3.7) into (3.6) we can write the equations (3.6) in the form

$$\begin{aligned}
&\begin{bmatrix}\Delta^\alpha x_1(k+1)\\ \Delta^\beta x_2(k+1)\end{bmatrix}=\begin{bmatrix}A_{11}&A_{12}\\ A_{21}&A_{22}\end{bmatrix}\begin{bmatrix}x_1(k)\\ x_2(k)\end{bmatrix}+\begin{bmatrix}B_1\\ B_2\end{bmatrix}u(k)\\
&y(k)=\begin{bmatrix}C_1 & C_2\end{bmatrix}\begin{bmatrix}x_1(k)\\ x_2(k)\end{bmatrix}+Du(k)
\end{aligned} \tag{3.9}$$

where

$$A_{11}=\begin{bmatrix}0&1&0&\ldots&0\\ 0&0&1&\ldots&0\\ \vdots&\vdots&\vdots&\ddots&\vdots\\ 0&0&0&\ldots&1\\ a_{0,n_2}&a_{1,n_2}&a_{2,n_2}&\ldots&a_{n_1-1,n_2}\end{bmatrix}\in R^{n_1\times n_1},$$

$$A_{12}=\begin{bmatrix}0&0&\ldots&0&0\\ 0&0&\ldots&0&0\\ \vdots&\vdots&\vdots&\vdots&\vdots\\ 0&0&\ldots&0&0\\ 1&0&\ldots&0&0\end{bmatrix}\in R^{n_1\times 2n_2},$$

$$A_{21}=\begin{bmatrix}\bar a_{0,n_2-1}&\bar a_{1,n_2-1}&\bar a_{2,n_2-1}&\ldots&\bar a_{n_1-1,n_2-1}\\ \bar a_{0,n_2-2}&\bar a_{1,n_2-2}&\bar a_{2,n_2-2}&\ldots&\bar a_{n_1-1,n_2-2}\\ \vdots&\vdots&\vdots&\vdots&\vdots\\ \bar a_{00}&\bar a_{10}&\bar a_{20}&\ldots&\bar a_{n-1,0}\\ \bar b_{0,n_2-1}&\bar b_{1,n_2-1}&\bar b_{2,n_2-1}&\ldots&\bar b_{n_1-1,n_2-1}\\ \bar b_{0,n_2-2}&\bar b_{1,n_2-2}&\bar b_{2,n_2-2}&\ldots&\bar b_{n_1-1,n_2-2}\\ \vdots&\vdots&\vdots&\vdots&\vdots\\ \bar b_{00}&\bar b_{10}&\bar b_{20}&\ldots&\bar b_{n_1-1,0}\end{bmatrix}\in R^{2n_2\times n_1},$$

$$A_{22}=\begin{bmatrix}
a_{n_1,n_2-1}&1&0&0&\ldots&0&0&0&0&0&0&0&\ldots&0&0&0\\
a_{n_1,n_2-2}&0&1&0&\ldots&0&0&0&0&0&0&0&\ldots&0&0&0\\
\vdots&\vdots&\vdots&\vdots&\vdots&\vdots&\vdots&\vdots&\vdots&\vdots&\vdots&\vdots&\vdots&\vdots&\vdots&\vdots\\
a_{n_1,2}&0&0&0&\ldots&0&1&0&0&0&0&0&\ldots&0&0&0\\
a_{n_1,1}&0&0&0&\ldots&0&0&1&0&0&0&0&\ldots&0&0&0\\
a_{n_1,0}&0&0&0&\ldots&0&0&0&0&0&0&0&\ldots&0&0&0\\
b_{n_1,n_2-1}&0&0&0&\ldots&0&0&0&0&1&0&0&\ldots&0&0&0\\
b_{n_1,n_2-2}&0&0&0&\ldots&0&0&0&0&0&1&0&\ldots&0&0&0\\
\vdots&\vdots&\vdots&\vdots&\vdots&\vdots&\vdots&\vdots&\vdots&\vdots&\vdots&\vdots&\vdots&\vdots&\vdots&\vdots\\
b_{n_1,2}&0&0&0&\ldots&0&0&0&0&0&0&0&\ldots&0&1&0\\
b_{n_1,1}&0&0&0&\ldots&0&0&0&0&0&0&0&\ldots&0&0&1\\
b_{n_1,0}&0&0&0&\ldots&0&0&0&0&0&0&0&\ldots&0&0&0
\end{bmatrix}$$
$$\in R^{2n_2\times 2n_2},$$

$$B_1=\begin{bmatrix}0\\0\\\vdots\\0\\1\end{bmatrix}\in R^{n_1\times 1},\quad B_2=\begin{bmatrix}a_{n_1,n_2-1}\\a_{n_1,n_2-2}\\\vdots\\a_{n_1,0}\\b_{n_1,n_2-1}\\b_{n,n_2-2}\\\vdots\\b_{n_1,0}\end{bmatrix}\in R^{2n_2\times 1},$$

$$C_1=\begin{bmatrix}\bar{b}_{0,n_2} & \bar{b}_{1,n_2} & \dots & \bar{b}_{n_1-1,n_2}\end{bmatrix}\in R^{1\times n},\qquad (3.10)$$

$$C_2=\begin{bmatrix}C_{21} & C_{22}\end{bmatrix}\in R^{1\times 2n_2},\quad D=\begin{bmatrix}b_{n_1,n_2}\end{bmatrix}\in R^{1\times 1}$$

and

$$C_{21}=\begin{bmatrix}b_{n_1,n_2} & 0 & \dots & 0\end{bmatrix}\in R^{1\times n_2},\quad C_{22}=\begin{bmatrix}1 & 0 & \dots & 0\end{bmatrix}\in R^{1\times n_2}\qquad (3.11)$$

where

$$\bar{a}_{i,j}=a_{i,j}+a_{i,n_2}a_{n_1,j},\ \bar{b}_{i,j}=b_{i,j}+a_{i,n_2}b_{n_1,j}\ \text{for}$$

$$i=0,1,\dots,n_1-1;\ j=0,1,\dots,n_2-1.\qquad (3.12)$$

Taking under consideration that $A_{1\alpha}=A_{11}+\alpha I_{n_1}$, $A_{1\beta}=A_{22}+\beta I_{n_2}$ the following theorem has been proved.

Theorem 3.1. There exists a positive realization (2.5) of the 2D different orders fractional system (2.1) with $0<\alpha<1$, $0<\beta<1$ if all coefficients of the numerator and denominator of the transfer function $T(w_\alpha, w_\beta)$ are nonnegative.

If the assumptions of Theorem 3.1 are satisfied then a positive realization (2.5) of (2.11) can be found by the use of the following procedure.

Procedure 3.1.

Step 1. Write the transfer function $T(w_\alpha, w_\beta)$ in the form (3.3) and the equations (3.5).

Step 2. Using (3.5) draw the state variable diagram shown in Fig. 3.1.

Step 3. Choose the state variables and write equations (3.4).

Step 4. Using (3.10) to (3.12) find the realization (3.10).

Step 5. Knowing fractional orders α, β and using (2.4) to matrices (3.10) compute the desired positive realization of the transfer function (2.11).

Example 3.1. Find a positive realization (2.5) of the proper transfer function where $\alpha=\beta=0{,}5$.

$$T(w_\alpha,w_\alpha)=\frac{6w_\alpha{}^2w_\beta+5w_\alpha{}^2+4w_\alpha w_\beta+3w_\alpha+2w_\beta+1}{w_\alpha{}^2w_\beta-0.5w_\alpha{}^2-0.4w_\alpha w_\beta-0.3w_\alpha-0.2w_\beta-0.1}\qquad (3.13)$$

In this case $n_1=2$ and $n_2=1$.

Using Procedure 3.1 we obtain the following.

Step 1. Multiplying the nominator and denominator of Transfer function (3.13) by $w_\alpha^{-2}w_\beta^{-1}$ we obtain

$$T(s,z)=\frac{Y}{U}$$
$$=\frac{6+5w_\beta^{-1}+4w_\alpha^{-1}+3w_\alpha^{-1}w_\beta^{-1}+2w_\alpha^{-2}+w_\alpha^{-2}w_\beta^{-1}}{1-0.5w_\beta^{-1}-0.4w_\alpha^{-1}-0.3w_\alpha^{-1}w_\beta^{-1}-0.2w_\alpha^{-2}-0.1s^{-2}w_\beta^{-1}}\qquad (3.14)$$

and

$$E=U+(0.5w_\beta^{-1}+0.4w_\alpha^{-1}+0.3w_\alpha^{-1}w_\beta^{-1}+0.2w_\alpha^{-2}+0.1s^{-2}w_\beta^{-1})E$$
$$Y=(6+5w_\beta^{-1}+4w_\alpha^{-1}+3w_\alpha^{-1}w_\beta^{-1}+2w_\alpha^{-2}+w_\alpha^{-2}w_\beta^{-1})E\qquad (3.15)$$

Step 2. State variable diagram has the form shown in Fig. 3.2

Step 3. Using state variable diagram we can write the following different orders fractional equations

$$\Delta^\alpha x_{1,1}(k+1)=x_{1,2}(k)$$
$$\Delta^\alpha x_{1,2}(k+1)=0.2x_{1,1}(k)+0.4x_{1,2}(k)+x_{2,1}(k)+u(k)$$
$$\Delta^\beta x_{2,1}(k+1)=0.2x_{1,1}(k)+0.5x_{1,2}(k)+0.5x_{2,1}(k)+0.5u(k)$$
$$\Delta^\beta x_{2,2}(k+1)=2x_{1,1}(k)+5x_{1,2}(k)+5x_{2,1}(k)+5u(k)$$
$$y(k)=3.2x_{1,1}(k)+6.4x_{1,2}(k)+6x_{2,1}(k)+x_{2,2}(k)+6u(k)\qquad (3.16)$$

Step 4. Defining state vectors

$$x_1(k)=\begin{bmatrix}x_{1,1}(k)\\x_{1,2}(k)\end{bmatrix},\quad x_2(k)=\begin{bmatrix}x_{2,1}(k)\\x_{2,2}(k)\end{bmatrix}\qquad (3.17)$$

we can write the equations (3.16) in the form

$$\begin{bmatrix}\Delta^\alpha x_1(k+1)\\\Delta^\beta x_2(k+1)\end{bmatrix}=\begin{bmatrix}0 & 1 & 0 & 0\\0.2 & 0.4 & 1 & 0\\0.2 & 0.5 & 0.5 & 0\\2 & 5 & 5 & 0\end{bmatrix}\begin{bmatrix}x_{1,1}(k)\\x_{1,2}(k)\\x_{2,1}(k)\\x_{2,2}(k)\end{bmatrix}+\begin{bmatrix}0\\1\\0.5\\5\end{bmatrix}u(k)$$
$$=\begin{bmatrix}A_{11} & A_{12}\\A_{21} & A_{22}\end{bmatrix}\begin{bmatrix}x_1(k)\\x_2(k)\end{bmatrix}+\begin{bmatrix}B_1\\B_2\end{bmatrix}u(k)$$
$$y(k)=\begin{bmatrix}3.2 & 6.4 & 6 & 1\end{bmatrix}\begin{bmatrix}x_{1,1}(k)\\x_{1,2}(k)\\x_{2,1}(k)\\x_{2,2}(k)\end{bmatrix}+[6]u(k)\qquad (3.18)$$
$$=\begin{bmatrix}C_1 & C_2\end{bmatrix}\begin{bmatrix}x_1(k)\\x_2(k)\end{bmatrix}+Du(k)$$

and

$$A_{11}=\begin{bmatrix}0 & 1\\0.2 & 0.4\end{bmatrix},\quad A_{12}=\begin{bmatrix}0 & 0\\1 & 0\end{bmatrix},$$
$$A_{21}=\begin{bmatrix}0.2 & 0.5\\2 & 5\end{bmatrix},\quad A_{22}=\begin{bmatrix}0.5 & 0\\5 & 0\end{bmatrix},\qquad (3.19)$$
$$B_1=\begin{bmatrix}0\\1\end{bmatrix},\quad B_2=\begin{bmatrix}0.5\\5\end{bmatrix},\quad C_1=\begin{bmatrix}3.2 & 6.4\end{bmatrix}$$
$$C_2=\begin{bmatrix}6 & 1\end{bmatrix},\quad D=[6].$$

Step 5. Knowing that $\alpha = \beta = 0.5$ and using (2.4) we have

$$A_{1\alpha} = A_{11} + \alpha I_{n_1} = \begin{bmatrix} 0 & 1 \\ 0.2 & 0.4 \end{bmatrix} + 0.5 \begin{bmatrix} 1 & 0 \\ 0 & 1 \end{bmatrix} = \begin{bmatrix} 0.5 & 1 \\ 0.2 & 0.9 \end{bmatrix},$$
$$A_{1\beta} = A_{22} + \beta I_{n_2} = \begin{bmatrix} 0.5 & 0 \\ 5 & 0 \end{bmatrix} + 0.5 \begin{bmatrix} 1 & 0 \\ 0 & 1 \end{bmatrix} = \begin{bmatrix} 1 & 0 \\ 0.5 & 0.5 \end{bmatrix}. \quad (3.20)$$

The conditions of Theorem 2.1 are satisfied and obtained realization (3.19) with (3.20) is positive.

4. CONCLUDING REMARKS

A method for computation of a positive realization of a given proper transfer matrix of 2D different orders fractional discrete-time linear systems has been proposed. Sufficient conditions for the existence of a positive realization of this class of systems have been established. A procedure for computation of a positive realization has been proposed. The effectiveness of the procedure has been illustrated by a numerical example. In general case the proposed procedure does not provide a minimal realization of a given transfer matrix. An open problem is formulation of the necessary and sufficient conditions for the existence of positive minimal realizations for 2D fractional systems in the general case as well as connection between minimal realization and controllability (observability) of this class of systems.

REFERENCES

1. **Benvenuti L. Farina L.** (2004), A tutorial on the positive realization problem, *IEEE Trans. Autom. Control*, vol. 49, no. 5, 651-664.
2. **Engheta N.** (1997), On the role of fractional calculus in electromagnetic theory, *IEEE Trans. Atenn. Prop.*, vol. 39, No. 4, 35-46.
3. **Farina L., Rinaldi S.** (2000), *Positive Linear Systems*, Theory and Applications, J. Wiley, New York.
4. **Ferreira N.M.F, Machado J.A.T.** (2003), Fractional-order hybrid control of robotic manipulators, *Proc. 11th Int. Conf. Advanced Robotics, ICAR*, Coimbra, Portugal, 393-398.
5. **Gałkowski K., Kummert A.** (2005), Fractional polynomials and nD systems, *Proc IEEE Int. Symp. Circuits and Systems, ISCAS*, Kobe, Japan, CD-ROM.
6. **Kaczorek T.** (2002), *Positive 1D and 2D Systems*, Springer-Verlag, London.
7. **Kaczorek T.** (2004), Realization problem for positive discrete-time systems with delay, *System Science*, vol. 30, no. 4, 117-130.
8. **Kaczorek T.** (2005), Positive minimal realizations for singular discrete-time systems with delays in state and delays in control, *Bull. Pol. Acad. Sci. Techn.*, vol 53, no. 3, 293-298.
9. **Kaczorek T.** (2006a), A realization problem for positive continues-time linear systems with reduced numbers of delay, *Int. J. Appl. Math. Comp. Sci.*, Vol. 16, No. 3, pp. 325-331.
10. **Kaczorek T.** (2006b), Computation of realizations of discrete-time cone systems, *Bull. Pol. Acad. Sci. Techn.*, vol. 54, no. 3, 2006, 347-350.
11. **Kaczorek T.** (2006c), Realization problem for positive multivariable discrete-time linear systems with delays in the state vector and inputs, *Int. J. Appl. Math. Comp. Sci.*, vol. 16, no. 2, 101-106.
12. **Kaczorek T.** (2007), Positive 2D hybrid linear systems, *Bull. Pol. Acad. Sci. Techn.*, vol 55, no. 4, 351-358.
13. **Kaczorek T.** (2008a), Fractional positive continuous-time linear systems and their reachability, *Int. J. Appl. Math. Comput. Sci.*, vol. 18, no. 2, 223-228.
14. **Kaczorek T.** (2008b), Realization problem for fractional continuous-time systems, *Archives of Control Sciences*, vol. 18, no. 1, 43-58.
15. **Kaczorek T.** (2008c), Realization problem for positive 2D hybrid systems, *COMPEL*, vol. 27, no. 3, 613-623.
16. **Kaczorek T.** (2008d), Realization problem for positive fractional discrete-time linear systems, *Pennacchio S. (Ed.): Emerging Technologies, Robotics and Control Systems, Int. Society for Advanced Research*, 226-236.
17. **Kaczorek T.** (2008e), Positive fractional 2D hybrid linear systems, *Bull. Pol. Acad. Sci. Techn.*, vol 56, no. 3, 273-277.
18. **Kaczorek T.** (2009a), Fractional positive linear systems, *Kybernetes: The International Journal of Systems & Cybernetics*, vol. 38, no. 7/8, 1059–1078.
19. **Kaczorek T.** (2009b), *Wybrane zagadnienia teorii układów niecałkowitego rzędu*. Oficyna Wydawnicza Politechniki Białostockiej, Rozprawy Naukowe Nr 174, Białystok.
20. **Kaczorek T.** (2011), Selected Problems in Fractional Systems Theory, Springer-Verlag.
21. **Klamka J.** (2002), Positive controllability of positive systems, *Proc. of American Control Conference*, ACC-2002, Anchorage, (CD-ROM).
22. **Klamka J.** (2005), Approximate constrained controllability of mechanical systems, *Journal of Theoretical and Applied Mechanics*, vol. 43, no. 3, 539-554.
23. **Miller K.S., Ross B.** (1993), *An Introduction to the Fractional Calculus and Fractional Differenctial Equations*. Willey, New York.
24. **Nishimoto K.** (1984), *Fractional Calculus*, Decartess Press, Koriama.
25. **Oldham K. B., Spanier J.** (1974), *The Fractional Calculus*. Academmic Press, New York:.
26. **Ortigueira M. D.** (1997), Fractional discrete-time linear systems, *Proc. of the IEE-ICASSP*, Munich, Germany, IEEE, New York, vol. 3, 2241-2244.
27. **Ostalczyk P.** (2000), The non-integer difference of the discrete-time function and its application to the control system synthesis, *Int. J. Syst, Sci.*, vol. 31, no. 12, 1551-1561.
28. **Oustaloup A.** (1993), *Commande CRONE*, Hermés, Paris.
29. **Podlubny I.** (1999), *Fractional Differential Equations*, Academic Press, San Diego.
30. **Podlubny I., Dorcak L., Kostial I.** (1997), On fractional derivatives, fractional order systems and $PI^{\lambda}D^{\mu}$-controllers, *Proc. 36th IEEE Conf. Decision and Control*, San Diego, CA, 4985-4990.
31. **Rogowski K., Kaczorek T.** (2010), Positivity and stabilization of fractional 2D linear systems described by the Roesser model, *International Journal of Applied Mathematics and Computer Science*, vol. 20, no. 1, 85-92.
32. **Sajewski Ł.** (2010), Realizacje dodatnie dyskretnych liniowych układów niecałkowitego rzędu w oparciu o odpowiedź impulsową, *Measurement Automation and Monitoring*, vol. 56, no. 5, 404-408.
33. **Zaborowsky V. Meylaov R.** (2001), Informational network traffic model based on fractional calculus, *Proc. Int. Conf. Info-tech and Info-net, ICII*, Beijing, China, vol. 1, 58-63.

Acknowledgments: This work was supported by Ministry of Science and Higher Education in Poland under work No. N N514 6389 40.

DISCRETE FRACTIONAL ORDER ARTIFICIAL NEURAL NETWORK

Dominik SIEROCIUK[*], Grzegorz SARWAS[*], Andrzej DZIELIŃSKI[*]

[*]Institute of Control and Industrial Electronics, Warsaw University of Technology, Koszykowa 75, 00-662 Warsaw, Poland

dsieroci@isep.pw.edu.pl, sarwasg@isep.pw.edu.pl, adziel@isep.pw.edu.pl

Abstract: In this paper the discrete time fractional order artificial neural network is presented. This structure is proposed for simulating the dynamics of non-linear fractional order systems. In the second part of this paper several numerical examples are shown. The final part of the paper presents the discussion on the use of fractional or integer discrete time neural network for modelling and simulating fractional order non-linear systems. The simulation results show the advantages of the proposed solution over the classical (integer) neural network approach to modelling of non-linear fractional order systems.

1. INTRODUCTION

Extending a highly desirable genericity of linear dynamic systems models to non-linear systems has for quite some time occupied control theorist. The main reason of the problems with obtaining generic models for non-linear systems is the complex behaviour associated with nonlinearity and its intrinsic locality. Thus the search for a universal non-linear model is highly non-trivial, as is the underlying problem of classification of non-linear systems. An important feature of a candidate for such a model is that it be parameterised to make finite-dimensional identification techniques applicable. Moreover, the model should be tractable from the control point of view as it is only an auxiliary step in the overall closed-loop system design. In this context we attempt to analyse and extend the application of neural networks for control. The neural networks can be treated as candidates for a generic, parametric, nonlinear model of a broad class of non-linear plants (see e.g. Hunt et al. (1995); Żbikowski and Hunt (1996); Kalkkuhl et al. (1997); Nørgaard et al. (2000)). Neural networks have modelling capabilities to a desired accuracy, however it is not entirely clear how they represent the plant's system properties. A remarkable progress in the investigations on the representational capabilities of neural networks in recent years not only validate them as the models, but also give interesting and practical suggestions for further research. Boroomand and Menhaj (2009); and Benoit-Marand et al. (2006) present continuous time description of neural networks for modelling nonlinear fractional order systems. In this paper the discrete approach is considered.

In many cases the use of feedforward neural networks for non-linear control is based on the input-output discrete-time description of the systems

$$y_{k+n} = f(y_k, \dots, y_{k-n+1}; u_k, \dots, u_{k-m+1}). \quad (1)$$

However, this model has rather limited capabilities for modelling the fractional order systems. Thus, in this paper we suggest the use of the fractional order calculus to built a model of a non-linear system in the form

$$\Delta^{n\alpha} y_{k+n} = f(\Delta^{(n-1)\alpha} y_{k+n-1}, \dots, \Delta^{\alpha} y_{k+1}, y_k, u_k). \quad (2)$$

The model proposed may turn out to be of lower order and may better reflect the dynamic properties of the fractional order system modelled.

2. DISCRETE FRACTIONAL ORDER NON-LINEAR SYSTEM

To present fractional order discrete time neural network we have to introduce discrete fractional order non-linear system. In this paper the following definition of the fractional order difference is used (see e.g. Oldham and Spanier (1974), Podlubny (1999)):

Definition 1. Fractional order difference is given as follows:

$$\Delta^{\alpha} x_k = \sum_{j=0}^{k} (-1)^j \binom{\alpha}{j} x_{k-j} \quad (3)$$

where, $\alpha \in \boldsymbol{R}$ is a fractional order and $k \in \boldsymbol{N}$ is a number of sample for which the difference is obtained.

In our case the artificial neural network is used to model the fractional order non-linear systems. Using fractional order difference the following non-linear discrete fractional order system in the state-space description is defined:

Definition 2. The non-linear discrete fractional order system in a state-space representation is given by the following set of equations:

$$\Delta^{\alpha} x_{k+1} = f(x_k, u_k) \quad (4)$$

$$x_{k+1} = \Delta^{\alpha} x_{k+1} - \sum_{j=1}^{k+1} (-1)^j \binom{\alpha}{j} x_{k+1-j} \quad (5)$$

$$y_k = h(x_k) \quad (6)$$

The system which we take into consideration is given as the following relation:

$$\Delta^{n\alpha} y_{k+n} = g(\Delta^{(n-1)\alpha} y_{k+n-1}, \dots, \Delta^{\alpha} y_{k+1}, y_k, u_k) \quad (7)$$

which can be rewritten as:

$$\begin{aligned} \Delta^{\alpha} y_{1,k+1} &= x_{2,k} \\ \Delta^{\alpha} y_{2,k+1} &= x_{3,k} \\ &\vdots \\ \Delta^{\alpha} x_{n,k+1} &= g(y_k, x_{2,k}, \dots, x_{n,k}, u_k) \end{aligned} \quad (8)$$

This system can be modelled using the artificial neural network presented in the next section.

3. DISCRETE TIME FRACTIONAL ORDER NEURAL NETWORKS

Neural networks have good properties to model the dynamics of the non-linear systems. In fact they are treated as a candidate for a generic, parametric, non-linear model of a broad class of non-linear systems, because they have modelling capabilities to a desired accuracy. Irrespective of system order so far the system scientists have proposed the integer order neural network for modelling integer or non-integer order system. In case of using standard (integer order) neural network for fractional systems modelling the network structure is complicated and the accuracy can be insufficient. Better solution can be achieved using fractional order neural network of the form.

This structure is a combination of a standard neural network and a linear discrete fractional order state-space system (DFOSS) defined below.

Definition 3. Linear discrete fractional order system in the state-space representation is given as follows (see e.g. Sierociuk and Dzieliński (2006)):

$$\Delta^{\alpha} x_{k+1} = Ax_k + Bu_k \tag{9}$$

$$x_{k+1} = \Delta^{\alpha} x_{k+1} - \sum_{j=1}^{k+1} (-1)^j \binom{\alpha}{j} x_{k-j+1} \tag{10}$$

$$y_k = Cx_k + Du_k \tag{11}$$

where, $\alpha \in \boldsymbol{R}$ is a system order.

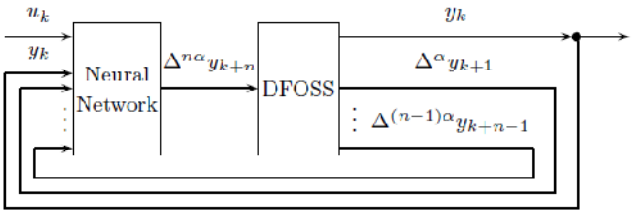

Fig. 1. Discrete time fractional neural network

Fig. 1 presents the architecture useful to simulate the fractional order neural network. It can be noticed, that the neural network is a traditional structure which choice is dependent on the modelled system. The neural network input signals are the system input and output data for the k sample (u_k, y_k) and the vector differences between previous outputs from $\Delta^{(n-1)\alpha} y_{k+n-1}$ to $\Delta^{\alpha} y_{k+1}$. In the output of the neural network we obtain the prediction of the next step difference $\Delta^{n\alpha} y_{k+n}$. Using this value DFOSS calculates the value of the system output and a new vector of differences. DFOSS blocks' sizes depend on the modelled system structure and the system matrices we can be obtained in the following way:

$$A = \begin{bmatrix} 0 & 1 & 0 & 0 & \cdots & 0 \\ 0 & 0 & 1 & 0 & \cdots & 0 \\ \vdots & \vdots & \vdots & \vdots & \ddots & \vdots \\ 0 & 0 & 0 & 0 & \cdots & 1 \\ 0 & 0 & 0 & 0 & \cdots & 0 \end{bmatrix}, \mathrm{B} = \begin{bmatrix} 0 \\ \vdots \\ 0 \\ 1 \end{bmatrix}, C = [I], D = [0]. \tag{12}$$

The structure discussed in this section can be used for offline simulation of the modelled non-integer order dynamics. In order to apply it to an on-line application in control one needs to use $\Delta^{n\alpha} y_{k+n}$ (output of the network) to calculate the system output using only previous signals samples which are available.

In the next section we present the numerical example which illustrates the operation of the proposed structure.

4. NUMERICAL EXAMPLE

For all the simulations two groups of input signals were prepared. The first group of four signals was meant for learning process and the second group of two signals was used for testing process. The learning and testing signals are presented in Fig. 2 and Fig. 3 respectively. Final results of neural modelling were obtained by on-line simulations in Simulink using Neural Network Toolbox and Fractional State-Space Toolkit (FSST) (see e.g. Sierociuk (2005)).

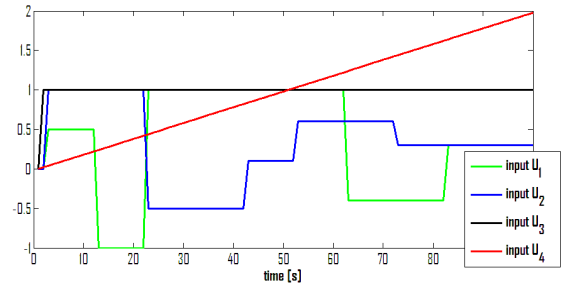

Fig. 2. Input learning signals $\boldsymbol{U_1, U_2, U_3, U_4}$

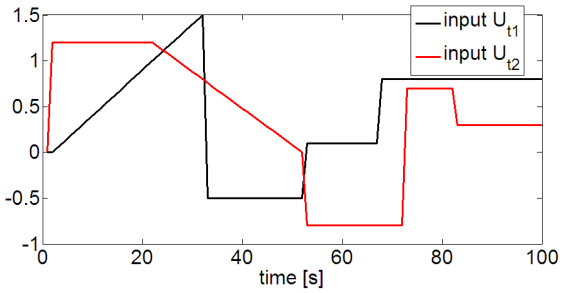

Fig. 3. Input testing signals $\boldsymbol{U_{t1}, U_{t2}}$

Example 1. Modelling of the fractional system by a discrete fractional order neural network

The system is given by the following equation:

$$\Delta^{0.5} y_{k+1} = -0.1 y_k^3 + u_k \tag{13}$$

For modelling the non-linear function in this system a two-layer neural network with two inputs and one output was used. The network consists of three neurons with nonlinear (tansign) activation function in the input layer and one linear neuron in the output layer.

The input vector for the fractional neural network for this case has the following form:

$$P = \begin{bmatrix} u_0 & u_1 & \cdots & u_k \\ y_0 & y_1 & \cdots & y_k \end{bmatrix} \tag{14}$$

The output vector has the form:

$$T = [\Delta^{0.5} y_1 \; \Delta^{0.5} y_2 \; \cdots \Delta^{0.5} y_{k+1}] \tag{15}$$

The DFOSS block has the following matrices:

$$A = [0], B = [1], C = [1], D = [0]. \quad (16)$$

The order of this block is equal to $\alpha = 0.5$ and is the same as the order of the given system equation.

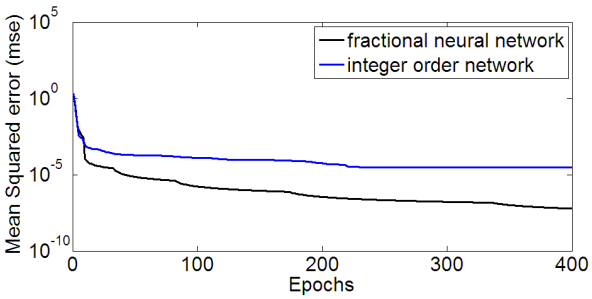

Fig. 4. Learning error for fractional and integer order neural network

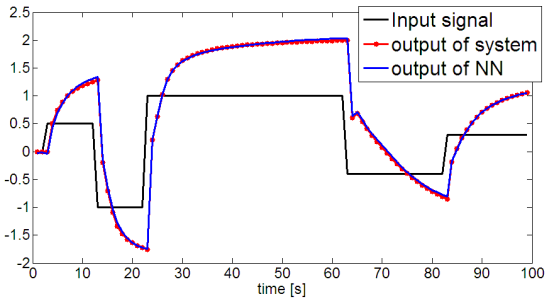

Fig. 5. Output of the fractional neural network for learning signal $\boldsymbol{U_1}$

For training the neural network the Levenberg-Marquardt and backpropagation algorithms (implemented in function TRAINLM in Neural Network Toolbox) were used for 400 epochs. The results of the performance of the network during learning process is presented in Fig. 4 (together with results of integer order neural network). As it could be seen the final error is very small, about 10^{-7}. Fig. 5 presents a comparison between the responses of the fractional neural network with original output for input signal U_1 from the group of learning signals. As it could be seen the accuracy of modelling is very high. Moreover, the Fig. 6 and Fig. 7 present analogical results for test signals U_{t1} and U_{t2} respectively. This results prove very high accuracy of modelling and confirm that the neural network has been properly taught. This also shows that the network is able to properly generalize data, which is the main feature of neural networks. Fig. 8 and Fig. 9 present results of neural modelling of the non-linear function. Fig. 8 presents the original non-linear function of the system equation, whereas Fig. 9 presents the modelling error, the difference between original function and the one modelled by neural network.

Example 2. Modelling of the same fractional system as in Example 1 by a discrete integer order neural network. In this example the traditional approach will be presented in which we try to model non-linear fractional order system by a non-linear integer order system with some (usually big) number of delays. Let us take into consideration the neural network with 5 inputs and one output. The neural network used has the following structure: input layer has 6 tansign neurons, output layer has one linear neuron. In this case the modelled equation has the form:

$$y_{k+4} = f(y_{k+3}, y_{k+2}, y_{k+1}, y_k, u_k) \quad (17)$$

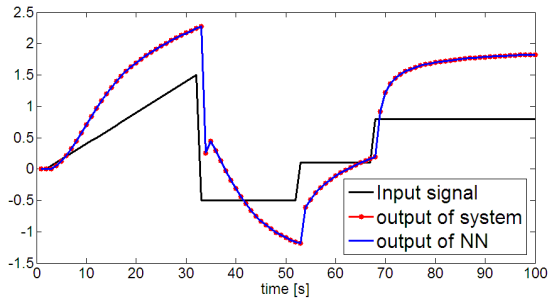

Fig. 6. Output of the fractional neural network for testing signal $\boldsymbol{U_{t1}}$

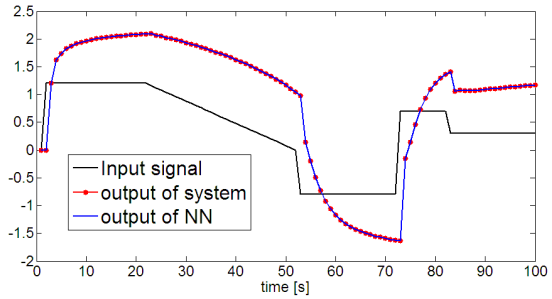

Fig. 7. Output of the fractional neural network for testing signal $\boldsymbol{U_{t2}}$

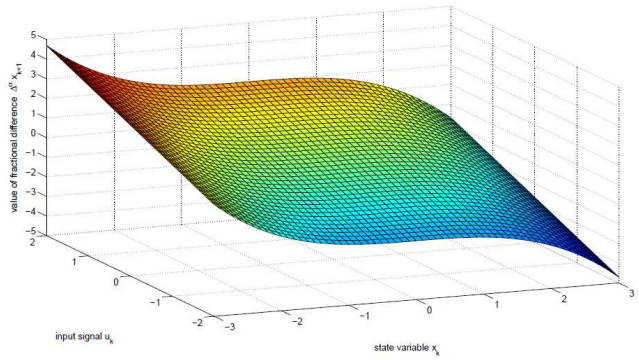

Fig. 8. Original non-linear function

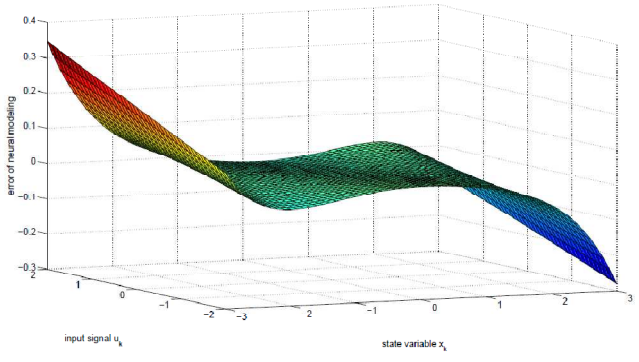

Fig. 9. Error of neural modelling

The results of the neural network performance during learning process are presented in Fig. 4. Fig. 10 presents results of simulation for one signal U_1 from learning group. As it may be seen the accuracy is acceptable. Additionally, the Fig. 11 and Fig. 12 present analogical results for the test signals U_{t1} and U_{t2} respectively. As it may be noticed, obtained results show unacceptable accuracy. In this case the integer order neural network is not able to properly generalize the data of the system, despite of the more complicated structure of a neural network. This justifies the main advantage of the proposed algorithm.

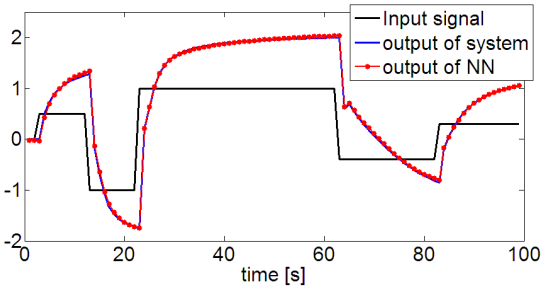

Fig. 10. Output of the integer order neural network for learning signal $\boldsymbol{U_1}$

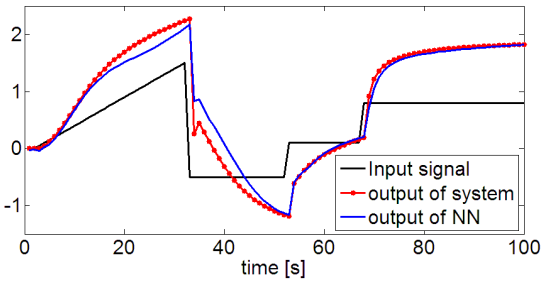

Fig. 11. Output of the integer order neural network for testing signal $\boldsymbol{U_{t1}}$

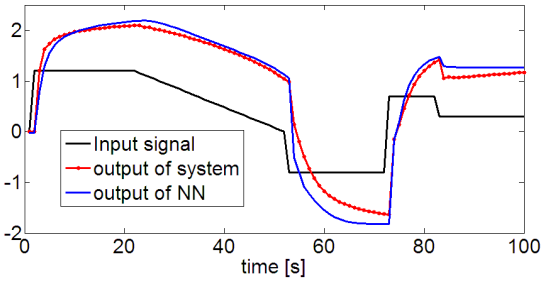

Fig. 12. Output of the integer order neural network for testing signal $\boldsymbol{U_{t2}}$

Example 3. Modelling of the fractional system with two state variables (one hidden) by the discrete fractional order neural network

Let us assume the system is given by the following equation:

$$\Delta^1 x_{1,k+2} = -0.1x_{2,k}^3 + u_k \tag{18}$$

where

$$x_{2,k} = \Delta^{0.5} y_{1,k+2} \tag{19}$$

In this case for modelling the non-linear function the two layer neural network with 3 inputs and one output was used. This network consisted of 3 neurons with non-linear (tansign) activation function in input layer and one linear neuron in output layer.

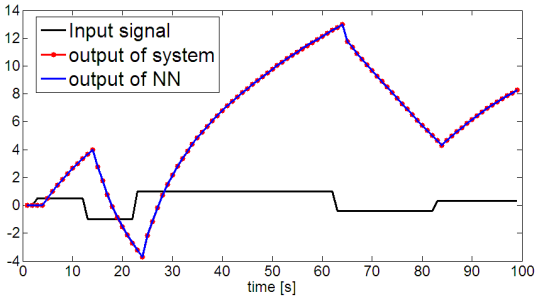

Fig. 13. Output of the fractional order neural network for learning signal $\boldsymbol{U_1}$

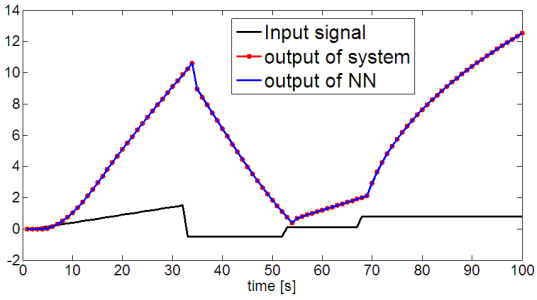

Fig. 14. Output of the fractional order neural network for testing signal $\boldsymbol{U_{t1}}$

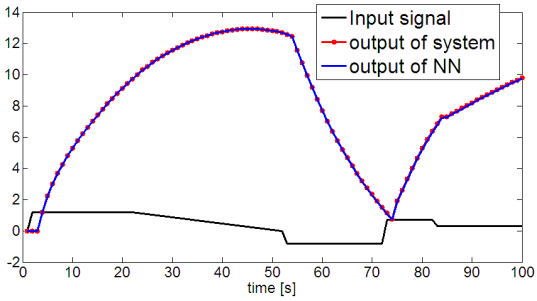

Fig. 15. Output of the fractional order neural network for testing signal $\boldsymbol{U_{t2}}$

The input vector for the fractional neural network has the following form:

$$P = \begin{bmatrix} u_0 & u_1 & \cdots & u_k \\ \Delta^{0.5} y_1 & \Delta^{0.5} y_2 & \cdots & \Delta^{0.5} y_{k+1} \\ y_0 & y_1 & \cdots & y_k \end{bmatrix} \tag{20}$$

The output vector has the form:

$$T = [\Delta^1 y_2 \ \Delta^1 y_3 \ \cdots \ \Delta^1 y_{k+2}] \tag{21}$$

The DFOSS block has the following matrices:

$$A = \begin{bmatrix} 0 & 1 \\ 0 & 0 \end{bmatrix}, B = \begin{bmatrix} 0 \\ 1 \end{bmatrix}, C = \begin{bmatrix} 1 & 0 \\ 0 & 1 \end{bmatrix}, D = \begin{bmatrix} 0 \\ 0 \end{bmatrix} \tag{22}$$

For training the neural network the same conditions as in previous examples were used. The results of an on-line simulation for one of the learning input signals

is presented in Fig. 13, while Fig. 14 and Fig. 15 present results for the testing input signals. As it may be seen the accuracy of neural modelling is very high.

5. CONCLUSIONS

In the paper we proposed a discrete time fractional order neural network. The structures given can be used to model the nonlinear fractional order dynamic systems. We have shown the appropriateness of the approach by the numerical examples. Also the advantages in modelling the fractional order discrete-time dynamic systems with the structure proposed over the traditional neural network coupled with the tapped-delay line have been shown in several example cases. Further research is needed to show the theoretical properties and advantages (and limitations) of the approach suggested.

REFERENCES

1. **Benoit-Marand F., Signac L., Poinot T., Trigeassou J.C**. (2006), Identification of non linear fractional systems using continuous time neural networks, *Proceedings of 2nd IFAC Workshop on Fractional Differentiation and its Applications*, IFAC FDA'06.
2. **Boroomand A., Menhaj M. B.** (2009), *Fractional order hopfield neural networks*, Lecture Notes in Computer Science: Advances in Neuro-Information Processing, 5506, 883–8902.
3. **Hunt K., Irwin G. Warwick K.** (1995), *Neural Network Engineering in Dynamic Control Systems*, Springer.
4. **Kalkkuhl J., Hunt K., Zbikowski R., Dzieliński A.** (1997), *Applications of neural adaptive control technology*, World Scientific.
5. **Nørgaard M., Ravn O., Poulsen N., Hansen L.** (2000), *Neural Networks for Modelling and Control of Dynamic Systems*, Springer.
6. **Oldham K., Spanier J.** (1974), *The Fractional Calculus. Academic Press*, New York.
7. **Podlubny I.** (1999), *Fractional Differential Equations*, Academic Press, San Diego.
8. **Sierociuk D.** (2005). Fractional Order Discrete State-Space System Simulink Toolkit User Guide http://www.ee.pw.edu.pl/˜dsieroci/fsst/fsst.htm
9. **Sierociuk D., Dzieliński A.** (2006), Fractional Kalman filter algorithm for states, parameters and order of fractional system estimation, *International Journal of Applied Mathematics and Computer Science*, 16(1), 129–140.
10. **Żbikowski R,. Hunt K.** (1996), *Neural adaptive control technology*, World Scientific.

This work was partially supported by the Polish Ministry of Science and Higher Education grant number 4125/B/T02/2009/36 and the European Union in the framework of European Social Fund through the Warsaw University of Technology Development Programme (by Centre for Advanced Studies WUT).

ABSTRACTS

Marek Błasik, Małgorzata Klimek
On Application of the Contraction Principle to Solve the Two-Term Fractional Differential Equations

We solve two-term fractional differential equations with left-sided Caputo derivatives. Existence-uniqueness theorems are proved using newly-introduced equivalent norms/metric on the space of continuous functions. The metrics are modified in such a way that the space of continuous functions is complete and the Banach theorem on a fixed point can be applied. It appears that the general solution is generated by the stationary function of the highest order derivative and exists in an arbitrary interval [0,b]

Tomasz Błaszczyk, Ewa Kotela, Matthew R. Hall, Jacek Leszczyński
Analysis and Applications of Composed Forms of Caputo Fractional Derivatives

In this paper we consider two ordinary fractional differential equations with composition of the left and the right Caputo derivatives. Analytical solution of this type of equations is known for particular cases, having a complex form, and therefore is difficult in practical calculations. Here, we present two numerical schemes being dependent on a fractional order of equation. The results of numerical calculations are compared with analytical solutions and then we illustrate convergence of our schemes. Finally, we show an application of the considered equation.

Mikołaj Busłowicz
Stability of State-Space Models of Linear Continuous-Time Fractional Order Systems

The paper considers the stability problem of linear time-invariant continuous-time systems of fractional order, standard and positive, described by the state space model. Review of previous results is given and some new methods for stability checking are presented. Considerations are illustrated by numerical examples and results of computer simulations.

Stefan Domek
Fuzzy Predictive Control of Fractional-Order Nonlinear Discrete-Time Systems

At the end of the 19th century Liouville and Riemann introduced the notion of a fractional-order derivative, and in the latter half of the 20th century the concept of the so-called Grünewald-Letnikov fractional-order discrete difference has been put forward. In the paper a predictive controller for MIMO fractional-order discrete-time systems is proposed, and then the concept is extended to nonlinear processes that can be modelled by Takagi-Sugeno fuzzy models. At first nonlinear and linear fractional-order discrete-time dynamical models are described. Then a generalized nonlinear fractional-order TS fuzzy model is defined, for which equations of a predictive controller are derived.

Marcin Graba
The Influence of Geometry of the Specimen and Material Properties on the Q-Stress Value Near the Crack Tip for SEN(T) Specimen

In the paper the short theoretical backgrounds about elastic-plastic fracture mechanics were presented and the O'Dowd-Shih theory was discussed. Using ADINA System program, the values of the Q-stress determined for various elastic-plastic materials for SEN(T) specimen – single edge notched plates in tension – were presented. The influence of kind of the specimen, crack length and material properties (work-hardening exponent and yield stress) on the Q-parameter were tested. The numerical results were approximated by the closed form formulas. Presented in the paper results are complementary of the two papers published in 2007 (Graba, 2007) and in 2010 (Graba, 2010), which show and describe influence of the material properties and crack length for the Q-stress value for SEN(B) and CC(T) specimens respectively. Presented and mentioned papers show such catalogue of the Q-stress value, which may be used in engineering analysis for calculation of the real fracture toughness.

Piotr Grześ
Partition of Heat in 2D Finite Element Model of a Disc Brake

In this paper nine of formulas (theoretical and experimental) for the heat partition ratio were employed to study the temperature distributions of two different geometrical types of the solid disc brake during emergency brake application. A two-dimensional finite element analysis incorporating specific values of the heat partition ratios was carried out. The boundary heat flux uniformly distributed over the circumference of a rubbing path to simulate the heat generated at the pad/disc interface was applied to the model. A number of factors over the heat partition ratio that affects the temperature fields are included and their importance is discussed.

Tadeusz Kaczorek
Positivity and Reachability of Fractional Electrical Circuits

Conditions for the positivity of fractional linear electrical circuits composed of resistors, coils, condensators and voltage (current) sources are established. It is shown that: 1) the fractional electrical circuit composed of resistors, coils and voltage source is positive for any values of their resistances, inductances and source voltages if and only if the number of coils is less or equal to the number of its linearly independent meshes, 2) the fractional electrical circuit is not positive for any values of its resistances, capacitances and source voltages if each its branch contains resistor, capacitor and voltage source, It is also shown that the fractional positive electrical circuits of *R*, *C*, *e* type are reachable if and only if the conductances between their nodes are zero and the fractional positive electrical circuits of *R*, *L*, *e* type are reachable if and only if the resistances belonging to two meshes are zero.

Tadeusz Kaczorek
Necessary and Sufficient Stability Conditions of Fractional Positive Continuous-Time Linear Systems

Necessary and sufficient conditions for the asymptotic stability of fractional positive continuous-time linear systems are established. It is shown that the matrix A of the stable fractional positive system has not eigenvalues in the part of stability region located in the right half of the complex plane.

Jerzy Klamka
Local Controllability of Fractional Discrete-Time Semilinear Systems

In the paper unconstrained local controllability problem of finite-dimensional fractional discrete-time semilinear systems with constant coefficients is addressed. Using general formula of solution of difference state equation sufficient condition for local unconstrained controllability in a given number of steps is formulated and proved. Simple illustrative example is also presented.

Zbigniew Kulesza
FPGA Based Active Magnetic Bearings Controller

The article discusses main problems of implementing the PID control law in the FPGA integrated circuit. Consecutive steps of discretizing and choosing the fixed-point representation of the continuous, floating-point PID algorithm are described. The FPGA controller is going to be used in the active hetero-polar magnetic bearings system consisting of two radial and one axial bearings. The results of the experimental tests of the controller are presented. The dynamic performance of the controller is better when compared with the dSPACE controller, that was used so far. The designed hardware and software, the developed implementation procedure and the experience acquired during this stage of the whole project are going to be used during the implementation of more sophisticated control laws (e.g. robust) in the FPGA for AMB controllers.

Wojciech Mitkowski
Approximation of Fractional Diffusion-Wave Equation

In this paper we consider the solution of the fractional differential equations. In particular, we consider the numerical solution of the fractional one dimensional diffusion-wave equation. Some improvements of computational algorithms are suggested. The considerations have been illustrated by examples.

Dorota Mozyrska, Ewa Pawłuszewicz
Linear q-Difference Fractional-Order Control Systems with Finite Memory

The formula for the solution to linear q-difference fractional-order control systems with finite memory is derived. New definitions of observability and controllability are proposed by using the concept of extended initial conditions. The rank condition for observability is established and the control law is stated.

Zbigniew Oksiuta
Microstructural Changes of Ods Ferritic Steel Powders During Mechanical Alloying

The ODS ferritic steel powder with chemical composition of Fe-14Cr-2W-0.3Ti-0.3Y2O3 was mechanically alloyed (MA) either from elemental or pre-alloyed powders in a planetary ball mill. Different milling parameters have been used to investigate their influence on the morphology and microstructure of the ODS ferritic steel powder. The time of MA was optimized by studying the structural evolution of the powder by means of X-ray diffractometry and TEM. In the case of elemental powder very small, about 10 µm in diameter, spherical particles with a large surface area have been obtained. Flakey-like particles with an average size of about 45 µm were obtained in the case of the pre-alloyed powder. The lattice strain calculated from XRD spectra of the elemental and pre-alloyed powders exhibits a value of about 0.51 % and 0.67, respectively. The pre-alloyed powder after consolidation process showed the highest density and microhardness value.

Piotr Ostalczyk
Variable-, Fractional-Orders Closed-Loop Systems Description

In this paper we explore the linear difference equations with fractional orders, which are functions of time. A description of closed-loop dynamical systems described by such equations is proposed. In a numerical example a simple control strategy based on time-varying fractional orders is presented.

Piotr Ostalczyk, Dariusz Brzeziński
Numerical Evaluation of Fractional Differ-Integral of Some Elementary Functions via Inverse Transformation

This paper presents methods of calculating fractional differ-integrals numerically. We discuss extensively the pros and cons of applying the Riemann-Liouville formula, as well as direct approach in form of The Grünwald-Letnikov method. We take closer look at the singularity, which appears when using classical form of Riemann-Liouville formula. To calculate Riemann-Liouville differ-integral we use very well-known techniques like The Newton-Cotes Midpoint Rule. We also use two Gauss formulas. By implementing transformation of the core integrand of Riemann-Liouville formula (we called it “the inverse transformation”), we would like to point the possible way of reducing errors when calculating it. The core of this paper is the subject of reducing the absolute error when calculating Riemann-Liouville differ-integrals of some elementary functions; we use our own C++ programs to calculate them and compare obtained results of all methods with, where possible, exact values, where not – with values obtained using excellent method of integration incorporated in Mathematica. We will not discuss complexity of numerical calculations. We will focus solely on minimization of the absolute errors.

Ivo Petráš, Dagmar Bednárová
Control of Fractional-Order Nonlinear Systems: A Review

This paper deals with the control of the fractional-order nonlinear systems. A list of the control strategies as well as synchronization of the chaotic systems is presented. An illustrative example of sliding mode control (SMC) of the fractional-order (commensurate and incommensurate) financial system is described and commented together with the simulation results.

Paweł Piątek, Jerzy Baranowski
Investigation of Fixed-Point Computation Influence on Numerical Solutions of Fractional Differential Equations

In this paper the problem of the influence of fixed point computation on numerical solutions of linear differential equations of fractional order is considered. It is a practically important problem, because of potential possibilities of using dynamical systems of fractional order in the tasks of control and filtering. Discussion includes numerical method is based on the Grünwald-Letnikov fractional derivative and how the application of fixed-point architecture influences its operation. Conclusions are illustrated with results of floating-point arithmetic with double precision and fixed point arithmetic with different word lengths.

Yuriy Povstenko
Solutions to Time-Fractional Diffusion-Wave Equation in Spherical Coordinates

Solutions to time-fractional diffusion-wave equation with a source term in spherical coordinates are obtained for an infinite medium. The solutions are found using the Laplace transform with respect to time t, the finite Fourier transform with respect to the angular coordinate φ, the Legendre transform with respect to the spatial coordinate μ, and the Hankel transform of the order n+1/2 with respect to the radial coordinate r. In the central symmetric case with one spatial coordinate r the obtained results coincide with those studied earlier.

Krzysztof Rogowski
General Response Formula for Fractional 2D Continuous-Time Linear Systems Described by the Roesser Model

A new class of fractional two-dimensional (2D) continuous-time linear systems is introduced. The general response formula for the system is derived using a 2D Laplace transform. It is shown that the classical Cayley-Hamilton theorem is valid for such class of systems. Usefulness of the general response formula to obtain a solution of the system is discussed and illustrated by a numerical example.

Andrzej Ruszewski, Tomasz Nartowicz
Stabilization of Inertial Plant with Time Delay Using Fractional Order Controller

The paper presents the problem of designing of a fractional order controller satisfying the conditions of gain and phase margins of the closed-loop system with time-delay inertial plant. The transfer function of the controller follows directly from the use of Bode's ideal transfer function as a reference transfer function for the open loop system. Using the classical D-partition method and the gain-phase margin tester, a simple computational method for determining stability regions in the controller parameters plane is given. An efficient analytical procedure to obtain controller parameter values for specified gain and phase margin requirements is also given. The considerations are illustrated by numerical examples computed in MATLAB/Simulink.

Łukasz Sajewski
Positive Realization of SISO 2D Different Orders Fractional Discrete-Time Linear Systems

The realization problem for single-input single-output 2D positive fractional systems with different orders is formulated and a method based on the state variable diagram for finding a positive realization of a given proper transfer function is proposed. Sufficient conditions for the existence of a positive realization of this class of 2D linear systems are established. A procedure for computation of a positive realization is proposed and illustrated by a numerical example.

Dominik Sierociuk, Grzegorz Sarwas, Andrzej Dzieliński
Discrete Fractional Order Artificial Neural Network

In this paper the discrete time fractional order artificial neural network is presented. This structure is proposed for simulating the dynamics of non-linear fractional order systems. In the second part of this paper several numerical examples are shown. The final part of the paper presents the discussion on the use of fractional or integer discrete time neural network for modelling and simulating fractional order non-linear systems. The simulation results show the advantages of the proposed solution over the classical (integer) neural network approach to modelling of non-linear fractional order systems.